

AD-A063 986

SOUTH CAROLINA UNIV COLUMBIA COASTAL RESEARCH DIV
HYDRAULICS AND DYNAMICS OF NORTH INLET, SOUTH CAROLINA, 1975-76--ETC(U)
SEP 78 D NUMMEDAL, S M HUMPHRIES

F/G 8/3

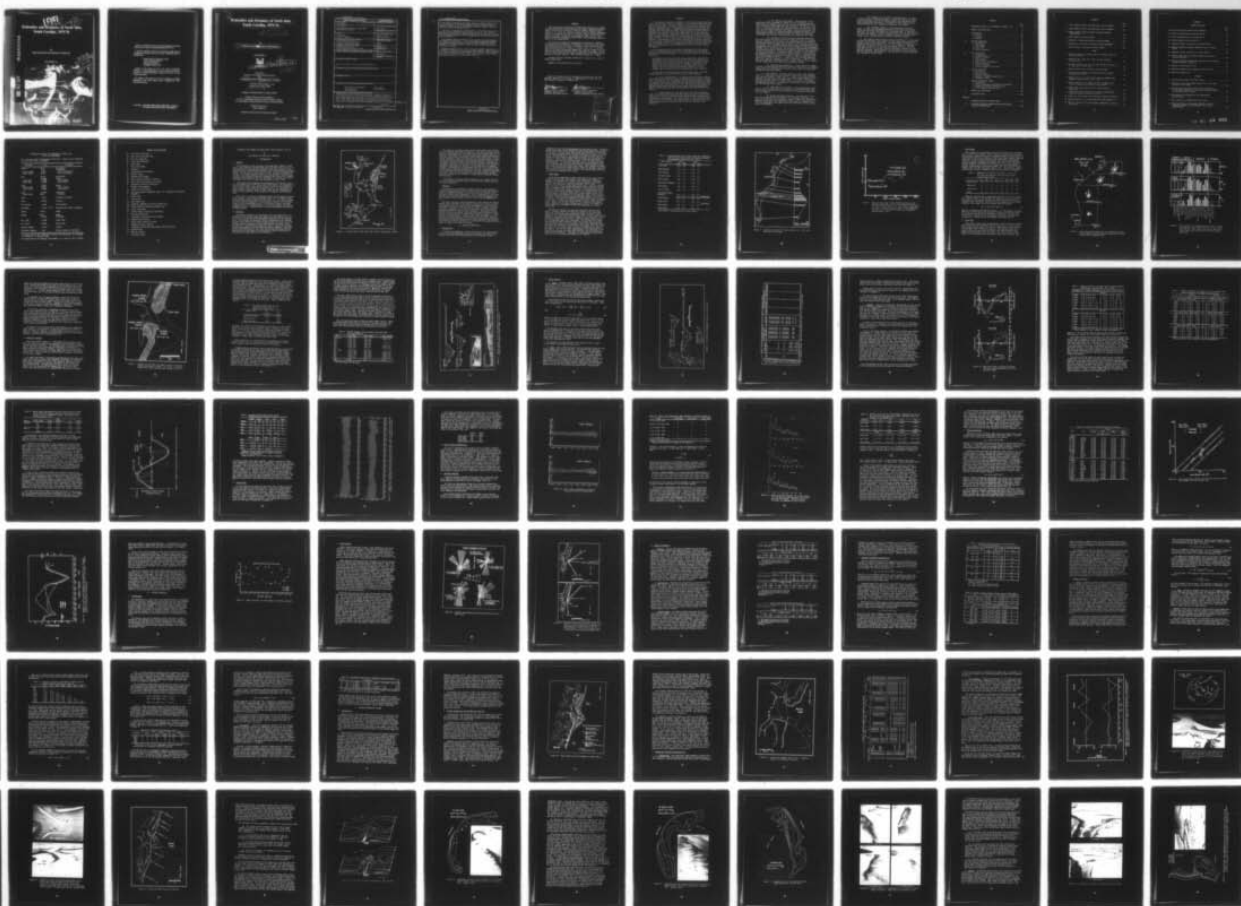
DACW72-72-C-0032

UNCLASSIFIED

WES-GITI-16

NL

1 OF 3
ADA
063986



LEVEL

A0 334912

Hydraulics and Dynamics of North Inlet, South Carolina, 1975-76

AD A063986

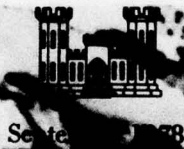
by

Dag Nummedal and Stanley M. Humphries

GITI REPORT 16

DDC
JAN 30 1979
UNIVERSITY OF SOUTH CAROLINA

DDC FILE COPY



September 1978

Research Center

DACW72-74-0018

by

University of South Carolina
Columbia, South Carolina 29208

GENERAL INVESTIGATION OF TIDAL INLETS

A Program of Research Conducted Jointly by

U.S. Army Coastal Engineering Research Center, Fort Belvoir, Virginia
U.S. Army Engineer Waterways Experiment Station, Vicksburg, Mississippi

Department of the Army
Corps of Engineers

NOT FOR PUBLICATION UNLESS SPECIFICALLY AUTHORIZED

29 060

Reprint or republication of any of this material shall give appropriate credit to the U.S. Army Coastal Engineering Research Center.

Limited free distribution within the United States of single copies of this publication has been made by this Center. Additional copies are available from:

*National Technical Information Service
ATTN: Operations Division
5285 Port Royal Road
Springfield, Virginia 22151*

Contents of this report are not to be used for advertising, publication, or promotional purposes. Citation of trade names does not constitute an official endorsement or approval of the use of such commercial products.

The findings in this report are not to be construed as an official Department of the Army position unless so designated by other authorized documents.

Cover Photo: North Inlet, South Carolina, March 1975. Courtesy of the National Aeronautics and Space Administration.

⑥
**Hydraulics and Dynamics of North Inlet,
South Carolina, 1975-76.**

⑨ Final rept.,

by

⑩ Dag/Nummedal [redacted] Stanley M./Humphries

GITI REPORT 16



⑪ September 1978

⑱ WES

⑲ GITI-16

⑫ 18p.

Prepared for

U.S. Army Coastal Engineering Research Center

under

⑮ Contract Nos. DACW72-72-C-0032 [redacted] DACW72-74-C-0018

by

University of South Carolina *New*
Columbia, South Carolina 29208
Coastal Research Div

GENERAL INVESTIGATION OF TIDAL INLETS

A Program of Research Conducted Jointly by

U.S. Army Coastal Engineering Research Center, Fort Belvoir, Virginia
U.S. Army Engineer Waterways Experiment Station, Vicksburg, Mississippi

Department of the Army
Corps of Engineers

APPROVED FOR PUBLIC RELEASE; DISTRIBUTION UNLIMITED

411 049

7012

UNCLASSIFIED

SECURITY CLASSIFICATION OF THIS PAGE (When Data Entered)

REPORT DOCUMENTATION PAGE		READ INSTRUCTIONS BEFORE COMPLETING FORM
1. REPORT NUMBER GITI Report 16	2. GOVT ACCESSION NO.	3. RECIPIENT'S CATALOG NUMBER
4. TITLE (and Subtitle) HYDRAULICS AND DYNAMICS OF NORTH INLET, SOUTH CAROLINA, 1975-76		5. TYPE OF REPORT & PERIOD COVERED Final Report
		6. PERFORMING ORG. REPORT NUMBER
7. AUTHOR(s) Dag Nummedal Stanley M. Humphries		8. CONTRACT OR GRANT NUMBER(s) DACW72-72-C-0032 DACW72-74-C-0018
9. PERFORMING ORGANIZATION NAME AND ADDRESS Coastal Research Division University of South Carolina Columbia, South Carolina 29208		10. PROGRAM ELEMENT, PROJECT, TASK AREA & WORK UNIT NUMBERS F31019
11. CONTROLLING OFFICE NAME AND ADDRESS Department of the Army Coastal Engineering Research Center Kingman Building, Fort Belvoir, Virginia 22060		12. REPORT DATE September 1978
		13. NUMBER OF PAGES 214
14. MONITORING AGENCY NAME & ADDRESS (if different from Controlling Office)		15. SECURITY CLASS. (of this report) UNCLASSIFIED
		15a. DECLASSIFICATION/DOWNGRADING SCHEDULE
16. DISTRIBUTION STATEMENT (of this Report) Approved for public release, distribution unlimited.		
17. DISTRIBUTION STATEMENT (of the abstract entered in Block 20, if different from Report)		
18. SUPPLEMENTARY NOTES		
19. KEY WORDS (Continue on reverse side if necessary and identify by block number) Beach and inlet morphology Tidal inlets North Inlet, S.C. Wave parameters Tidal hydraulics		
20. ABSTRACT (Continue on reverse side if necessary and identify by block number) North Inlet, South Carolina, was selected as a natural tidal inlet for investigation within the scope of the Army Corps of Engineers' program on General Investigations of Tidal Inlets. Over a 2-year period, from July 1974 to June 1976, eight 2-week intensive field sessions were conducted at the inlet. Three tide gages provided nearly continuous water surface elevation records for the ocean and tidal creeks throughout the period of investigation. (continued)		

CONT →

DD FORM 1 JAN 73 1473

EDITION OF 1 NOV 65 IS OBSOLETE

UNCLASSIFIED

SECURITY CLASSIFICATION OF THIS PAGE (When Data Entered)

UNCLASSIFIED

SECURITY CLASSIFICATION OF THIS PAGE(When Data Entered)

CONT

→ The analysis presented in this report focuses on three attributes of the inlet environment: (a) the inlet hydraulics, (b) the longshore currents adjacent to the inlet, and (c) the seasonal morphologic change of the North Inlet tidal deltas and adjacent beaches.

North Inlet is hydraulically ebb dominated. For the throat section, the peak ebb velocity exceeded the peak flood by a factor of 1.22. The model presented to account for this difference explains the ebb dominance as a result of the different efficiency of water exchange between the ocean and the bay at high and low tide.

The longshore currents off Debidue Island were found to be significantly controlled by the wind stress. In a multiple stepwise regression procedure, the longshore component of wind velocity was found to explain more of the variance in the observed longshore current velocity than any other measured environmental parameter.

→ Topographic mapping of inlet shoals and adjacent beaches, combined with bathymetric profiling of the throat and the major channels, suggest that there is a sediment exchange between the channels and the beaches. During periods of fair weather, the beaches accrete and the channels appear to scour. During high-energy conditions, the reverse seems to occur.

UNCLASSIFIED

2

SECURITY CLASSIFICATION OF THIS PAGE(When Data Entered)

FOREWORD

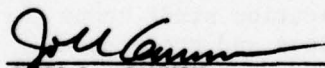
This report results from work performed under Contract Nos. DACW72-72-C-0032 and DACW72-74-C-0018 between the Coastal Engineering Research Center (CERC) and the University of South Carolina, Columbia, South Carolina. It is one in a series of reports from the Corps of Engineers' General Investigation of Tidal Inlets (GITI), which is under the technical surveillance of CERC and is conducted by CERC, the U.S. Army Engineer Waterways Experiment Station (WES), other government agencies, and by private organizations.

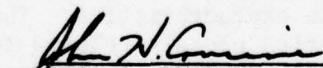
The report was prepared by Dag Nummedal and Stanley M. Humphries. M.O. Hayes served as principal investigator on the contracts and supervised preparation of the report. Assistance in data collection and analysis was provided by J. Knoth, J. Sexton, and F. Lee. B. Kjerfve and R. Finley made many helpful suggestions. Logistics support was provided by the Coastal Research Division, Department of Geology, and the Belle W. Baruch Institute for Marine Biology and Coastal Studies of the University of South Carolina. CERC technical monitor was C. Mason.


Technical Directors of CERC and WES were T. Saville, Jr., and F.R. Brown, respectively.

Comments on the publication are invited.

Approved for publication in accordance with Public Law 166, 79th Congress, approved 31 July 1945, as supplemented by Public Law 172, 88th Congress, approved 7 November 1963.


JOHN L. CANNON
Colonel, Corps of Engineers
Commander and Director
Waterways Experiment Station


JOHN H. COUSINS
Colonel, Corps of Engineers
Commander and Director
Coastal Engineering Research Center

ACCESSION for	
NTIS	File Section <input checked="" type="checkbox"/>
DDC	Ref Section <input type="checkbox"/>
UNANNOUNCED	<input type="checkbox"/>
PUBLICATION	<input type="checkbox"/>
BY	
DISTRIBUTION/AVAILABILITY CODES	
Dist	SPECIAL
	

PREFACE

1. The Corps of Engineers, through its Civil Works program, has sponsored, over the past 23 years, research into the behavior and characteristics of tidal inlets. The Corps' interest in tidal inlet research stems from its responsibilities for navigation, beach erosion prevention and control, and flood control. Tasked with the creation and maintenance of navigable U.S. waterways, the Corps dredges millions of cubic yards of material each year from tidal inlets that connect the ocean with bays, estuaries, and lagoons. Design and construction of navigation improvements to existing tidal inlets are an important part of the work of many Corps' offices. In some cases, design and construction of new inlets are required. Development of information concerning the hydraulic characteristics of inlets is important not only for navigation and inlet stability, but also because inlets, by allowing for the ingress of storm surges and egress of flood waters, play an important role in the flushing of bays and lagoons.

2. A research program, the General Investigation of Tidal Inlets (GITI), was developed to provide quantitative data for use in design of inlets and inlet improvements. It is designed to meet the following objectives:

To determine the effects of wave action, tidal flow, and related phenomena on inlet stability and on the hydraulic, geometric, and sedimentary characteristics of tidal inlets; to develop the knowledge necessary to design effective navigation improvements, new inlets, and sand transfer systems at existing tidal inlets; to evaluate the water transfer and flushing capability of tidal inlets; and to define the processes controlling inlet stability.

3. The GITI is divided into three major study areas: (a) inlet classification, (b) inlet hydraulics, and (c) inlet dynamics.

a. Inlet Classification. The objectives of the inlet classification study are to classify inlets according to their geometry, hydraulics, and stability, and to determine the relationships that exist among the geometric and dynamic characteristics and the environmental factors that control these characteristics. The classification study keeps the general investigation closely related to real inlets and produces an important inlet data base useful in documenting the characteristics of inlets.

b. Inlet Hydraulics. The objectives of the inlet hydraulics study are to define tide-generated flow regime and water level fluctuations in the vicinity of coastal inlets and to develop techniques for predicting these phenomena. The inlet hydraulics study is divided into three areas: (1) idealized inlet model study, (2) evaluation of state-of-the-art physical and numerical models, and (3) prototype inlet hydraulics.

(1) The Idealized Inlet Model. The objectives of this model study are to determine the effect of inlet configurations and structures on discharge, head loss and velocity distribution for a number of realistic inlet shapes and tide conditions. An initial set of tests in a trapezoidal inlet was conducted between 1967 and 1970. However, in order that subsequent inlet models are more representative of real inlets, a number of "idealized" models representing various inlet morphological classes are being developed and tested. The effects of jetties and wave action on the hydraulics are included in the study.

(2) Evaluation of State-of-the-Art Modeling Techniques. The objectives of this part of the inlet hydraulics study are to determine the usefulness and reliability of existing physical and numerical modeling techniques in predicting the hydraulic characteristics of inlet-bay systems, and to determine whether simple tests, performed rapidly and economically, are useful in the evaluation of proposed inlet improvements. Masonboro Inlet, North Carolina, was selected as the prototype inlet which would be used along with hydraulic and numerical models in the evaluation of existing techniques. In September 1969 a complete set of hydraulic and bathymetric data was collected at Masonboro Inlet. Construction of the fixed-bed physical model was initiated in 1969, and extensive tests have been performed since then. In addition, three existing numerical models were applied to predict the inlet's hydraulics. Extensive field data were collected at Masonboro Inlet in August 1974 for use in evaluating the capabilities of the physical and numerical models.

(3) Prototype Inlet Hydraulics. Field studies at a number of inlets are providing information on prototype inlet-bay tidal hydraulic relationships and the effects of friction, waves, tides, and inlet morphology on these relationships.

c. *Inlet Dynamics.* The basic objective of the inlet dynamics study is to investigate the interactions of tidal flow, inlet configuration, and wave action at tidal inlets as a guide to improvement of inlet channels and nearby shore protection works. The study is subdivided into four specific areas: (1) model materials evaluation, (2) movable-bed modeling evaluation, (3) reanalysis of a previous inlet model study, and (4) prototype inlet studies.

(1) Model Materials Evaluation. This evaluation was initiated in 1969 to provide data on the response of movable-bed model materials to waves and flow to allow selection of the optimum bed materials for inlet models.

(2) Movable-Bed Model Evaluation. The objective of this study is to evaluate the state-of-the-art of modeling techniques, in this case movable-bed inlet modeling. Since, in many cases, movable-bed modeling is the only tool available for predicting the response of an inlet to improvements, the capabilities and limitations of these models must be established.

(3) Reanalysis of an Earlier Inlet Model Study. In 1975, a report entitled, "Preliminary Report: Laboratory Study of the Effect of an Uncontrolled Inlet on the Adjacent Beach," was published by the Beach Erosion Board (now CERC). A reanalysis of the original data is being performed to aid in planning of additional GITI efforts.

(4) Prototype Dynamics. Field and office studies of a number of inlets are providing information on the effects of physical forces and artificial improvements on inlet morphology. Of particular importance are studies to define the mechanisms of natural sand bypassing at inlets, the response of inlet navigation channels to dredging and natural forces, and the effects of inlets on adjacent beaches.

4. This report presents results of the second phase of a field study to define the hydraulics and dynamics of North Inlet, South Carolina, a natural Atlantic coast tidal inlet. Detailed bathymetric mapping of the intertidal and shallow subtidal zones is used to define the seasonal morphologic variability of the inlet and adjacent beaches. Wave and tidal data are used to correlate observed bathymetric changes with the causative processes, and to provide basic information on wave conditions and inlet hydraulic characteristics. Results for the 1974-75 field year were included in Finley (1976).

CONTENTS

	Page
CONVERSION FACTORS, U.S. CUSTOMARY TO METRIC (SI)	12
SYMBOLS AND DEFINITIONS	13
I INTRODUCTION.	15
1. General.	15
2. Processes.	15
3. Response	17
II REGIONAL VARIABILITY.	17
1. Introduction	17
2. Tidal Range.	18
3. Wave Energy.	22
4. Inlet Size	22
5. Storm Frequencies.	25
III TIDAL HYDRAULICS.	25
1. Introduction	25
2. Hydraulic Geometry	27
3. Tidal Currents	32
4. Tidal Curves	43
5. Water Surface Differentials.	45
6. Spectral Analysis.	45
7. Inlet Equilibrium.	50
8. Seasonal Changes in Sea Level.	53
IV LITTORAL PROCESSES.	56
1. Introduction	56
2. Wind Patterns.	58
3. Breaker Parameters	61
4. Longshore Sediment Transportation.	63
5. Longshore Currents	65
V SEASONAL MORPHOLOGIC CHANGE	72
1. Introduction	72
2. General Morphology and Sediment Distribution	73
3. Morphologic Response Characteristics	75
4. Process Response Interactions.	102
VI SUMMARY AND CONCLUSIONS	105
LITERATURE CITED.	109
APPENDIX	
A FATHOMETER PROFILES AT NORTH INLET.	117
B TIME-SERIES DATA ON CURRENT VELOCITIES AND WATER SURFACE DIFFERENTIALS.	130

CONTENTS

	Page
C TIDAL CURRENT VELOCITY AND PHASE DATA, 1975-76 SEASON	146
D TIDAL CURRENT VELOCITY AND PHASE DATA, 1974-75 SEASON	157
E HOURLY CURRENT VELOCITY READINGS AND WATER SURFACE DIFFERENTIALS.	166
F WATER SURFACE ELEVATION RECORDS	174
G SPECTRA OF 2-WEEK WATER SURFACE ELEVATION RECORDS	191
H DESCRIPTIVE STATISTICS OF LITTORAL PROCESS PARAMETERS	197
I BEACH PROFILES AT DEBIDUE AND NORTH ISLANDS	204

TABLES

1 Spring and mean tidal ranges along the southeast coast of the United States.	19
2 Deepwater wave energy flux values for the southeast United States.	22
3 Bay water surface area, A_b , and inlet throat flow area, A_c , as functions of water level.	29
4 Monthly channel cross-sectional areas below MSL	30
5 North Inlet hydrography measurements and water surface differentials, 1975-76	34
6 Summary statistics on North Inlet current parameters and hydraulic lag constants, 1974 to 1976.	37
7 Summary statistics, by channel section, on North Inlet current parameters and hydraulic lag constants	38
8 Median phase lags measured at the throat section at North Inlet.	41
9 Correlation matrices between water surface differential values and current velocities, 1975-76	43
10 Water level time-series data subjected to spectral analysis . .	47
11 Radian frequency, f , in cycles per hour versus period, T	47
12 Spectral densities for tidal harmonic components M_1 , M_2 , M_4 , M_6 , and M_8	49

CONTENTS

TABLES--Continued

	Page
13 North Inlet ebb and flood tidal discharge	51
14 Percent spilling waves at station DBI-25.	62
15 Percent plunging waves at station DBI-25.	62
16 Breaker heights at station DBI-25	62
17 Longshore energy flux factors at station DBI-25	64
18 Computed longshore sediment transport rates at station DBI-25	64
19 Longshore current velocities at station DBI-25.	67
20 Variable names used in multiple regression analysis of littoral processes	68
21 Pearson correlation coefficients between littoral process variables defined in Table 20.	69
22 Percent of the variance in VEL.	70
23 Regression equations for longshore current velocity	72
24 Quarterly sediment data	77

FIGURES

1 Location map of North Inlet and vicinity.	16
2 Variation in mean tidal range along the U.S. east coast from New York to Miami	20
3 Observed mean tidal range versus offshore distance to the 200-meter bathymetric contour for selected stations of the eastern United States	21
4 Wave energy flux diagrams for the southeastern United States.	23
5 Size variation in southeastern tidal inlets	24
6 Annual probability of hurricane landfalls within 80- kilometer segments on the southeast coast of the United States.	26

CONTENTS
FIGURES--Continued

	Page
7 Location of the three tide gages relative to the main channels and barrier islands	28
8 Typical profiles of the 5 bathymetric sections monitored during the study	31
9 Location of hydrography stations at North Inlet	33
10 Time-series data of current velocities and water surface differentials at Town and Jones Creeks	36
11 Histograms summarizing the distribution of high water and low water tidal lag at the North Inlet throat section.	40
12 Diagram illustrating the "typical" tidal cycle at North Inlet.	42
13 Sample water elevation records for the Jones Creek gage	44
14 Water surface differential curves for the period 28 April to 12 May 1976	46
15 Spectral density functions for 2-week records off the ocean, Town Creek, and Jones Creek gages.	48
16 Tidal prisms versus throat cross-sectional areas for North Inlet between July 1974 and May 1976	52
17 Measured tidal prism versus ocean tidal range	54
18 Annual variation in MSL computed from available 2-week tide gage records of the ocean, Jones Creek, and Town Creek gages.	55
19 Annual variation in tide ranges at the three stations	57
20 Seasonal distributions of wind directions observed at North Inlet.	59
21 Resultant wind vectors for each 2-week field period	60
22 Major depositional environments at North Inlet.	74
23 Location of sediment sample sites	76
24 Changes in cross-sectional areas of Town Creek and Jones Creek.	79

CONTENTS
FIGURES--Continued

	Page
25 Diagram of a flood tidal delta and oblique air photo of the North Inlet flood tidal delta, June 1975	80
26 Topographic map of the North Inlet flood tidal delta.	81
27 Diagram of an ebb tidal delta and oblique air photo of the North Inlet tidal delta, January 1976.	83
28 Beach and offshore profile locations.	84
29 North Inlet nearshore bathymetry in 1964 and 1976	86
30 Topographic map and oblique air photo of the northern channel-margin linear bar at North Inlet, 13 January 1966. . .	87
31 Topographic map and oblique air photo of the northern channel-margin linear bar at North Inlet, 18 March 1976. . . .	89
32 Topographic map of the southern channel-margin linear bar, 18 March 1976.	90
33 Seasonal changes in configuration of the southern channel- margin linear bar.	91
34 Configuration of swash bar complex off North Island	93
35 Oblique air photo and topographic map of swash bar complex off North Island, 1 October 1975	94
36 Oblique air photo and topographic map illustrating beach progradation at the point of bar attachment, 17 January 1976.	95
37 Topographic map of the area of bar attachment at North Island and the adjacent swash bar, 17 March 1976	96
38 Oblique air photo and topographic map of Debidue Island recurved spit, 28 September 1975	98
39 Oblique air photo and topographic map of Debidue Island recurved spit, 11 January 1976	99
40 Oblique air photo and topographic map of Debidue Island recurved spit, 19 March 1976	100
41 Trends of beach erosion and deposition on Debidue and North Islands from June 1975 to May 1976	101
42 Seasonal change in position of the shoreline of the Debidue Island recurved spit	103
43 Seasonal changes of the beach face on North Island where bar attachment dominated nearshore morphology.	104
44 Average trends in beach erosion and deposition on Debidue and North Islands and channel cross sections	106

CONVERSION FACTORS, U.S. CUSTOMARY TO METRIC (SI)
UNITS OF MEASUREMENT

U.S. customary units of measurement used in this report can be converted to metric (SI) units as follows:

Multiply	by	To obtain
inches	25.4	millimeters
	2.54	centimeters
square inches	6.452	square centimeters
cubic inches	16.39	cubic centimeters
feet	30.48	centimeters
	0.3048	meters
square feet	0.0929	square meters
cubic feet	0.0283	cubic meters
yards	0.9144	meters
square yards	0.836	square meters
cubic yards	0.7646	cubic meters
miles	1.6093	kilometers
square miles	259.0	hectares
knots	1.852	kilometers per hour
acres	0.4047	hectares
foot-pounds	1.3558	newton meters
millibars	1.0197×10^{-3}	kilograms per square centimeter
ounces	28.35	grams
pounds	453.6	grams
	0.4536	kilograms
ton, long	1.0160	metric tons
ton, short	0.9072	metric tons
degrees (angle)	0.01745	radians
Fahrenheit degrees	5/9	Celsius degrees or Kelvins ¹

¹To obtain Celsius (C) temperature readings from Fahrenheit (F) readings, use formula: $C = (5/9) (F - 32)$.

To obtain Kelvin (K) readings, use formula: $K = (5/9) (F - 32) + 273.15$.

SYMBOLS AND DEFINITIONS

A_b	bay water surface area
A_c	inlet cross-sectional area
a_b	bay tidal amplitude
a_o	ocean tidal amplitude
d	water depth
F	tidal form number
f	frequency
g	gravitational acceleration
H_b	breaker height
H_o	deepwater wave height
H_1	water surface elevation in the bay
H_2	water surface elevation in the ocean
K	Kuelegan's repletion coefficient
k	breaker form parameter
L_c	length of inlet channel
M_i	i th tidal harmonic component, where M_1 designates the diurnal component
m	beach slope
P	tidal prism
P_f	wave energy flux
P_{ls}	longshore component of the wave energy flux
Q_s	annual longshore sediment transport rate
R_o	ocean tidal range
r	product-moment correlation coefficient
r'	friction coefficient
T	semidiurnal tidal period (12.42 hours)
T_o	deepwater wave period
u	mean current velocity in inlet
V	longshore current velocity
W	discharge into the bay from sources other than inlet
α_b	breaker angle
ρ	density of water
σ	bed shear stress

HYDRAULICS AND DYNAMICS OF NORTH INLET, SOUTH CAROLINA, 1975-76

by

Dag Nummedal and Stanley M. Humphries

I. INTRODUCTION

1. General.

Tidal hydraulics, wave processes, and morphologic changes at North Inlet, South Carolina, were monitored from July 1974 to May 1976, to define the physical environmental parameters characterizing this stable, unmodified, tidal inlet on the mesotidal coast of the southeastern United States. Results from the first year of study, including the geological setting, the littoral process variability, the hydraulic parameters of the inlet, and detailed analysis of longshore wave energy flux, sediment transport characteristics, and the development of the inlet and associated shoals over historic time, are presented in Finley (1976).

The present report completes the presentation of hydraulic, littoral, and morphologic data for the 2-year study period. To complement the work of Finley (1976), this report focuses on a more detailed analysis of the travel of the tidal wave through the inlet, the relationship between seasonal changes in mean sea level (MSL) and the morphologic response, and the question of the mechanics of longshore current generation.

North Inlet is located in Georgetown County, South Carolina, and provides drainage to the Atlantic Ocean for about 24×10^6 square meters of marsh behind Debidue and North Islands (Fig. 1). The marsh is bounded to the south by Winyah Bay, a large estuary formed at the confluence of the Pee Dee and Waccamaw Rivers. To the west or north, the marsh borders directly on Pleistocene units of the lower Coastal Plain physiographic province. Further details on local stratigraphy are provided in Finley (1976).

2. Processes.

The hydraulic behavior of a mesotidal inlet like North Inlet is a function of the adjacent ocean tidal range, the wave climate, the size of the bay, and the degree of development of marsh within the drainage area. To facilitate an evaluation of how representative the findings at North Inlet would be for other southeast inlets of similar size, the regional process variability between Cape Hatteras and south Florida was reviewed. North Inlet was found to occupy a transitional position between wave-dominated and tide-dominated coastal segments. Therefore, process characterization of the inlet system entailed documenting the mean values and the ranges of all pertinent variables describing the nearshore wave climate and the inlet currents.

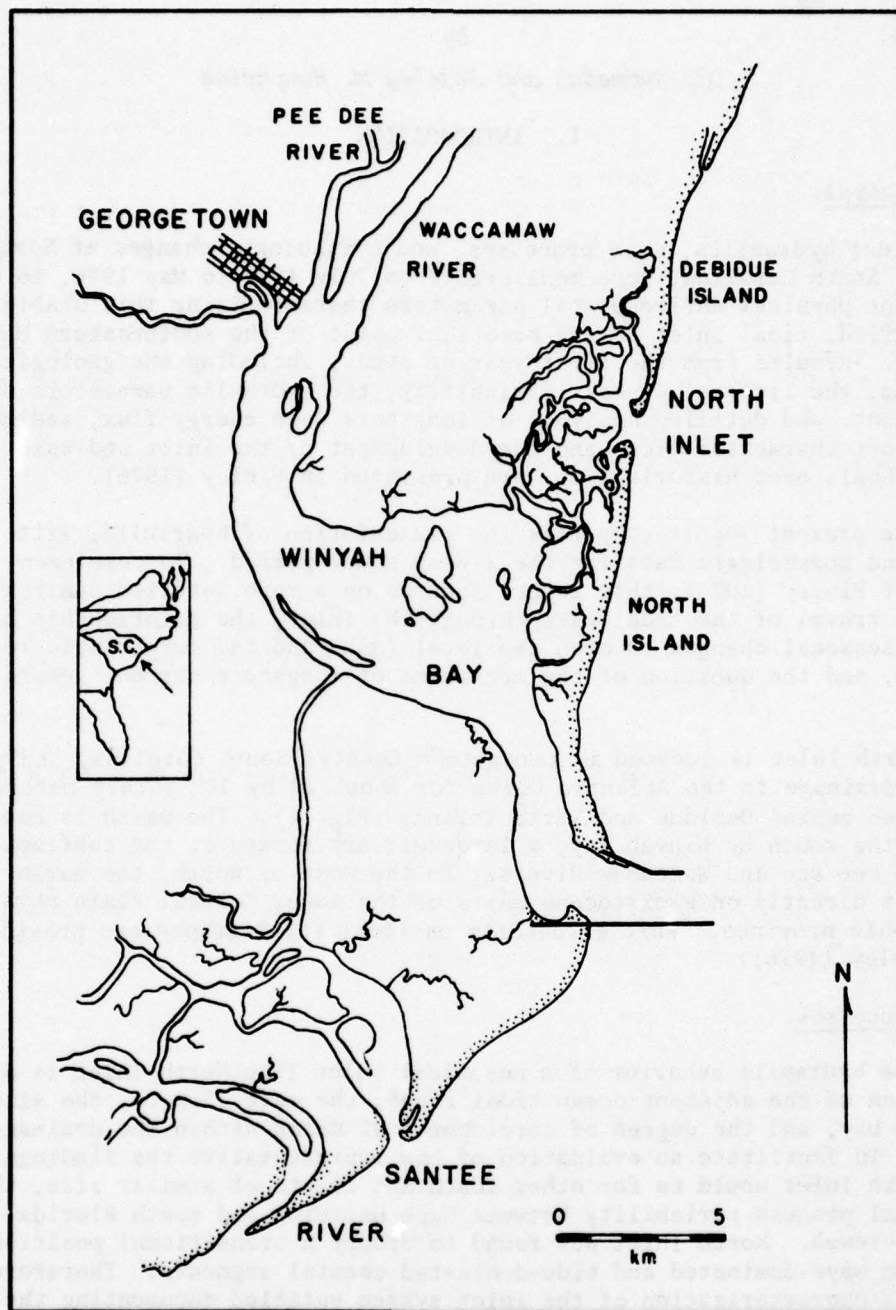


Figure 1. Location map of North Inlet and vicinity (from Finley, 1976).

The hydraulics questions asked in this study address the problems of time asymmetry and velocity asymmetry in the inlet currents, the effects of the propagation of the tidal wave through shallow water on its harmonic constituents, the relation between water surface differentials and tidal creek current velocities, inlet throat equilibrium, and the annual variations in MSL as recorded by the tide gage network. Because the wave process measurements were designed primarily to document environmental conditions rather than performing specific studies of the surf zone, the analysis of this data set was limited to one question of fundamental importance—the mechanics of the generation of longshore currents. The existence of an extensive data set at one location for a wide range of conditions provided the basis for a statistical evaluation of the observed current velocities. Stepwise regression procedures were used to test how the dependent variable (the observed current velocity) correlates with a series of simultaneously measured independent variables.

In addition to characterizing the dynamics of the North Inlet system, the parameters provide a data base for testing a number of basic scientific hypotheses.

3. Response.

The monitoring of morphologic response over the study period included recording channel cross-sectional profiles, beach and nearshore profiles, topographic mapping of selected intertidal features, and quarterly oblique aerial photography. Basic documentation of the variability was the primary objective, and all pertinent morphologic data have therefore been included, either as text or in data Appendixes A to I.

The basic scientific question addressed in the analysis of the morphologic data pertained to the seasonal variability in selected intertidal features and their significant, and apparently cyclic, pattern of change in response to the fluctuations in MSL. Seasonal sea level fluctuation apparently has a much more profound effect on intertidal sediment distribution than has been recognized. The monthly surveys of beach profiles and channel cross-sectional profiles provide a data base for testing Escoffier's (1940) basic stability concept: If inlet stability is maintained by increased tidal scour subsequent to an infilling of the main channel by increased wave action, then channel profiles and beach profiles adjacent to the inlet should be out of phase with respect to erosion and accretion. The North Inlet morphologic data appear to support this stability concept.

II. REGIONAL VARIABILITY

1. Introduction.

Processes and morphology at North Inlet reflect its location relative to the global atmospheric circulation pattern, the tides of the Atlantic Ocean and their transformation by the southeast Atlantic

Continental Shelf, and the physiography of the Coastal Plain. On this regional scale, North Inlet occupies an interesting transitional location: to the north, the Outer Banks are clearly wave dominated; to the south, the shores of southern South Carolina and Georgia are clearly tide dominated. Physiographically, the coastal zone north of North Inlet is characterized by either straight beaches eroding the Pleistocene mainland (e.g., Myrtle Beach; Brown, 1975) or narrow Holocene barriers fringing a system of wide shallow lagoons (e.g., the Outer Banks and Pamlico Sound). To the south, the South Carolina and Georgia coasts have stubby Holocene and Pleistocene barrier islands backed by extensive intertidal marsh and tidal creeks (Hoyt, 1967; Hubbard and Barwis, 1976). These marsh-filled bays create a hydraulic geometry similar to that studied by Oliveira (1970) for bays with sloping banks, and tend to develop ebb-dominated tidal inlets.

2. Tidal Range.

Based on the morphology of sandy shorelines of the world, Davies (1964) recognized that tidal range is the single most diagnostic variable. He proposed the following class boundaries: microtidal (spring tidal range 0 to 2 meters), mesotidal (tidal range 2 to 4 meters), and macrotidal (tidal range greater than 4 meters). Accordingly, the coast of the southeastern United States would be mesotidal only in southern South Carolina and Georgia, and microtidal at North Inlet and farther north (Table 1; Fig. 2). By defining mesotidal estuaries as those where sedimentary forms due to deposition by tidal currents begin to dominate those built by waves (Hayes, 1975), it is found that the lower boundary of the mesotidal range in the southeastern United States should be adjusted downward, perhaps as far as to 1.6 meters. The North Inlet morphology (spring tidal range 1.8 meters) clearly fits the mesotidal models proposed by Oertel (1972) and Hayes, et al. (1973). The low wave energy of the southeast United States coast, compared to the world average (Davies, 1973), is probably the reason behind the development of mesotidal morphology at a lower tidal range.

The observed increase in tidal range southward from the Outer Banks to Georgia reflects the effect of shoaling of the tidal wave across the increasingly wider Continental Shelf. Silvester (1974) reported a fair correlation between shelf width and tidal range for the margins of all major world oceans. Figure 3 is a scatter plot illustrating the offshore distance of the 200-meter depth contour versus the corresponding open-coast tidal range. As the tidal wave travels onto the United States southeast shelf, the cotidal lines intersect the bathymetric contours at a relatively steep angle (Redfield, 1958). Therefore, the "effective" shelf width of any coastal tide station may be larger than the values given in Figure 3, accounting for some of the scatter. The coastal tidal range depends on the amplitude of the deepwater ocean tide, the actual shelf profile, and the influence of local coastal embayments. Therefore, the relationship derived from Figure 3 does not necessarily pertain to all shelves.

Table 1. Spring and mean tidal ranges along the southeastern coast of the United States (from National Oceanic and Atmospheric Administration, 1977).

Ocean station	Spring		Mean	
	(m)	(ft)	(m)	(ft)
Kitty Hawk	1.16	3.8	0.93	3.2
Cape Hatteras	1.25	4.1	1.04	3.4
Cape Lookout	1.34	4.4	1.13	3.7
Atlantic Beach	1.31	4.3	1.10	3.6
Myrtle Beach	1.83	6.0	1.55	5.1
Winyah Bay entrance	1.65	5.4	1.40	4.6
Cape Romain	1.68	5.5	1.43	4.7
Isle of Palms	1.86	6.1	1.58	5.2
Charleston Harbor entrance	1.86	6.1	1.58	5.2
Edisto Beach	2.10	6.9	1.80	5.9
Fripp Inlet	2.23	7.3	1.89	6.2
Hilton Head	2.38	7.8	2.01	6.6
Tybee Light	2.44	8.0	2.07	6.8

Microtidal¹

Mesotidal¹

¹According to classification by Davies (1964).

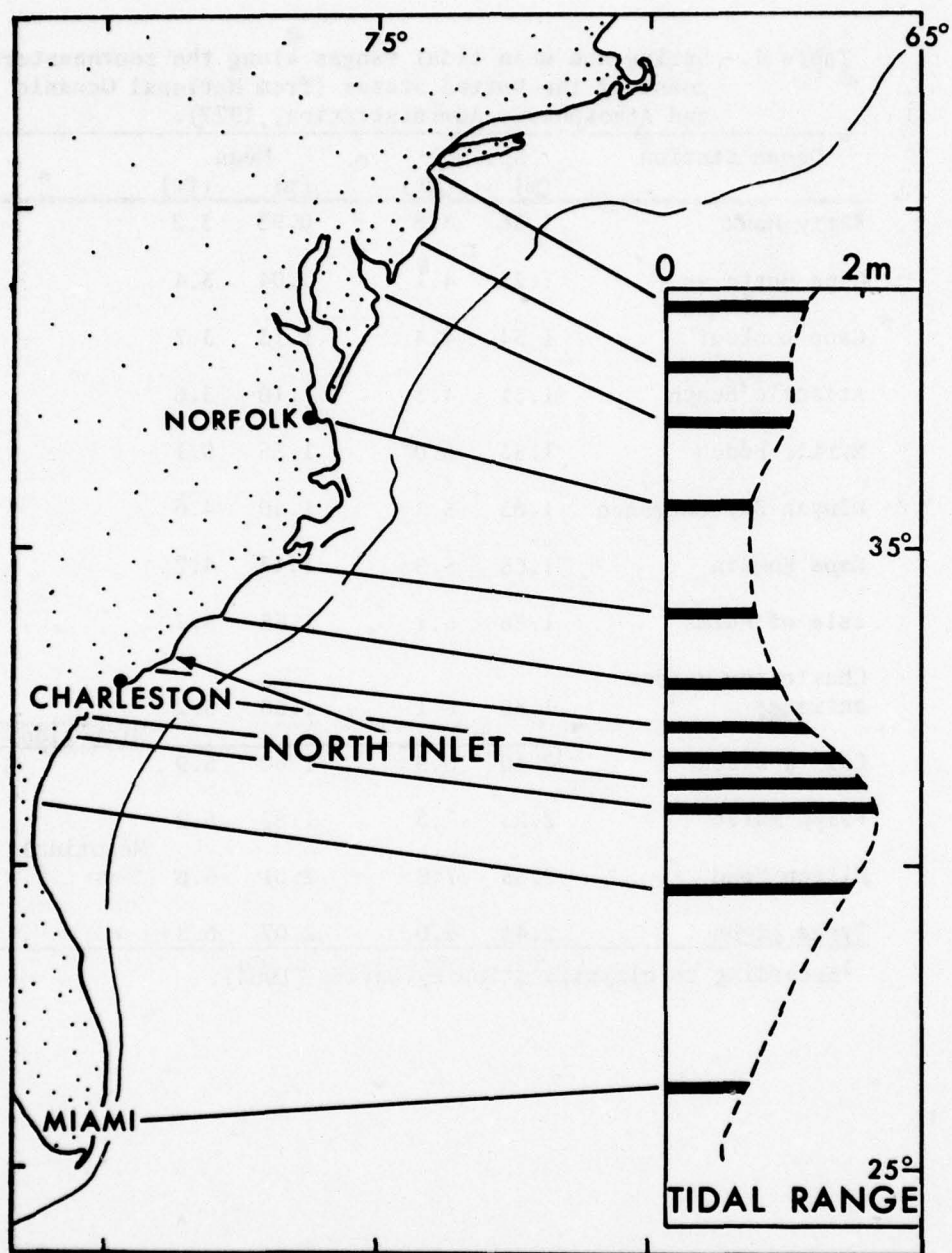


Figure 2. Variation in mean tidal range along the U.S. east coast from New York to Miami.

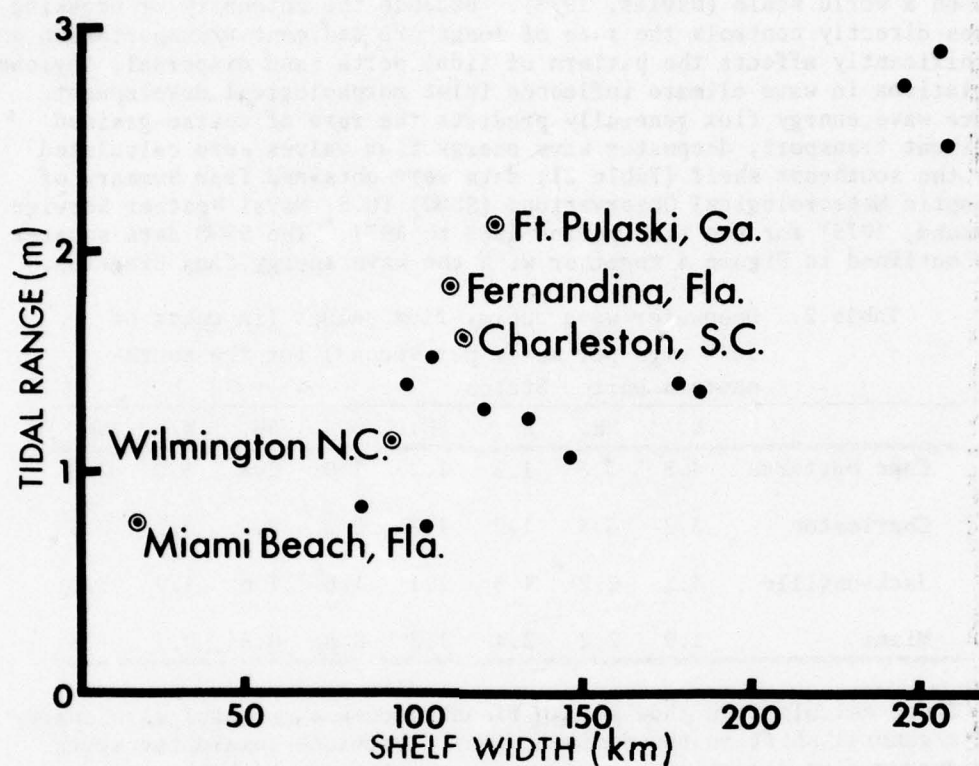


Figure 3. Observed tidal range versus offshore distance to the 200-meter bathymetric contour for selected stations of the eastern United States. All data refer to open-coast stations. Circled data points refer to the identified tide stations (from National Oceanic and Atmospheric Administration, 1977).

3. Wave Energy.

Wave energies on the southeast shelf of the United States are moderate on a world scale (Davies, 1973). Because the intensity of breaking waves directly controls the rate of longshore sediment transportation and significantly affects the pattern of tidal delta sand dispersal, regional variations in wave climate influence inlet morphological development. Since wave energy flux generally predicts the rate of coarse-grained sediment transport, deepwater wave energy flux values were calculated for the southeast shelf (Table 2); data were obtained from Summary of Synoptic Meteorological Observations (SSMO) (U.S. Naval Weather Service Command, 1975) for the time period 1963 to 1971. The SSMO data squares are outlined in Figure 4 together with the wave energy flux diagrams.

Table 2. Deepwater wave energy flux values (in units of 10^{10} ergs per meter per second) for the southeastern United States.

	N.	NE.	E.	SE.	S.	SW.	W.	NW.
Cape Hatteras	4.8	3.3	1.3	1.2	1.9	2.8	3.0	2.8
Charleston	3.2	3.5	1.9	1.3	2.2	2.5	3.2	2.6
Jacksonville	4.2	2.2	1.3	1.1	1.8	1.6	1.9	3.2
Miami	1.9	2.2	2.4	1.2	0.8	0.8	0.7	1.3

These calculations show a significant decrease in total wave energy and a general shift in the dominant flux directions toward the south. The energy flux directions are given as those from which the waves are coming and are, therefore, consistent with the common format for wind diagrams. Wave energy flux is calculated from the equation:

$$P_f = 9.58 \times 10^9 \times H_0^2 \times T_0 \quad (1)$$

where H_0 is deepwater wave height (meters), T_0 is wave period (seconds), and P_f is the wave energy flux expressed in ergs per meter per second. An in-depth discussion of the procedures, assumptions, and errors involved in the calculations of wave energy flux values from SSMO data is presented in Walton (1973) and Nummedal and Stephen (1976).

4. Inlet Size.

Tidal range, coastal plain geomorphology, and wave energy variations have caused a distinct regional trend in inlet size. This size variation is expressed in Figure 5 in terms of tidal prisms, cross sections, and hydraulic radii of the inlet throats. The data are taken from Jarrett (1976), Finley (1976) for North Inlet, and FitzGerald, Nummedal and Attaway (1977) for Price Inlet. The significance of tidal range as an overriding factor controlling inlet size is evident when

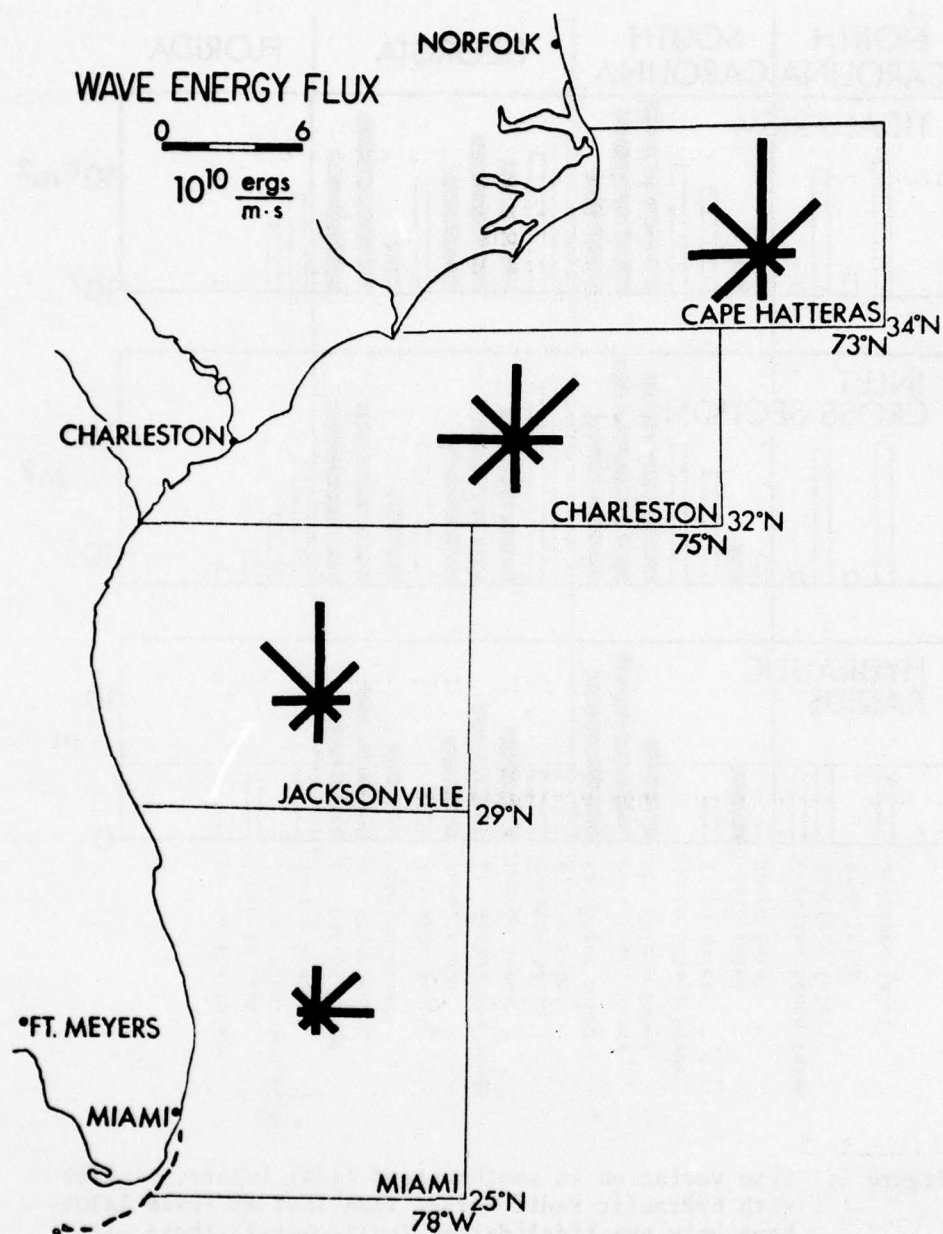


Figure 4. Wave energy flux diagrams for the southeastern United States (energy flux calculated from data in U.S. Naval Weather Service Command, 1975).

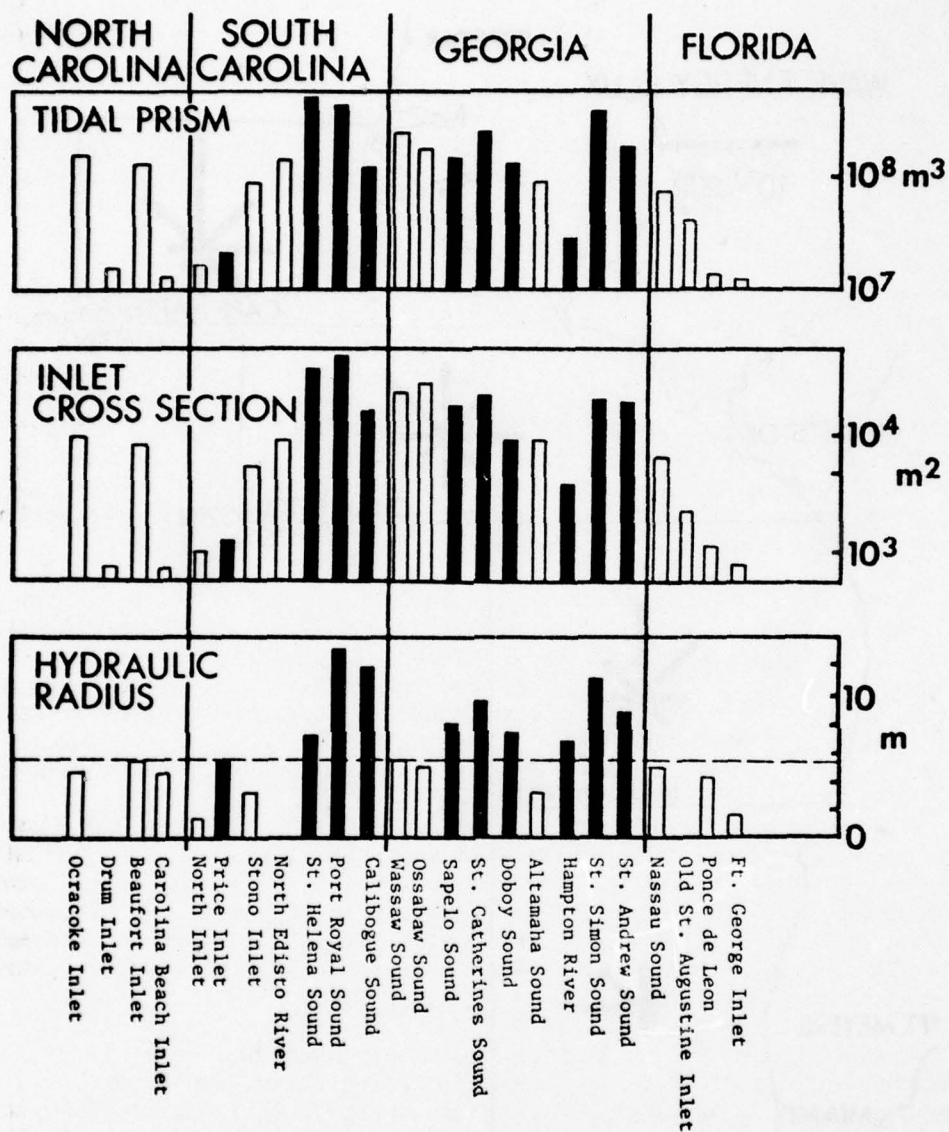


Figure 5. Size variation in southeastern tidal inlets. Inlets with hydraulic radii larger than that at Price Inlet have only ebb tidal deltas (solid bars); those with smaller radii have both ebb and flood tidal deltas (open bars).

comparing the distributions in Figures 2 and 5. In all measures of size, the inlets reach a maximum in southern South Carolina and Georgia and then decrease rapidly into Florida and, to a lesser extent, into North Carolina. Inlet shoal development shows an interesting relationship to the depth of the main channel. All inlets listed in Figure 5, which are at least as deep as Price Inlet (hydraulic radius equal to 5.2 meters), appear only to have developed ebb tidal deltas (outer shoals); the inlets shallower than Price have developed both ebb tidal and flood tidal deltas (inner shoals).

5. Storm Frequencies.

Since the initiation of geological studies at North Inlet in 1972, only two storm events have caused significant morphological changes at, and adjacent to, the inlet. The storm of 10 and 11 February 1973, which was classified as a moderate to severe storm (U.S. Army, Corps of Engineers, Coastal Engineering Research Center, 1977), caused erosion up to 31.3 cubic meters per linear meter of beach (Finley, 1976). Another storm on 23 and 24 September 1974, classified as light to moderate, caused up to 13.0 cubic meters of erosion per linear meter (Kana, 1977). Hurricane Hazel, by comparison, eroded up to 52 cubic meters per meter at Myrtle Beach in 1954 (U.S. Congress, 1966).

These observations indicate that despite intensive sediment transportation and redeposition during storm events, such events may be too rare to significantly affect the long-term morphologic development of a system like North Inlet. As pointed out by Davies (1973), the South Carolina coast is south of the American east coast storm environment. Fox and Davis (1976) also reported that most extratropical cyclones ("northeast" storms) pass to the north of the South Carolina coast.

Tropical storms and hurricanes do occasionally hit the South Carolina coast; however, the frequency is substantially less than that at the Outer Banks (Fig. 6). According to Meyers (1975), the annual probability of hurricane force winds (windspeed in excess of 120 kilometers per hour) striking within an 80-kilometer segment of coast in northern South Carolina is about 0.050. This corresponds to the one hurricane landfall every 20 years.

It was assumed at the initiation of this study that 2 weeks of measurements every season would give representative samples of the annual population of process parameters controlling inlet morphologic response. The low frequency of cyclones (tropical and extratropical) crossing the shoreline near North Inlet appears to justify that assumption.

III. TIDAL HYDRAULICS

1. Introduction.

One fundamental objective of the North Inlet project was to document the hydraulic conditions of this unmodified tidal inlet. Three tide

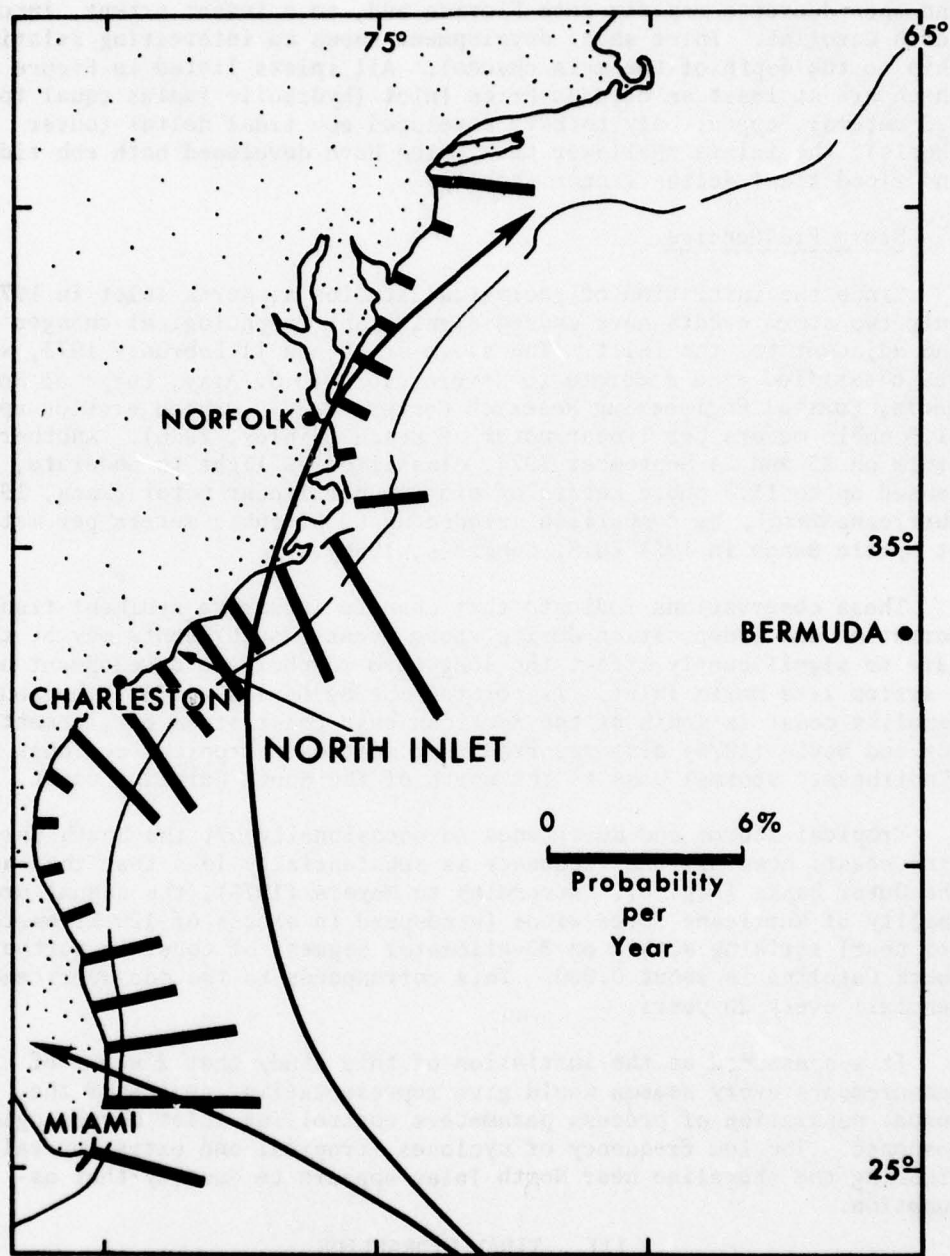


Figure 6. Annual probability of hurricane landfalls within 80-kilometer segments on the southeast coast of the United States (from Meyers, 1975).

gages were operated throughout the study period from July 1974 to May 1976. Leupold and Stevens float gages in 30-centimeter culverts supported by 5-centimeter water pipes jetted into the channel bed were installed at the intersection of Town and Debidue Creeks and at Jones Creek (Fig. 7). A Bristol bubbler gage with the orifice just seaward of North Island (Fig. 7) was used to record tidal fluctuations in the ocean.

To complement the tide gaging program, current velocities were monitored with an ENDECO directional current meter for a number of 13-hour periods at stations located at the inlet throat and at cross sections of Town and Jones Creeks. Changes in the hydraulic geometry of the inlet system over time were measured by repetitive longitudinal and transverse channel surveys with a Bludworth fathometer.

Finley (1976) presented a comprehensive analysis of the first year's tidal hydraulics data in terms of (a) the relationship between inlet throat cross-sectional area and the tidal prism, (b) the variations in tidal prism with tidal phase, (c) the relation between ocean-bay water surface differentials and current velocities for hydrographic measurement periods, (d) variation in channel friction coefficient (Manning's n) over the same tidal cycles, and (e) the efficiency of tidal exchange through the inlet expressed by Keulegan's (1967) repletion coefficient.

The analysis of the second year's tidal hydraulics data emphasizes other aspects of the hydraulics as well as some of Finley's points in order to achieve as complete a characterization of inlet behavior as possible. Computer printouts of a large number of both raw and reduced hydraulic data are given in Appendixes A to G.

2. Hydraulic Geometry.

North Inlet drains about 23.7×10^6 square meters of marsh, channels, and shallow bays (based on planimetry of U.S. Department of Agriculture vertical air photos). The drainage boundary between the southern part of the North Inlet system and the tributaries to Winyah Bay is poorly defined and fluctuates somewhat, depending on the stage of the rivers draining into the bay, the tidal phase, and seasonal fluctuations in sea level. These factors may introduce about 5-percent variability into the above figure.

The ocean tidal wave is distorted by passage through the tidal inlet (Boon, 1973; Byrne and Boon, 1976; Nummedal, FitzGerald, and Humphries, 1976) due to the presence of water level dependent impedance factors like changing channel cross section, variations in bay surface area, and bottom friction. As demonstrated by Brown (1928) and Keulegan (1967), the ratio between the bay surface area, A_b , and the inlet throat cross-sectional area, A_c , significantly affects the efficiency

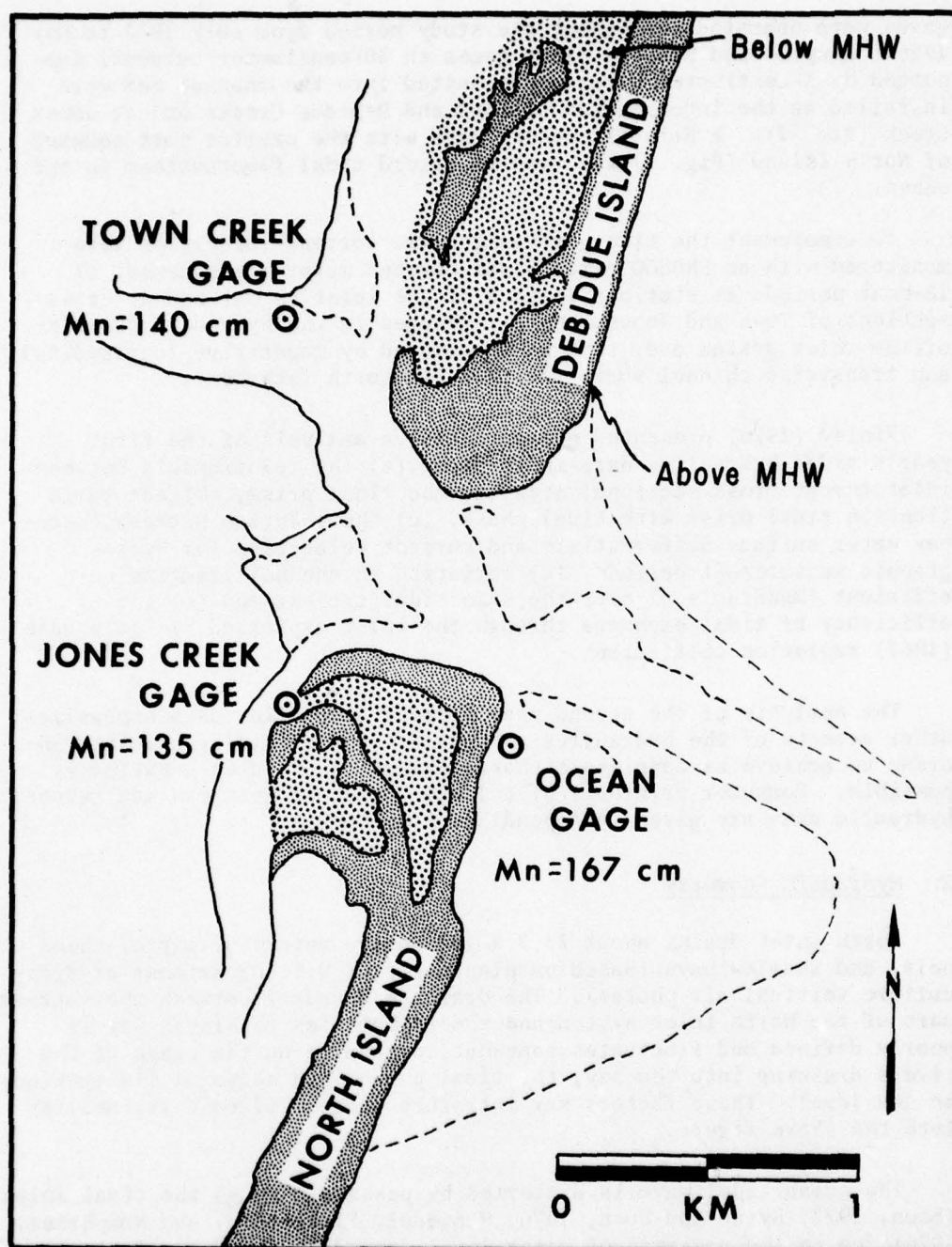


Figure 7. Location of the three tide gages relative to the main channels and barrier islands. Mn refers to the mean annual tidal ranges determined at the gage stations.

of water exchange between the ocean and the marsh (bay). Values for A_b were obtained by planimetry of the creek surface area on one vertical air photo (CDW 2K) taken near mean low water (MLW) and another (USDA A40) obtained near MSL. Unfortunately, A_b could not be determined for spring low water. For any water stage above MSL, significant parts of the marsh are inundated, and A_b cannot be estimated except at spring high tide when the vegetation change at the high water line can be used to trace the entire marsh outline. A_c values were directly obtained from fathometer records at the inlet throat, calibrated by the surveyed distance between two transect end markers. To relate A_b and A_c to the same tide stages, spring high was taken as 90 centimeters above MSL, and MLW was set at 70 centimeters below MSL. Table 3 summarizes the results.

Table 3. Bay water surface area, A_b , and inlet throat flow area, A_c , as functions of water level.

Water level	A_b (10^6 m^2)	A_c (m^2)
Spring high water	23.66	1,680
Mean sea level	7.33	1,475
Mean low water	6.32	1,330

A_b varies by a factor of 3.74 through the tidal cycle; A_c only changes by about 1.26 for the same water level range. Therefore, the ratio A_b/A_c , which controls inlet impedance according to Keulegan's (1967) analysis, is 2.9 times larger at spring high than at MLW. These variations appear to be typical for South Carolina inlets. Fitzgerald, Nummedal, and Kana (1977) documented the A_b/A_c ratio for Price Inlet as about 2.7 times larger at spring high than at MLW.

These conditions are at variance with the geometry of the Wachapreague Inlet system in Virginia (Byrne, Bullock, and Tyler, 1975), which includes large open bays that reduce A_b variations.

A complicating factor which is not pursued any further in this study is the time of travel of the tidal wave in the shallow creek system. The distance from the North Inlet throat section to the most distant head of a tidal creek is about 6 kilometers, with a "typical" channel depth at low water of 2 meters. The celerity of a free wave in such a channel is 4.43 meters per second, giving a maximum traveltime of 22 minutes for the tidal wave to reach the perimeter of the tidal system. Water level adjustments on the shallow interchannel marsh surface are substantially slower. Therefore, at any tide stage, there are water surface slopes within the tidal creek-marsh system which affect the hydraulics at the measured sections in an unknown way.

The rapid changes in channel hydraulic geometry required repetitive surveys of designated cross sections on a monthly basis. Figure 8 shows the locations of the monitored sections as well as the "typical" profile for the 1975-76 field year. All fathometer profiles have been tied to a common reference datum used for the tide gages by means of the gage record obtained at the time of each survey. Appendix A contains profiles obtained for (a) the inlet throat, (b) Town Creek, (c) Jones Creek, and (d) the flood tidal delta, from June 1975 to May 1976.

The inlet throat profile shows a distinct separation between the nearly 8-meter-deep main ebb channel to the south and a wide intertidal to shallow subtidal platform made up of the channel-margin linear bar and marginal flood channel to the north. Only a small percentage of the tidal prism passes over the intertidal platform. However, large variations in throat cross-section area are accounted for by depth changes on this platform. The total throat cross section varies by a factor of 1.34 between a high of 1,679 square meters in November and an alltime low of 1,255 square meters in May. This variation is probably a reflection of the seasonal change in MSL. High MSL in November increases the mean daily tidal prism and scours the channel floor. However, the low MSL in May reduces the tidal prism. The throat section, in turn, adjusts by a decrease in size in accordance with Escoffier's (1940) stability concept.

The cross-sectional areas of Town and Jones Creeks (Table 4) appear to undergo seasonal variations in phase with the throat section. DeAlteris and Byrne (1975) recorded a seasonal pattern of variation in inlet flow area consistent with the one detected at North Inlet.

Table 4. Monthly channel cross-sectional areas below MSL (in square meters).

Date	Town Creek	Jones Creek	Inlet Throat
June 1975	1,091 (+4) ¹	490 (-2)	1,585 (+7)
July	1,087 (+3)	520 (+4)	-----
Aug.	1,034 (-2)	470 (-6)	-----
Sept.	1,124 (+7)	483 (-4)	-----
Oct.	1,238 (+15)	510 (+2)	1,445 (-2)
Nov.	1,056 (+5)	500 (0)	1,679 (+12)
Dec.	-----	-----	-----
Jan. 1976	862 (-18)	407 (-19)	-----
Feb.	1,177 (+11)	548 (+9)	1,298 (-12)
Mar.	863 (-18)	515 (+3)	1,676 (+12)
Apr.	1,033 (-2)	593 (+16)	1,388 (-6)
May	956 (-9)	473 (-6)	1,255 (+15)
Mean	1,051	501	1,475

¹Percent change from the mean.

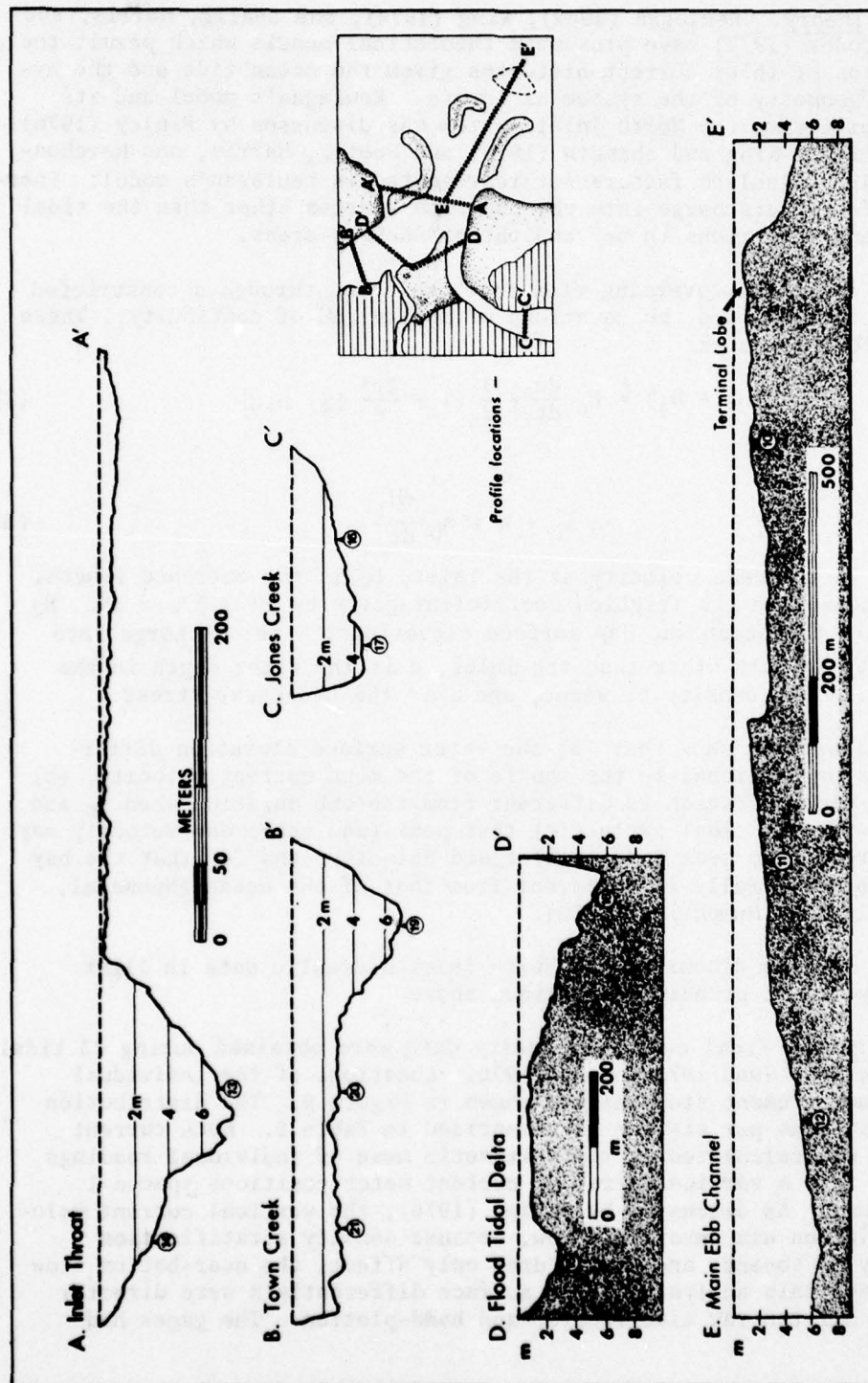


Figure 8. Typical profiles of the five bathymetric sections monitored during this study. Circled data designates sediment sample locations.

3. Tidal Currents.

a. Theory. Keulegan (1967), King (1974), and Seelig, Harris, and Herchenroder (1977) have presented theoretical models which permit the derivation of inlet current histories given the ocean tide and the hydraulic geometry of the system as inputs. Keulegan's model and its applicability to the North Inlet system was discussed by Finley (1976). The models by King and Shemdin (1975) and Seelig, Harris, and Herchenroder (1977) include factors not represented in Keulegan's model: inertial effects, discharge into the bay from sources other than the tidal inlet, and variations in bay and throat section areas.

The equations governing flow from the ocean through a constricted inlet into a bay are the equations of motion and of continuity. These can be formulated as:

$$g(H_2 - H_1) = L_c \frac{du}{dt} + \frac{1}{2} \left(1 + \frac{2r'}{d} L_c\right) u|u| \quad (2)$$

and

$$u A_c + W = A_b \frac{dH_1}{dt}, \quad (3)$$

where u is the mean velocity at the inlet, L_c is the entrance length, r' is the square law friction coefficient given by $r' = \sigma/\rho \times u^2$. H_2 and H_1 are the ocean and bay surface elevations, W is discharge into the bay by sources other than the inlet, d is the water depth in the inlet, ρ is the density of water, and σ is the bed shear stress.

The equations show that (a) the water surface elevation differential is proportional to the square of the mean current velocity, (b) that the flood duration is different from the ebb duration when A_c and A_b vary over the tidal cycle, (c) that peak (and mean) ebb velocity may be different from peak (and mean) flood velocity, and (d) that the bay tidal range generally is different from that of the ocean (Nummedal, FitzGerald, and Humphries, 1976).

This section discusses the North Inlet hydraulic data in light of the hydraulic principles outlined above.

b. Data. Tidal current velocity data were obtained during 23 tidal cycles between June 1975 and May 1976. Locations of the individual current measurement stations are shown in Figure 9. The distribution of observations per station is summarized in Table 5. Each current velocity was calculated as the arithmetic mean of individual readings obtained from a vertical array of current meter positions spaced 1 meter apart. As discussed by Finley (1976), the vertical current velocity variation was invariably low, because density stratification generally is absent, and bottom drag only affects the near-bottom flow layer. For this analysis, water surface differentials were directly measured off the raw tide records and hand-plotted. The gages had

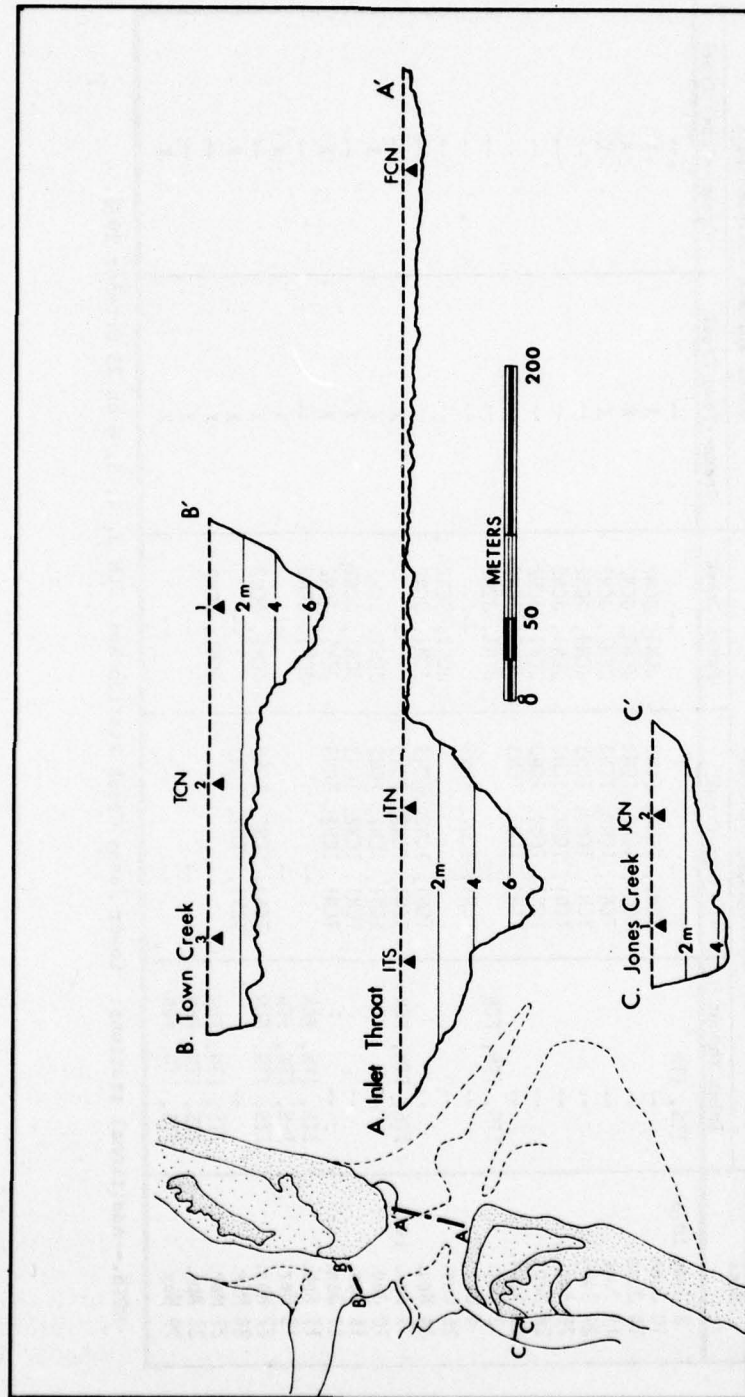


Figure 9. Location of hydrography stations at North Inlet.

Table 5. North Inlet hydrography measurements and water surface differentials, 1975-76.

Date	Hydrography stations			Water surface differentials	
	Inlet throat	Town Creek	Jones Creek	Ocean--Town Creek	Ocean--Jones Creek
2 June 1975	ITS, ITN	TCN1, TCN2, TCN3	JCN1, JCN2	--	--
10 June	--	TCN1, TCN2, TCN3	JCN1, JCN2	X	X
14 June	--	TCN1, TCN2, TCN3	JCN1, JCN2	X	X
17 June	--	TCN1, TCN2, TCN3	JCN1, JCN2	X	X
29 July	--	TCN1, TCN2, TCN3	JCN1, JCN2	--	--
26 Aug.	--	TCN1, TCN2, TCN3	JCN1, JCN2	--	--
26 Sept.	--	TCN1, TCN2, TCN3	JCN1, JCN2	--	--
29 Sept.	--	TCN1, TCN2, TCN3	JCN1, JCN2	--	--
2 Oct.	ITS, ITN, FCN	TCN1, TCN2, TCN3	JCN1, JCN2	--	--
4 Oct.	--	TCN1, TCN2, TCN3	JCN1, JCN2	--	--
25 Oct.	--	TCN1, TCN2, TCN3	JCN1, JCN2	--	--
24 Nov.	--	TCN1, TCN2, TCN3	JCN1, JCN2	--	--
7 Jan. 1976	ITS, ITN, FCN	TCN1, TCN2, TCN3	JCN1, JCN2	X	--
10 Jan.	--	TCN1, TCN2, TCN3	JCN1, JCN2	X	X
15 Jan.	--	TCN1, TCN2, TCN3	JCN1, JCN2	X	X
17 Jan.	--	TCN1, TCN2, TCN3	JCN1, JCN2	X	X
17 Feb.	ITS, ITN, FCN	TCN1, TCN2, TCN3	JCN1, JCN2	--	--
15 Mar.	ITS, ITN, FCN	TCN1, TCN2, TCN3	JCN1, JCN2	X	X
22 Mar.	ITS, ITN, FCN	TCN1, TCN2, TCN3	JCN1, JCN2	X	X
24 Mar.	--	TCN1, TCN2, TCN3	JCN1, JCN2	X	X
27 Mar.	ITS, ITN, FCN	TCN1, TCN2, TCN3	JCN1, JCN2	X	X
27 Apr.	ITS, ITN, FCN	TCN1, TCN2, TCN3	JCN1, JCN2	X	X
19 May	ITS, ITN, FCN	TCN1, TCN2, TCN3	JCN1, JCN2	X	X

NOTE.--Additional stations: Lower Jones Creek station Nos. JCN 3, 4, 5, 6 on 25 October 1976.

been surveyed to a common reference datum (Finley, 1976). The discontinuous tide records made it impossible to derive water surface differential time series for more than half of the data sets (Table 5).

Sample plots of current velocities versus the corresponding water surface differentials are shown in Figure 10; the complete data set is contained in Appendix B.

The water surface differential plotted in the Jones Creek figures refers to that between the ocean and Jones Creek gages. The differential used in the Town Creek and inlet throat figures refers to that between the ocean and Town Creek gages.

c. Analysis. Figure 10 and Appendix B demonstrate that the current velocity curves are asymmetric with higher ebb than flood velocities. They are also asymmetric in time, with peak ebb velocity occurring about halfway between ocean high and low water; peak flood velocity occurs shortly before ocean high. The flood, consequently, lasts longer than the ebb. Examples of similar time-velocity asymmetries are known from many tidal systems (Klein, 1970; Hayes, et al., 1973; Boothroyd and Hubbard, 1975; Hine, 1975) and reflect the presence of differential impedance to inlet flow at high and low water.

A number of environmental factors affect each set of tidal hydrographic observations. Therefore, reliable quantification of hydraulic process parameters must be based on a statistical analysis of a representative sample.

For the statistical analysis, the following variables were defined from Appendix C: VFMAX, peak flood velocity in a given tidal cycle (centimeters per second); VEMAX, peak ebb velocity (centimeters per second); DELTF, time (in hours) between peak flood velocity and subsequent high water in the ocean; DELTE, time between high water in the ocean and subsequent peak ebb velocity; LAGH, time between ocean high tide and subsequent station slack; LAGL, time between ocean low tide and subsequent station slack. Data sets of 100 for the 1975-76 season (App. C) and 45 for the 1974-75 season were obtained. Summary statistics are presented in Table 6. Both years, peak ebb velocities exceeded peak flood. For all velocity stations combined, the peak ebb velocity in 1975-76 was 82.8 centimeters per second which was compared to 70.7 centimeters per second for the flood, an average peak ebb velocity 1.17 times the average peak flood. In 1974-75, the peak ebb velocity exceeded peak flood by as much as 1.26. Peak velocities during individual tidal cycles covered a wide range. Over the 2 years of study, peak ebb velocities ranged from 30 to 156 centimeters per second; peak flood velocities ranged from 24 to 128 centimeters per second.

The ebb dominance of the inlet circulation is even more pronounced when the individual velocity sections are considered separately

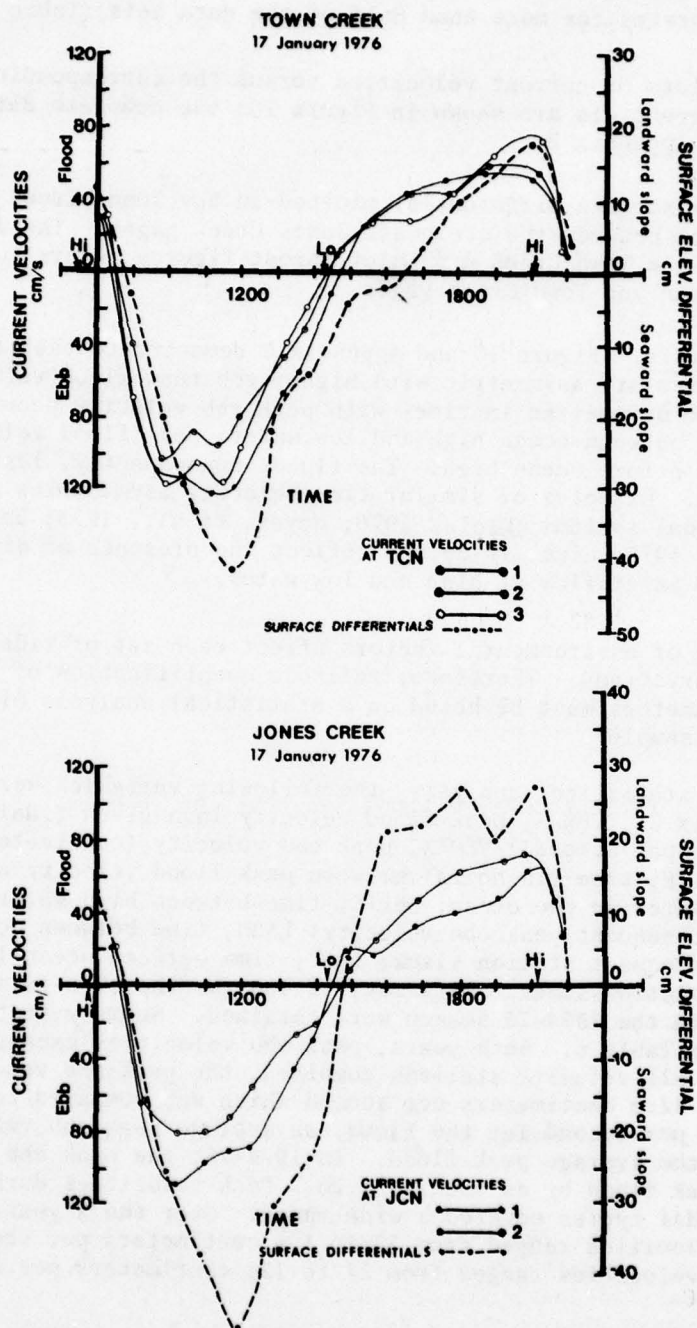


Figure 10. Time-series data of current velocities and water surface differentials at Town and Jones Creeks.

Table 6. Summary statistics on North Inlet current parameters and hydraulic lag constants, 1974 to 1976.

Variable ¹	N	Mean	Median	Std. dev.	Min.	Max.
1974-75						
VFMAX	45	70.60	70	22.94	26	128
VEMAX	40	88.43	84	18.10	59	156
DELTF	42	1.55	1.6	0.65	0.2	2.9
DELTE	32	3.45	3.3	0.45	2.5	4.4
LAGH	35	0.86	0.75	0.39	0.1	2.0
LAGL	20	0.87	0.65	0.54	0.3	2.1
1975-76						
VFMAX	92	70.74	67	22.60	24.0	125
VEMAX	91	82.80	80	25.57	30.0	150
DELTF	92	1.33	1.25	0.62	0.0	3.0
DELTE	82	3.06	3.05	0.72	0.9	4.8
LAGH	89	0.81	0.8	0.37	0.0	1.9
LAGL	58	0.52	0.45	0.32	0.0	1.6

¹Names defined in text, symbols listing, and Appendix C.

(Table 7). For the throat section, the peak ebb velocity exceeded the peak flood by a factor of 1.32 in 1974-75 and 1.22 in 1975-76.

This degree of ebb current dominance over flood currents through the inlet throat is comparable to Price Inlet where FitzGerald, Nummedal, and Attaway (1977) document an average peak ebb velocity 16 percent larger than the average flood over a data set of 12 complete tidal cycles. However, New Corpus Christi Pass, connecting the microtidal Gulf of Mexico to the open Corpus Christi Bay, is dominated by floodtides. The average peak flood velocity, over eight tidal cycles measured in 1972-73, exceeds the ebb by as much as 33 percent (Behrens, Watson, and Mason, 1977). These current asymmetries are consistent with equations (2) and (3) when A_b and A_c vary during the tidal cycle in accordance with local hydraulic geometries.

Currents at the Town Creek and Jones Creek velocity sections are weaker than those at the throat section by about 83 and 76 percent, respectively, for peak flood, and by 79 and 70 percent, respectively, for peak ebb. Calculations indicate that about 7 percent of the mean tidal prism (including flow up Sixty Bass Creek) is stored between the throat and the two velocity sections, and that the combined flow areas of Town Creek and Jones Creek are 5 percent larger than the cross section at the throat (Table 5). These two factors appear adequate to explain the reduced current velocities in the tidal creeks.

Table 7. Summary statistics, by channel section, on North Inlet current parameters and hydraulic lag constants.

Variable ¹	1974-75			1975-76		
	N	Mean	Std. dev.	N	Mean	Std. dev.
Inlet throat (ITN, ITS)				(FCN, ITN, ITS)		
VFMAX	6	85.13	33.36	25	83.05	24.89
VEMAX	6	112.00	26.37	24	101.05	23.48
DELTF	6	1.58	0.60	25	1.63	0.71
DELTE	6	3.68	0.58	20	2.94	0.59
LAGH	6	1.02	0.39	22	0.80	0.32
LAGL	4	0.68	0.53	14	0.34	0.15
Town Creek (TCN1, TCN2, TCN3)				(TCN1, TCN2, TCN3)		
VFMAX	24	72.74	18.83	37	66.79	20.55
VEMAX	21	87.86	11.78	37	80.57	25.44
DELTF	21	1.70	0.62	37	1.34	0.52
DELTE	15	3.42	0.42	37	3.05	0.69
LAGH	18	0.79	0.26	41	0.85	0.39
LAGL	8	0.69	0.30	28	0.59	0.36
Jones Creek (JCN1, JCN2)				(JCN1, JCN2)		
VFMAX	15	61.33	20.58	30	65.57	19.96
VEMAX	13	78.46	6.74	30	70.17	0.61
DELTF	15	1.28	0.70	28	1.10	0.69
DELTE	11	3.35	0.46	30	2.84	0.35
LAGH	11	0.86	0.76	25	0.74	0.31
LAGL	8	1.09	0.74	17	0.53	

¹Names defined in text, symbols listing, and Appendix C.

Frequency distributions for variables VFMAX and VEMAX (Apps. C and D) illustrate a pronounced unimodal distribution, consistent with semi-diurnal tides with only minor diurnal inequality.

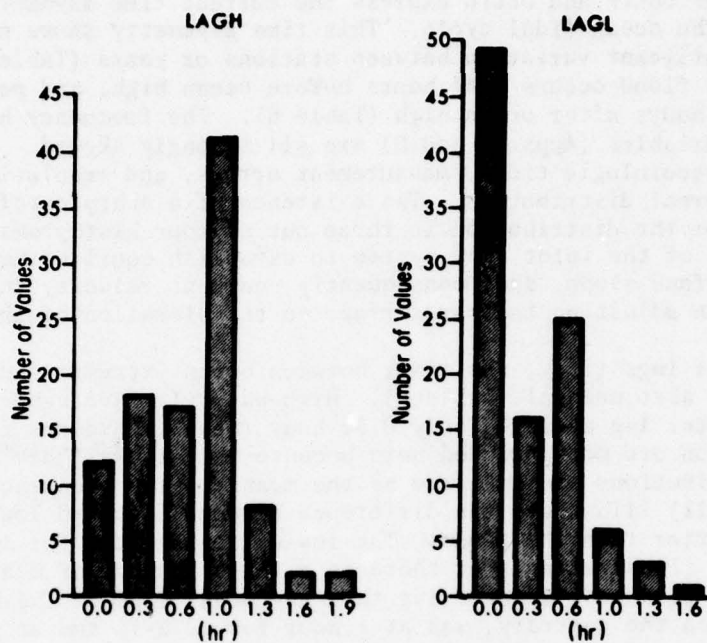
Variables DELTF and DELTE express the current time asymmetry with respect to the ocean tidal cycle. This time asymmetry shows no statistically significant variation between stations or years (Table 7). Generally, peak flood occurs 1.44 hours before ocean high, and peak ebb occurs 3.26 hours after ocean high (Table 6). The frequency histograms for these variables (Apps. C and D) are all strongly skewed. Random factors like meteorologic tides, measurement errors, and resolution limits produce a normal distribution. The existence of a sharp cutoff on the right side of the distribution in three out of four histograms reflects the tendency of the inlet flow system to establish equilibrium by increasing surface slope, and, consequently, current velocity in response to a delay in adjusting the bay surface to the elevation of the ocean.

The tidal lags (i.e., the times between ocean extremes and station slacks) were also unequal (Table 6). High water lag averaged 0.81 hour; low water lag averaged only 0.52 hour (mean lag values for the 1974-75 season are not included here because the standard deviations of the distributions are as large as the means). The frequency histograms (Fig. 11) illustrate the difference between high and low water lags even better than the means. The low water lag mode for 1975-76 was at zero, illustrating that there is a larger number of measured tidal cycles with no low water lag than any other class. The high water mode, on the contrary, was at 1 hour for 1975-76 and at 0.86 hour for 1974-75. Equations (2) and (3) predict less flow impedance (or greater exchange efficiency) at low values of A_b/A_c than at high; i.e., the bay water level adjusted much more easily to that of the ocean at low water than at high. This agrees with the observations.

Different lags for high and low water were also observed at Government Cut, Florida (O'Brien and Dean, 1972). At high tide, the lag was 52° or 1.79 hours. At low tide, it was 60° or 2.07 hours. The fact that low tide lag exceeded high tide lag was probably due to the hydraulic geometry of the system. Government Cut links the ocean to the large Miami Harbor and Biscayne Bay rather than a marsh-tidal creek system.

It is apparent at this point that knowing the average lag and the average Keulegan repletion coefficient for a tidal cycle is not adequate. Net sediment discharge and, consequently, the morphological development of the entire inlet system, are controlled by the flow asymmetry which is related to the "variation" in the lag and repletion coefficient over time. Table 8 summarizes the high tide and low tide median lag values for North Inlet for the 1974-75 seasons (median values represent the central tendency of skewed distributions like those in Fig. 11 better than the mean). K is consistently larger at low water than at high, demonstrating a more efficient water exchange.

1975—1976



1974—1975

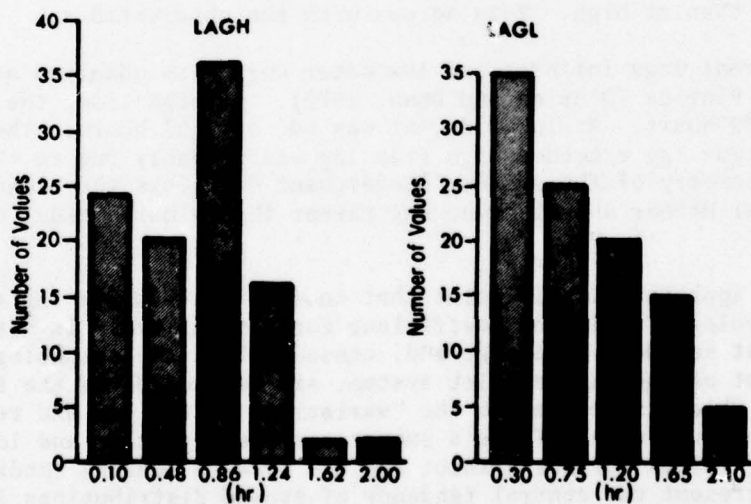


Figure 11. Histograms summarizing the distribution of high water and low water tidal lag at the North Inlet throat section.

Table 8. Median phase lags measured at the throat section at North Inlet; predicted Keulegan repletion coefficients (K) and relative bay tidal amplitude (a_b/a_o) (K and a_b/a_o from O'Brien and Dean, 1972).

Season	Tidal stage	Lag		K	a_b/a_o
		Hours	Degrees		
1974-75	Low	0.65	18.6	1.32	0.95
	High	0.77	22.3	1.22	0.92
1975-76	Low	0.45	13.1	1.60	0.98
	High	0.78	22.6	1.22	0.92

The predicted tidal amplitudes compare fairly well to those actually observed. The average of the Jones and Town Creek amplitudes relative to that in the ocean is 0.95 for the 1974-75 data (Finley, 1976) and 0.92 for the 1975-76 data.

To summarize the discussion of tidal lags and time velocity asymmetry, Figure 12 illustrates the "average" conditions at North Inlet. This tidal cycle has a period of 12.4 hours, and the ocean tide is at MSL at time $t = 0$ hour. At $t = 1.66$ hours, a peak flood velocity of 84 centimeters per second is attained; 1.44 hours later, at $t = 3.1$ hours, the ocean tide is at its high with bay high being attained 0.77 hour later or at $t = 3.87$ hours. At 3.26 hours after ocean high, a peak ebb current of 107 centimeters per second occurs, and 2.94 hours after that, at $t = 9.3$ hours, the ocean reaches low tide. However, the bay continues to ebb to reach low water 0.55 hour later; i.e., at $t = 9.85$ hours. At $t = 12.4$ hours, the ocean surface returns to MSL. For this tidal cycle, the inlet currents flood for a total of 6.42 hours and ebb for 5.98 hours, a difference of 0.44 hour or 26 minutes. This compares to an average duration difference of 42 minutes at Price Inlet (FitzGerald, Nummedal, and Attaway, 1977) and 26 minutes at Wachapreague Dock in Virginia (Boon, 1973).

To test for the correlation between inlet current velocities and water surface differentials, hourly velocity readings at each individual station and the corresponding surface differentials (App. E) were analyzed by a simple correlation routine. Table 9 is a simplified output matrix; a complete correlation matrix and some scattergrams are included in Appendix E. Variable names DELTOW and DELJON refer to water surface differentials at Town Creek and Jones Creek, respectively. DIFT and DIFJ refer to the absolute values of same. VELT, VELJ, VELM and AVELT, AVELJ, AVELM refer to the mean velocities and the absolute values of the mean velocities at Town Creek, Jones Creek, and the inlet throat, respectively.

The linear correlations between the mean velocities of any section and the corresponding water surface differentials are fair. For example, the correlation is 0.78 between the instantaneous mean velocity at the Town Creek section (VELT) and the water surface differential between

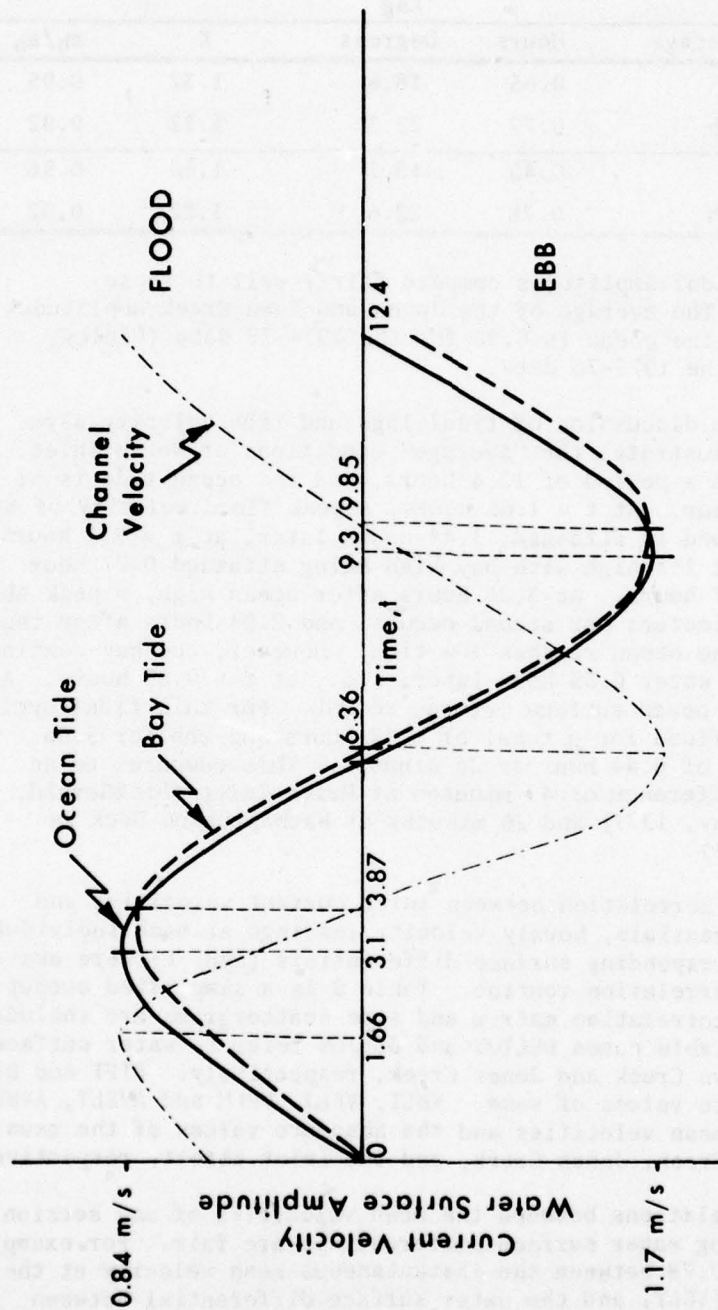


Figure 12. Diagram illustrating the "typical" tidal cycle at North Inlet.

Table 9. Correlation matrices between water surface differential values and current velocities, 1975-76.¹

	DELTOW	DELJON	VELT	VELJ	VELM
DELTOW ²	1	190	91	87	64
DELJON	0.81	1	93	89	69
VELT	0.78	0.75	1	66	11
VELJ	0.79	0.83	0.97	1	22
VELM	0.86	0.88	0.95	0.98	1
	DIFT	DIFJ	AVELT	AVELJ	
DIFT	1	190	91	87	
DIFJ	0.63	1	93	89	
AVELT	0.54	0.38	1	66	
AVELJ	0.50	0.53	0.90	1	

¹Numbers below the diagonal give the Pearson correlation coefficients. Numbers above give the number of data pairs used in the same calculations.

²Names are defined in text, symbol listing, and Appendix E.

the ocean and Town Creek gages (DELTOW). Similar correlation coefficients characterize the other linear regressions. However, the correlation coefficients decrease when the absolute values of the variables are considered. The correlations between the water surface differentials and the square of the velocities are also poor. Equation (2) indicates that the square of the current velocity is proportional to the water surface differential. However, the fact that both variable ranges in these correlations are reduced to about one-half by using the absolute (or square) values gives the data an apparent increase in scatter. The good linear correlation does support equation (2); failure to obtain improved correlation by using the velocity squared does not contradict it.

4. Tidal Curves.

All tide records were digitized and hourly water surface elevation values were output on cards and verified. Tidal curves were plotted from the punched records. All output was plotted on a monthly basis regardless of the duration of the record. Sample outputs are shown in Figure 13, and the complete set of plotted curves is in Appendix F. All tidal curves are referenced to a common datum of 205 centimeters below the "INLET" triangulation station. The tidal curves are not continuous because of logistics problems. The availability of tide records for each gage is summarized in Appendix F.

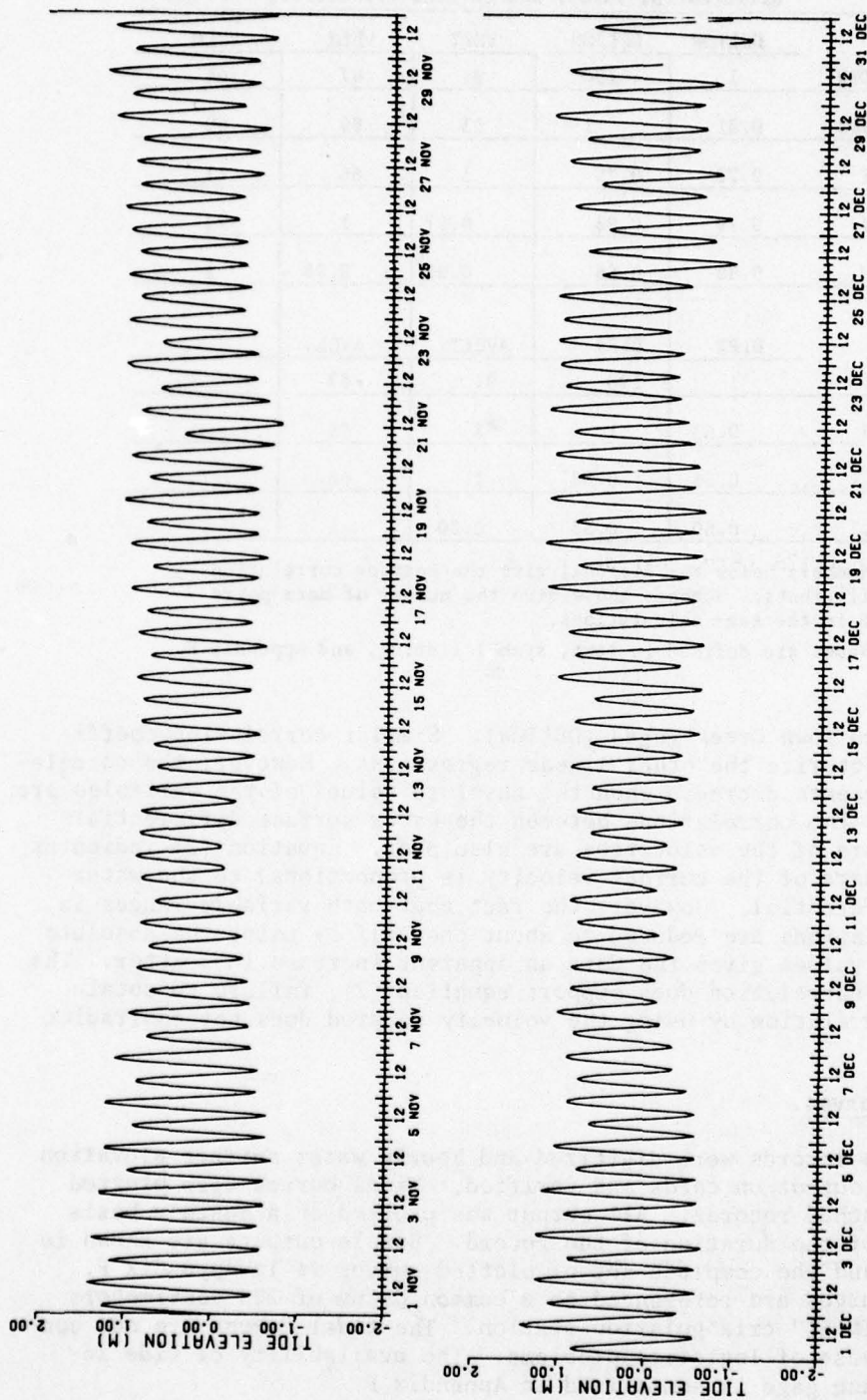


Figure 13. Sample water elevation records for the Jones Creek gage. The tide curves are referenced relative to a datum which is 205 centimeters below the "INLET" triangulation station.

The curves illustrate well the semidiurnal tide, the variations in diurnal inequality, and the tidal range fluctuations. For the ocean gage, the diurnal inequality at tropical tides can reach 55 centimeters with most of the inequality generally due to unequal high water levels. At equatorial tides, the inequality is all but nonexistent. The daily mean tidal range varies by as much as 60 centimeters from an average spring range of 175 centimeters to a neap range of only 117 centimeters. The mean tidal range and MSL were calculated for selected 2-week periods. The mean annual tidal ranges were computed, in turn, as the arithmetic mean of the 2-week ranges. Tidal ranges for the 1975-76 field year and 1974-75 (from Finley, 1976) are:

	1975-76 (cm)	1974-75 (cm)
Ocean gage	167	151
Town Creek	140	145
Jones Creek	135	140

5. Water Surface Differentials.

Scarcity of overlapping tide records limits the number of differential curves. Computer-plotted differential curves for the period 28 April to 12 May 1976 (Fig. 14) demonstrate good correspondence with the hand-plotted differentials in Appendix B. Typically, peak differentials ranged from about 10 to 20 centimeters at neap tides (1 to 4 May) to about 30 centimeters at spring (12 May). The jaggedness of the differential curves is probably attributed to random errors. Normally, most irregularities occur near slack water (0 differential) at a time when both measurement error and weather-induced level fluctuations are most noticeable. Figure 14 demonstrates that throughout most of the time period, peak ebb differentials seem to equal those for peak flood. At springtides, however, the seaward slopes are clearly the dominant ones. This indicates that the ebb flow dominance and the consequent net seaward sediment transport are to a large extent caused by the spring tides.

6. Spectral Analysis.

A spectral analysis was made of the water level time-series data for a number of 2-week periods of overlapping tide records for the ocean gage and at least one of the two bay gages (Table 10).

The first six time periods (Table 10) of records contained 360 hourly water level observations. The absolute value of the calculated spectral density function was compared from one record to another, and an increase or a decrease in the relative contribution of a given harmonic component was determined.

The procedure adjusts the mean of the sample to zero and then creates a raw periodogram and a spectral density function as measures of the variance explained by a simple harmonic oscillation of a given

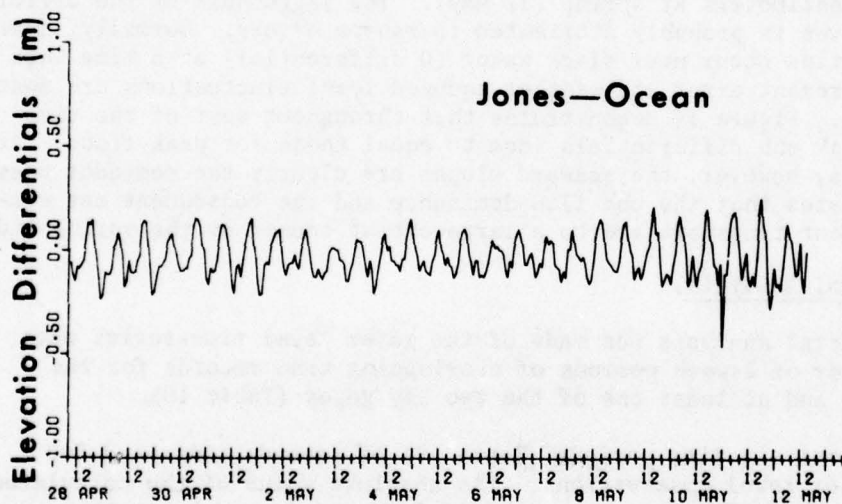
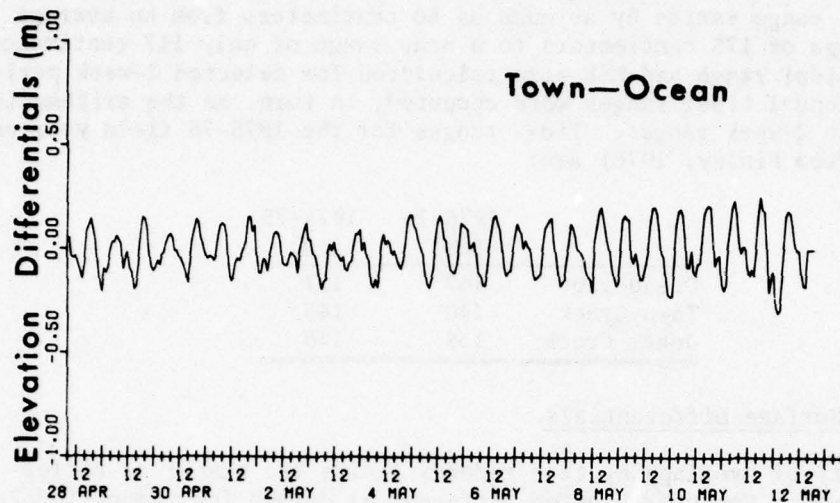


Figure 14. Water surface differential curves for the period 28 April to 12 May 1976.

Table 10. Water level time-series data subjected to spectral analysis.¹

Date	Ocean gage	Town Creek	Jones Creek
9 to 23 July 1975	x	-	x
26 Oct. to 10 Nov. 1975	x	x	x
8 to 23 Dec. 1975	x	-	x
2 to 17 Jan. 1976	-	x	x
14 to 29 Mar. 1976	x	x	x
1 to 15 May 1976	x	x	x
26 Oct. to 31 Dec. 1975	-	-	x

¹Spectra are presented in Figure 15 and Appendix G.

frequency. The cutoff frequency is that corresponding to twice the observation interval. In this analysis, T cutoff equals 2 hours. Since

$$f = \frac{2\pi}{T} \quad (4)$$

$$f \text{ cutoff} = \pi .$$

Calculations were made for 180 frequency values less than π ; the frequency interval between each successive spectral density estimate was 0.0175 cycle per hour. To facilitate reading Figure 15 and the spectra in Appendix G, Table 11 presents the relation between frequency and period calculated according to equation (4).

Table 11. Radian frequency, f, in cycles per hour versus period, T.

f	3.14	2.09	1.57	1.26	1.05	0.89	0.78	0.70	0.63	0.57	0.52
T	2	3	4	5	6	7	8	9	10	11	12

The ordinate of the spectral density diagrams is expressed in units of meters squared times hours or $(2\pi/f)$ meters squared.

The distinctly semidiurnal tidal characteristics at North Inlet are expressed by the dominance of the 0.5 cycle per hour peak which corresponds to a period of 12.4 hours. Typically, the spectral density value for this semidiurnal peak is about 50 times larger than that for the diurnal peak (Table 12). The semidiurnal solar constituent, S_2 , and the lunar constituent, M_2 , are too similar in frequency to be resolved by the bandwidths used; the same applies to the diurnal components, S_1 and M_1 . However, it is not necessary for these components to be resolved. An approximate tidal form number

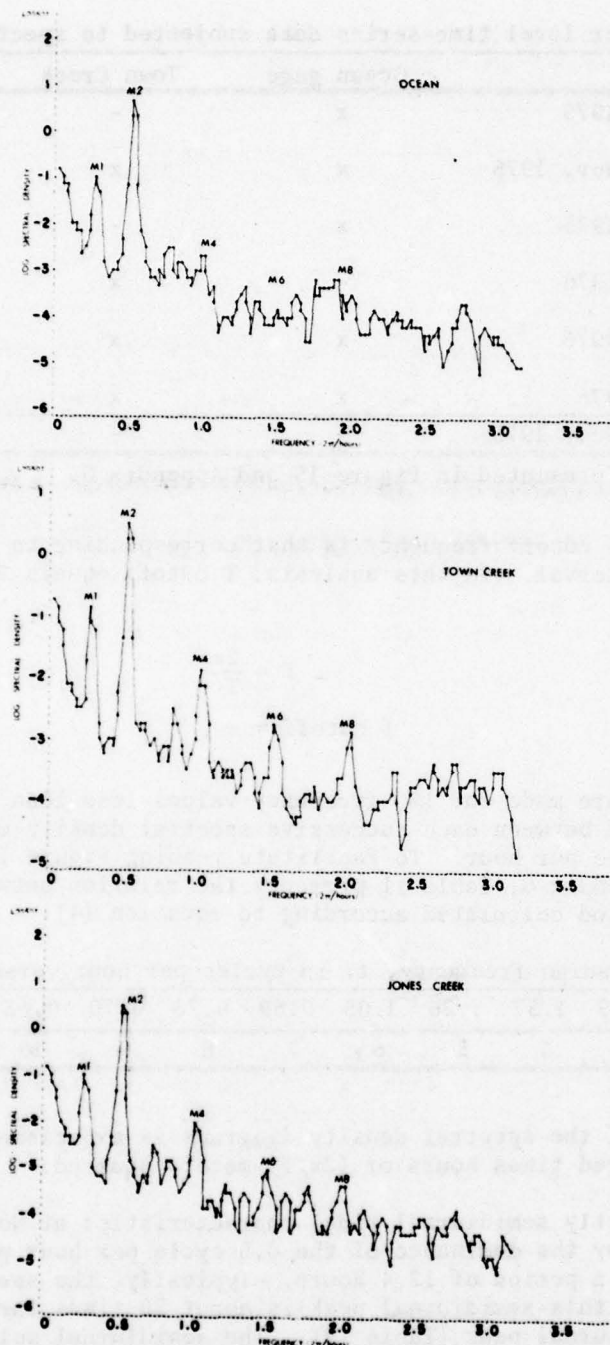


Figure 15. Spectral density functions for 2-week records (1 to 15 May 1976) off the ocean, Town Creek, and Jones Creek gages. Spectral density (ordinate) is expressed in log-10 scales.

Table 12. Spectral densities for tidal harmonic components M_1 , M_2 , M_4 , M_6 , and M_8 at ocean gage, Town Creek, and Jones Creek, 26 October to 10 November 1975.

Station	M_1	M_2	M_4	M_6	M_8
Ocean gage	0.08	5.5	0.004	0.0005	0.0003
Town Creek	0.07	3.6	0.01	0.003	0.0003
Jones Creek	0.08	3.6	0.01	0.003	0.0004
	M_1/M_2		M_4/M_2	M_6/M_2	M_8/M_2
Ocean gage	1.5×10^{-2}		7.3×10^{-4}	9.1×10^{-5}	5.5×10^{-5}
Town Creek	1.9×10^{-2}		2.8×10^{-3}	8.3×10^{-4}	8.3×10^{-5}
Jones Creek	2.2×10^{-2}		2.8×10^{-3}	8.3×10^{-4}	1.1×10^{-4}

(Defant, 1958) can be calculated if it is assumed that the M_1 and M_2 values of Table 12 equal the sum of the corresponding lunar and solar component values. The mean values of the form number F , defined as

$$F = \frac{M_1}{M_2}, \quad (5)$$

are F (ocean) equals 0.0145, F (Jones Creek) equals 0.0194, and F (Town Creek) equals 0.0222. All demonstrate a strong semidiurnal form.

Figure 15 and Appendix G demonstrate the presence of shallow-water tidal components of higher than semidiurnal frequency. These include the M_4 , M_6 , and M_8 components, the *overtides*, labeled on all spectra, as well as other peaks possibly due to interactions between the major tidal constituents. Table 12 summarizes the magnitude of the overtide spectral densities at the three gage sites for a "typical" 2-week period, 26 October to 10 November 1975. The high frequency overtides have spectral densities ranging from about 3×10^{-3} to 5×10^{-5} times that of the semidiurnal component. Therefore, the significance of these overtides is due more to their amplification with the passage of the tidal wave through the inlet, than their absolute magnitudes. Table 12 demonstrates that the amount of variance in the tide record, accounted for by the M_4 overtide, increases by a factor of 4 as the tidal wave progresses from the ocean to the bay gages. The other overtides considered, M_6 and M_8 , also appear to account for more of the variance in the bay spectra than in the ocean spectrum. Since the tidal wave had traveled across a wide shallow swash platform before it was recorded by the ocean gage (Fig. 7), significant shallow-water components were already present in this record. The total amplification of the overtides from deep ocean water to bay conditions was even larger than indicated by these figures.

Low-frequency harmonics (periods more than 12 hours) do not change much due to tidal wave progress through the inlet (Fig. 15 and Table 12). Therefore, the tidal inlet acts as a low-pass filter for tidal wave travel from the ocean to the bay-marsh system. The amplification of the overtides suggests that inlet impedance is a time-varying factor introducing higher order harmonics, through a series of nonlinear terms in the flow equations (eqs. 2 and 3). The results of the spectral analysis are conceptually consistent with the hydraulic data presented in this section and Figure 11. The amplification of overtide amplitudes in shallow water has also been found at Wachapreague (Boon, 1973) and at Chesterfield Inlet, Northwest Territories (Budgell, 1976).

7. Inlet Equilibrium.

Empirical studies of Pacific coast inlets by O'Brien (1931) demonstrated that the cross-sectional area of the inlet throat is proportional to the tidal prism, according to the equation:

$$A_c = 4.69 \times 10^{-4} P^{0.85} , \quad (6)$$

where A_c is the minimum flow section of the inlet (throat) measured below MSL (in square feet), and P is the diurnal or spring tidal range (in cubic feet). O'Brien (1969) and Johnson (1973) introduced slightly different equations expressing the same equilibrium concept.

Escoffier (1940) and Inman and Frautschy (1966) discussed the equilibrium concept in detail, stating that a stable inlet cross section is maintained by a balance between the amount of sediment scoured by tidal currents and the amount supplied as wave-generated longshore drift. Therefore, an inlet equilibrium equation should include both tidal prism and wave energy as independent variables. A development in this direction has been provided by Jarrett (1976) who investigated 108 tidal inlets along the coast of the United States. Jarrett concluded that natural or single-jettied inlets on the Atlantic coast have larger cross sections for a given tidal prism than on the Pacific coast, presumably because of the lower wave energy on the east coast. Using the same symbols and units as in equation (6), Jarrett's equation for east coast natural inlets is:

$$A = 5.37 \times 10^{-6} P^{1.07} . \quad (7)$$

Based on channel hydrography measurements and throat section fathometer profiles, the flood, ebb, and mean daily tidal prisms were calculated (Table 13) for each data set between May 1975 and May 1976. Throat cross sections were precisely measured during 11 hydrography periods. These data sets and Finley's (1976) data for the previous year were plotted on Jarrett's (1976) equilibrium diagram (Fig. 16).

All data points plot well within the 95-percent confidence limit on Jarrett's empirical diagram, indicating that North Inlet is at a state of long-term stability. The scatter of the data points reflects measurement errors, meteorologic tides, tidal exchange between the North Inlet system and Winyah Bay, and significant annual variations in sea level.

Table 13. North Inlet ebb and flood tidal discharge.

Date	Tide	Prism			
		Flood	Ebb	Mean	Mean
		Millions of m ³			10 ⁸ ft ³
1975					
24 May	Spring	24.066	15.724	19.895	7.025
10 June	Spring	29.088	21.773	25.430	8.979
14 June	Mean	19.894	21.341	20.617	7.280
17 June	Neap	18.464	19.123	18.794	6.636
21 June ¹	Mean	15.631	12.820	14.225	5.023
29 June	Mean	12.942	18.918	15.930	5.625
26 Aug.	Mean	13.658	15.311	14.490	5.116
26 Sept.	Mean	14.630	16.092	15.360	5.424
29 Sept.	Neap	18.446	18.706	18.580	6.561
2 Oct. ¹	Mean	24.926	23.022	23.980	8.467
4 Oct.	Spring	19.336	24.008	21.672	7.652
24 Nov.	Mean	18.630	21.186	19.908	7.029
1976					
7 Jan. ¹	Mean	11.700	10.800	11.250	3.972
10 Jan. ¹	Neap	8.071	8.586	8.329	2.941
15 Jan.	Mean	18.515	23.274	20.894	7.378
17 Jan.	Spring	19.555	29.530	24.543	8.666
17 Feb. ¹	Spring	20.534	21.614	21.070	7.439
15 Mar. ¹	Spring	21.395	18.047	19.721	6.964
22 Mar. ¹	Mean	10.393	7.844	9.119	3.220
24 Mar.	Neap	8.550	8.233	8.392	2.963
27 Mar. ¹	Mean	11.963	14.854	13.410	4.735
27 Apr. ¹	Mean	15.732	10.145	12.940	4.569
19 May ¹	Mean	13.104	12.880	12.992	4.588

¹Based on throat section stations.

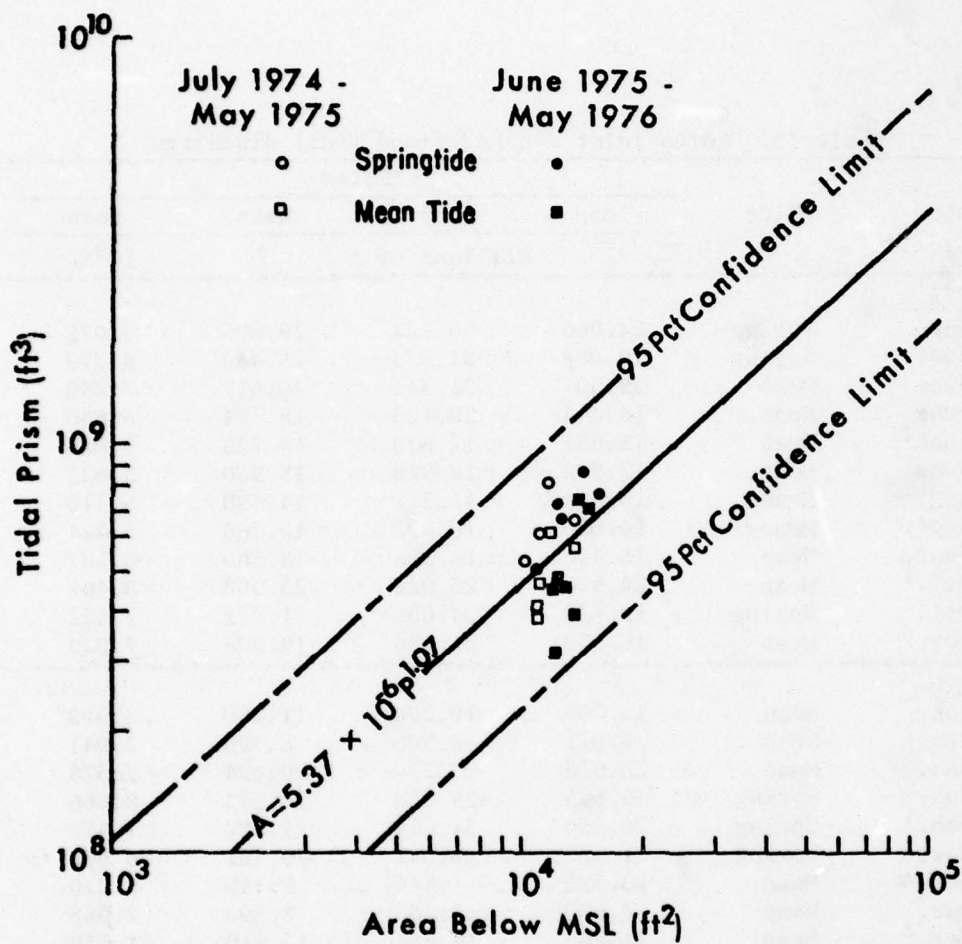


Figure 16. Tidal prisms versus throat cross-sectional areas for North Inlet between July 1974 and May 1976.

Figure 17 presents a correlation diagram of 10 measurements of tidal prism and the ocean tidal range, R_0 , using both the data in Table 13 and the recorded tidal ranges. The regression equation is:

$$P = 12R_0 - 5.10 \quad (8)$$

where P is measured in 10^6 cubic meters and R_0 in meters. The Pearson product moment correlation coefficient, r , equals 0.94. This correlation clearly demonstrates that tidal prism is a direct function of the available storage volume in the marsh-creek system. A good linear correlation for Price Inlet was demonstrated by FitzGerald, Nummedal, and Kana (1977) by averaging hourly water level readings.

8. Seasonal Changes in Sea Level.

MSL (relative to a reference datum) was calculated for 2-week cycles from the available ocean, Town Creek, and Jones Creek gage records. The resulting MSL curve is shown in Figure 18. A seasonal pattern of high sea level in the fall, an alltime low in mid-winter, and a secondary high in mid-spring is quite evident. The measured annual range at the creek gages is about 34 centimeters, the inferred ocean range is about 45 centimeters. Annual sea level changes significantly affect the sedimentation and patterns of morphologic change of the intertidal zone (Sec. V, 4). To assess the applicability of certain North Inlet morphologic results to inlets in general, the geographic variations in and reasons for the sea level fluctuations will be discussed in some detail.

Pronounced seasonal variations in sea level are found at nearly all coastal locations (Marmer, 1952; Pattullo, et al., 1955; Pattullo, 1966), although the pattern of variation changes from place to place. For Charleston Harbor, Pattullo, et al. (1955) reported an annual high in October of 17 centimeters above MSL and a low in January of 8.7 centimeters below MSL, based on tide records from 1921 to 1946. There was no indication of a secondary spring high in that record. In the Gulf of Mexico, an interesting increase in the secondary spring high toward the west was observed (Marmer, 1952; Pattullo, et al. 1955). At Key West, no spring high was observed. At Port Isabel (Marmer, 1952), and at the New Corpus Christi Pass (Behrens, Watson, and Mason, 1977), a pronounced spring high was observed. The sea level curve in Behrens, Watson, and Mason (1977) corresponds closely to the one for North Inlet (Fig. 18).

A number of factors can contribute to annual changes in sea level. Pattullo (1966) listed (a) variations in water temperature, (b) variations in salinity, and (c) changes in local atmospheric pressure; Meade and Emery (1971) listed river runoff in the eastern United States. Each individual factor can cause seasonal deviations in sea level of about 20 centimeters. Behrens, Watson, and Mason (1977) qualitatively attribute the changes at Corpus Christi to seasonal variations in onshore and longshore winds, factors which Pattullo

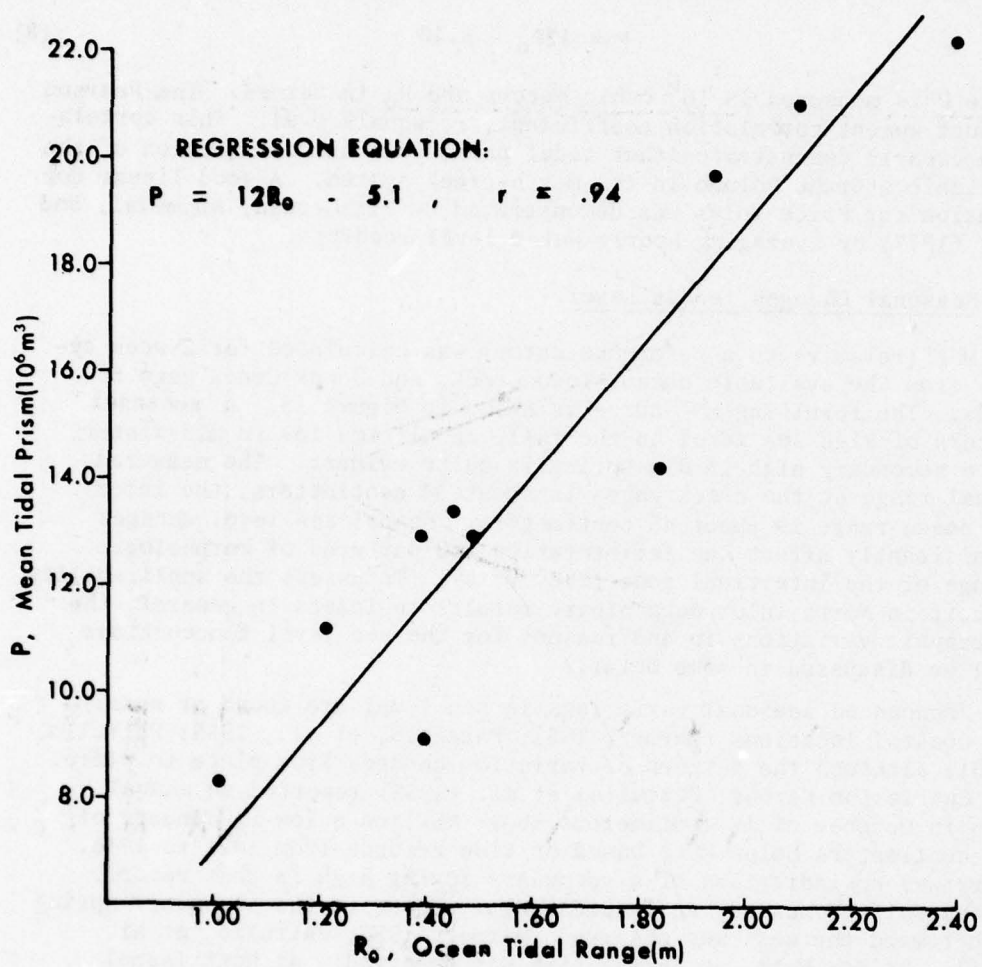


Figure 17. Measured tidal prism versus ocean tidal range.

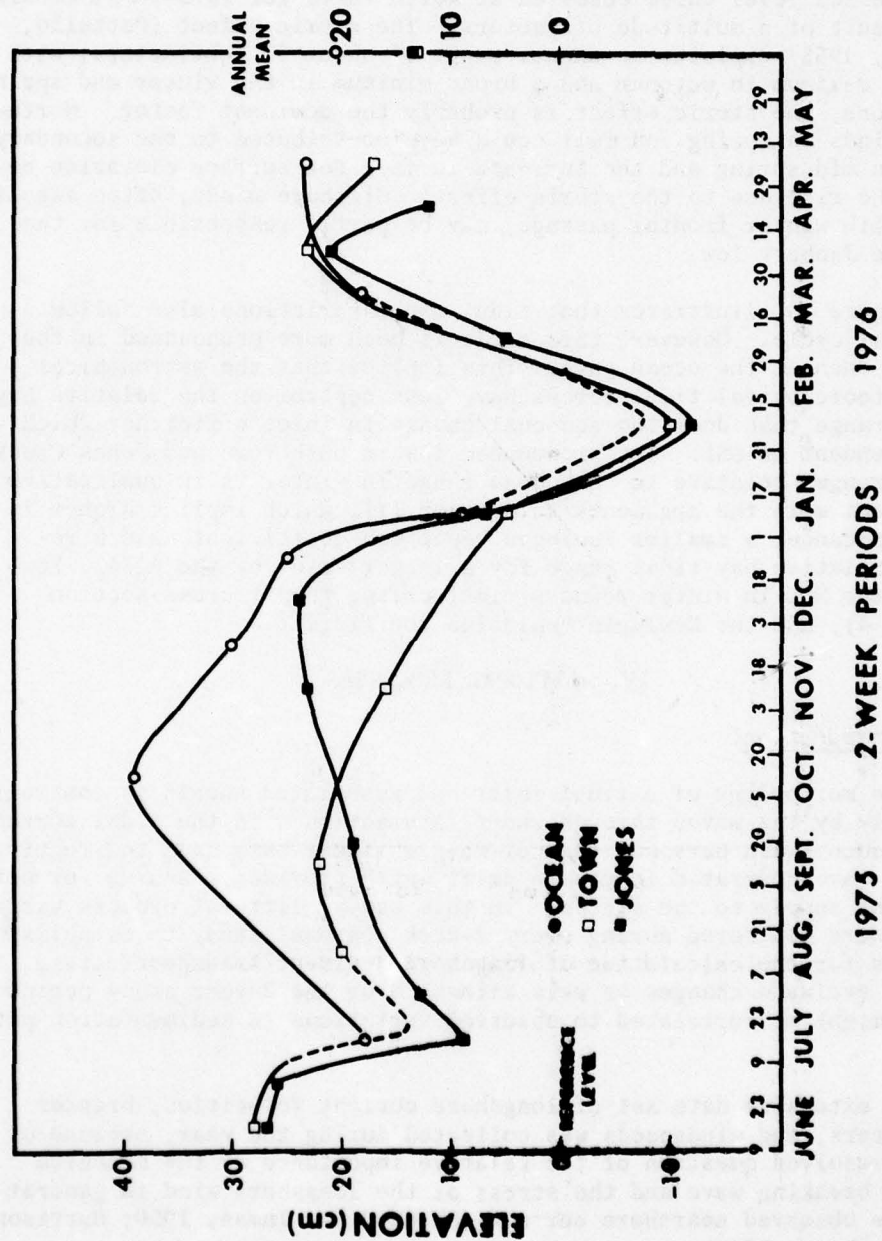


Figure 18. Annual variation in MSL computed from available 2-week tide gage records of the ocean, Jones Creek, and Town Creek gages. Dashed line indicates missing ocean tide records.

(1966) was unable to assess quantitatively. An additional set of factors known to have a significant influence on sea level is the upwelling and geostrophic effects of ocean currents (Wyrski, 1973; Komar, 1976).

The sea level curve observed at North Inlet for 1975-76 is clearly the result of a multitude of factors. The steric effect (Pattullo, et al., 1955) explains an annual range of about 25 centimeters, with a single maximum in October and a broad minimum in the winter and spring. Therefore, the steric effect is probably the dominant factor. Northeast winds in spring and fall could have contributed to the secondary peak in mid-spring and the increase in fall sea surface elevation beyond the rise due to the steric effect. Offshore winds, often associated with winter frontal passage, may be partly responsible for the extreme January low.

Figure 19 illustrates that tidal range variations also follow a seasonal cycle. However, this cycle is much more pronounced in the creeks than at the ocean gage. This implies that the astronomical and meteorological tidal forces have less control on the relative bay tidal range than does the seasonal change in inlet efficiency which is dependent on MSL. The pronounced low in both Town and Jones Creek tidal ranges relative to the ocean range in winter is in qualitative agreement with the arguments in Section III, which implies higher inlet impedance, a smaller Keulegan repletion coefficient, and a reduced relative bay tidal range for a larger value of the A_b/A_c . Lowering the MSL in winter reduces tidal prism, throat cross section (Table 4), and the Keulegan repletion coefficient.

IV. LITTORAL PROCESSES

1. Introduction.

The morphology of a tidal inlet and associated shoals is controlled directly by the waves through their interaction with the tidal currents to produce swash bars and channel-margin linear bars and, indirectly, by the wave-generated longshore drift which provides a source for net sediment supply to the system. In this study, littoral process variations were monitored during every 2-week seasonal study to establish a basis for the calculation of longshore sediment transport rates, and to evaluate changes in wave climate over the 2-year study period which might be correlated to observed variations in sedimentation patterns.

An extensive data set of longshore current velocities, breaker parameters, and windspeeds was collected during the year, because of the unresolved question of the relative importance of the momentum of the breaking wave and the stress of the longshore wind in generating the observed nearshore current (Shepard and Inman, 1950; Harrison and Krumbein, 1964).

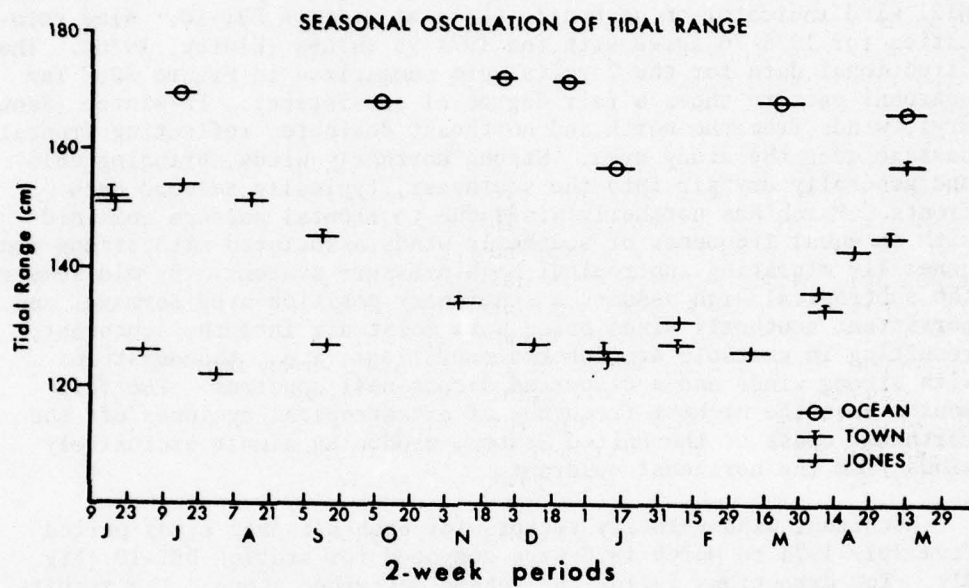


Figure 19. Annual variation in tidal ranges at the three stations.

2. Wind Patterns.

Annual offshore wind data (Finley, 1976) demonstrate that South Carolina coastal winds dominantly come from the northeast and the southwest. The former component is largely due to extratropical cyclones, most of which are far to the northeast of South Carolina but control the wind pattern along the entire east coast of the United States. South and southwesterly winds are generally anticyclonic summer winds associated with a strong Bermuda high.

Wind velocities and directions were measured by a Weather Measure W121 wind indicator on an hourly basis at station DBI-10. Wind velocities for 1975-76 agree with the 1974-75 values (Finley, 1976). The directional data for the 2 years were summarized in Figure 20. The seasonal pattern shows a fair degree of consistency. In winter (January), winds from the north and northeast dominate, reflecting frontal passage over the study area. Strong northerly winds, bringing cold and generally dry air into the southeast, typically succeed such fronts. March has northerly winds due to frontal passage combined with an equal frequency of southerly winds associated with strong and generally migrating subtropical high-pressure systems. By mid-summer, the subtropical high assumes a stationary position over Bermuda, and persistent southerly winds bring warm moist air into the southeast, resulting in unstable atmospheric conditions; i.e., thunderstorms with strong winds and a dispersed directional spectrum. The fall months have the highest frequency of extratropical cyclones off the northeast coast of the United States, producing almost exclusively winds from the northeast quadrant.

Resultant wind velocity vectors for each seasonal study period from July 1974 to March 1976 were computed for station DBI-10 (Fig. 21). The directions follow the scheme described above. The resultant wind vectors for the summer and fall were rather consistent for the 2 years. Due to an onshore (azimuth 71°) wind vector in January 1975, as compared to the offshore (azimuth 130°) vector in January 1976, the annual resultant wind vector for 1974-75 was much larger than the one for 1975-76 and, more significantly, oriented nearly perpendicular to the local shoreline. The magnitude of the annual resultant wind vector is a measure of the directional variation throughout the year, which differs from the scalar quantity of wind-speed. The mean windspeed was not significantly different the 2 years. However, the smaller contribution of northerly winds in January 1975, as compared to January 1976, caused the 1974-75 resultant vector to rotate 24° clockwise from the 1975-76 vector. Based on this wind pattern, the total wave energy flux was comparable for the 2 years. However, the *net longshore* energy flux, oriented to the south both years, was significantly higher in 1975-76 than in 1974-75.

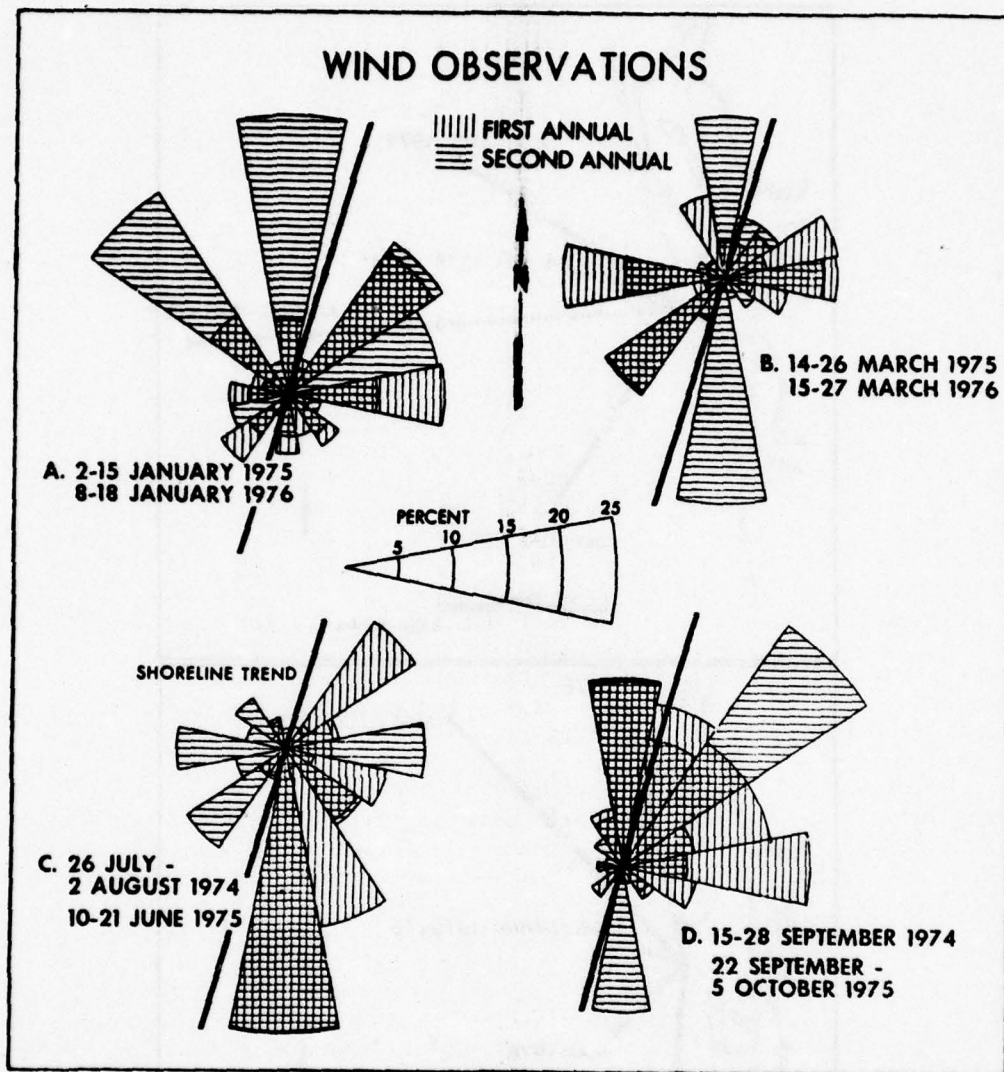


Figure 20. Seasonal distributions of wind directions observed at North Inlet.

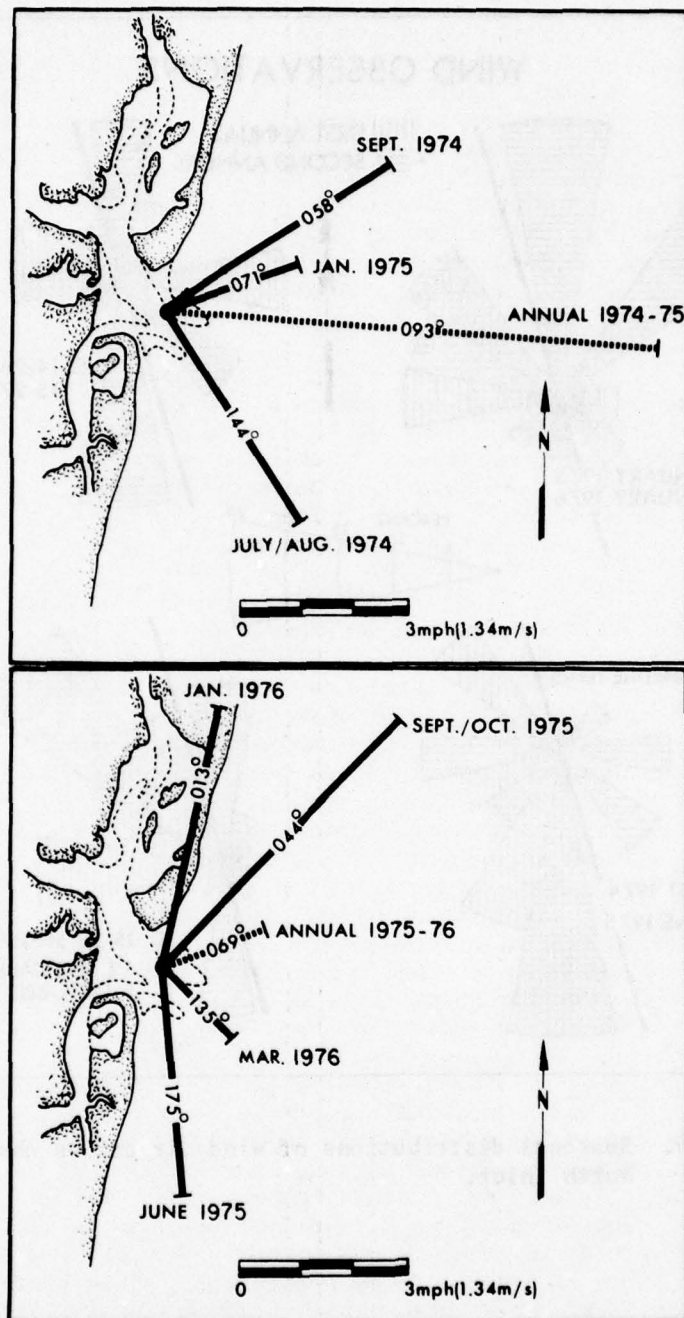


Figure 21. Resultant wind vectors for each 2-week field period. Note the significant difference in both magnitude and direction of the two annual vectors. (The vector for March 1975 is obscured by the one for September 1974).

3. Breaker Parameters.

a. General. Recently developed instrumentation has provided a means of recording directional wave spectra on a continuous basis (Seymour, et al., 1976). More commonly, however, wave recorders are all nondirectional (Harris, 1972) and estimates of directionally dependent parameters like energy flux are based on visual observations of the near-shore wave field. Littoral processes at North Inlet were measured by observers standing in the breaker zone. Every 2 daylight hours during the 2-week seasonal observation period, the observers recorded breaker heights and depths by holding a graduated rod at the primary breaker. Breaker angle was measured by a hand-held protractor or Brunton compass, and longshore currents by tracing the movement of a neutrally buoyant rubber float in the surf. Periods were measured by counting 11 successive wave crests passing a fixed point in the surf. To release personnel for tidal hydraulics measurements and morphological mapping, littoral processes in 1975-76 were only recorded at station DBI-25 which was least influenced by shoaling and refraction around the ebb tidal delta. Therefore, the parameter statistics presented in this section should reflect conditions at a straight segment of beach without any complicating nearshore bathymetry.

b. Breaker Type. Breakers were classified as spilling and plunging (Galvin, 1972). Surging and collapsing breakers were not observed. The beach slope at station DBI-25 was gentle; most variations in the primary breaker form were due to the changing deepwater steepness of the waves. Long-period swell arriving from offshore areas of generation more commonly formed plunging breakers. Locally generated steeper waves commonly break by spilling. Summary statistics (Tables 14 and 15) for 2 years of observation (July 1974 to March 1976) indicate that the breakers were evenly distributed, half were spilling and half were plunging. The standard error of the mean is quite large, so the percentage differences with respect to wave approach direction are not statistically significant. There are no statistically significant differences between the seasonal percentages either, which indicates that locally generated wind waves and distant swell account for about the same relative amount of the observed breakers at all seasons.

c. Breaker Height. The breaker height statistics were better than those for breaker type, and significant seasonal variations were detected (Table 16). The 2-year adjusted average was 59 centimeters with seasonal variations ranging from a low of 54 centimeters in March to a high of 70 centimeters in September. This is consistent with the wind climate. Weak, variable, and commonly offshore winds in spring tend to generate small waves. A high frequency of northeast winds in fall tends to generate larger waves reaching shore from the northeast. These results vary somewhat with those of U.S. Army, Corps of Engineers, Coastal Engineering Research Center (1977) which indicated that the south Atlantic coast has a

Table 14. Percent spilling waves at station DBI-25.

	Direction ¹	N ²	Mean	Std. dev.	Median
July 1974 - March 1976	S	141	46.6	33.0	49.3
	N	210	54.2	29.4	50.5
	//	112	40.2	34.5	30.1
	Average		48.9	32.2	50.0

Analysis by season								
	July 1974	June 1975	Sept.		Jan.		Mar.	
			1974	1975	1975	1976	1975	1976
Mean	----- ³	48.9	56.4	55.0	44.5	46.0	36.0	52.5
Std. Dev.	----	32.6	28.4	31.8	32.7	32.4	27.8	35.2

¹ N = Wave approach direction between east and north;

S = Wave approach direction between east and south;

// = Wave approach direction parallel to shoreline.

² Number of observations.³ No reading.

Table 15. Percent plunging waves at station DBI-25.

Direction ¹		N ²	Mean	Std. dev.	Median
July 1974 - March 1976	S	141	53.4	33.0	50.7
	N	210	45.5	29.5	40.5
	//	112	59.8	34.5	69.9
	Average		51.1	32.2	50.0

Analysis by season								
	July 1974	June 1975	Sept.		Jan.		Mar.	
			1974	1975	1975	1976	1975	1976
Mean	----- ³	51.0	43.6	45.0	55.5	54.0	64.0	47.5
Std. Dev.	----	32.7	28.4	31.8	32.7	32.4	27.8	35.2

¹ N = Wave approach direction between east and north;

S = Wave approach direction between east and south;

// = Wave approach direction parallel to shoreline.

² Number of observations.³ No reading.

Table 16. Breaker heights (in meters) at station DBI-25.

	Direction ¹	N ²	Mean	Std. dev.	Median
July 1974 - March 1976	S	141	0.55	0.17	0.52
	N	209	0.65	0.26	0.60
	//	112	0.53	0.19	0.50
	Average		0.59	0.23	0.56

Analysis by season								
	July 1974	June 1975	Sept.		Jan.		Mar.	
			1974	1975	1975	1976	1975	1976
Mean	----- ³	0.57	0.69	0.71	0.59	0.55	0.52	0.53

¹ N = Wave approach direction between east and north;

S = Wave approach direction between east and south;

// = Wave approach direction parallel to shoreline.

² Number of observations.³ No reading.

minimum wave height of about 43 centimeters in July and a maximum of about 56 centimeters in September. Since these latter figures are averages from a number of U.S. Coast Guard stations over a large region with variable deepwater waves and refraction and shoaling characteristics, this level of difference is expected. Breaker depth, angle between the crest of the breaker and the shoreline, and wave period were measured, but not tabulated in this report. However, they were used in following calculations.

4. Longshore Sediment Transportation.

The best established predictive equation for the transportation of sediment on beaches is based on the longshore component of wave energy flux (Komar, 1976; Galvin and Vitale, 1977). Since wave observations in this study were made at the surf, and the significant wave heights were recorded, the correct expression is:

$$P_{1s} = 2.78 \times 10^{-2} \times H_b^{5/2} \times \sin 2\alpha_b \quad (9)$$

where P_{1s} is the longshore energy flux *factor* measured in joules per second per meter of beach front (U.S. Army, Corps of Engineers, Coastal Engineering Research Center, 1977), H_b is the breaker height (in meters), and α_b is the breaker angle.

Longshore energy flux factors at station DBI-25 for the eight seasonal field studies are summarized in Table 17. Since P_{1s} does not scale linearly with H_b or α_b , no mean values were used in the calculations. P_{1s} was calculated for each observation to include all observation variability; the P_{1s} values, in turn, were averaged for specified time periods. Mean values in Table 17 refer to the mean of all readings giving either a northerly or southerly flux component. The resultant vector, on the other hand, is the arithmetic mean of all calculated P_{1s} values, with (+) assigned to all flux vectors oriented to the right (south) and (-) assigned to all flux vectors oriented to the left (north).

Using only field studies where a precise relationship between P_{1s} and the volumetric rate of longshore sand transport had been established, the U.S. Army, Corps of Engineers, Coastal Engineering Research Center (1977) arrived at the following rating equation:

$$Q_s = 1.28 \times 10^3 \times P_{1s} \quad (10)$$

where Q_s is the annual longshore transport rate (in cubic meters). Applying equation (10) to the data in Table 17, sediment transport rates at station DBI-25 were calculated (Table 18). Transport to the north (Q north) and south (Q south), respectively, was computed from the mean energy flux factors to the north and south for each 2-week period. The net and gross transport rates were obtained as the difference and sum, respectively, of Q north and Q south. To estimate the annual transport rates, the calculated values for each 2-week period were assumed to be representative for an entire 3-month season. The validity of this as-

Table 17. Longshore energy flux factors (in Joules per second per meter) at station DBI-25.

Date	Direction ¹	N ²	Mean	Resultant vector ³
July 1974 - Mar. 1976	N	141	250	+182
	S	211	451	
Analysis by season				
July 1974	N	---	---	----
	S	---	---	
June 1975	N	28	157	+141
	S	21	540	
Sept. 1974	N	4	324	+344
	S	46	391	
1975	N	18	124	+281
	S	39	469	
Jan. 1975	N	22	449	-42
	S	27	289	
1976	N	26	87	+160
	S	33	355	
Mar. 1975	N	16	244	+184
	S	18	565	
1976	N	32	180	-32
	S	27	144	

¹Direction along shoreline.

²Number of observations.

³(+) values indicate flux toward the south.

⁴(-) values indicate flux toward the north.

Table 18. Computed longshore sediment transport rates at station DBI-25.

Date	Gross (m ³ /yr)	Net (m ³ /yr)	Direction		
June 1974 - May 1975	882,500	87,500	S		
June 1975 - May 1976	761,500	392,100	S		
Mean	822,000	239,800	S		
Rates per quarterly (2 weeks) field period (m ³)					
Date	Q north	Q south	Gross	Net	Net direction
July 1974	----- ¹	-----	-----	-----	-
June 1975	7,640	30,600	38,240	22,960	S
Sept. 1974	16,020	19,340	35,360	3,314	S
Sept. 1975	6,290	32,110	38,410	25,820	S
Jan. 1975	22,140	14,280	36,430	7,860	N
Jan. 1976	4,980	24,650	29,620	19,670	S
March 1975	12,050	27,890	29,950	15,840	S
March 1976	11,880	8,770	20,660	3,109	N

¹No reading.

sumption should be judged both in light of the breaker height data (Table 16), which indicate a distinct and clearly repetitive seasonal pattern, and the low frequency of shoreline crossing extratropical or tropical cyclones.

The computed total rate for each year indicates a consistent gross transport of about 8×10^5 cubic meters. In the 1974-75 project year, the net transport to the south was only 8.7×10^4 cubic meters or about 10 percent of the gross. This result is consistent with the wind climate studies which indicated that the resultant wind vector for 1974-75 was oriented nearly perpendicular to the local shoreline with only a small southward component (Fig. 21). However, the wind vector for 1975-76 is more oblique to the shoreline, with a much larger southward component, consistent with a net transport to the south of about 50 percent of the gross for that year, or about 3.9×10^5 cubic meters. Transport rates on the United States east coast are about 2.0×10^5 cubic meters per year, generally to the south (Wiegel, 1964). The average net transport rate for 2 years at North Inlet is 2.4×10^5 cubic meters. Studies of the growth of Debidue spit and the North Inlet ebb tidal delta from 1925 to 1964 (Finley, 1976) indicate an annual rate of increase of 4.3×10^5 cubic meters per year.

5. Longshore Currents.

a. Theory. Longshore current velocities measured in the surf zone at station DBI-25 are the vector resultant of velocity components due to the oblique approach of the breaking wave, the nearshore cell circulation system, currents generated directly in the nearshore zone by wind stress and, perhaps, components of a regional circulation system. It is generally assumed that the dominant factor in the generation of longshore currents is the oblique approach of the breaking wave. The two most important parameters determining the longshore current velocity are the wave height and the angle between the wave crest and the shoreline (U.S. Army, Corps of Engineers, Coastal Engineering Research Center, 1977). A number of theories explain the generation of such currents and predict their magnitude. These theories are grouped according to their considerations of (a) conservation of mass, (b) conservation of energy flux, or (c) consideration of momentum flux (Galvin, 1967). Empirical equations, based on statistical analysis of parameters describing the breaking wave, have also been constructed (Harrison, 1968; Fox and Davis, 1972), though such equations are generally of limited value outside the specific area of formulation.

The objective of this section was to evaluate, through the use of a stepwise multiple-linear regression procedure, whether parameters descriptive of the surf zone field adequately explain the observed variability in longshore currents, or if the inclusion of additional environmental parameters could significantly improve the ability to predict such current velocity. Linear combinations of breaker param-

eters and three proposed equations for prediction of longshore current velocity were used in the evaluation. Galvin (1963), basing his model on the continuity of water mass, arrived at:

$$V = k \times g \times m \times T_b \times \sin 2\alpha_b \quad (11)$$

where V is longshore current velocity, g is the acceleration of gravity, m is beach slope, α_b is breaker angle, and k is a parameter of the breaker form, here taken as 1.0 (Galvin and Eagleson, 1965).

The equation by Longuet-Higgins (1970) was derived by considerations of the conservation of momentum flux for breaking waves. The U.S. Army, Corps of Engineers, Coastal Engineering Research Center (1977) empirically determined the proportionality constant in Longuet-Higgins' equation by fitting it to laboratory data by Galvin and Eagleson (1965) and field data from Putnam, Munk, and Traylor (1949). Thus, the "modified" Longuet-Higgins equation reads:

$$V = 20.7 m(g H_b)^{1/2} \sin 2\alpha_b \quad (12)$$

Fox and Davis' (1972) empirical equation for their Lake Michigan data set,

$$V = 2.98 \frac{H_b}{T_b} \sin 4\alpha_b \quad (13)$$

was also included in the testing. This equation accounted for 77.8 percent of the variance in the current velocity data at Sheboygan, Lake Michigan.

b. Data. Descriptive summary statistics for all longshore current velocity readings obtained between July 1974 and March 1976 are presented in Table 19. The mean longshore current is stronger to the south (35.8 centimeters per second versus 23.8 centimeters to the north). Extreme variability in current velocities is demonstrated by the fact that the standard deviation almost equals the mean. Inman and Quinn (1952) also found in their study of longshore current variability on the Pacific coast that the standard deviation often equaled or exceeded the mean. There is an indication in the data that fall current velocities are slightly higher than those at other seasons.

Appendix H shows that the 1975-76 current velocity data ranged from 73 centimeters per second to the left (north) to 151 centimeters per second to the right (south), with 5 percent of currents set to the north stronger than 51 centimeters per second and 5 percent of those set to the south stronger than 85 centimeters per second.

The 1974-75 current data were not included in the following analysis because of the large number of missing wind observations. The 1975-76 data set included only those velocity readings which occurred at least 3 hours after sudden reversals in wind direction; there was a lag

Table 19. Longshore current velocities (in centimeters per second) at station DBI-25.

Date	Direction ¹	N ²	Mean	Std. dev.	Median	Resultant vectors ³
Analysis by season						
July 1974 - Mar. 1976	N	176	23.8	17.0	19.6	
	S	271	35.8	27.9	28.4	+12.3
Analysis by season						
July 1974	N	0	----	----		----
	S	0	----	----		----
June 1975	N	120	22.6	15.0		
	S	98	37.3	28.7		+4.3
Sept. 1974	N	21	13.8	0.0		
	S	152	46.4	33.0		+39.2
1975	N	58	26.3	16.1		
	S	137	45.5	30.7		+24.1
Jan. 1975	N	61	22.7	14.0		
	S	107	33.8	21.4		+13.5
1976	N	57	17.2	13.2		
	S	136	34.9	25.6		+19.5
Mar. 1975	N	72	24.4	18.3		
	S	64	27.1	17.4		-0.2
1976	N	117	31.3	19.7		
	S	103	25.7	16.3		-4.6

¹Current direction along shoreline. N is to the north, S to the south.

²Number of observations.

³(+) values indicate direction to the south. (-) values indicate direction to the north.

⁴No reading.

of some hours between reversals in the longshore wind component and corresponding reversals in the current. A total sample of 250 data sets remained.

c. Analysis. Three regression procedures were utilized in this data analysis:

(a) Simple correlation was used to test for linear relationships between any pair of variables. The Pearson correlation coefficient is a measure of the degree of proportionality between two variables.

(b) Stepwise regression enters one independent variable at a time until all are entered simultaneously. Their order of inclusion is determined by the computer--the independent variable which explains the largest amount of variance in the dependent variable is entered first. The others are then entered in order of decreasing variance. The proportion of the total variance in the dependent variable explained by an independent variable, or a combination of variables, is expressed by the multiple correlation coefficient, r^2 .

(c) Multiple regression enters one independent variable at a time in any order specified by the investigator. Thus, the amount of variance explained by any independent variable of particular interest can be assessed.

The variable names used in the computations and the following analysis are defined in Table 20.

Table 20. Variable names used in multiple regression analysis of littoral processes.

Name	Definition
VEL	Observed longshore current velocity (in centimeters per second). (+) indicates current to the right (south); (-) indicates current to the left (north).
HGT	Breaker height (in centimeters).
PER	Breaker period (in seconds).
WIND	Wind velocity (miles per hour).
WINDL	Longshore component of wind velocity (miles per hour).
ANGL	Angle of wave orthogonal relative to shoreline.
WAVL	Sine of the breaker angle.
VGAL	Velocity calculated by Galvin's (1963) formula (eq. 11).
VELH	Velocity calculated by Louquet-Higgins' (1970) formula (eq. 12).
VEFD	Velocity calculated by Fox and Davis' (1972) formula (eq. 13).

Table 21 is a matrix of the Pearson product-moment correlation coefficients for these 10 variables for the 1975-76 annual data set of 250 observations.

Table 21. Pearson correlation coefficients between littoral process variables defined in Table 20.

	VEL	HGT	PER	WINDL	WAVL	VGAL	VELH
VEL	-----						
HGT	0.37	-----					
PER	-0.11	-0.06	-----				
WINDL	0.83	0.36	-0.07	-----			
WAVL	0.68	0.27	-0.09	0.68	-----		
VGAL	0.64	0.27	-0.01	0.66	0.97	-----	
VELH	0.69	0.38	-0.07	0.70	0.97	0.95	-----
VEFD	0.70	0.46	-0.12	0.69	0.88	0.81	0.93

The measured surf zone current velocity correlates better with the longshore component of the wind velocity than with any other variable ($r = 0.83$). Wave height, period, and the sine of the breaker angle all show a poor correlation with the current velocity. When these latter parameters are combined as suggested in equations (10), (11), and (12), the predicted and observed longshore velocities show correlations ranging from r equals 0.64 for Galvin's (1963) formula to r equals 0.70 for Fox and Davis' (1972) formula.

Bivariate data plots produced by the computer "SCATTERGRAM" procedure (App. H) give further information on the nature of these correlations. The plots of wave height and period versus current velocity show hardly any discernible trend. Clearly, these parameters do not exert a dominant control on the current velocity. Wind velocity correlates with the longshore current velocity at r equals 0.32. A large amount of scatter is observed at low wind velocities. As expected, wave angle shows a negative correlation ($r = 0.45$) with the velocity because of the direction convention. The variable ANGL (Table 20) refers to the orientation of the incoming wave orthogonal relative to the shoreline; thus, for ANGL $< 90^\circ$, the breaking wave will generate a momentum flux and a longshore current to the right (positive direction). For ANGL $> 90^\circ$, the wave-generated longshore current should be directed to the left (negative). The longshore component of the wind velocity correlates with the current velocity at r equals 0.83. The scatter is rather uniform over the entire range of wind velocities.

If the longshore component of the wind is considered as the only independent variable, a simple regression equation for the longshore current velocity can be written as:

$$VEL = 3.42 \times WINDL + 6.32 \quad (14)$$

This is a wholly empirical equation, and all parameters affecting the longshore current velocity are lumped into WINDL. Equation (14) does not indicate how much is due to the oblique breaking of the wind-generated waves. However, the equation is of predictive value for longshore currents off Debidue Island (and probably elsewhere under similar environmental conditions).

The correlation coefficients between observed current velocity and that predicted by the three equations tested are all reasonably high. This indicates proportionality. However, the magnitude of the predicted velocity generally differs substantially from that observed as evidenced by the proportionality factors in the following three regression equations (all velocities are in centimeters per second).

$$VEL = 0.33 VGAL + 5.18, r = 0.57 \quad (15)$$

$$VEL = 0.45 VELH + 4.6, r = 0.68 \quad (16)$$

$$VEL = 2.0 VEFD + 4.1, r = 0.70 \quad (17)$$

Galvin's (1963) and Longuet-Higgins' (1970) equations are both semiempirical; their derivations are based on the assumption that the longshore current is caused by the breaking of the obliquely incident wave. Both equations predict current velocities higher than those observed at Debidue Island. The empirical equation of Fox and Davis (1972) predicts current velocities which are generally too low by a factor of $\frac{1}{2}$.

To test for the relative importance of the independent variables in explaining the variance in the dependent one, a stepwise regression analysis was used. The test was performed both for the pooled annual process data and for each seasonal data set. Results are summarized in Table 22.

Table 22. Percent of the variance in VEL.¹

Variable	Annual	1975		1976	
		June	Sept.	Jan.	Mar.
WINDL	70	81	63	57	69
VGAL	1	0	0	2	2
VELH	2	0	1	2	4
VEFD	4	0	7	1	6

¹Explained by each of four independent variables entered successively in a stepwise regression analysis.

For all data sets, the longshore component of the wind velocity, WINDL, proved to be the independent variable explaining most of the observed variance in current velocity, VEL. The multiple correlation coefficient (r^2), for VEL versus WINDL ranged from 0.81 for the June 1975 data set to 0.57 for the January 1976 data. Expectedly, data

noise was at a maximum in January and minimum in June because of the different weather conditions under which the field observers had to operate. It is quite significant to note that for the data set which was expected to be the most reliable (June 1975), WINDL alone explained 81 percent of the variance. For this data set, the inclusion of breaker parameters combined into the predictive equations of Galvin (1963), Longuet-Higgins (1970), and Fox and Davis (1972), does not improve the multiple correlation coefficient. For the other data sets, these variables add a few percentages of explained variance.

Based on these considerations, the best predictive equation for longshore current velocities at Debidue Island appears to be that derived from the data set of 62 observations from June 1975. This equation is:

$$VEL = 4.36 \times WINDL + 12.9 \quad (18)$$

In both equations (14) and (18), VEL is measured in centimeters per second and WINDL in miles per hour. For a longshore wind velocity of 10 miles per hour, equation (18) predicts a current velocity of 56.5 centimeters per second; whereas, equation (14) predicts 40.6 centimeters per second, a difference of 39 percent. For wind velocities above 30 miles per hour, the difference between the two predicted current velocities becomes less than 30 percent.

Using a standard multiple regression to test for the amount of variance explained by VGAL, VELH, and VEFD, if they are entered as the first independent variable in three separate calculations, VGAL can explain 32 percent of the variance, VELH, 46 percent, and VEFD, 49 percent for the annual data set.

d. Discussion. A series of regression equations can be developed depending on which variables or combinations of variables are included. Table 23 summarizes the two types of equations derived in this study; the first (eq. 19) is the regression equation derived by treating each measured environmental parameter as an independent variable; the three subsequent equations (eqs. 20, 21, and 22) are derived by combining the pertinent breaker parameters as suggested in Galvin's (1963), Longuet-Higgins' (1970), and Fox and Davis' (1972) predictive formulas. Breaker parameters not accounted for in the predictive formulas are included as independent variables. The amount of variance in VEL explained by each parameter combination is indicated.

Based on a similar analysis, Harrison (1968) derived a regression equation for longshore current velocity at Virginia Beach, Virginia. However, simultaneous wind measurements were not obtained in his study, and the question of wind stress or breaking wave dominance in current generation was left unexplained. Based on earlier studies by Sonu, McCloy, and McArthur (1967), at Nags Head, North Carolina, Harrison discounted the importance of wind stress. The results at Debidue Island

Table 23. Regression equations for longshore current velocity.¹

Eq. No.	Equation	r ²
19	VEL = 2.78 WINDL + 44.2 WAVL + 0.12HGT - 0.85 PER + 5.94	0.722
20	VEL = 2.73 WINDL + 0.69 VEFD + 4.72	0.726
21	VEL = 2.83 WINDL + 0.13 VELH - 0.94 PER + 13.28	0.719
22	VEL = 2.91 WINDL + 0.06 VGAL + 0.12HGT - 1.15	0.714

¹All measured environmental parameters were included in the analysis.
r² is the total proportion of variance explained.

clearly demonstrate that wind stress can be a most significant factor in nearshore current generation. The statistical approach, unfortunately, does not explain the actual mechanism of energy transfer from the wind to the current system. All current measurements were obtained by surface floats. Further research is needed to test the three-dimensional structure of this flow field and to evaluate various genetic mechanisms.

V. SEASONAL MORPHOLOGIC CHANGE

1. Introduction.

Mapping of the intertidal morphology at North Inlet during the quarterly field studies (June 1975 to May 1976), low aerial overflights, and profiling of the channels and inlet-associated beaches on a monthly basis provided the data base for the evaluation of the seasonal changes in morphologic characteristics. Sedimentary subenvironments were established according to the strand-plain classification of Fisher and Brown (1972) and the tidal delta models of Hayes, et al. (1973). To facilitate a systematic evaluation of morphological development over the year, a detailed description of the observed change in each subenvironment was made.

Tidal deltas and associated characteristic beach features are formed as a result of the interruption to the continuous longshore sediment transport system by strong tidal currents flowing essentially perpendicular to the regional shoreline. Although additional research is needed on the origin and initial development of the tidal deltas once an inlet channel has been cut, the characteristics of morphology and sediment transport patterns on established tidal deltas are well documented. Hayes, et al. (1973) and Oertel (1972) documented how the typical ebb tidal delta morphology of mesotidal inlets results from the balance between a seaward transportation of sediment by the ebb flow and a landward transport due to wave swash and flood currents. Hayes (1975) considered the changes in inlet morphology with tidal range and developed models for microtidal, mesotidal, and macrotidal estuaries. Detailed studies of tidal delta bed-form distributions and migration patterns have been done at a number of mesotidal inlets (Oertel, 1972; Boothroyd and Hubbard, 1975; Hine, 1975; Hubbard, 1975; Finley, 1975, 1976). For some inlets, detailed sediment circulation patterns have been proposed (Masterson, Machemehl, and Cavaroc, 1973; Hine, 1975; FitzGerald,

Nummedal, and Kana, 1977). Past studies of inlet morphologic changes have been based on the assumption that MSL throughout the year is constant, which, as pointed out in Section III, 8, is not the case. Future inlet studies, involving interpretations of morphologic change, should consider the fact that sea level on the United States east coast varies some 40 centimeters during the year. The first objective of this analysis of North Inlet morphology was to document how this sea level fluctuation has affected particularly sensitive inlet sub-environments.

As pointed out by Escoffier (1940) and reiterated by Inman and Frautschy (1966) and others, a stable inlet appears to maintain a balance between the scouring actions of the tidal currents and the infilling by sediment supplied through the longshore drift system. If this concept is correct, it should be documented that the time histories of channel erosion and erosion on the inlet adjacent beaches are out of phase. The extensive morphological data collected at North Inlet over a year, involving a wide range of weather conditions, make such a test possible. This constituted the second objective of the morphologic analysis.

2. General Morphology and Sediment Distribution.

A depositional environment map (Fig. 22) was prepared from vertical aerial photos, data on historical changes in inlet morphology and field mapping. The terminology follows the strand-plain classification of Fisher and Brown (1972).

Abandoned flood tidal deltas and associated washover units were identified on the landward side of Debidue Creek. The inlet has migrated to the south, and Debidue Spit has been extended by about 2 kilometers since 1878 (Finley, 1976). The abandoned flood tidal deltas reflect short-term stillstands in the southward migration of the inlet. The present inlet is backed by a flood tidal delta and washover berm at the mouth of Sixty Bass Creek and flanked by supratidal barrier beaches with small washover fans and intertidal and shallow subtidal bars and platforms forming a seaward continuum of North and Debidue Islands; i.e., the ebb tidal delta.

Sediment size and distribution at North Inlet are related to a number of factors that vary on a regional scale. The inlet is located at the southern end of an arcuate shoreline that extends approximately 100 kilometers from the North Carolina border to Winyah Bay. For most of these 100 kilometers, the present beach borders Pleistocene upland except in the immediate vicinity of North Inlet and Murrells Inlet, 35 kilometers farther south. The Holocene-Pleistocene boundary at North Inlet is about 5 kilometers inland. Littoral drift along the coast is derived from mid-Pleistocene beach deposits. An average size of 2.48 phi (0.175 millimeter) was determined for these sediments (Brown, 1975). The arcuate strand is broken by few tidal inlets. No major rivers exist within this coastal segment. The

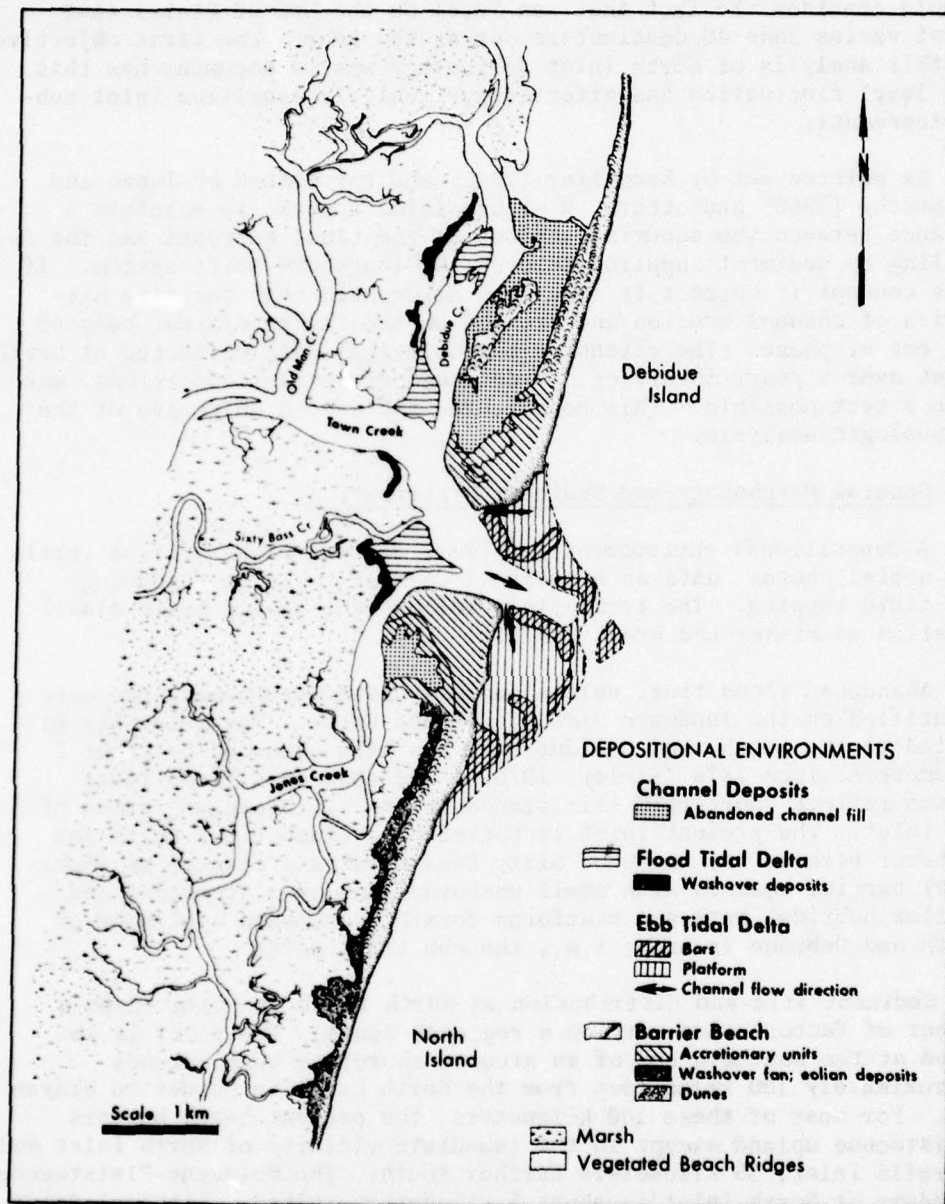


Figure 22. Major depositional environments at North Inlet.

nearest river sources are located south of North Inlet. Winyah Bay, an estuary for the Sampit, Pee Dee, Black, and Waccamaw Rivers, is connected to the sea approximately 15 kilometers to the south. About 15 kilometers farther south is the Santee River delta. Sand-size material reaching North Inlet from these sources is minimal; however, suspended fine-grained organic and inorganic sediments may reach the inlet (Finley, 1976). The presence of coarser sediment south of North Inlet (average size 2.01 phi or 0.248 millimeter) indicates a higher percentage of fluvially derived sand (Brown, 1975).

The sediment sampling program at North Inlet was designed to evaluate seasonal variations in sediment size. Locations of sediment sampling stations 1 to 21 are shown in Figure 23, with respect to the channel bathymetric profiles in Figure 8. Most sample stations were the same as those used by Finley (1976). The beach sediments were obtained midway between MSL and mean high water after removing the surface layer of coarse shell fragments and taking a 2-centimeter-deep sample immediately below. Channel bed samples were obtained with a Van Veen grab sampler. Standard sieving techniques were applied in the laboratory. Size parameters were calculated, using Folk's (1968) statistics. The percentage of shell hash coarser than 2 millimeters in each sample was recorded. The sample means and standard deviations (see Table 24) refer to the sand-sized fraction (particles less than 2 millimeters).

No significant seasonal variation in grain size was found at any environment sampled. However, there is a distinct difference between beach and channel sands. Beach sands have a total sample mean of 2.375 phi (0.19 millimeter); whereas, channel sands have a mean of 1.214 phi (0.43 millimeter), a difference of more than 1 phi unit. More than 90 percent of the beach samples were well sorted or very well sorted ($S = 0.50$ phi) in contrast to moderate to poor sorting ($S = 0.71$ to 2 phi) for more than 85 percent of the channel samples. Shell fragments or coarse shell hash was very diagnostic of the channel sands, ranging from 0.1 to 80 percent of the total sample weight. This type of variation is illustrated by the samples collected at station 13 (Table 24), where a large amount of shell hash is deposited in the thalweg of the main ebb channel. If this area was sampled continuously over a short period of time, a large variation in the amount and size of shell fragments would be found because of changes in current strength over the tidal cycle. Sediment characteristics at stations 17 and 19 (Fig. 23) are not properly defined by the statistics in Table 24 as these locations are at outcrops of firm, cohesive lagoonal muds. At these thalweg locations, gray mud was often brought up with the anchor.

3. Morphologic Response Characteristics.

a. Introduction. Four individual subenvironments at North Inlet were subjected to detailed morphologic mapping on a seasonal basis: inlet channels, flood and ebb tidal deltas, and barrier island beaches.

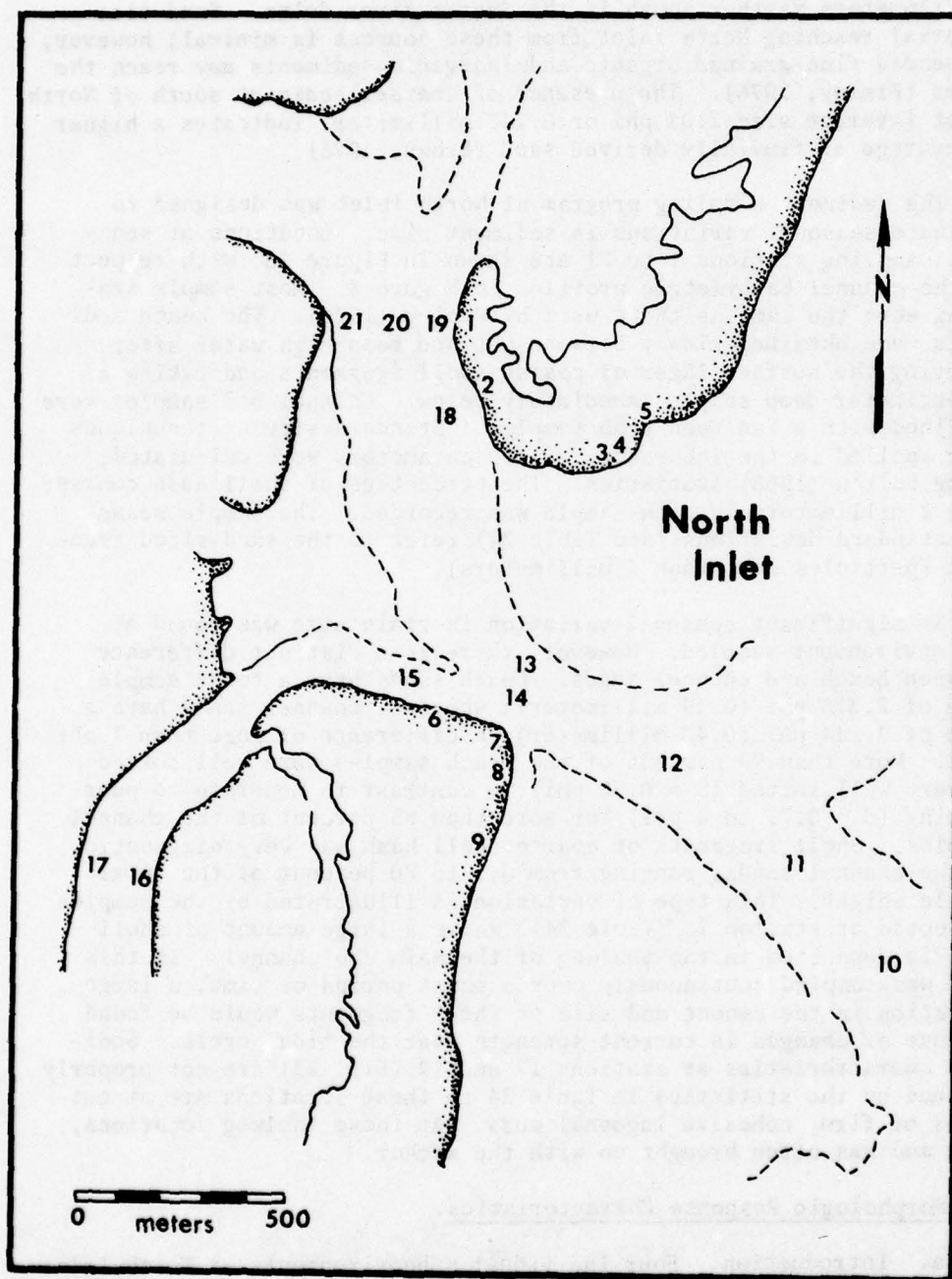


Figure 23. Location of sediment sample sites. Compare to Figure 8 for bathymetric profiles.

Table 24. Quarterly sediment data (expressed in phi units)

Station	Location	June 1975			Oct. 1975			Jan. 1976			Mar. 1976			Total Mean
		M1	S2		M	S		M	S		M	S		
1	TCN Beach	2.236	0.309		2.679	0.309		2.134	0.368		2.393	0.315		2.254
2	DBI FtD Beach	2.533	0.287		2.589	0.337		2.158	0.516		2.361	0.407		2.524
3	DBI TS	2.037	0.398		2.579	0.359		1.931	0.662		2.307	0.440		2.273
4	DBI 6	2.297	0.334		2.385	0.327		2.388	0.412		2.526	0.406		2.333
5	DBI 8	2.295	0.330		2.412	0.322		2.412	0.352		2.484	0.360		2.388
6	NI FtD Beach	2.464 (0.1) ³	0.302		2.620	0.256		2.067	0.397		2.099 (0.1)	0.477		2.308
7	NI TS Beach	2.434	0.295		2.545	0.321		2.528	0.505		2.610 (0.1)	0.338		2.440
8	NI 6	2.473	0.330		2.330	0.313		2.437	0.313		2.111	0.481		2.405
9	NI 8										2.540	0.451		2.445
10	MEC 3	1.026 (2.2)	0.830					1.106 (1.7)	0.749		0.952 (3.0)	0.544		1.028
11	MEC 2										0.338 (10.8)	0.879		0.338
12	MEC 1	0.334 (15.2)	0.863		0.982 (3.6)	0.715		1.700 (1.1)	0.628		1.283 (4.1)	1.029		1.074
13	ITN	0.523 (2.6)	0.826					0.199 (19.1)	1.035		0.848 (79.9)	1.572		0.523
14	ITS	2.023 (0.4)	0.744		1.064 (40.5)	1.106		0.734 (41.5)	0.958		0.336 (34.0)	1.068		1.039
15	NI FtD Channel	1.407 (1.6)	0.868		0.953 (5.0)	1.007		1.913	0.436		0.626 (18.1)	0.932		1.224
16	JCN 1	2.085 (0.1)	0.523		1.492 (1.6)	0.864		1.401 (2.2)	0.884		1.826 (0.1)	0.694		1.701
17	JCN 2				1.132 (1.8)	1.020								1.054
18	DBI FtD Channel	0.977 (1.2)	0.814		1.254 (15.2)	0.927		1.036 (6.5)	0.920		0.655 (13.8)	1.003		0.981
19	TCN 1				1.115 (17.8)	1.240								1.115
20	TCN 2	0.372 (12.3)	1.049		1.752 (1.5)	1.031		1.460 (0.6)	0.781		1.503 (0.4)	0.874		1.271
21	TCN 3	0.633 (0.7)	0.706		1.552 (3.5)	0.736		1.344 (5.6)	0.910		0.797 (4.4)	1.126		1.081

¹M = graphic mean.²S = graphic standard deviation (sorting).³Parentheses indicate percent shell hash.

NOTE:--See Figure 23 for location of stations.

To facilitate quantitative comparisons of morphology, a systematic, consistent, and accurate field surveying program was emphasized throughout the study.

b. Inlet Channels. Temporal fluctuations in cross-sectional areas for Town and Jones Creeks (summarized in Table 4) are graphically shown in Figure 24 to facilitate the discussion of annual changes. The cross-sectional change (in square meters) is plotted relative to the area of the June 1975 survey (chosen as 0). The mean cross-sectional area of Jones Creek is about half that of Town Creek. Consequently, the vertical scales in Figure 24 are adjusted such that a given amount of deviation represents the same relative change in the two channel flow areas.

Both channels underwent an 18-percent variation in flow area throughout the year, compared to 15 percent for the inlet throat section. The changes were roughly in-phase (Fig. 24). Channel cross sections were relatively stable through the summer, followed by a scouring trend in early fall. Deposition occurred in November and, apparently, continued through mid-winter to reach an alltime high in January. For the remainder of the winter and the spring, two cycles of erosion and deposition occurred, one from January to March, the other from March to May. Both creeks appear to respond to similar external events, and both have a clear seasonal pattern of channel fill and scour. An exact analysis of flow area changes of the inlet throat is impossible due to insufficient data, but inspection of the data indicates a seasonal behavior similar to that of the main creeks.

c. Flood Tidal Delta. Both the abandoned flood tidal deltas and the active one are similar in that each formed at the junction of tidal creeks, and washover deposits exist on their landward sides. The active flood tidal delta is formed at the junction of Jones and Town Creeks. The triangular planform geometry (Fig. 25) differs somewhat from the typically lobate flood tidal delta geometry described for New England (Hayes, 1975; Boothroyd and Hubbard, 1975; Hine, 1975) and the Outer Banks of North Carolina (Nummedal, et al., 1977). The typical flood tidal delta is generally located midchannel and is open to ebb process modification along its flank. As such, the complete symmetrical flood delta can only form in a large embayment or a wide channel (Barwis and Hubbard, 1976). Of the five components which characterize the typical flood tidal delta (i.e., flood channel, flood ramp, ebb spit, spillover lobe, and ebb shield), the ebb shield is the least developed at North Inlet (Fig. 25). This is due to the welding of the landward margin of the delta to the marsh.

Between July 1972 and March 1973, a 42-meter westward migration of the landward edge of the delta was measured (Finley, 1976). Continued monitoring the following 2 years indicated little farther migration, and only minor changes along the northern delta margin.

During the 1975-76 field season, the flood tidal delta changes were monitored by monthly fathometer transects (Fig. 8, profile D-D'), quarterly oblique aerial photography, and a theodolite and rod survey (Fig. 26).

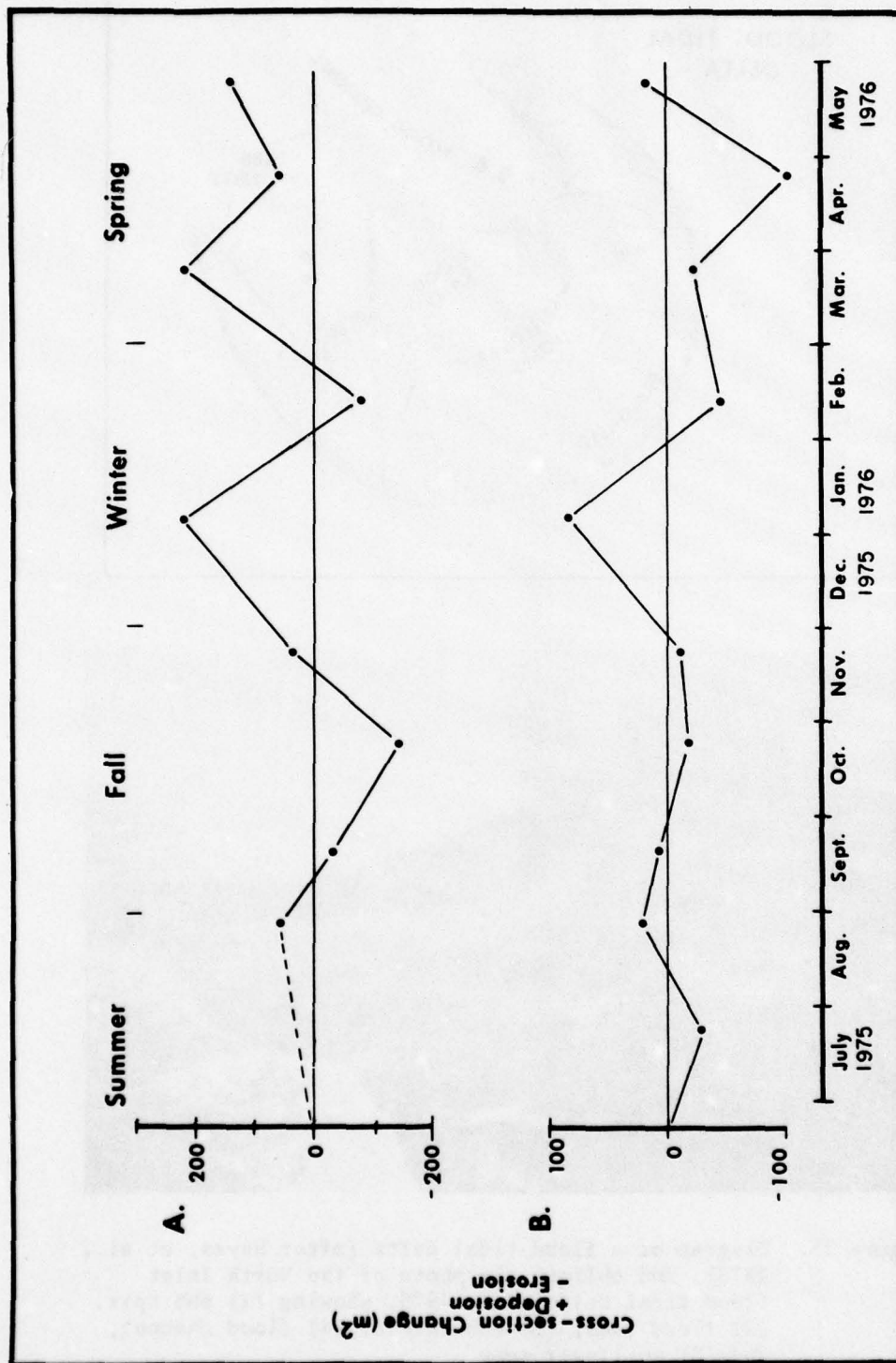


Figure 24. Changes in cross-sectional areas of Town Creek (A) and Jones Creek (B). Positive and negative slopes indicate deposition and erosion, respectively. (See Fig. 8 for section locations, profiles B-B' and C-C'.)

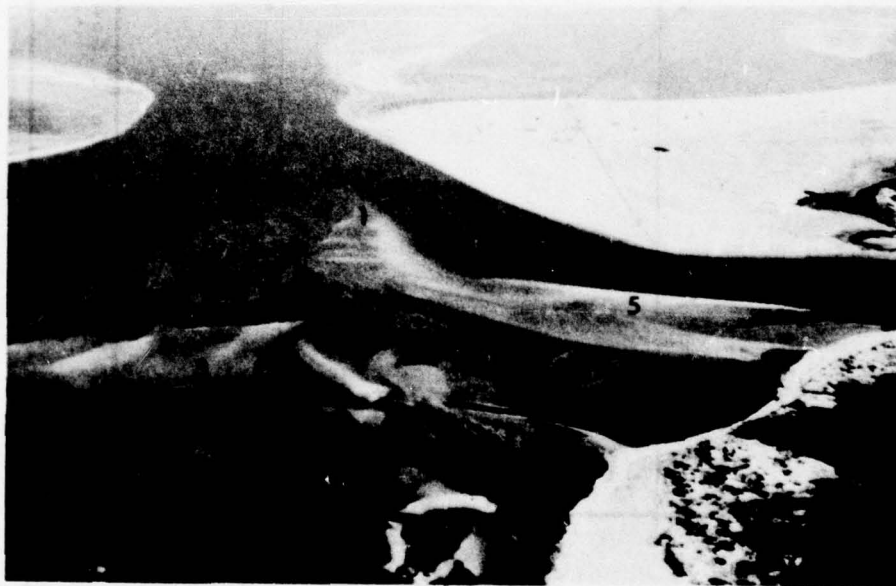
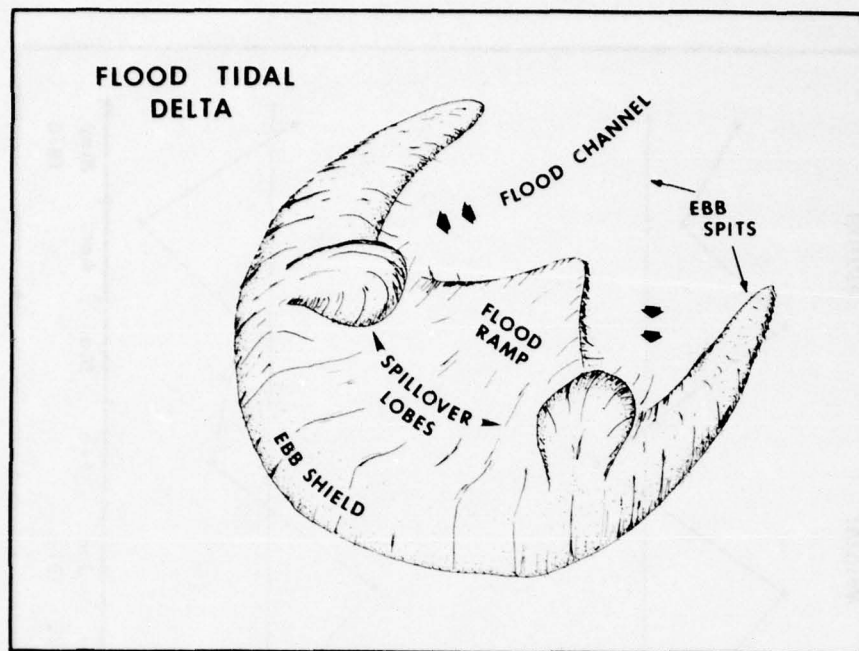


Figure 25. Diagram of a flood tidal delta (after Hayes, et al., 1973), and oblique air photo of the North Inlet flood tidal delta, June 1975, showing (1) ebb spit, (2) flood ramp, (3) ebb shield, (4) flood channel, and (5) spillover lobe.

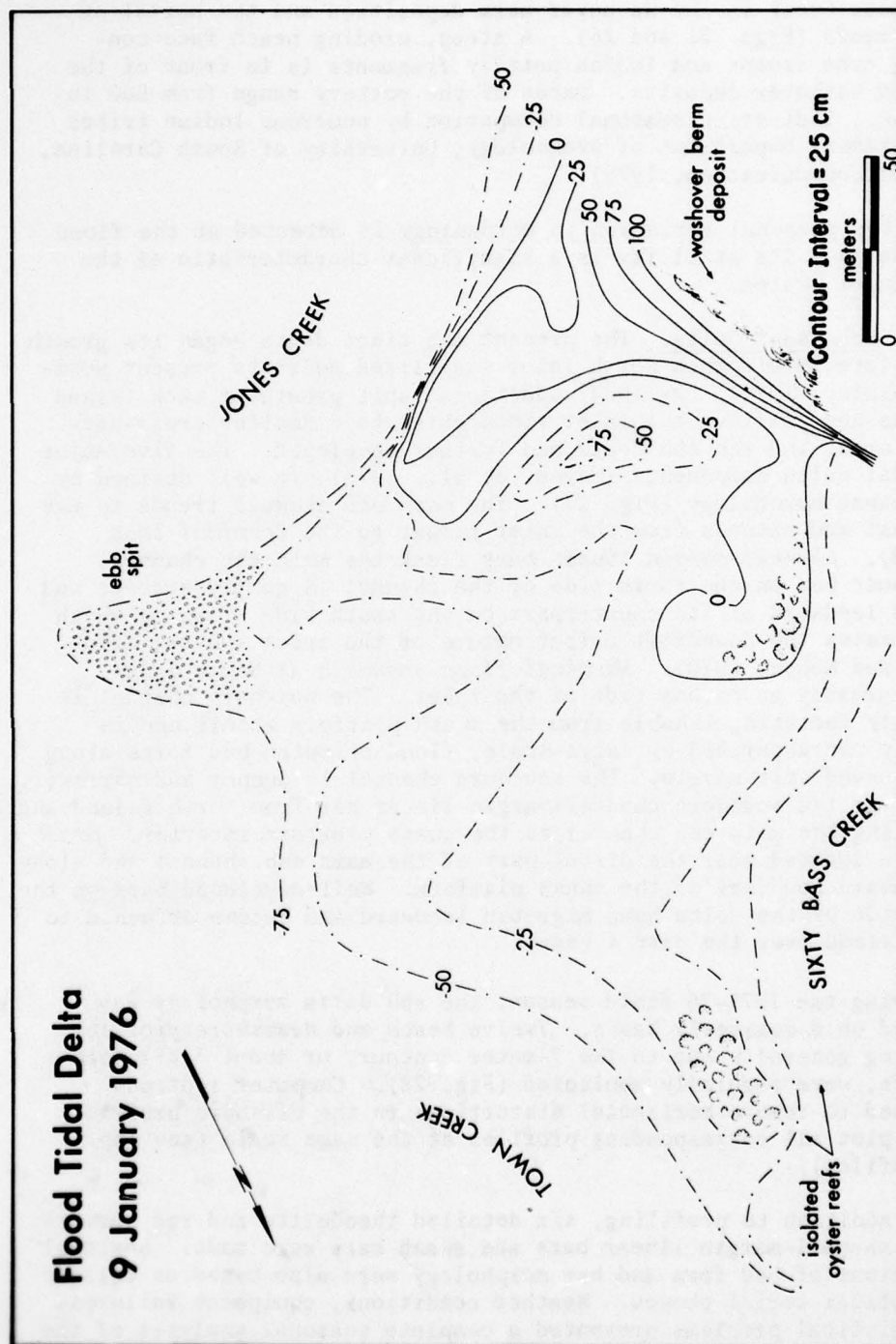


Figure 26. Topographic map of the North Inlet flood tidal delta

The bathymetry recorded by profile track D-D' shows the wide, shallow delta platform, or flood ramp, between the two creeks. Evidence of westward migration into the salt-marsh environment and into Sixty Bass Creek is the washover berm deposition and the burial of oyster reefs (Figs. 25 and 26). A steep, eroding beach face containing tree stumps and Indian pottery fragments is in front of the southern washover deposits. Dates of the pottery range from 500 to 1500 B.P., indicating seasonal occupation by numerous Indian tribes (R.J. Widmer, Department of Archeology, University of South Carolina, personal communication, 1976).

Little seasonal variation in morphology is detected at the flood tidal delta. Its stability is a significant characteristic of the North Inlet system.

d. Ebb Tidal Delta. The present ebb tidal delta began its growth in the late 1930's when North Inlet stabilized near its present position (Finley, 1976). By 1964, additional spit growth at each island terminus had confined the inlet tidal prism to a smaller cross-sectional area, and the ebb delta had further developed. The five major ebb tidal delta components (Hayes, et al., 1973) are well defined by the present morphology (Fig. 27). The *main ebb channel* trends to the southeast and extends from the inlet throat to the *terminal lobe* (Fig. 8). *Channel-margin linear bars* flank the main ebb channel. The linear bar on the north side of the channel is gently arcuate and located landward of its counterpart on the south side (Fig. 8) which demonstrates the downdrift offset nature of the inlet (Hayes, Goldsmith, and Hobbs, 1970). *Marginal flood channels* at North Inlet differ greatly on either side of the inlet. The northern channel is generally indistinguishable from the swash platform itself and is commonly characterized by large-scale, flood-oriented bed forms along the recurved spit margin. The southern channel is deeper and narrower, separating the southern channel-margin linear bar from North Island and connecting the main ebb channel to the swash platform interior. *Swash bars* are located near the distal part of the main ebb channel and along the seaward boundary of the swash platform. Well-developed bars on the south side of the delta have migrated landward and become attached to North Island over the past 4 years.

During the 1975-76 field season, the ebb delta morphology was recorded on a quarterly basis. Twelve beach and nearshore profiles, extending generally out to the 7-meter contour, or about 3 kilometers offshore, were regularly monitored (Fig. 28). Computer routines were used to remove horizontal distortions in the offshore profiles and to plot all corresponding profiles at the same scale (see App. I for profiles).

In addition to profiling, six detailed theodolite and rod surveys of the channel-margin linear bars and swash bars were made. Seasonal evaluations of bed form and bar morphology were also based on oblique and vertical aerial photos. Weather conditions, equipment failures, and logistical problems prevented a complete seasonal analysis of the

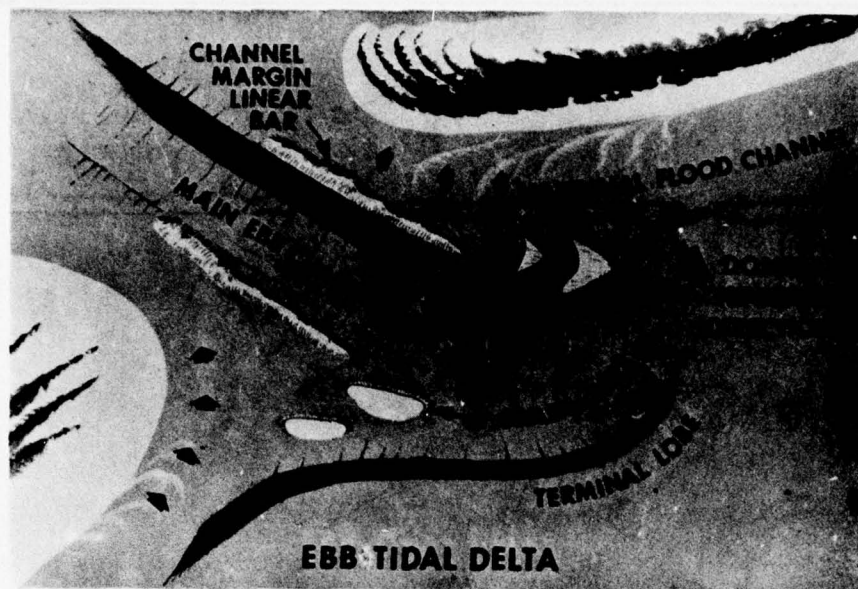


Figure 27. Diagram of an ebb tidal delta (after Hayes, et al., 1973), and oblique air photo of the North Inlet tidal delta, January 1976, showing (1) main ebb channel, (2) channel-margin linear bars, (3) marginal flood channels, (4) swash bars, and (5) terminal lobe.

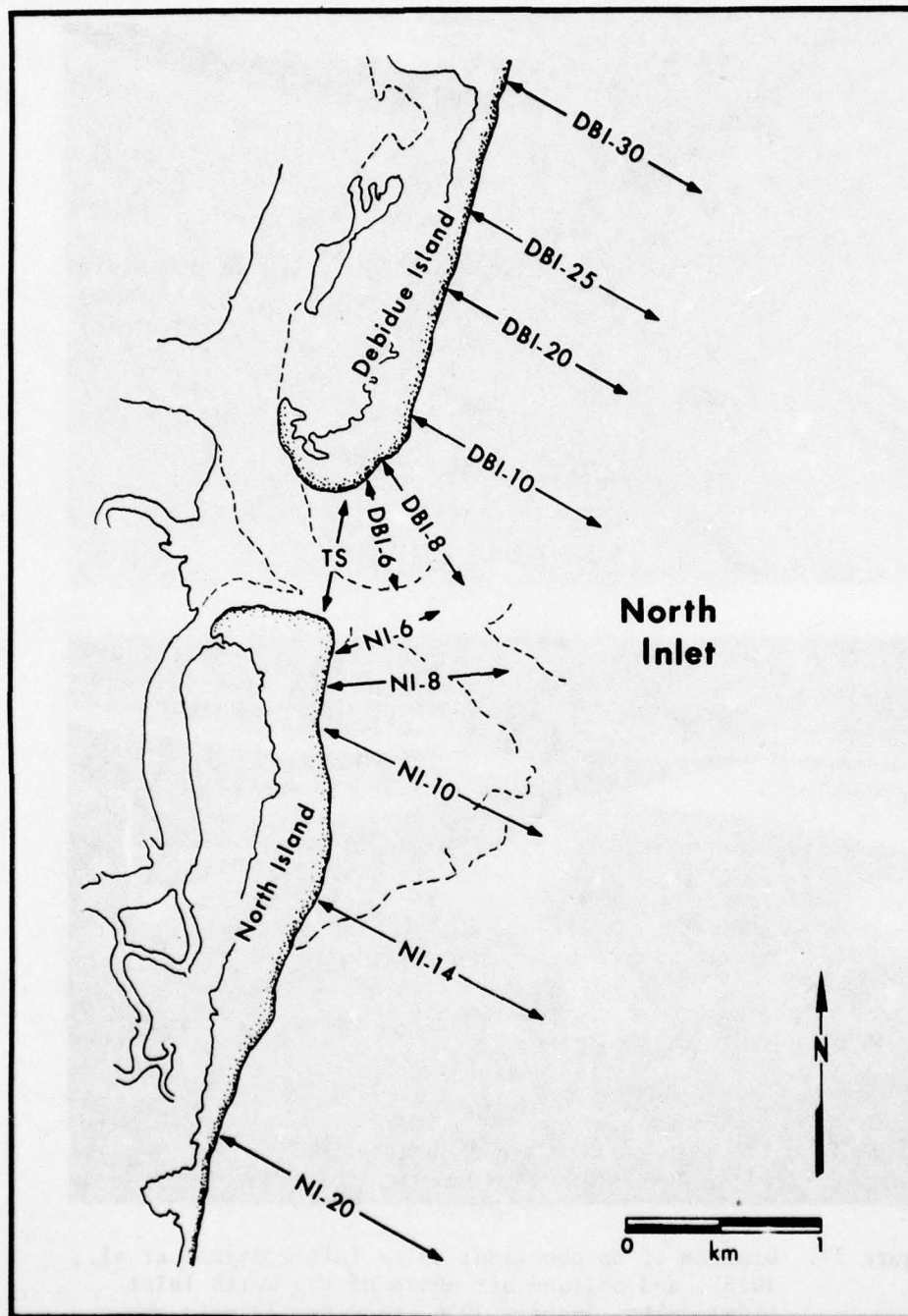


Figure 28. Beach and offshore profile locations.

entire ebb tidal delta. Sea conditions were often not favorable for the monitoring of offshore profiles, especially those located over the shoals. A detailed bathymetric map of the North Inlet ebb tidal delta was constructed from the January 1976 profile data (Fig. 29). The evaluation of the last 12 years of ebb delta development is based on the comparison between this 1976 map and that constructed from the 1964 U.S. Coast and Geodetic Survey, Chart No. 8838 (Fig. 29). The general bathymetric development of the ebb delta since 1964 provides the background for the short-term morphological change detected in the 1975-76 field season.

The following four major bathymetric changes have occurred since 1964:

(a) The 7-meter contour northeast of the inlet has moved landward along with the 5- and 6-meter contours. This represents steepening of the northeast delta margin relative to the 1964 configuration.

(b) In the southeast map area, a topographic high outlined by the 4-meter contour in 1976 occupies an area which was gently sloping seaward from 5 to 6 meters in 1964.

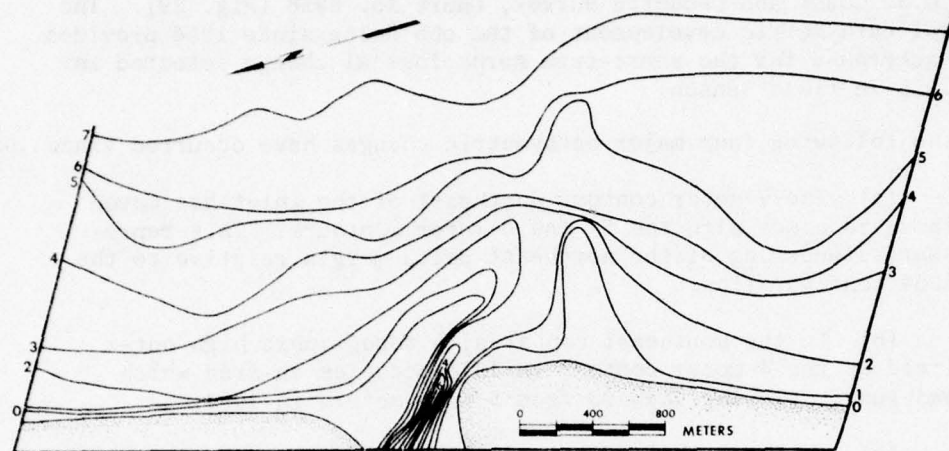
(c) At least three distinctive shoals (less than 2 meters deep) have developed adjacent to the main ebb channel, one at the terminal lobe and one at either side of the main channel on the swash platform.

(d) The main ebb channel has deepened and is now oriented straight toward the southeast.

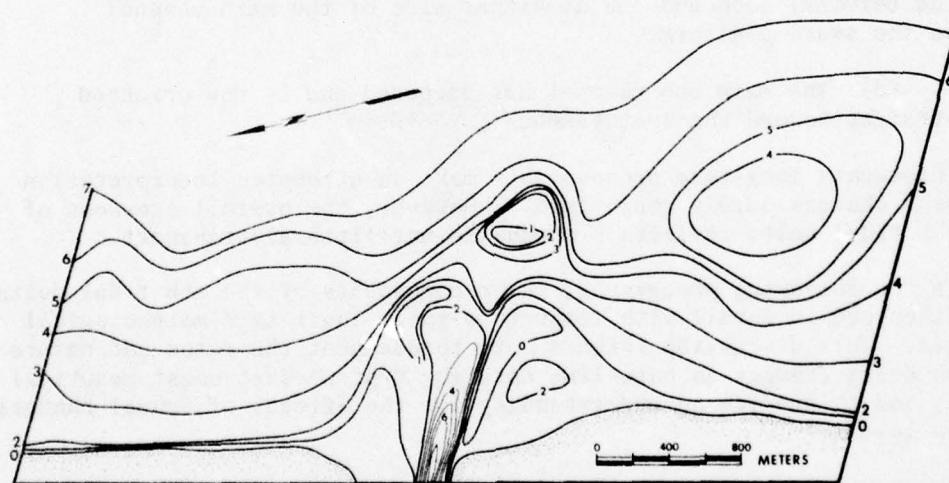
Inadequate long-term process data make an attempted interpretation of these changes purely conjectural. However, the overall skewness of the ebb tidal delta reflects a southward net littoral transport.

In the following paragraphs, three components of the ebb tidal delta are discussed in detail with respect to their short-term morphological changes. This discussion intends both to document the rates and nature of ebb delta changes as base-line data for typical east coast mesotidal inlets and to provide an understanding for the effects of annual changes in sea level.

The *northern channel-margin linear bar* has undergone growth toward the southwest, changes in surface elevation, and a widening of the spillover channel on its seaward side since observations began. Between July and September 1974, a 70-centimeter increase in bar margin elevation occurred, but by March 1975, there was a 70-centimeter decrease in elevation (Finley, 1976). This erosion was probably related to a northeast storm in September 1974. About a year later, between January and March 1976, a period of accretion occurred. Figure 30 is a photo and contour map of the bar morphology in January 1976, showing the broad and shallow slope toward the swash platform, the steep channel margin, and ridgelike



1964



1976

Contour Interval = -1 M

Figure 29. North Inlet nearshore bathymetry in 1964 and 1976.

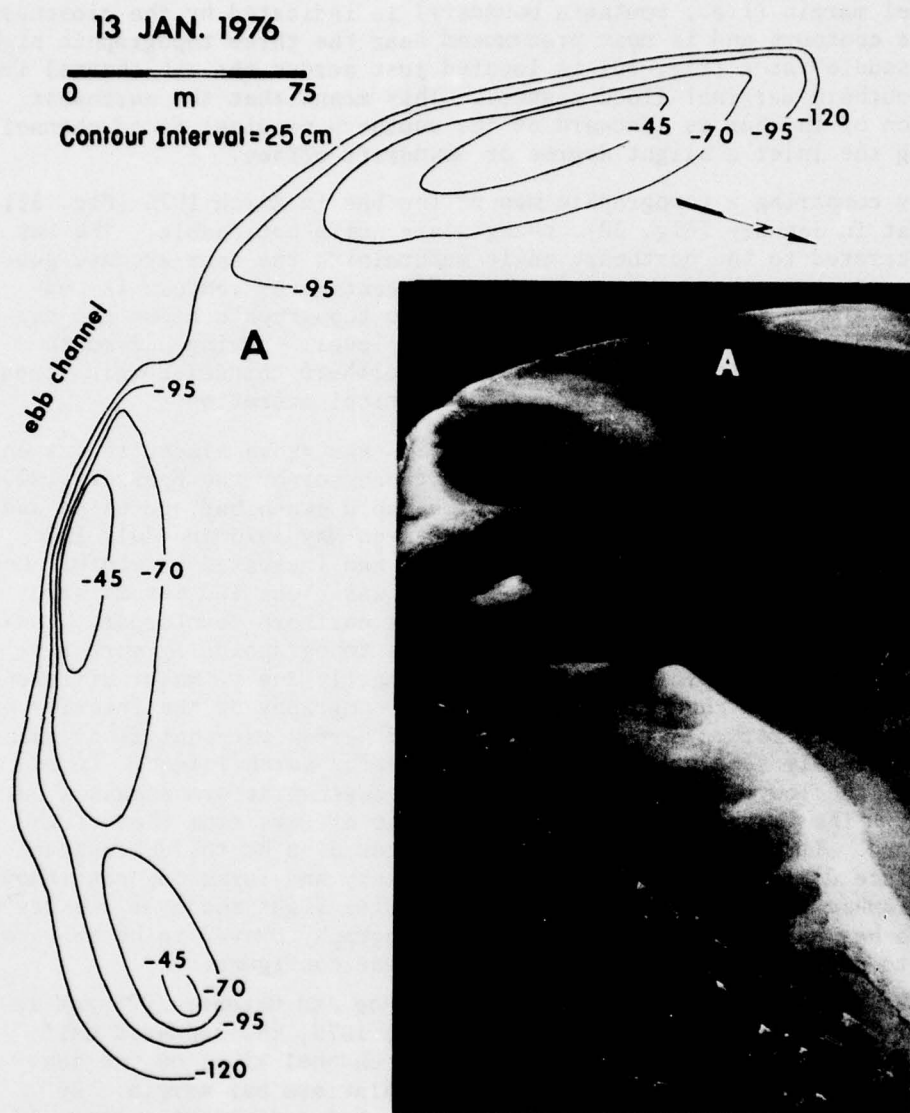


Figure 30. Topographic map and oblique air photo of the northern channel-margin linear bar at North Inlet, 13 January 1976. (Datum is MSL.)

topographic highs. Although the swash platform is not clearly represented by either the contour map or the photo, the open contours north of the bar imply a broad and shallow topography. The 120-centimeter contour defines well the overall arcuate geometry. The steepness of the channel margin (i.e., southern boundary) is indicated by the closeness of the contours and is most pronounced near the three topographic highs. The "saddle" at A (Fig. 30) is located just across the ebb channel from the southern marginal flood channel. This means that the northwest section of the bar is landward of the southern marginal flood channel, giving the inlet a slight degree of downdrift offset.

By comparing a topographic map of the bar in March 1976 (Fig. 31) to that in January (Fig. 30), changes are quite noticeable. The bar has accreted to the northeast while maintaining the same arcuate geometry and steep channel margin. The -70-centimeter contour is continuous around the entire bar, and the two topographic highs are separated only at the -45-centimeter contour level. During a 2-month period, in the late winter of 1976, the northern channel-margin linear bar underwent significant lateral and vertical accretion.

The *southern channel-margin linear bar* has grown almost in its entirety since the obliteration of its predecessor by the February 1973 northeast storm. Following that storm, rapid swash bar accretion and coalescence formed a long linear bar between May 1973 and July 1974 (Finley, 1976). By January 1975, the bar had increased in width. One year later (March 1976, Fig. 32), the bar was about 100 meters wide and had a length comparable to that of its northern counterpart. Unlike the northern bar, the southern bar is topographically more isolated on the swash platform. This is primarily due to major differences in marginal flood channel morphology and topography on the interior of the swash platform. A relatively deep and narrow marginal flood channel completely separates the southern bar from North Island. In addition, the low elevation of the adjacent swash platform enhances bar relief. The morphology of the southern bar differs from that of the northern. It has a gently sloping perimeter even at the ebb channel side, a surface dominated by plane beds or ripples, and forms one continuous topographic high. Because of the distinctive light shade of the dry sands of the bar crest at low tide, aerial photography proved to be an excellent tool to document the seasonal changes in bar configuration.

Oblique air photos were obtained in June and October 1975 and in January and March 1976 (Fig. 33). In June 1975, the landward half of the bar had a distinct crest along the channel side; on the seaward half, the crest formed at the swash platform bar margin. By October, only the landward half of the bar had a distinct crest. In January 1976, a continuous crest was present along the swash platform bar margin. In March, the crest had again moved over to the channel side of the bar at its landward part. Although the March morphology is not nearly as distinct as that of the previous June, it has the same general distribution of features. A distinct "cyclic" change in bar crest location characterized the annual changes of the morphology of the southern channel-margin linear bar.

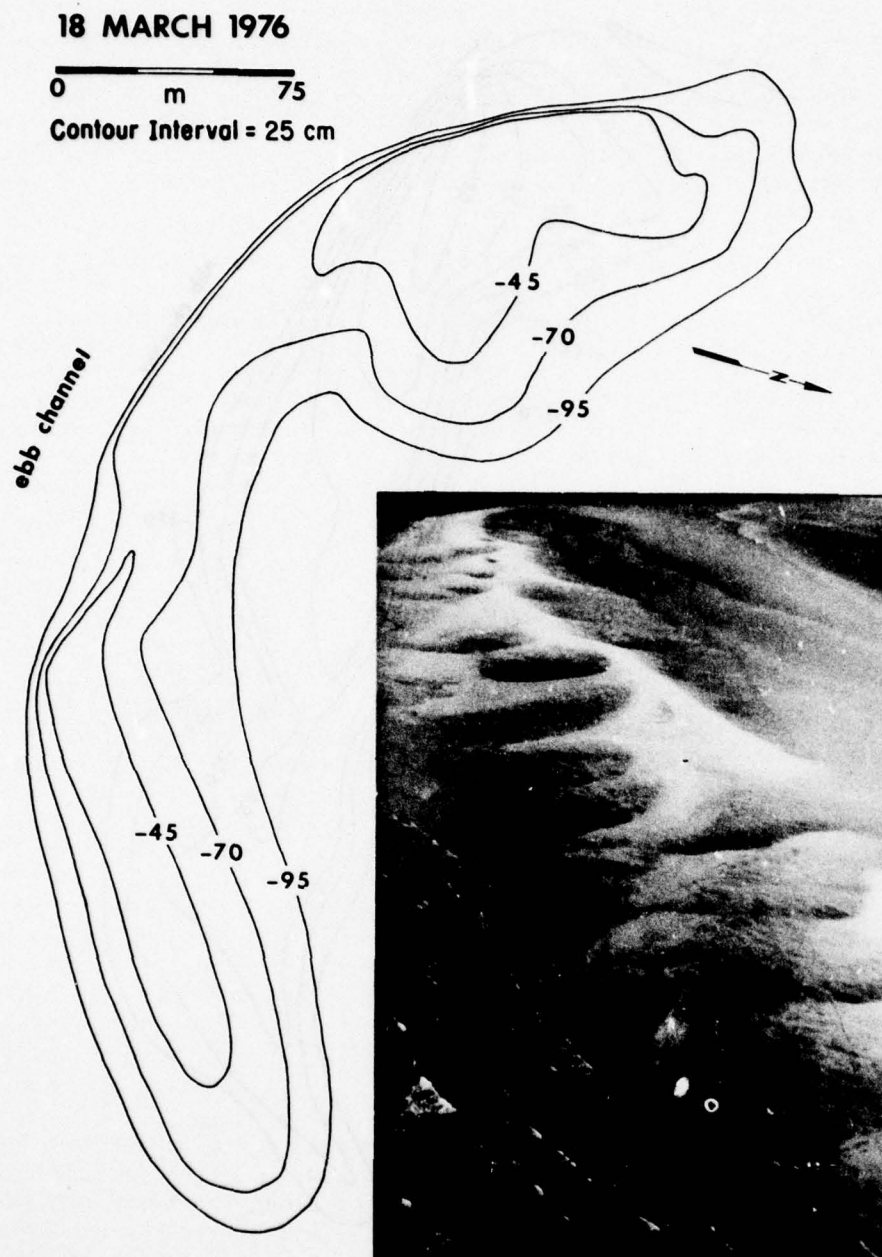


Figure 31. Topographic map and oblique air photo of the northern channel-margin linear bar at North Inlet, 18 March 1976. (Datum is MSL.)

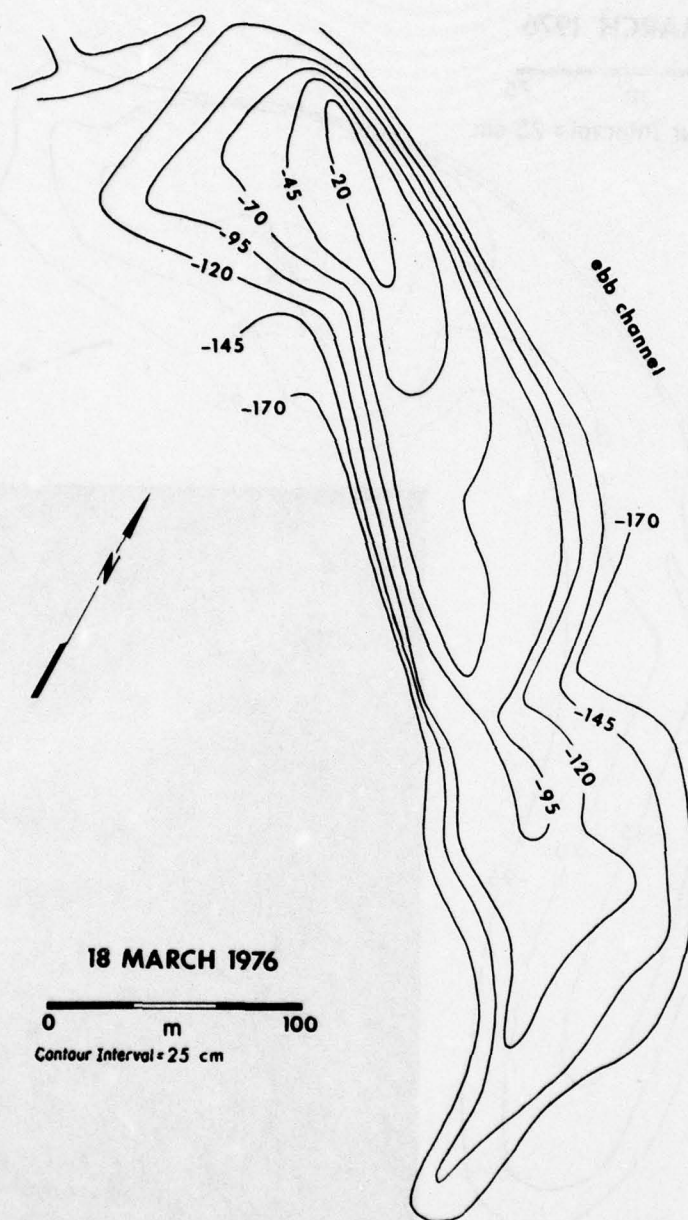


Figure 32. Topographic map of the southern channel-margin linear bar, 18 March 1976.



A. 11 June 1975



B. 4 October 1975



C. 12 January 1976



D. 21 March 1976

Figure 33. Seasonal changes in configuration of the southern channel-margin linear bar. Light areas are topographic highs.

The dominant processes controlling the morphologies of the northern and southern channel-margin linear bars were identified. Strong tidal currents and relatively weak wave action are responsible for the overall morphology and the large bed forms of the northern channel-margin linear bar. The southern, seaward offset channel-margin bar, on the contrary, is dominated by wave swash causing a smooth compacted surface with few bed forms, similar to a beach face.

The *North Island swash bar complex* has been monitored since 1974 when it was observed that the entire bar was moving landward and that its point of beach-face attachment was moving to the north. The large landward-pointed swash bar had been divided, and both parts were migrating landward by September 1974 (Fig. 34,A). In March 1975, changes in the southern part were apparent (Fig. 34,B). Vertical air photos taken in April 1974 and March 1975 were used to determine that the southern part had moved 417 meters or an average of 36.3 meters per month (Finley, 1976). The northernmost pointed feature moved much slower. During the 1975-76 field year, the following detailed changes were observed:

(a) In October 1975, an advanced stage of bar attachment to the beach face was evidenced by the presence of two large intertidal ridges only partly separated from the beach face by a narrow and short runnel (Fig. 35, point B). Immediately north of the point of bar attachment (Fig. 35, point A), the beach face is very steep.

(b) By January 1976, the runnel had been closed off by accretion (Fig. 36, point C) forming an isolated saltwater pond (point B). Rapid deposition had caused significant accretion and seaward displacement of the berm crest off point B. The second intertidal ridge (Fig. 37, point D) had become morphologically more distinct and undergone significant vertical accretion and landward migration as illustrated by the topographic maps in Figures 35 and 36.

(c) By March 1976 (Fig. 37), the topography of the site of the swash bar attachment had become similar to that in October 1975, the primary difference being that all features were displaced about 50 meters seaward of their October position. During this 6-month period, one episode of ridge welding had been carried to completion.

e. Beaches. The Debidue Island shore in the vicinity of the inlet consists of a recurved spit experiencing seaward progradation and landward retreat in response to migrating ridge-and-runnel systems. As these systems migrate shoreward, sediment is moved alongshore in discrete packages, and some is delivered to the inlet throat by currents in the marginal flood channel. This process has been well documented also at other inlets (Farrell, 1969; Kumar and Sanders, 1974). Surveys in June 1972 and July 1974 demonstrated landward retreat of the



A. September 1974



B. March 1975

Figure 34. Configuration of swash bar complex off North Island.

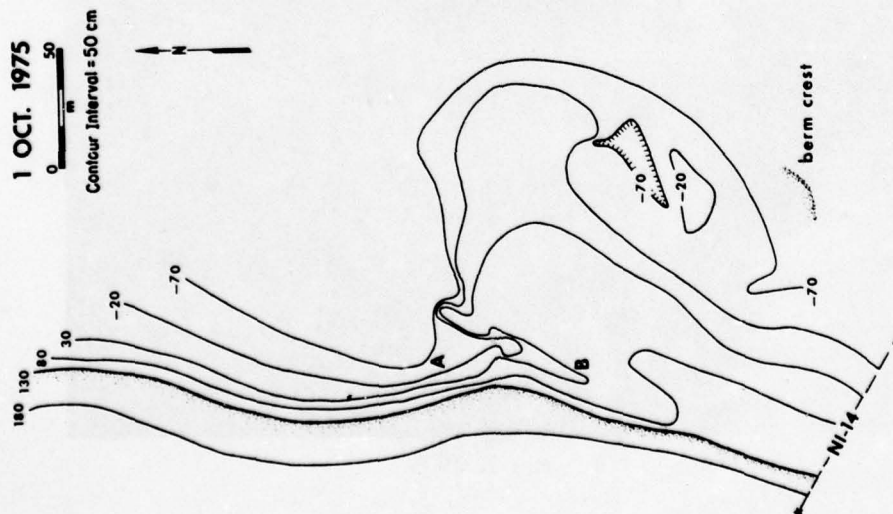


Figure 35. Oblique air photo and topographic map of swash bar complex off North Island, 1 October 1975. Late stage swash bar migration and beach attachment are characterized by steep beach face (A) and confined runnel (B). (Datum is MSL.)

AD-A063 986

SOUTH CAROLINA UNIV COLUMBIA COASTAL RESEARCH DIV
HYDRAULICS AND DYNAMICS OF NORTH INLET, SOUTH CAROLINA, 1975-76--ETC(U)
SEP 78 D NUMMEDAL, S M HUMPHRIES

F/G 8/3

DACW72-72-C-0032

UNCLASSIFIED

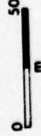
WES-GITI-16

NL

2 OF 3
ADA
063986



17 JAN. 1976



Contour Interval = 5.0 cm

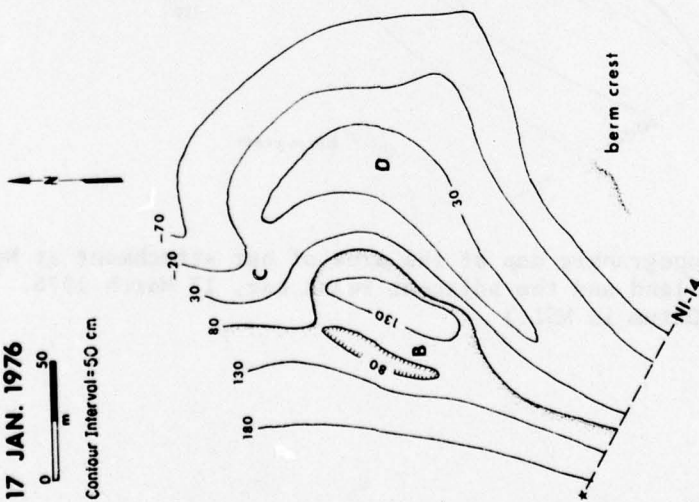


Figure 36. Oblique air photo and topographic map illustrating beach progradation at the point of bar attachment, 17 January 1976. Bar attachment is characterized by beach accretion at C, ponding at B, and the onshore migration of a second ridge at D. (Datum is MSL.)

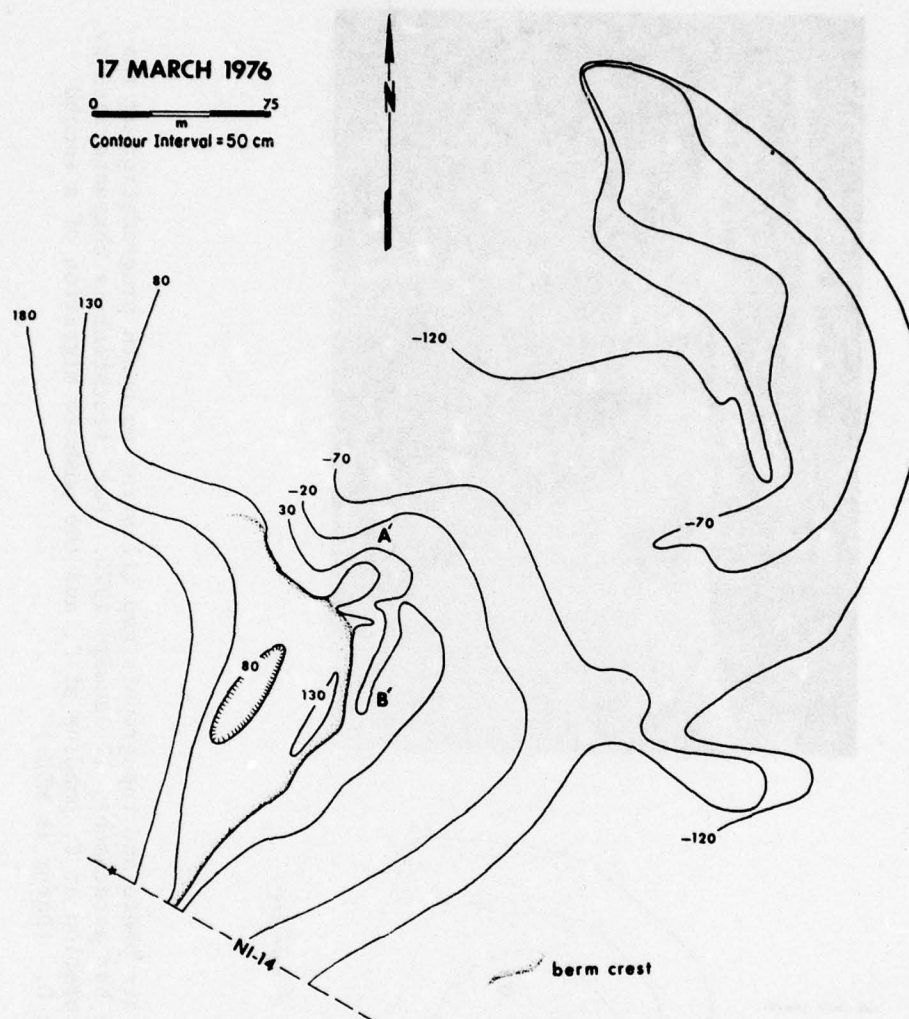


Figure 37. Topographic map of the area of bar attachment at North Island and the adjacent swash bar, 17 March 1976. (Datum is MSL.)

Debidue beach (Finley, 1976). During these 2 years, the base of the beach face had retreated about 60 meters along a 300-meter section. Although the volume of sand was not computed, a large amount of deposition probably occurred on the inlet shoals. More recently, between September 1975 and March 1976, a cycle of deposition and erosion was documented at the recurved spit. The area monitored in this recent survey was located to the west of the 1972-74 site at the landward extension of the inlet throat profile (Fig. 28, DBI-TS). The following is a discussion of variations in spit morphology at this site, referencing the air photos and topographic maps in Figures 38, 39, and 40:

(a) Figure 38, 28 September 1975: Along the western margin of the mapped spit area, a steep, irregular topography is illustrated by the spacing and curvature of the contours. A reentrant at A defines the western boundary of the lobate part of the spit. A small, partly enclosed runnel at B drained toward A. A well-defined berm crest existed only west of B. Broad washovers characterized the rest of the survey area and continued east of profile DBI-TS. Seaward of this broad overwash was a relatively steep beach face becoming gradually more gentle toward A.

(b) Figure 39, 11 January 1976: The survey area had undergone extensive deposition since September. Beach accretion had displaced the berm crest toward the inlet. A uniform beach-face topography characterized the arcuate margin of the spit. The reentrant at A had changed into a narrow runnel outlet draining a pond at B.

(c) Figure 40, 19 March 1976: Beach-face erosion characterized the entire survey area. About 25 meters of shoreline recession had occurred since January, leaving a uniformly sloping beach face from A around the recurve to profile DBI-TS. The berm crest along this margin had receded to within 10 meters of area B. Minor shoreline modification had occurred west of area A. Little evidence of the outlet channel between A and B was preserved, and B was a dry, isolated depression.

The two ocean-facing beaches adjacent to North Inlet have very similar intertidal morphology and quite similar response characteristics on a month-by-month basis. Beach morphology was monitored throughout the year at nine profile locations at Debidue and North Islands (Fig. 28). The individual profiles are included in Appendix I.

From the profiles, the amounts of erosion and deposition between consecutive surveys were computed (expressed as cubic meters of sand added or removed per running meter of beach). These results were plotted as a function of time using the beach profile for June 1975 as a reference datum (Fig. 41).

Profile DBI-25, which is the one farthest away from the inlet, is quite stable. Most other profiles recorded significant amounts

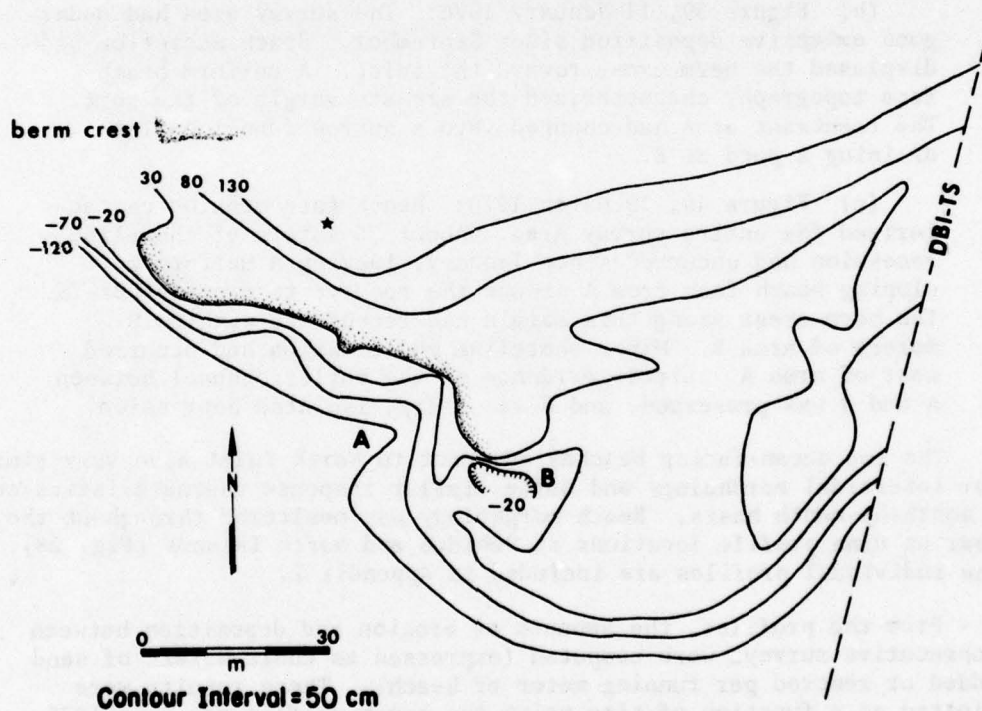


Figure 38. Oblique air photo and topographic map of Debidue Island recurved spit, 28 September 1975. Note shoreline reentrant at A and enclosed pond at B. (Datum is MSL.)

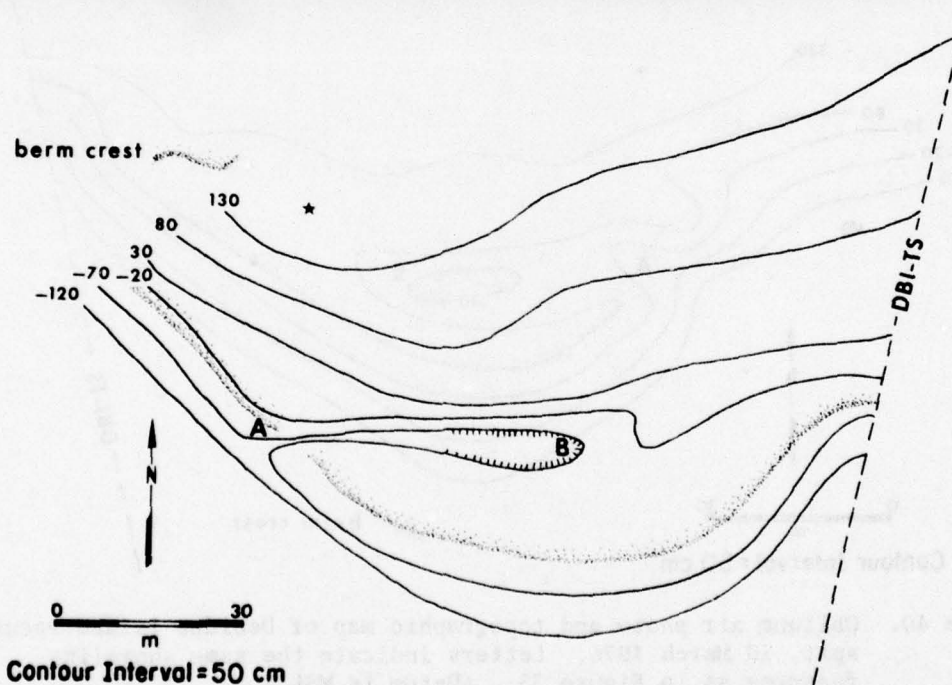


Figure 39. Oblique air photo and topographic map of Debidue Island recurved spit, 11 January 1976. Letters indicate the same shoreline features as in Figure 38. (Datum is MSL.)

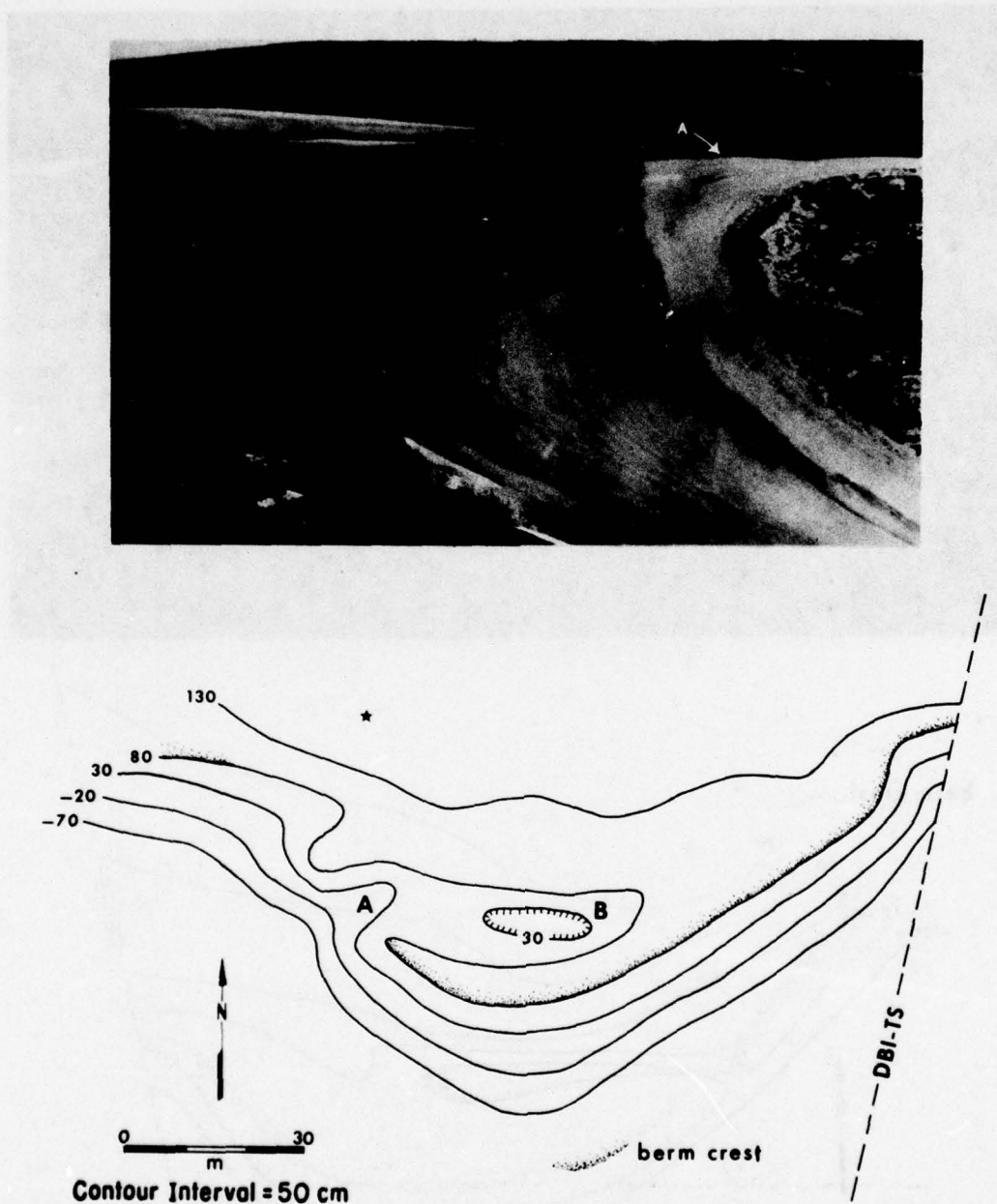


Figure 40. Oblique air photo and topographic map of Debidue Island recurved spit, 19 March 1976. Letters indicate the same shoreline features as in Figure 35. (Datum is MSL.)

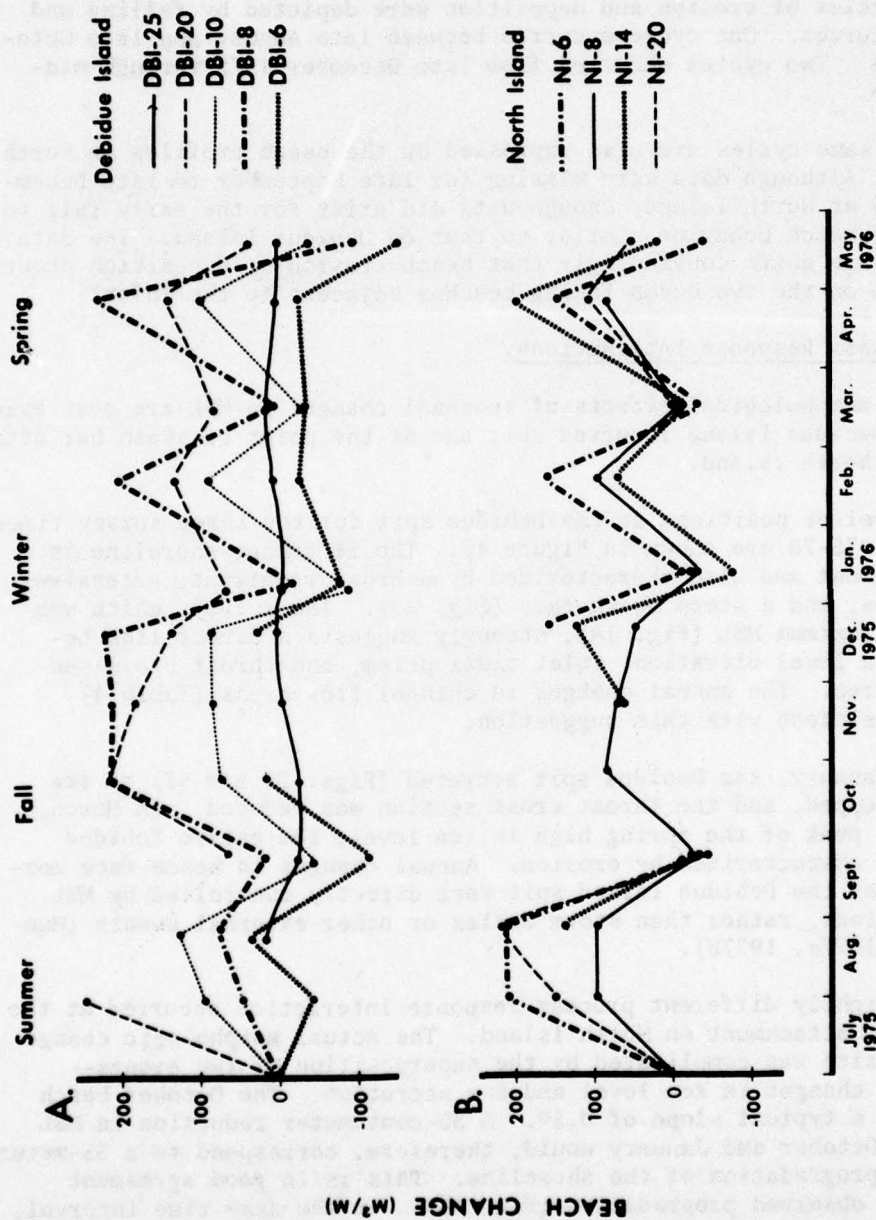


Figure 41. Trends of beach erosion and deposition on Debidue and North Islands from June 1975 to May 1976. Faint dotted lines indicate missing data. Positive values designate deposition; negative values indicate erosion.

of erosion and deposition during the year. Comparisons of the fluctuations in all profiles on Debidue Island show that variations are in phase.

From October to December 1975, relative stability was reflected by nearly all DBI profiles. For the remainder of the year, three distinct cycles of erosion and deposition were depicted by falling and rising curves. One cycle occurred between late August and late October 1975. Two cycles occurred from late December 1975 through mid-May 1976.

The same cycles are also expressed by the beach profiles on North Island. Although data were missing for late September to late December 1975 at North Island, enough data did exist for the early fall to indicate beach behavior similar to that on Debidue Island. The data demonstrate quite convincingly that beach erosion or deposition occurs in phase on the two ocean-facing beaches adjacent to the inlet.

4. Process Response Interactions.

The morphological effects of seasonal changes in MSL are most evident at the Debidue Island recurved spit and at the point of swash bar attachment on North Island.

Shoreline positions at the Debidue spit for the three survey times during 1975-76 are shown in Figure 42. The September shoreline is landwardmost and also characterized by a broad reentrant, extensive washovers, and a steep beach face (Fig. 38). The survey, which was made at maximum MSL (Fig. 18), strongly suggests a direct link between sea level elevation, inlet tidal prism, and throat cross-sectional area. The annual changes in channel flow areas (Table 4) were consistent with this suggestion.

By January, the Debidue spit accreted (Figs. 39 and 42) as sea level dropped, and the throat cross section was reduced. In March, near the peak of the spring high in sea level, the entire Debidue spit was characterized by erosion. Annual changes in beach-face morphology of the Debidue Island spit were directly controlled by MSL fluctuations, rather than storm cycles or other external events (Humphries, 1977a, 1977b).

A slightly different process response interaction occurred at the swash bar attachment on North Island. The actual morphologic change at this site was complicated by the superposition of two events--seasonal changes in sea level and bar accretion. The October beach face had a typical slope of 0.50. A 30-centimeter reduction in MSL between October and January would, therefore, correspond to a 35-meter seaward progradation of the shoreline. This is in good agreement with the observed progradation (Fig. 43). In the same time interval, significant vertical accretion occurred on the beach (Figs. 35 and 36)--a result of the landward migration of the swash bar complex.

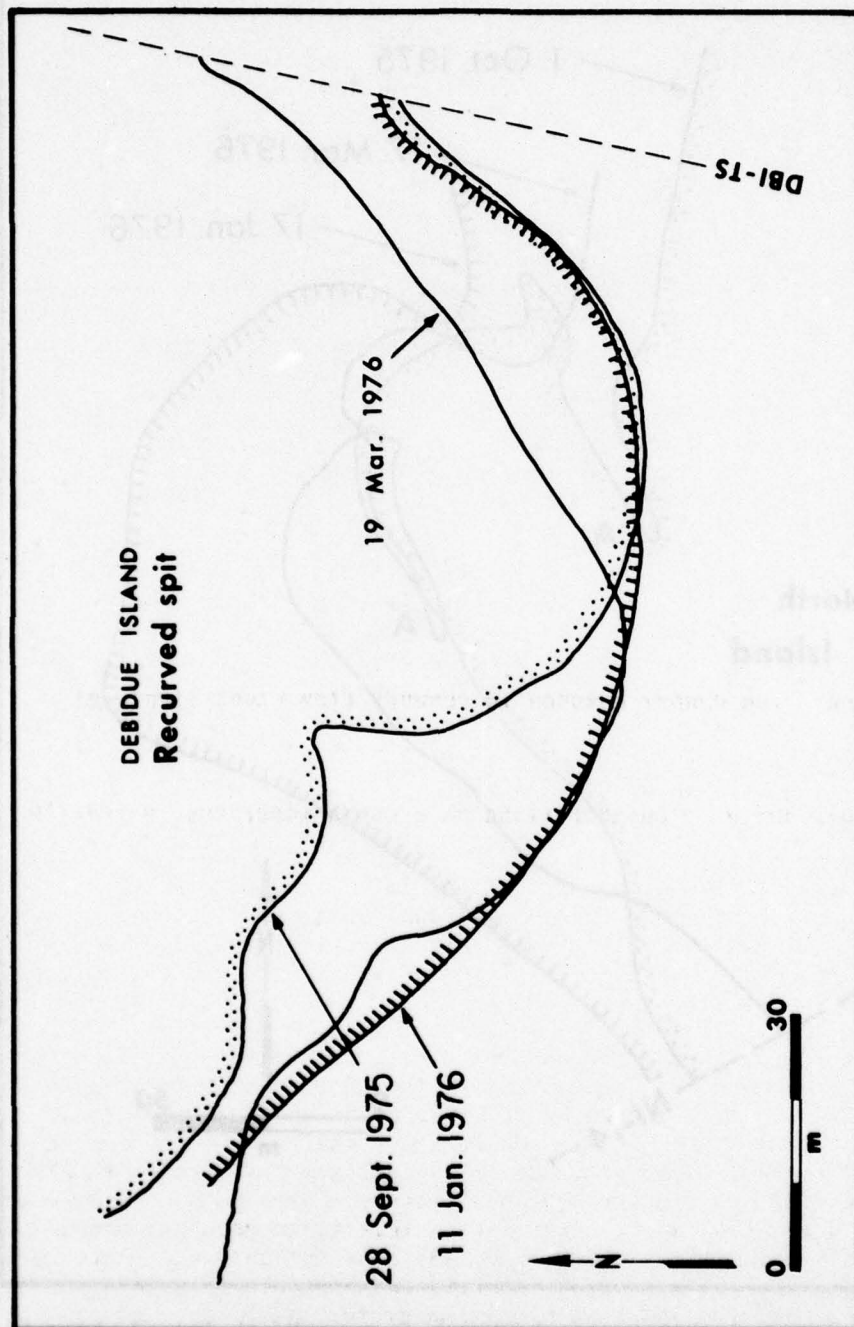


Figure 42. Seasonal change in position of the shoreline at the Debidue Island recurved spit (based on Figs. 21, 22, and 23). Monthly local MLW outlines the shoreline.

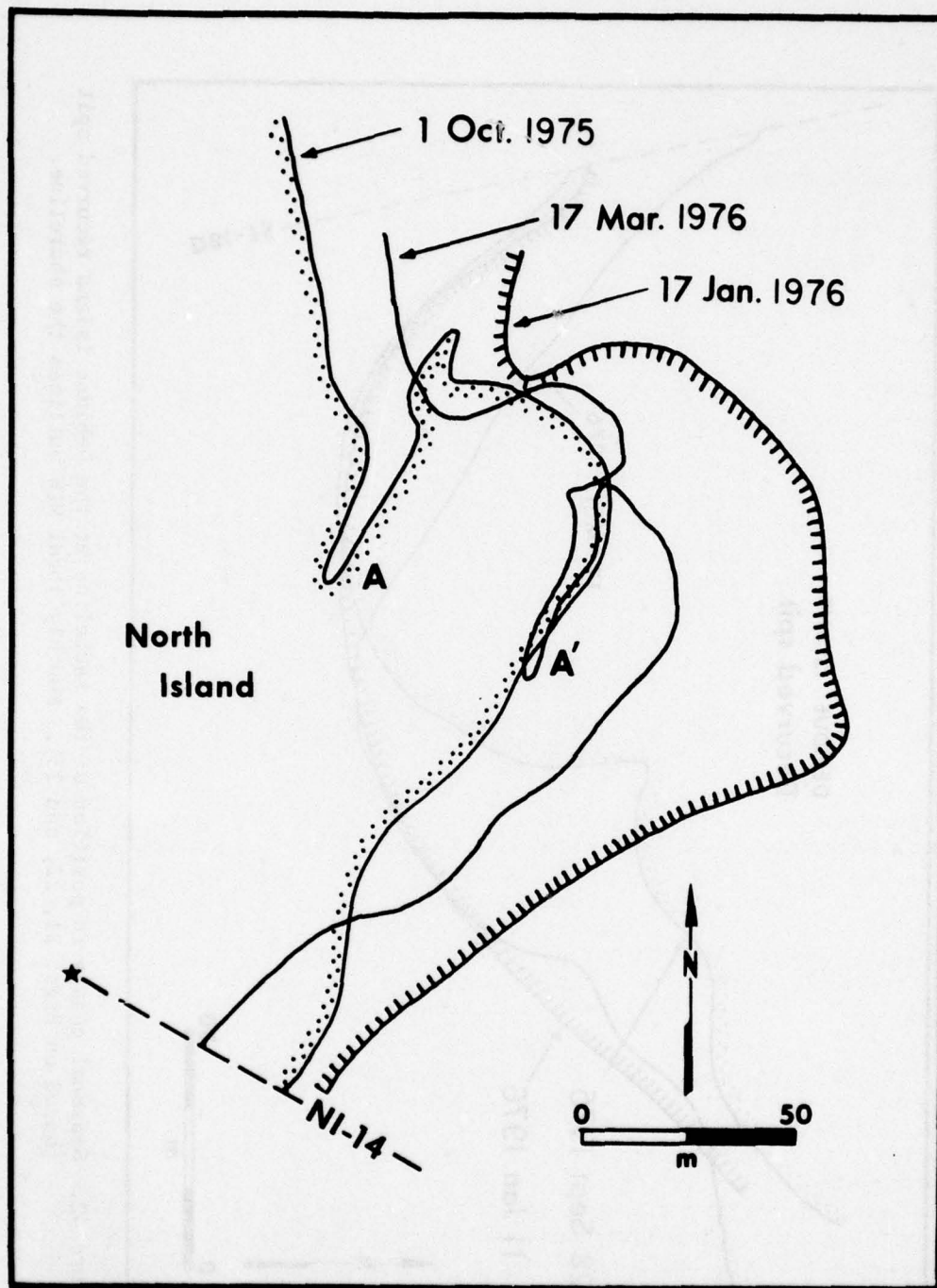


Figure 43. Seasonal changes of the beach face on North Island where bar attachment dominated nearshore morphology.

This steepened the beach face to about 1.2° such that the spring sea level rise was accompanied by, typically, only 20 meters of shore-line transgression (Fig. 43).

Perhaps the most significant response interaction was that which existed between inlet channel cross sections and the volume of the adjacent beaches. Figure 44 shows the 'average' pattern of erosion and deposition on the Debidue and North Island beaches (adapted from Fig. 41). Both beach volumes and channel cross sections fluctuated about a stable annual mean. The phase relationship between the fluctuations throughout the year was quite striking. Beach accretion (positive slope) corresponded rather consistently with channel erosion; beach erosion (negative slope) corresponded to channel infilling. (An exception to this trend appeared to exist for the fall months. However, the North Island data for this time period were rather sparse, and interpretations of phase relationships based on the fall trends could be misleading.) Although more closely spaced data points would have been desirable, the data strongly suggest an out-of-phase relationship between beach erosion and channel erosion. The data provided only speculation concerning the mechanisms of sediment exchange which tie inlet channel to beach morphology. A feasible chain of events is the following: Storm-induced beach erosion would be associated with the delivery of an increased sediment load to the inlet channels, thus reducing their flow areas. Subsequent decrease in wave action, in turn, would permit channel scour. This model is consistent with Escoffier's (1940) and Inman and Frautschy's (1960) inlet stability concepts.

VI. SUMMARY AND CONCLUSIONS

Both this report and Finley (1976) analyzed the basic hydraulic, morphologic, and littoral process characteristics of North Inlet, South Carolina. Data were obtained over a 2-year period from July 1974 to May 1976. Water level records from one ocean and two bay tide gages, combined with tidal channel hydrographic data, littoral process measurements, intertidal morphological maps, bathymetric profiles, and aerial photographic records (all obtained on a quarterly basis) provided the main data base for the study. Channel cross sections were monitored on a monthly basis.

North Inlet is located on the northern South Carolina coast, in a transition zone between the wave-dominated coast of North Carolina and the distinctly tide-dominated coast of southern South Carolina and Georgia. Although the mean ocean tidal range is only 167 centimeters, North Inlet is classified as mesotidal because tidal current-generated features, conforming to those of existing mesotidal inlet models, dominate the system. The low annual wave energy and the infrequent storm passage across the South Carolina coast appear to permit the development of a typical mesotidal morphology for a tidal range slightly below the proposed worldwide mesotidal interval.

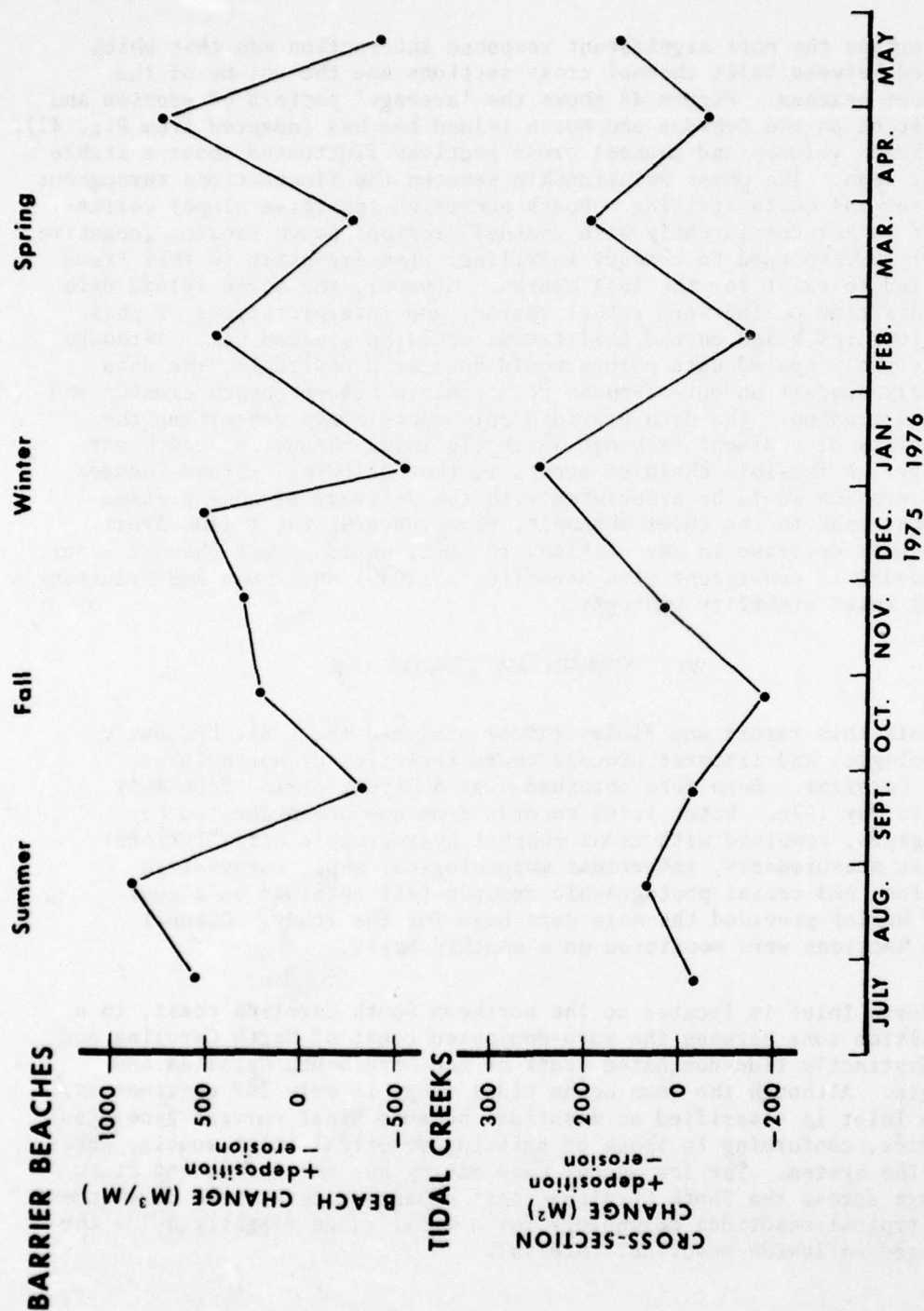


Figure 44. Average trends in beach erosion and deposition at Debidue and North Islands (top) and channel cross sections (bottom) (derived from data in Figs. 24 and 41).

Within the same seasons of the 2 consecutive years of observation, the weather and littoral process parameters were quite comparable. This justifies one of the implicit assumptions in the study methodology: the sampling of process parameters on a quarterly basis over 2 years will provide a representative measure of the total annual variability of the North Inlet environment.

North Inlet is hydraulically ebb dominated. For the throat section, the peak ebb velocity exceeded the peak flood by a factor of 1.22. Also, the ebb duration was shorter than the flood duration by an average of 26 minutes. A model is proposed, which explains the ebb dominance as a result of the different efficiency of water exchange between the ocean and the bay at high and low tide. Considering continuity, the existence of a much larger water surface area in the bay at high tide rather than at low tide results in a longer lag at high water than at low water, an average of 46 versus 33 minutes. This differential lag is consistent with the observed asymmetries in the duration and velocity of the flood and ebb.

Spectral analysis of the tide records further verify the model. Overtides, M_4 , M_6 , and M_8 components, are present in all the tide records. These are produced by propagation of the tidal wave in shallow water. However, their amplitudes are increased by one to two orders of magnitude as the tidal wave moved in through the inlet; this is due to the presence of nonlinear terms in the equations of motion for inlet flow. The development of an asymmetric bay tidal curve relative to the one in the ocean, is consistent with the amplification of the overtides.

Average surf zone conditions expressed in terms of breaker types, breaker heights, and longshore currents exhibited a consistent seasonal pattern from one year to the next. Mean breaker heights ranged from a low of 54 centimeters in March to a high of 70 centimeters in September. The longshore wave energy flux factor was computed from the littoral process measurements and used to estimate rates of longshore sediment transport. The gross transport was 800,000 cubic meters per year for both years of observation. The net transport for 1974-75 and 1975-76 was 87,000 and 390,000 cubic meters, respectively, both years to the south. This difference is also reflected in the annual resultant wind vectors derived from anemometer readings at Debidue Island during the quarterly field periods.

Literature reviews suggest that the role of wind stress in the generation of longshore currents is largely unknown. From the 250 complete data sets of littoral environmental observations for Debidue Island, stepwise regression analyses were performed to isolate the external variable that would explain the largest amount of variance in the observed longshore current velocities. In all regression analyses, the longshore component of the wind velocity was the parameter explaining most of the variance. Other littoral parameters, including

breaker angle and breaker height, used in previously developed theoretical or semiempirical longshore current velocity equations all explained far less of the observed variance. It appears that the longshore component of wind stress is at least as important as the momentum of the obliquely breaking wave in the generation of currents in the surf zone at Debidue Island, and probably in similar coastal environments.

Analysis of the tide gage records demonstrated a distinct pattern of seasonal variations in MSL. The measured bay variation was 34 centimeters, the inferred ocean variation about 45 centimeters. The annual high occurred in mid-fall, the low in January, and a secondary high occurred in mid-spring. A combination of steric effects, seasonal wind setups and, perhaps, river discharge, appears adequate to explain the observed sea level fluctuations.

Repetitive topographic mapping of the intertidal channel-margin linear bars, the Debidue Island recurved spit, and the swash bar complex welding on to North Island revealed a distinct seasonal pattern in the morphologic change. It is suggested that this morphologic pattern is, at least in part, a response to the seasonal changes in MSL. For example, the Debidue spit shoreline occupied its landwardmost position during the September 1975 survey. In January 1976, the spit shore had accreted several tens of meters. In March, it had retreated again. This suggests that the Debidue Spit eroded during periods of high sea level and consequent large tidal prism in North Inlet, and accreted during periods of low sea levels.

Existing concepts of inlet stability suggest that there is an exchange of sediment between the inlet channels and the adjacent beaches. Thus, during periods of high wave action, when the beaches will undergo erosion and retreat, sedimentation and shoaling should be evident in the tidal channels. During periods of fair weather, the beaches will accrete and the tidal creeks scour. Since MSL is not a constant, the effects of this sediment exchange pattern could be masked by changes due to water level fluctuations. Nevertheless, in the winter and spring of 1976, a clear out-of-phase relationship between beach erosion and channel scour was detected, in good agreement with the sediment exchange mechanism stated above.

LITERATURE CITED

- BARNIS, J.H., and HUBBARD, D.K., "The Relationship of Flood-Tidal Delta Morphology to the Configuration and Hydraulics of Tidal Inlet-Bay Systems," *Abstracts, Geological Society of America*, Northeast and Southeast Sections, 1976, pp. 128-129.
- BEHRENS, E.W., WATSON, R.L., and MASON, C., "Hydraulics and Dynamics of New Corpus Christi Pass, Texas: A Case History, 1972-73," GITI Report 8, U.S. Army, Corps of Engineers, Coastal Engineering Research Center, Fort Belvoir, Va., and U.S. Army Engineer Waterways Experiment Station, Vicksburg, Miss., Jan. 1977.
- BOON, J.D., III, "Sediment Transport Processes in a Salt Marsh Drainage System," Ph.D. Dissertation, College of William and Mary, Williamsburg, Va., 1973.
- BOOTHROYD, J.C., and HUBBARD, D.K., "Bed Form Development and Distribution Pattern, Parker and Essex Estuaries, Massachusetts," MP 1-74, U.S. Army, Corps of Engineers, Coastal Engineering Research Center, Fort Belvoir, Va., Feb. 1974.
- BOOTHROYD, J.C., and HUBBARD, D.K., "Genesis of Bedforms in Mesotidal Estuaries," *Estuarine Research*, Vol. II, Academic Press, New York, 1975, pp. 217-234.
- BROWN, E.I., "Inlets on Sandy Coasts," *Proceedings of the American Society of Civil Engineers*, Vol. 54, 1928, pp. 505-553.
- BROWN, P.J., "Coastal Morphology of South Carolina," M.S. Thesis, University of South Carolina, Columbia, S.C., 1975.
- BUDGEELL, W.P., "Tidal Propagation in Chesterfield Inlet, N.W.T.," Report Series No. 3, Canada Centre for Inland Waters, Burlington, Ontario, 1976.
- BYRNE, R.J., AND BOON, J.D., III, "Speculative Hypothesis on the Evolution of Barrier Island-Inlet-Lagoon Systems: II, A Case Study, Wachapreague, Virginia," *Abstracts, Geological Society of America*, Northeast and Southeast Sections, 1976, p. 144.
- BYRNE, R.J., BULLOCK, P., and TYLER, D.G., "Response Characteristics of a Tidal Inlet: A Case Study," *Estuarine Research*, Vol. II, Academic Press, New York, 1975, pp. 201-216.
- DAVIES, J.L., "A Morphogenetic Approach to World Shorelines," *Zeitschrift fur Geomorphologie*, Vol. 8, 1964, pp. 127-142.
- DAVIES, J.L., *Geographical Variation in Coastal Development*, Hafner, New York, 1973.

- DeALTERIS, J.T., and BYRNE, R.J., "The Recent History of Wachapreague Inlet, Virginia," *Estuarine Research*, Vol. II, Academic Press, New York, 1975, pp. 167-181.
- DEFANT, A., *Ebb and Flow*, The University of Michigan Press, Ann Arbor, Mich., 1958.
- ESCOFFIER, F.F., "The Stability of Tidal Inlets," *Shore and Beach*, Vol. 8, No. 4, 1940, pp. 114-115.
- FARRELL, S.C., "Growth Cycle of a Small Recurved Spit," Coastal Environments, N.E. Massachusetts and New Hampshire, Coastal Research Group, University of Massachusetts, Amherst, Mass., 1969, pp. 316-336.
- FINLEY, R.J., "Hydrodynamics and Tidal Deltas of North Inlet, South Carolina," *Estuarine Research*, Vol. II, Academic Press, New York, 1975, pp. 277-291.
- FINLEY, R.J., "Hydraulics and Dynamics of North Inlet, South Carolina, 1974-75," GITI Report 10, U.S. Army, Corps of Engineers, Coastal Engineering Research Center, Fort Belvoir, Va., and U.S. Army Engineer Waterways Experiment Station, Vicksburg, Miss., Sept. 1976.
- FINLEY, R.J., and HUMPHRIES, S.M., "Morphologic Development of North Inlet, South Carolina," Terrigenous Clastic Depositional Environments, 2d ed., 1976, Technical Report No. 11-CRD, University of South Carolina, Columbia, S.C., pp. II-172-II-184.
- FISHER, W.L., and BROWN, L.F., Jr., "Clastic Depositional Systems--A Genetic Approach to Facies Analysis," Bureau of Economic Geology, University of Texas, Austin, Tex., 1972.
- FITZGERALD, D.M., NUMMEDAL, D., and ATTAWAY, S., "Hydraulics and Morphology of Price Inlet, South Carolina," *Sedimentology* (manuscript in preparation) 1977.
- FITZGERALD, D.M., NUMMEDAL, D., and KANA, T.W., "Sand Circulation Pattern at Price Inlet, South Carolina," *Proceedings of the 15th Coastal Engineering Conference*, Vol. II, 1977, pp. 1868-1880.
- FOLK, R.L., *Petrology of Sedimentary Rocks*, Hemphill's, Austin, Tex., 1968.
- FOX, W.T., and DAVIS, R.A., Jr., "Coastal Processes and Beach Dynamics at Sheboygan, Wisconsin, July 1972," Technical Report No. 10, Williams College, Williamstown, Mass., 1972.
- FOX, W.T., and DAVIS, R.A., Jr., "Weather Patterns and Coastal Processes," *Beach and Nearshore Sedimentation*, Special Publication No. 24, Society of Economic Paleontologists and Mineralogists, Tulsa, Okla., 1976, pp. 1-23.

- GALVIN, C.J., Jr., "Experimental and Theoretical Study of Longshore Currents on a Plane Beach," Ph.D. Dissertation, Department of Geology and Geophysics, Massachusetts Institute of Technology, Cambridge, Mass., 1963.
- GALVIN, C.J., Jr., "Longshore Current Velocity: A Review of Theory and Data," *Reviews of Geophysics*, Vol. 5, No. 3, Aug. 1967, pp. 287-304.
- GALVIN, C.J., Jr., "Wave Breaking in Shallow Water," *Waves on Beaches and Resulting Sediment Transport*, Academic Press, New York, 1972, pp. 413-456.
- GALVIN, C.J., Jr., and EAGLESON, P.S., "Experimental Study of Longshore Currents on a Plane Beach," TM-10, U.S. Army, Corps of Engineers, Coastal Engineering Research Center, Washington, D. C., Jan. 1965.
- GALVIN, C.J., Jr., and VITALE, P., "Longshore Transport Prediction - SPM 1973 Equation," *Proceedings of the 15th Coastal Engineering Conference*, Vol. II, 1977, pp. 1133-1148.
- HARRIS, D.L., "Characteristics of Wave Records in the Coastal Zone," *Waves on Beaches and Resulting Sediment Transport*, Academic Press, New York, 1972, pp. 1-51.
- HARRISON, W., "Empirical Equation for Longshore Current Velocity," *Journal of Geophysical Research*, Vol. 73, No. 22, Nov. 1968, pp. 6929-6936.
- HARRISON, W., and KRUMBEIN, W.C., "Interactions of the Beach-Ocean-Atmosphere System at Virginia Beach, Virginia," TM-7, U.S. Army, Corps of Engineers, Coastal Engineering Research Center, Washington, D.C., Dec. 1964.
- HAYES, M.O., "Morphology of Sand Accumulation in Estuaries: An Introduction to the Symposium," *Estuarine Research*, Vol. II, Academic Press, New York, 1975, p. 3-22.
- HAYES, M.O., GOLDSMITH, V., and HOBBS, C.H., III, "Offset Coastal Inlets," *Proceedings of the 12th Coastal Engineering Conference*, Vol. II, 1970, pp. 1187-1200.
- HAYES, M.O., et al., "The Investigation of Form and Processes in the Coastal Zone," *Proceedings of the Third Annual Geomorphology Symposium*, 1973, Publications in Geomorphology, State University of New York, Binghamton, N.Y., pp. 11-41.
- HINE, A.C., "Bedform Distribution and Migration Patterns on Tidal Deltas in the Chatham Harbor Estuary, Cape Cod, Massachusetts," *Estuarine Research*, Vol. II, Academic Press, New York, 1975, pp. 235-252.

- HOYT, J.H., "Barrier Island Formation," *Bulletin of the Geological Society of America*, Vol. 78, No. 9, Sept. 1967, pp. 1125-1136.
- HUBBARD, D.K., "Morphology and Hydrodynamics of the Merrimack River Ebb-Tidal Delta," *Estuarine Research*, Vol. II, Academic Press, New York, 1975, pp. 253-266.
- HUBBARD, D.K., and BARWIS, J.H., "Discussion of Tidal Inlet Sand Deposits: Examples from the South Carolina Coast," Technical Report No. 11-CRD, Terrigenous Clastic Depositional Environments, Coastal Research Division, Department of Geology, University of South Carolina, Columbia, S.C., 1976, pp. II-128-II-142.
- HUMPHRIES, S.M., "Morphological Variability of North Inlet, South Carolina, 1975/76," M.S. Thesis, Department of Geology, University of South Carolina, Columbia, S.C., 1977a.
- HUMPHRIES, S.M., "Seasonal Hydraulic and Morphologic Variation of a Natural Inlet," *Abstracts, Geological Society of America, Southeast Section*, 1977b, pp. 149-150.
- INMAN, D.L., and FRAUTSCHY, J.D., "Littoral Processes and the Development of Shorelines," *Proceedings of the Coastal Engineering Specialty Conference*, 1966, pp. 511-536.
- INMAN, D.L., and QUINN, W.H., "Currents in the Surf Zone," *Proceedings of the Second Conference on Coastal Engineering*, 1952, pp. 24-36.
- JARRETT, J.T., "Tidal Prism-Inlet Area Relationships," GITI Report 3, U.S. Army, Corps of Engineers, Coastal Engineering Research Center, Fort Belvoir, Va., and U.S. Army Engineer Waterways Experiment Station, Vicksburg, Miss., Feb. 1976.
- JOHNSON, J.W., "Characteristics and Behavior of Pacific Coast Tidal Inlets," *Journal of the Waterways, Harbors and Coastal Engineering Division*, ASCE, Vol. 9, No. WW3, Aug. 1973, pp. 235-339.
- KANA, T.W., "Beach Erosion During a Minor Storm," *Journal of the Waterway, Port, Coastal and Ocean Division*, ASCE, Vol. 103, No. WW4, Nov. 1977, pp. 505-518.
- KEULEGAN, G.H., "Tidal Flow in Entrances: Water-Level Fluctuations of Basins in Communication with Seas," Technical Bulletin No. 14, Committee on Tidal Hydraulics, U.S. Army, Corps of Engineers, Vicksburg, Miss., July 1967.
- KING, D.J., Jr., "The Dynamics of Inlets and Bays," Technical Report No. 22, Coastal and Oceanographic Engineering Laboratory, University of Florida, Gainesville, Fla., Mar. 1974.

- KLEIN, G. deV., "Depositional and Dispersal Dynamics of Intertidal Sand Bars," *Journal of Sedimentary Petrology*, Vol. 40, No. 4, Dec. 1970, pp. 1095-1127.
- KOMAR, P.D., *Beach Processes and Sedimentation*, Prentice-Hall, Englewood Cliffs, N.J., 1976.
- KOMAR, P.D., and INMAN, D.L., "Longshore Sand Transport on Beaches," *Journal of Geophysical Research*, Vol. 75, No. 30, Oct. 1970, pp. 5914-5927.
- KUMAR, N., and SANDERS, J.E., "Inlet Sequence: A Vertical Succession of Sedimentary Structures and Textures Created by the Lateral Migration of Tidal Inlets," *Sedimentology*, Vol. 21, No. 4, Nov. 1974, pp. 491-532.
- LONGUET-HIGGINS, M.S., "Longshore Currents Generation by Obliquely Incident Sea Waves 1," *Journal of Geophysical Research*, Vol. 75, No. 33, Nov. 1970, pp. 6778-6789.
- MARMER, H.A., "Changes in Sea Level Determined from Tide Observations," *Proceedings of the Second Conference on Coastal Engineering*, 1952, pp. 62-67.
- MASTERSON, R.P., Jr., MACHEMEHL, J.L., and CAVAROC, V.V., "Sediment Movement in Tubbs Inlet, North Carolina," Report No. 73-2, Center for Marine and Coastal Studies, North Carolina State University, Raleigh, N.C., June 1973.
- MEADE, R.H., and EMERY, K.O., "Sea Level as Affected by River Run-off, Eastern United States," *Science*, Vol. 173, No. 3995, July 1971, pp. 425-427.
- MEYERS, V.A., "Storm Tide Frequencies on the South Carolina coast," Technical Report No. NWS-16, National Oceanic and Atmospheric Administration, Rockville, Md., 1975.
- NATIONAL OCEANIC AND ATMOSPHERIC ADMINISTRATION, "Tide Tables, East Coast of North and South America," National Ocean Survey, Rockville, Md., 1977.
- NUMMEDAL, D., and STEPHEN, M.F., "Coastal Dynamics and Sediment Transportation, Northeast Gulf of Alaska," Technical Report No. 9-CRD, Coastal Research Division, Department of Geology, University of South Carolina, Columbia, S.C., 1976.
- NUMMEDAL, D., FITZGERALD, D.M., and HUMPHRIES, S.M., "Hydraulics of Sediment Transportation in Meso-Tidal Inlets," *Abstracts, Geological Society of America*, Northeast and Southeast Sections, 1976, p. 236.

- NUMMEDAL, D., et al., "Tidal Inlet Variability--Cape Hatteras to Cape Canaveral," *Proceedings of Coastal Sediments '77*, 1977, pp. 543-562.
- O'BRIEN, M.P., "Estuary Tidal Prisms Related to Entrance Areas," *Civil Engineering*, Vol. 1, No. 8, May 1931, pp. 738-739.
- O'BRIEN, M.P., "Equilibrium Flow Areas of Inlets on Sandy Coasts," *Journal of Waterways, Harbors and Coastal Engineering Division*, ASCE, Vol. 95, No. WW1, Feb. 1969, pp. 43-52.
- O'BRIEN, M.P., and DEAN, R.G., "Hydraulics and Sedimentary Stability of Coastal Inlets," *Proceedings of the 13th Coastal Engineering Conference*, Vol. 11, 1972, pp. 761-779.
- OERTEL, G.F., "Sediment Transport on Estuary Entrance Shoals and the Formation of Swash Platforms," *Journal of Sedimentary Petrology*, Vol. 42, No. 4, Dec. 1972, pp. 858-868.
- OLIVEIRA, I.B.M., "Natural Flushing Ability in Tidal Inlets," *Proceedings of the 12th Coastal Engineering Conference*, Vol. II, 1970, pp. 1827-1844.
- PATTULLO, J.G., "Seasonal Changes in Sea Level," *The Sea*, Interscience, New York, 1966, pp. 485-496.
- PATTULLO, J.G., et al., "The Seasonal Oscillation in Sea Level," *Journal of Marine Research*, Vol. 14, 1955, pp. 88-155.
- PUTNAM, J.A., MUNK, W.H., and TRAYLOR, M.A., "The Prediction of Longshore Currents," *Transactions of the American Geophysical Union*, Vol. 30, 1949, pp. 337-345.
- REDFIELD, A.C., "The Influence of the Continental Shelf on the Tides of the Atlantic Coast of the United States," *Journal of Marine Research*, Vol. 17, 1958, pp. 432-448.
- SEELIG, W.N., HARRIS, D.L., and HERCHENRODER, B.E., "A Spatially Integrated Numerical Model of Inlet Hydraulics," GITI Report 14, U.S. Army, Corps of Engineers, Coastal Engineering Research Center, Fort Belvoir, Va., and U.S. Army Engineer Waterways Experiment Station, Vicksburg, Miss., Nov. 1977.
- SEYMOUR, R.J., et al., "Coastal Engineering Data Network," Sea Grant Publication No. 50, Institute of Marine Resources, University of California, La Jolla, Calif., July 1976.
- SHEPARD, F.P., and INMAN, D.L., "Nearshore Water Circulation Related to Bottom Topography and Wave Refraction," *Transactions of the American Geophysical Union*, Vol. 31, No. 2, 1950, pp. 196-212.

SILVESTER, R., *Coastal Engineering*, 2, Elsevier, Amsterdam, 1974.

SONU, C.J., McCLOY, J.M., and McARTHUR, D.S., "Longshore Currents and Nearshore Topographies," *Proceedings of the 10th Conference on Coastal Engineering*, 1967, pp. 524-549.

U.S. ARMY, CORPS OF ENGINEERS, COASTAL ENGINEERING RESEARCH CENTER, *Shore Protection Manual*, 3d ed., Stock No. 008-022-00113-1, U.S. Government Printing Office, Washington, D.C., 1977, 1,262 pp.

U.S. CONGRESS, "Other Coastal Beaches, South Carolina--Interim Hurricane Survey," House Document No. 422, Apr. 1966.

U.S. NAVAL WEATHER SERVICE COMMAND, "Summary of Synoptic Meteorological Observations, North American Coastal Marine Areas," Vol. 3, May 1975.

WALTON, T.L., Jr., "Littoral Drift Computations Along the Coast of Florida by Means of Ship Wave Observations," Technical Report No. 15, Coastal and Oceanographic Engineering Laboratory, University of Florida, Gainesville, Fla., Feb. 1973.

WIEGEL, R.L., *Oceanographical Engineering*, Prentice-Hall, Englewood Cliffs, N.J., 1964.

WYRTKI, K., "Teleconnections in the Equatorial Pacific Ocean, *Science*, Vol. 180, 1973, pp. 66-68.

APPENDIX A

FATHOMETER PROFILES AT NORTH INLET

The profiles were measured by a Bludworth precision depth recorder (Figs. A-1 to A-12). A map of channel profile locations is given in Figure 8. Offshore profile locations are shown in Figure 28. All profiles are computer reduced to the same scale.

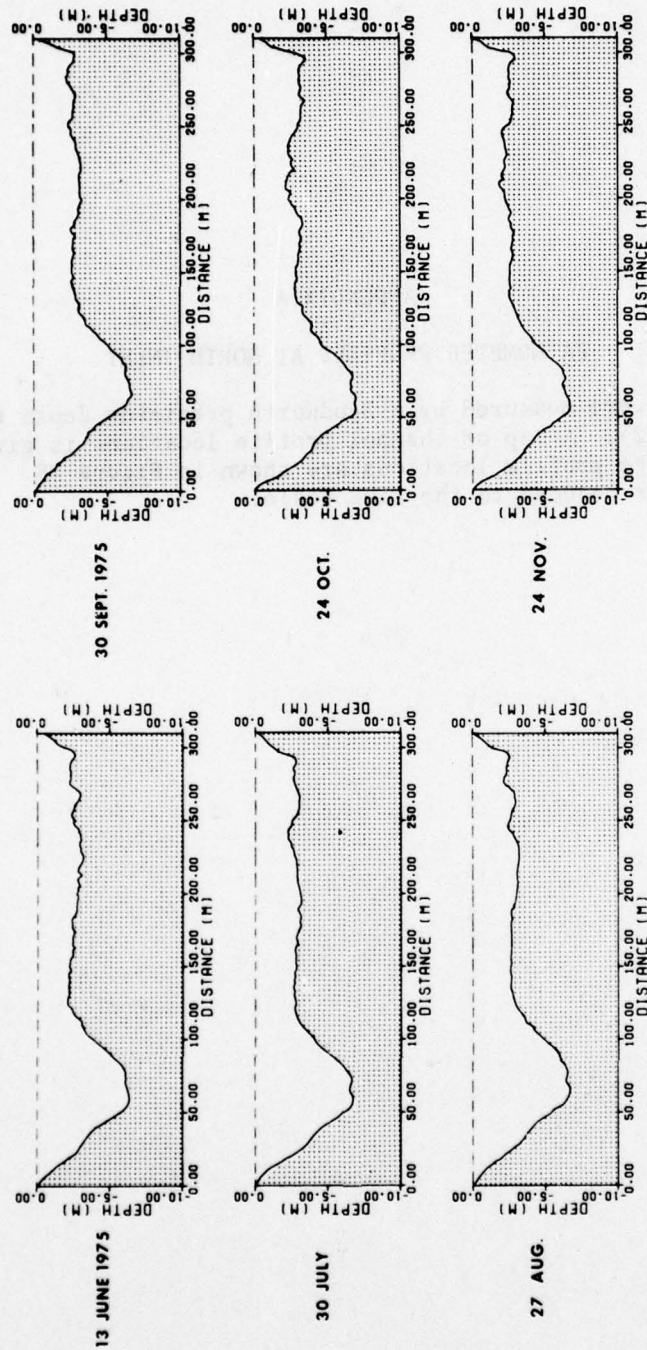


Figure A-1. Town Creek, 13 June to 24 November 1975.

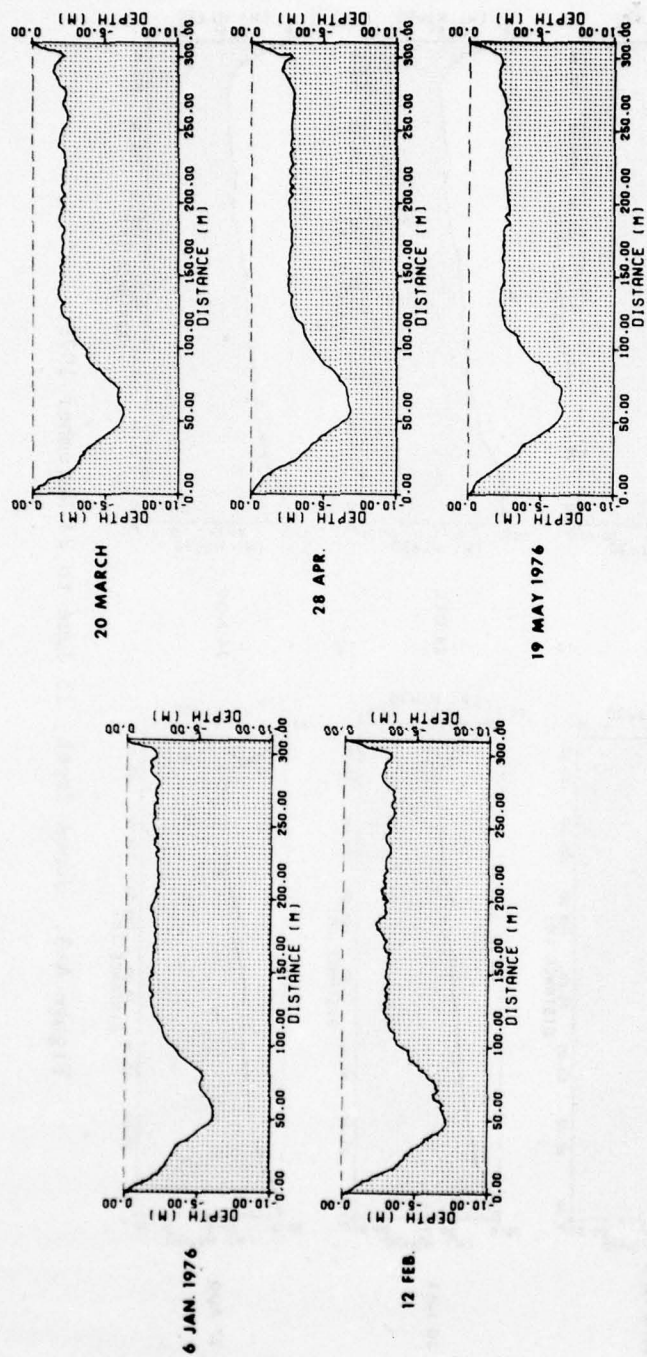


Figure A-2. Town Creek, 6 January to 19 May 1976.

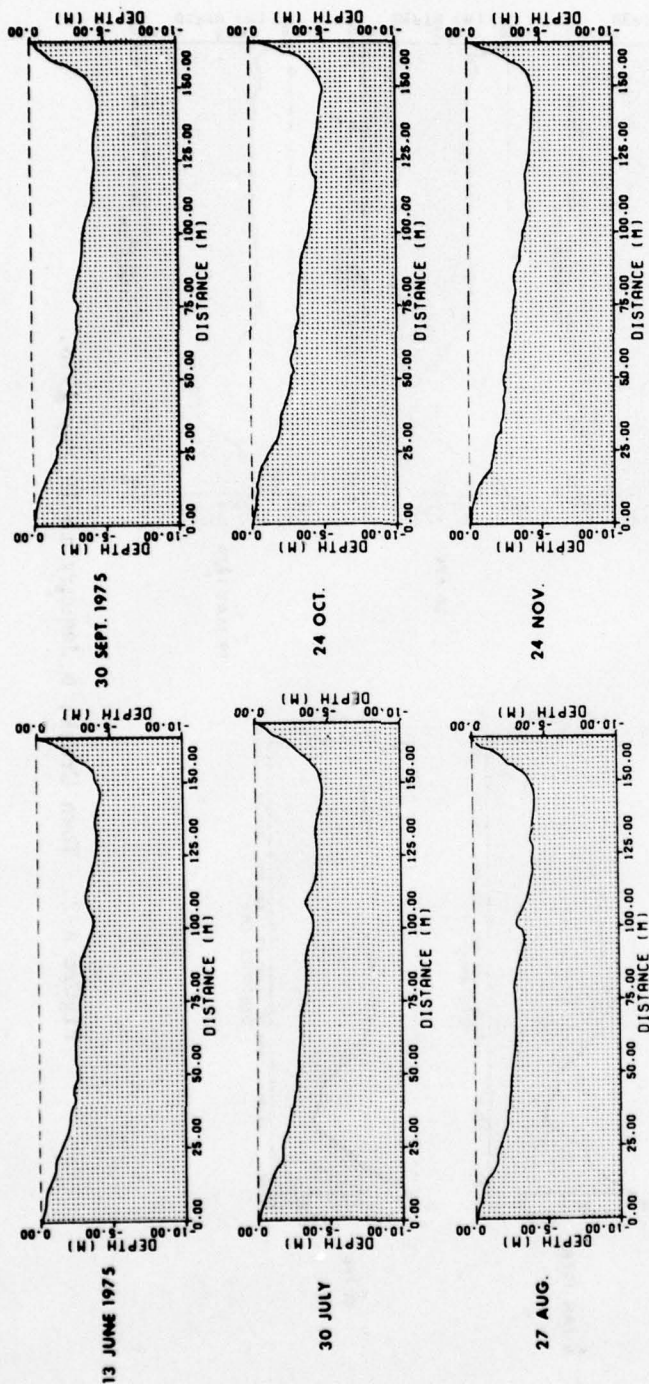


Figure A-3. Jones Creek, 13 June to 24 November 1975.

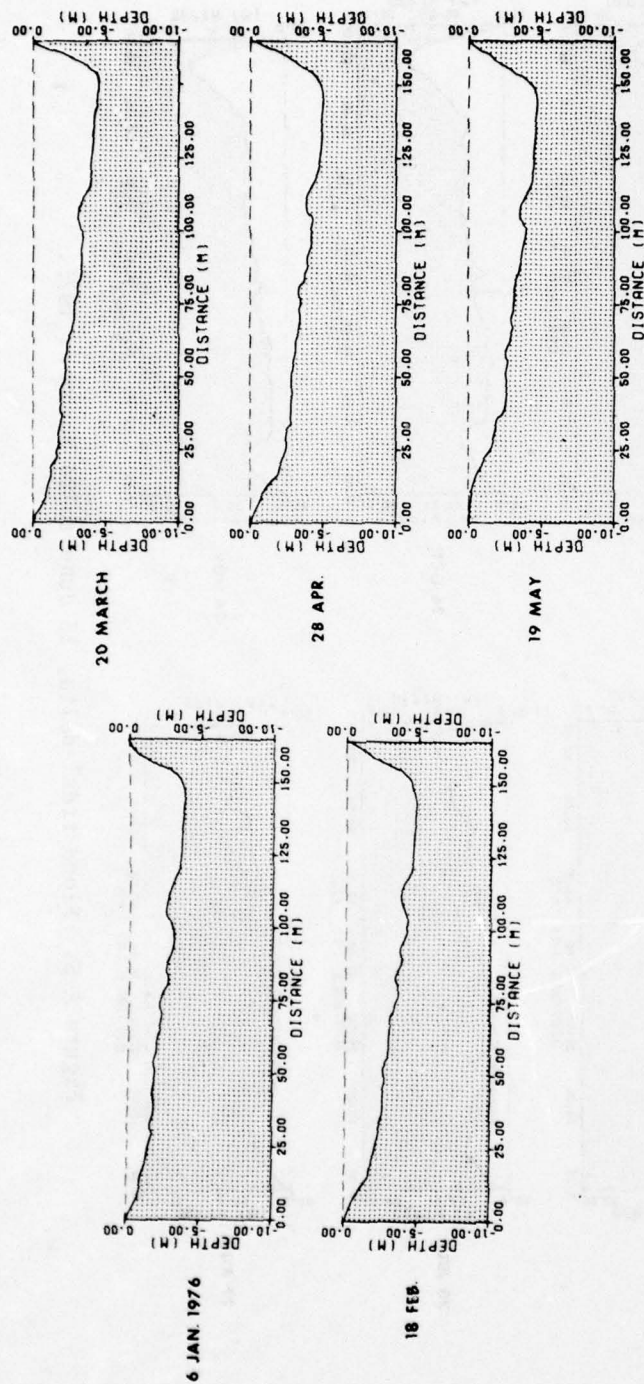


Figure A-4. Jones Creek, 6 January to 19 May 1976.

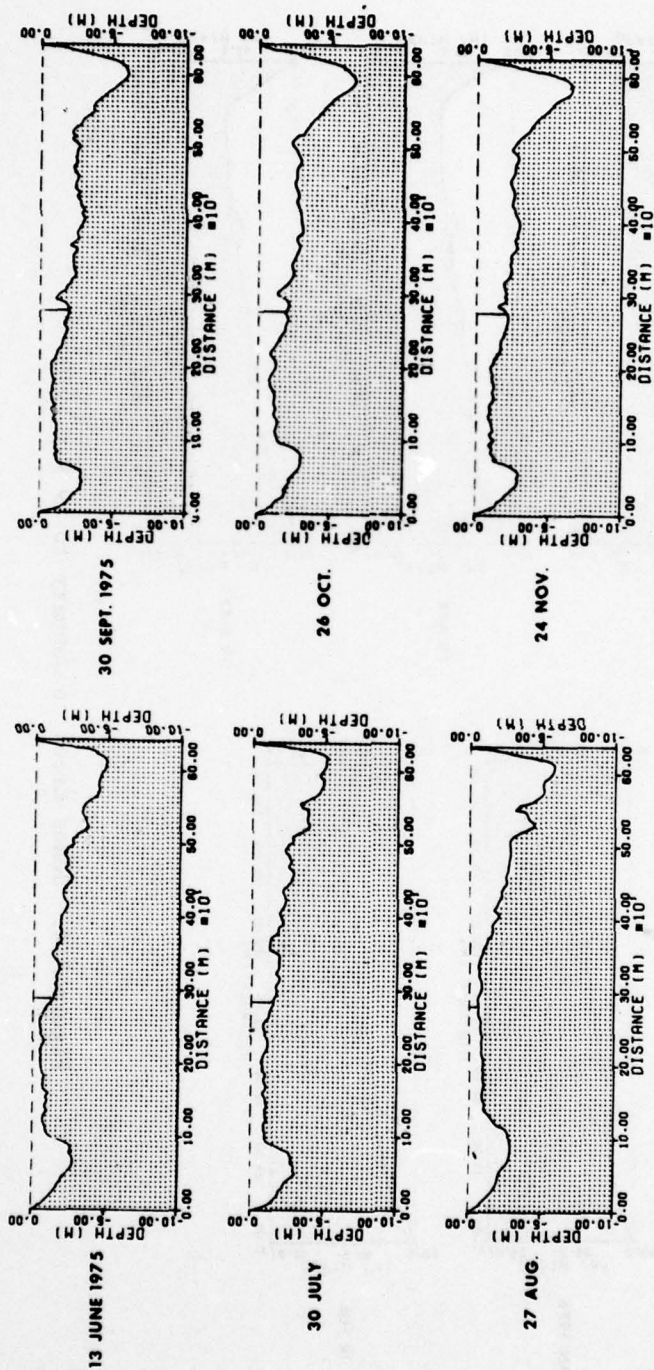


Figure A-5. Flood tidal delta, 13 June to 24 November 1975.

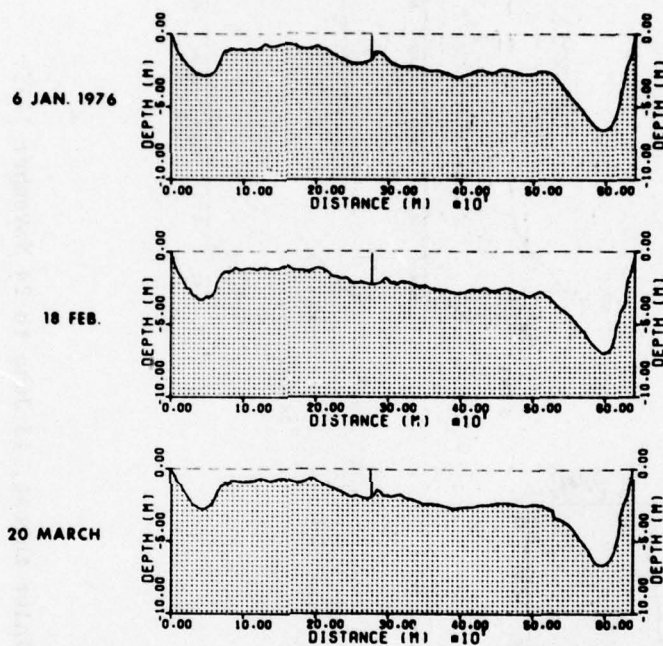


Figure A-6. Flood tidal delta, 6 January to 20 March 1976.

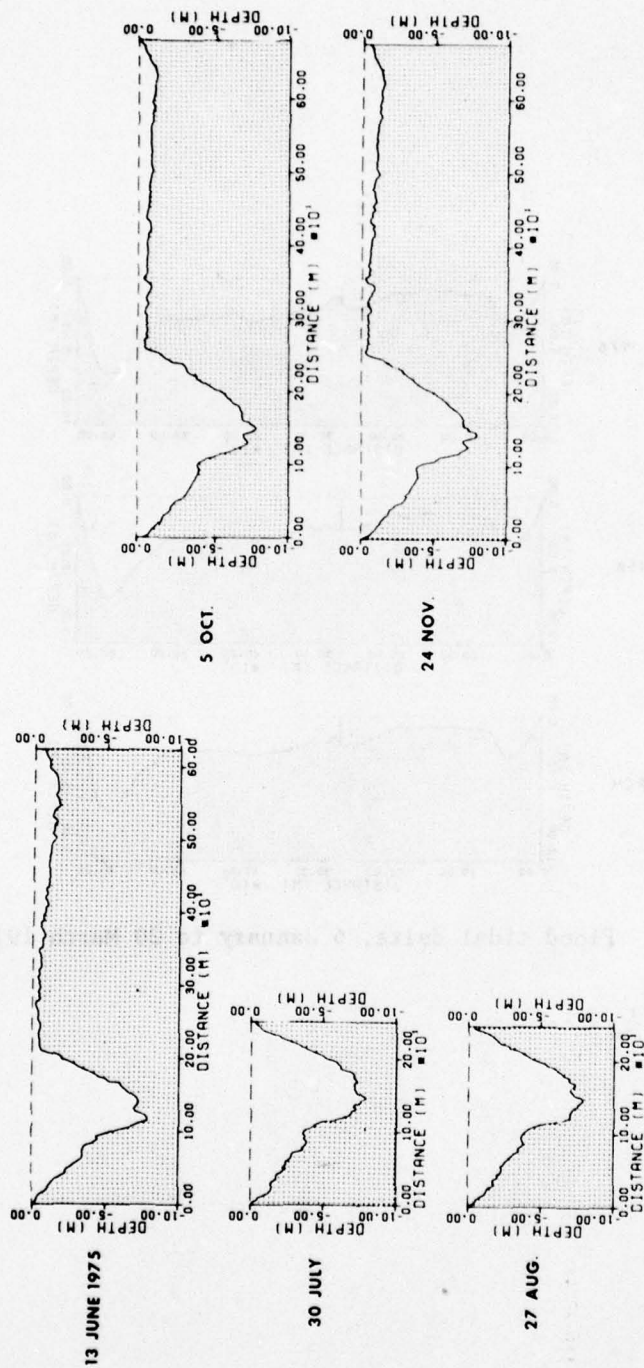


Figure A-7. Inlet throat, 13 June to 24 November 1975.

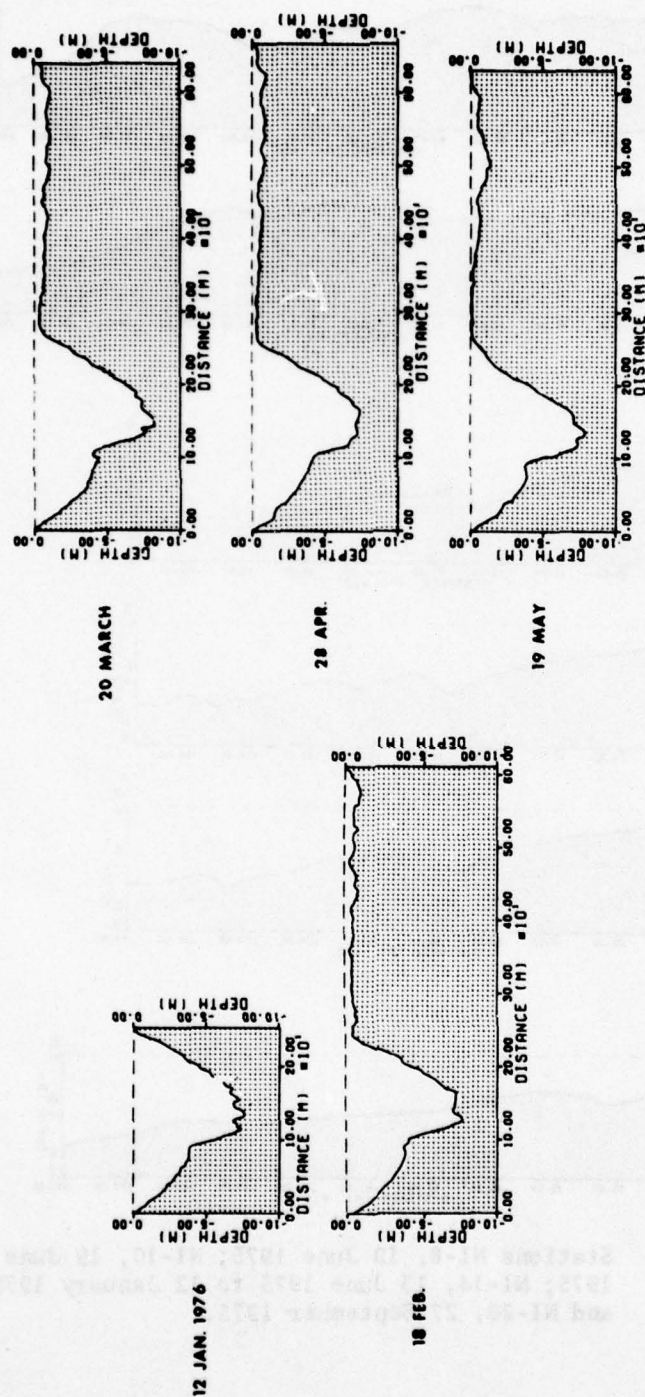


Figure A-8. Inlet throat, 12 January to 19 May 1976.

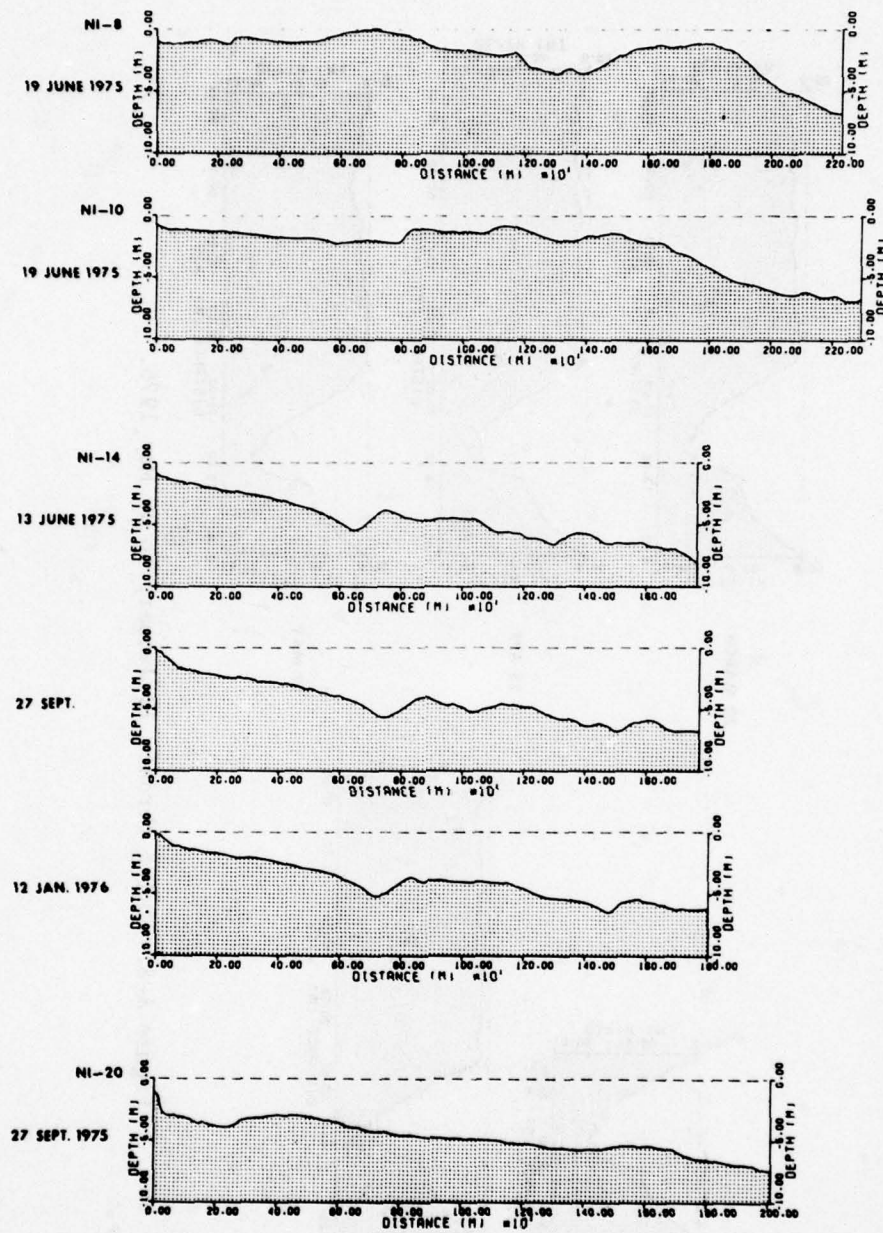


Figure A-9. Stations NI-8, 19 June 1975; NI-10, 19 June 1975; NI-14, 13 June 1975 to 12 January 1976; and NI-20, 27 September 1975.

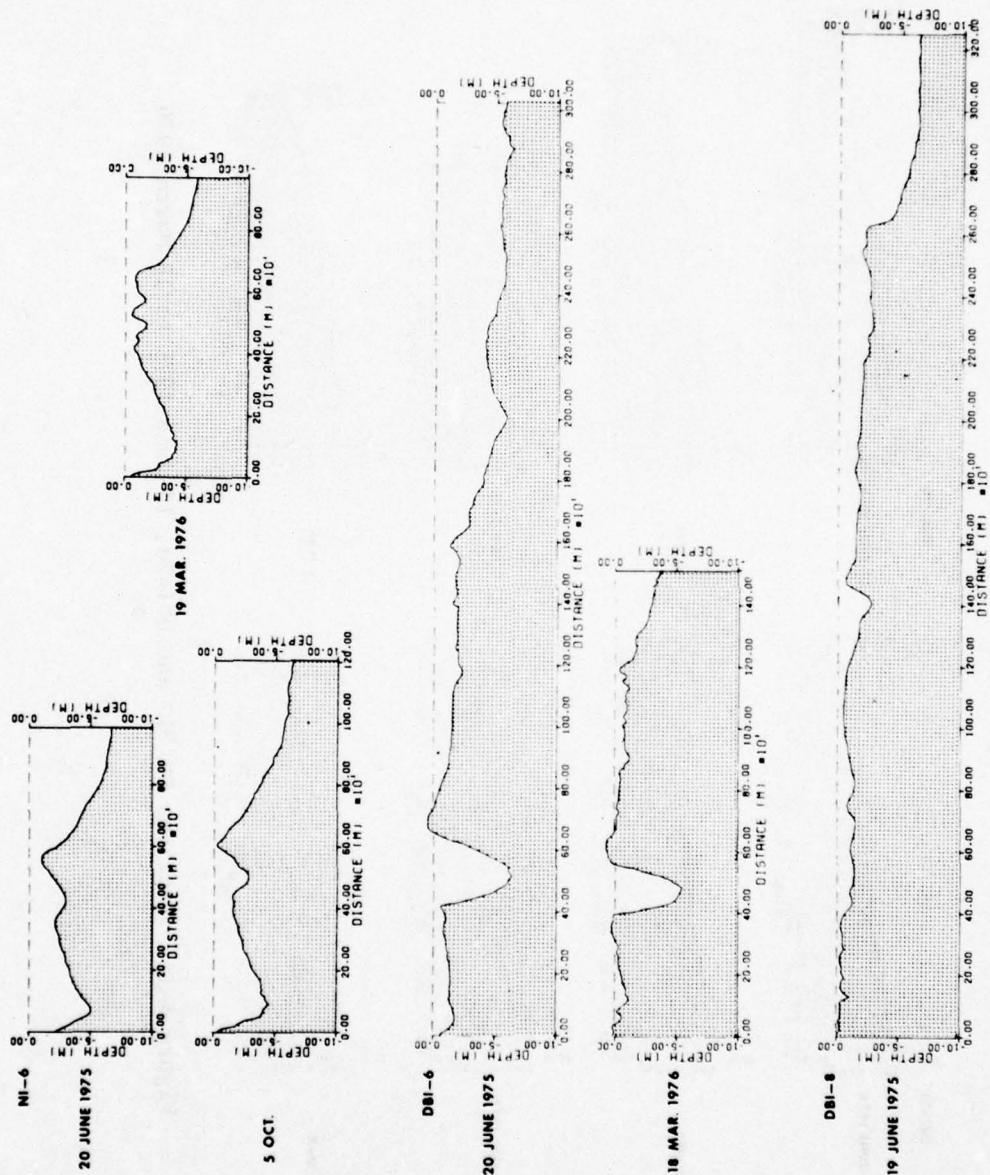


Figure A-10. Stations NI-6, June 1975 to 19 March 1976; DBI-6, 20 June 1975 and 18 March 1976; and DBI-8, 19 June 1975.

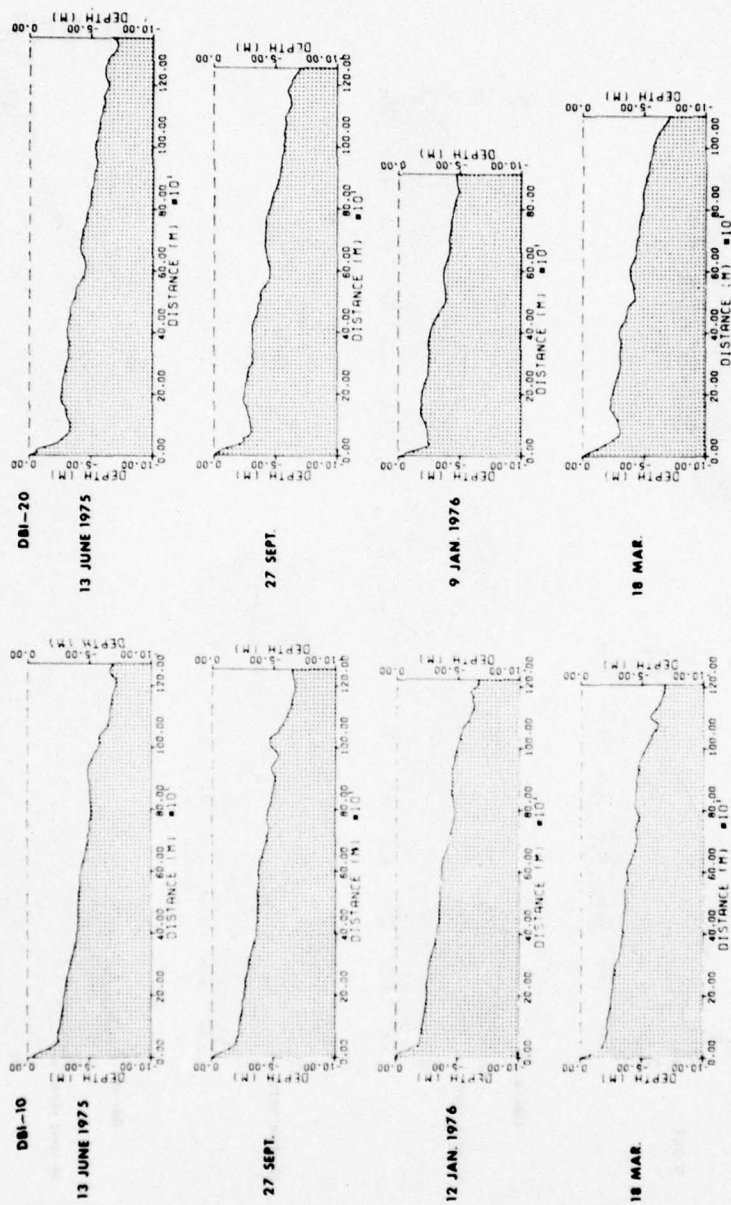


Figure A-11. Stations DBI-10 and DBI-20, 13 June 1975 to 18 March 1976.

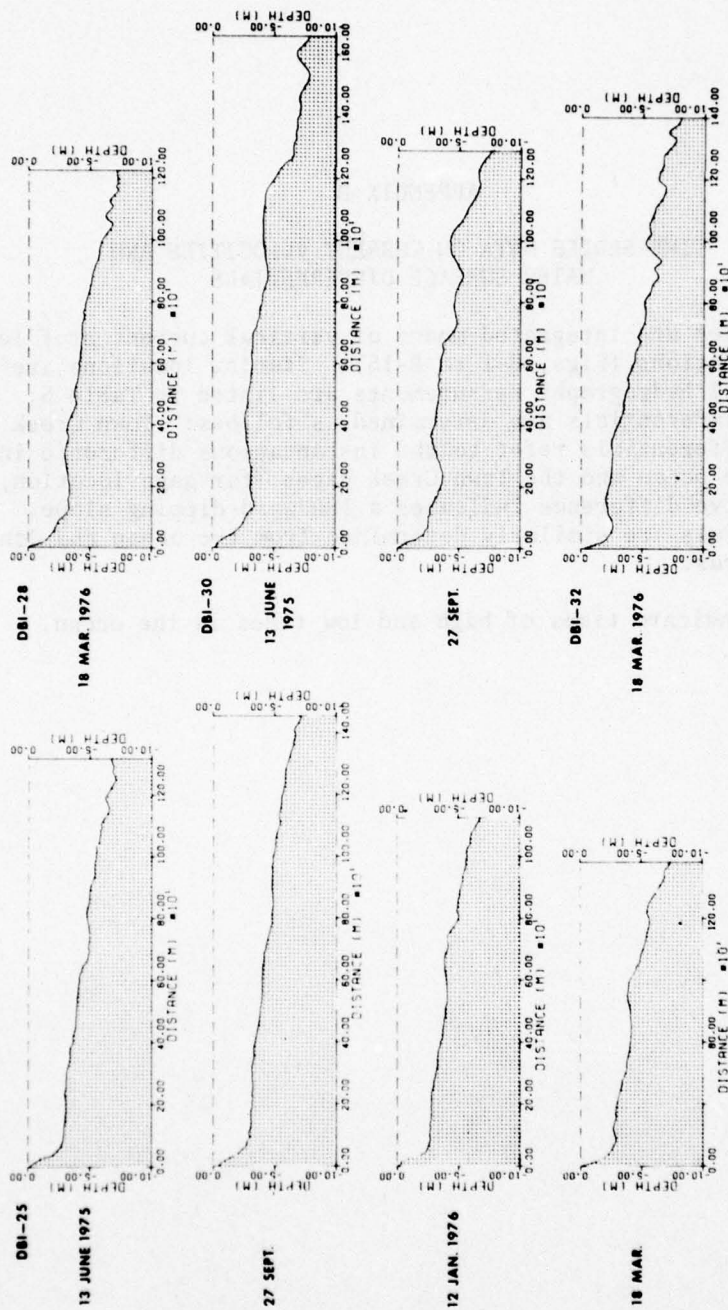


Figure A-12. Stations DBI-24, 13 June 1975 to 18 March 1976; DBI-28, 18 March 1976; DBI-30, 13 June and 27 September 1975; and DBI-32, 18 March 1976.

APPENDIX B

TIME-SERIES DATA ON CURRENT VELOCITIES AND WATER SURFACE DIFFERENTIALS

The velocities are integrated means of vertical current profiles at the indicated stations (Figs. B-1 to B-15). Station locations are shown in Figure 9. All hydrography measurements are listed in Table 5. The water surface differentials are determined as follows: Town Creek and Inlet Throat differentials refer to the instantaneous difference in water elevation at the ocean and the Town Creek gages (for gage location, see Fig. 7); a positive difference indicates a landward-dipping slope. Jones Creek differentials are similarly determined from the ocean and Jones Creek gage records.

Hi and Lo indicate times of high and low tides in the ocean.

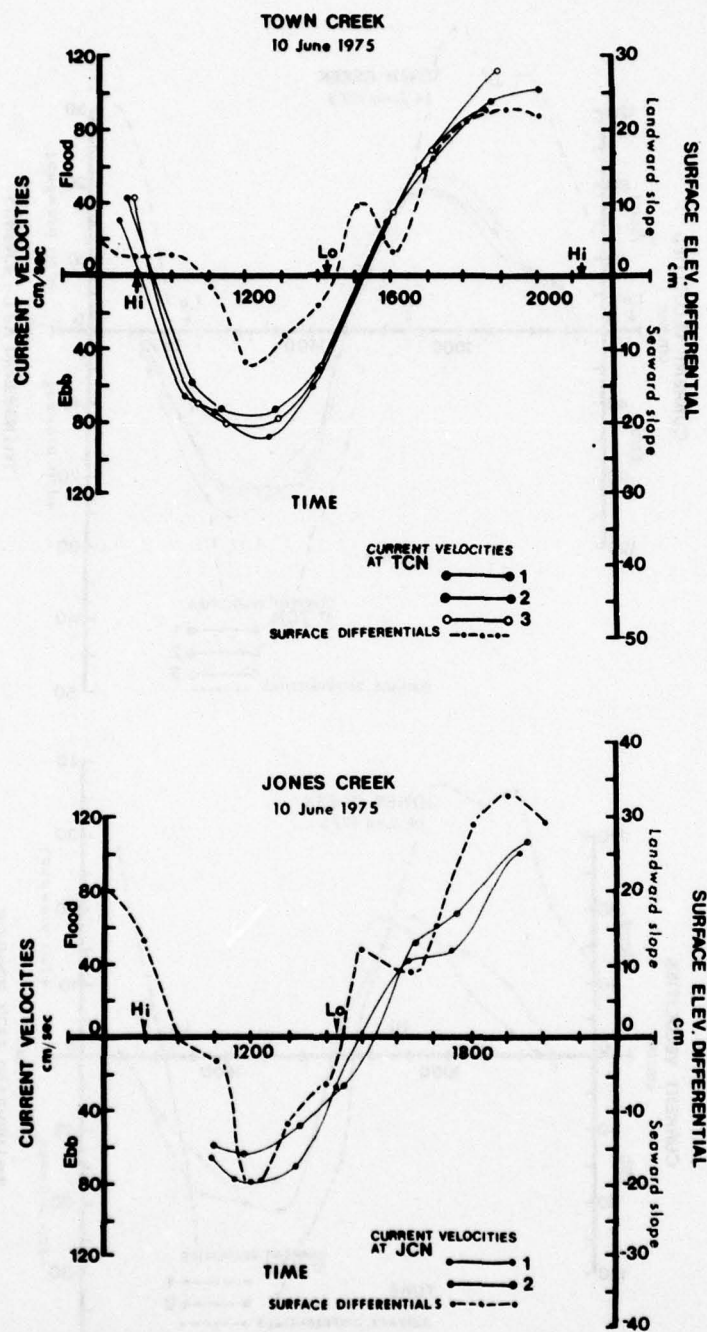


Figure B-1. Current velocity time series and surface differentials at Town and Jones Creeks, 10 June 1975.

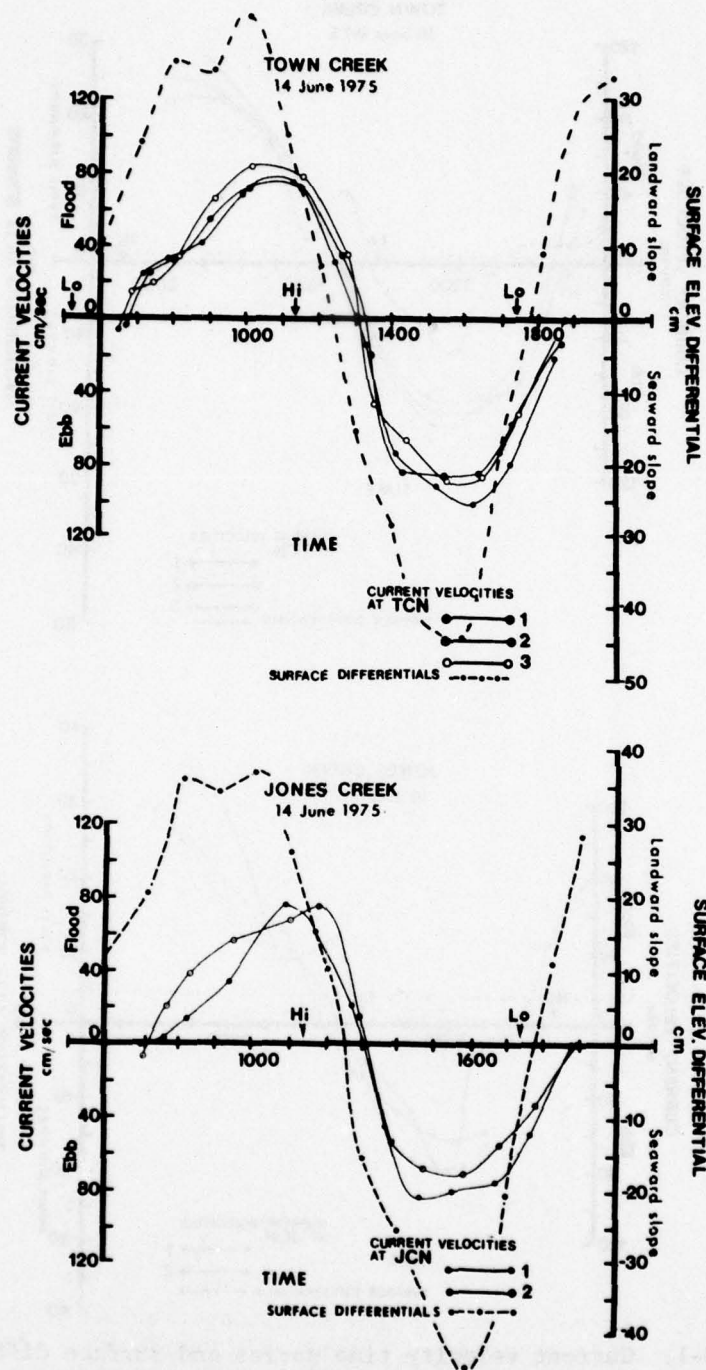


Figure B-2. Current velocity time series and surface differentials at Town and Jones Creeks, 14 June 1975.

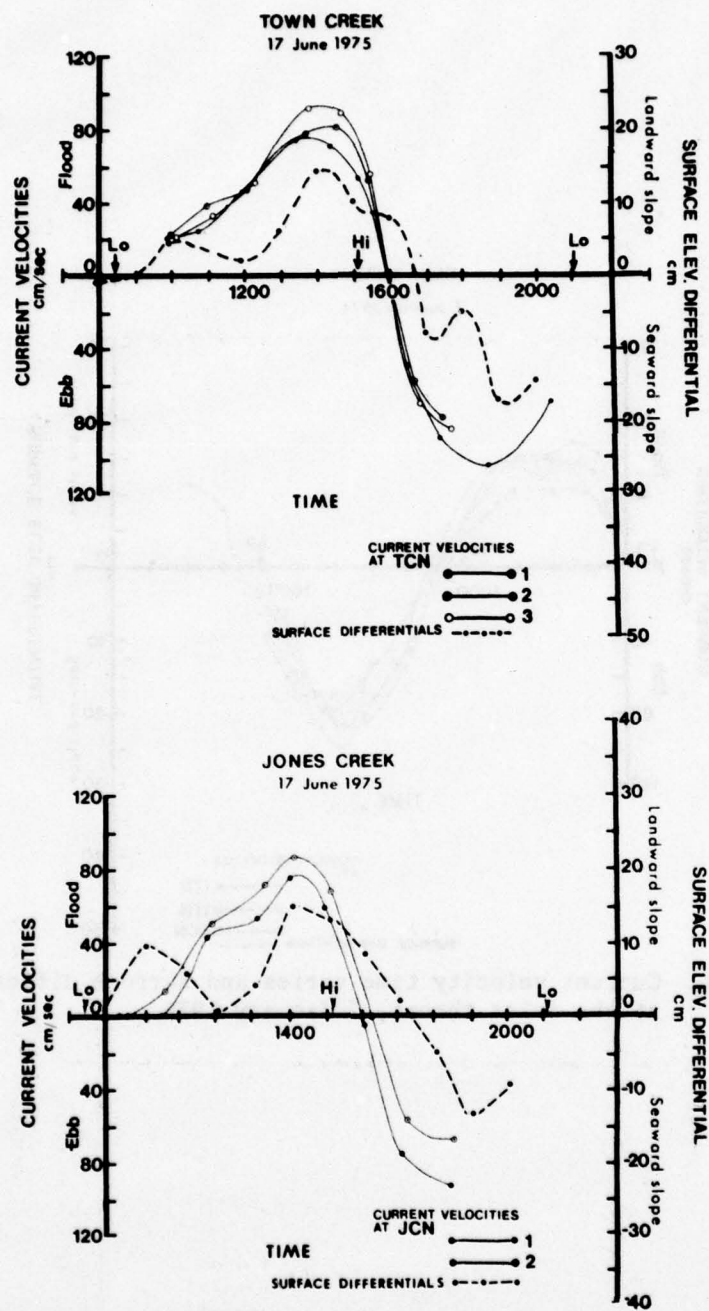


Figure B-3. Current velocity time series and surface differentials at Town and Jones Creeks, 17 June 1975.

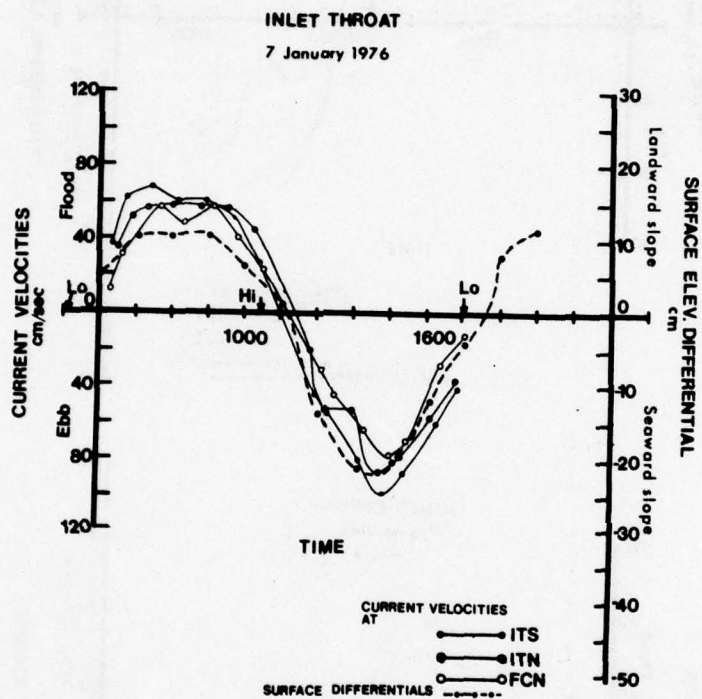


Figure B-4. Current velocity time series and surface differentials at the inlet throat, 7 January 1976.

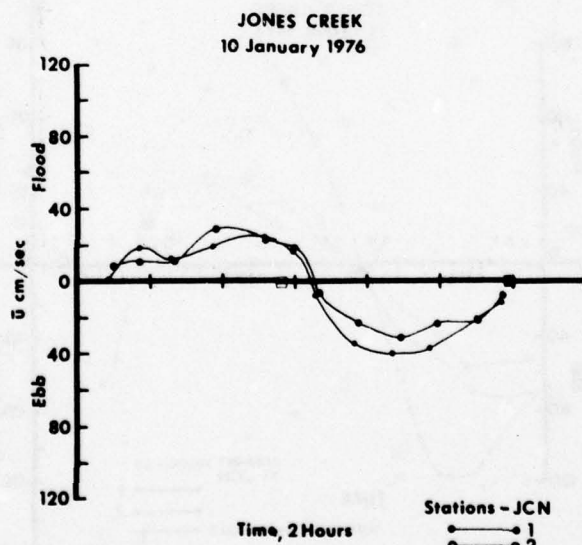
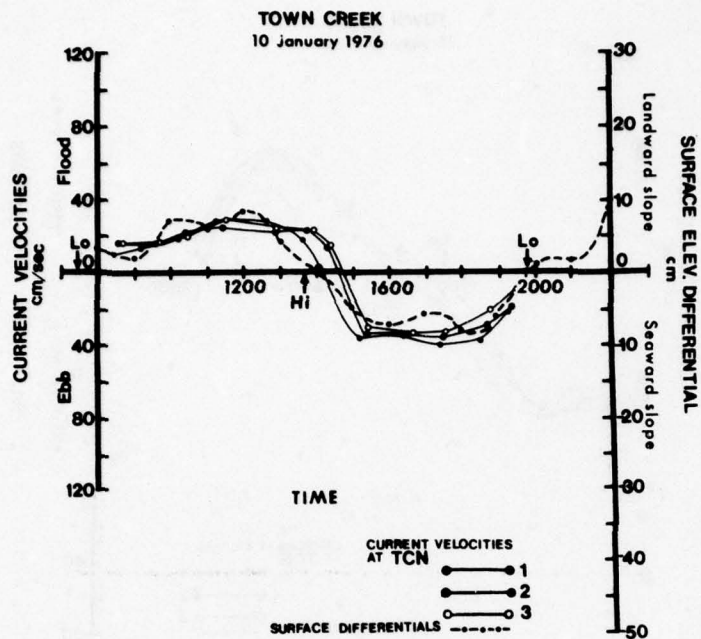


Figure B-5. Current velocity time series and surface differentials at Town and Jones Creeks, 10 January 1976.

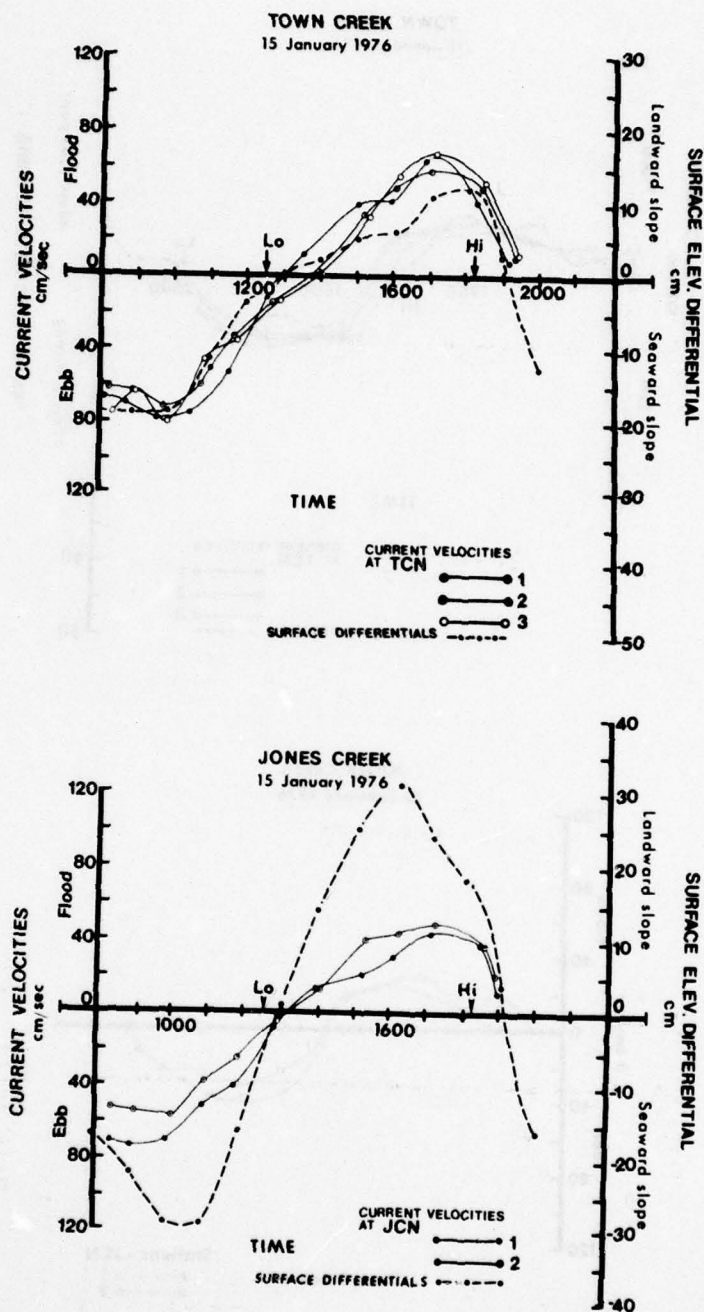


Figure B-6. Current velocity time series and surface differentials at Town and Jones Creeks, 15 January 1976.

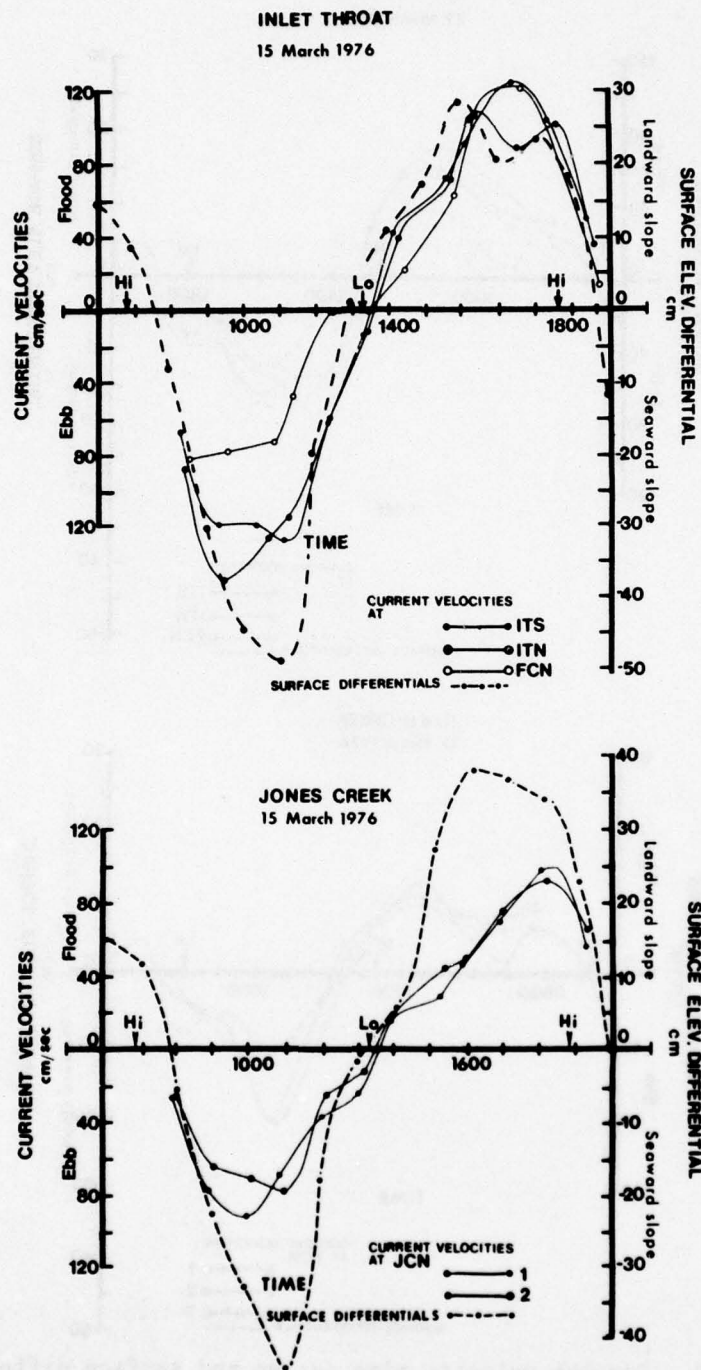


Figure B-7. Current velocity time series and surface differentials at the inlet throat and Jones Creek, 15 March 1976.

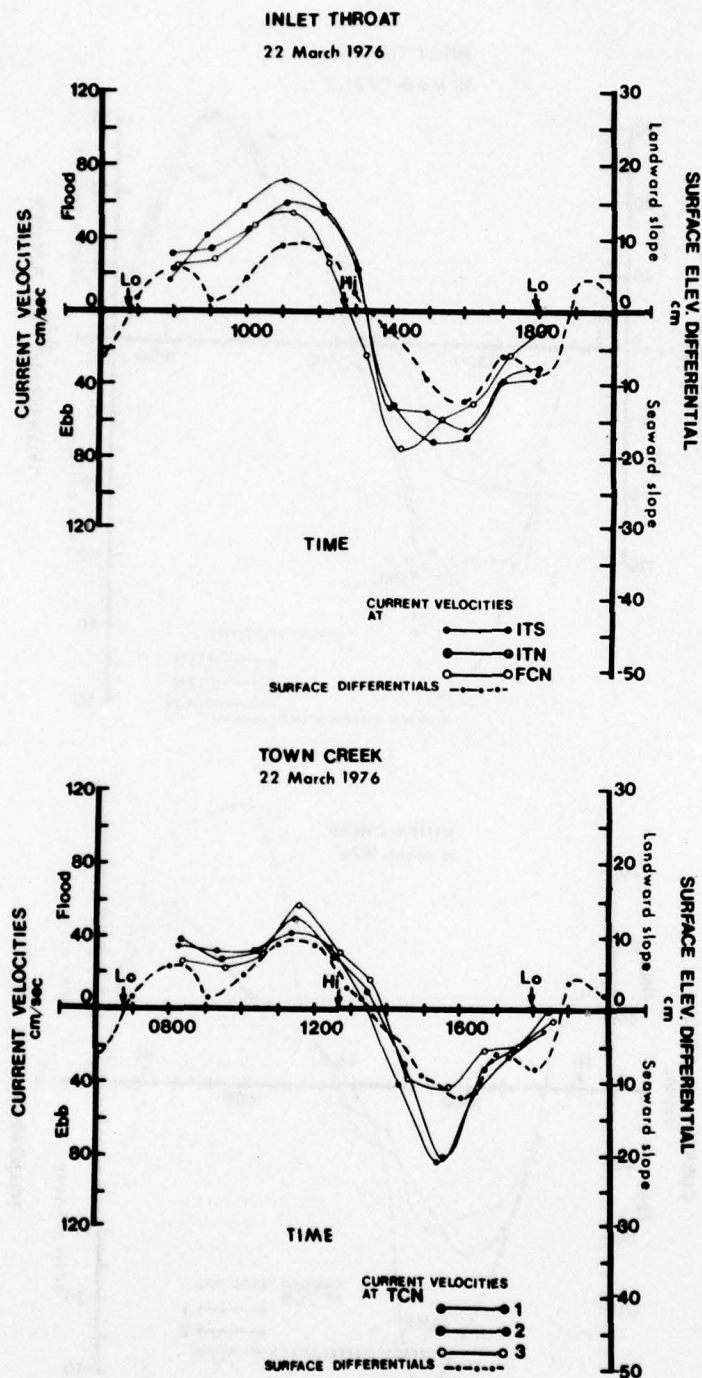
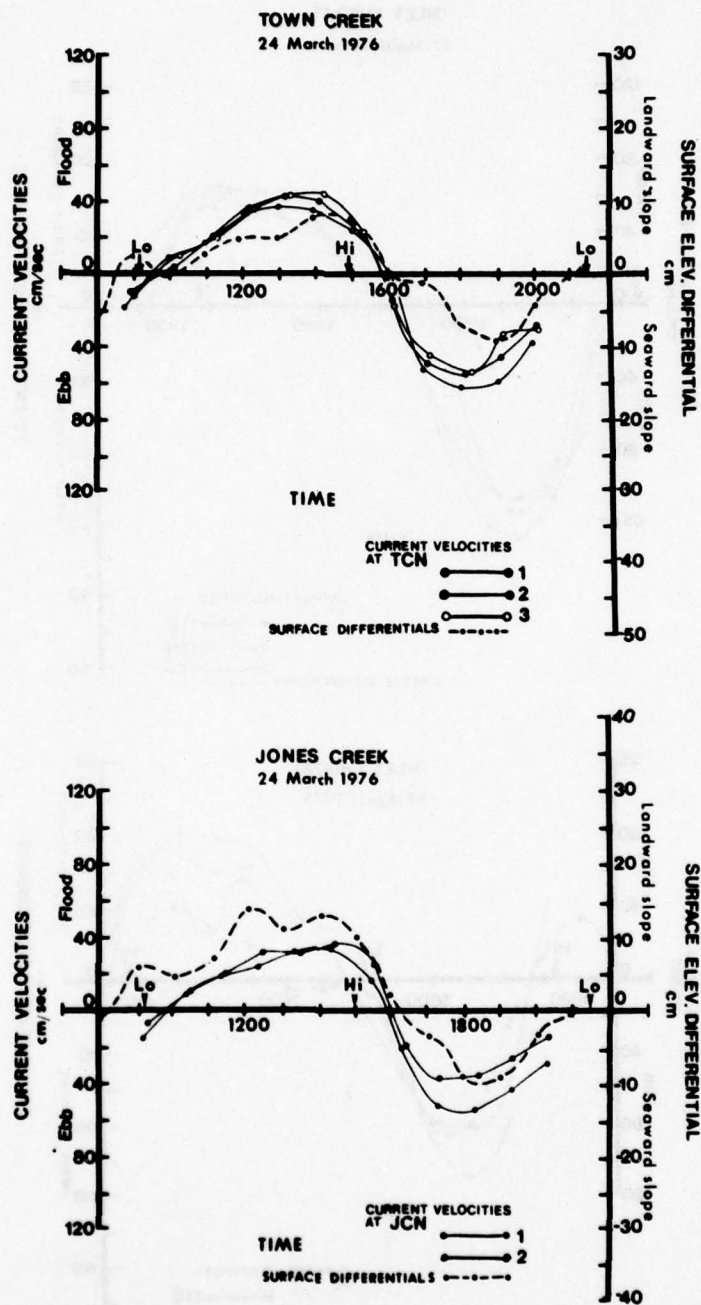


Figure B-8. Current velocity time series and surface differentials at the inlet throat and Town Creek, 22 March 1976.



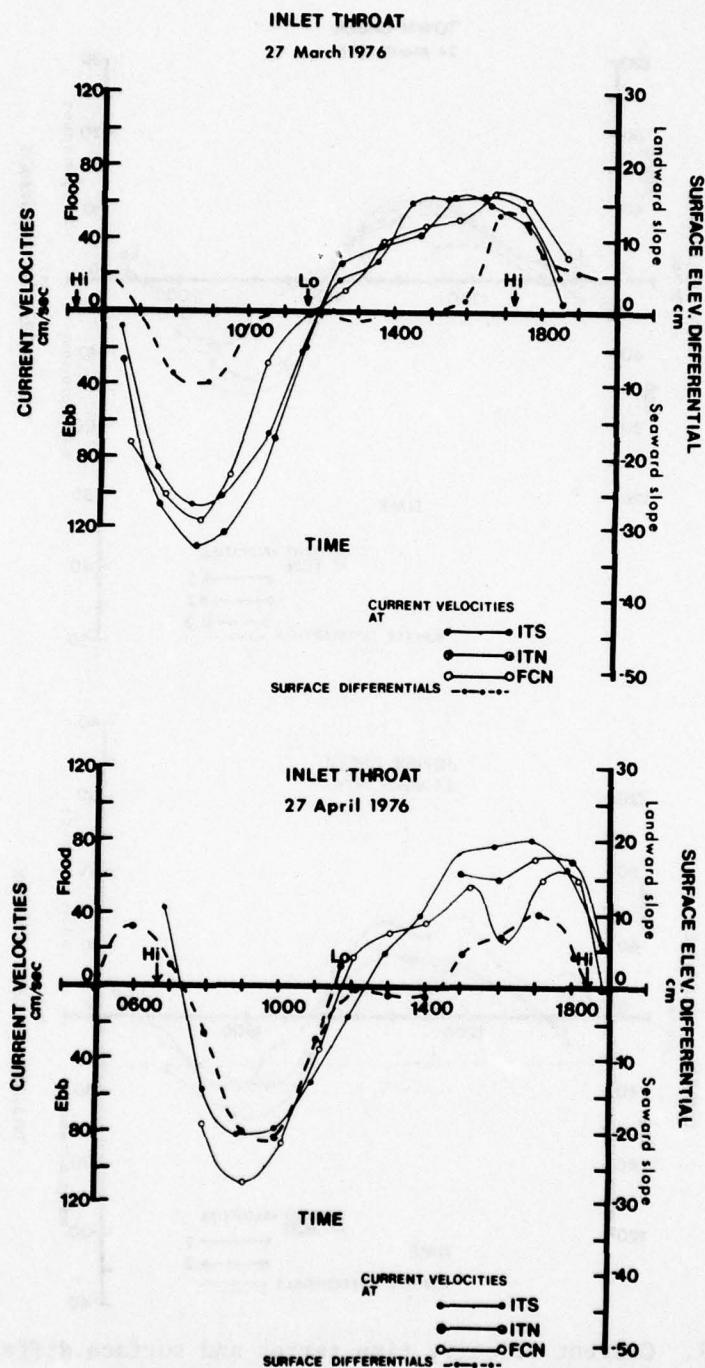


Figure B-10. Current velocity time series and surface differentials at the inlet throat, 27 March and 27 April 1976.

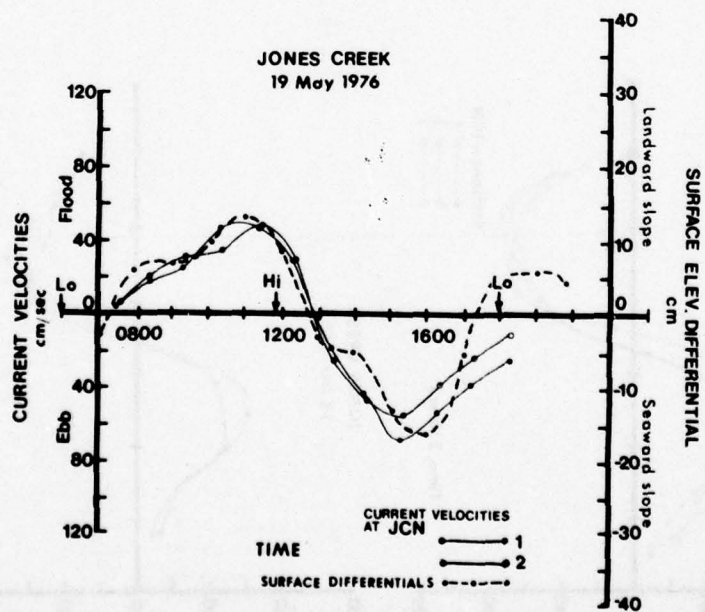
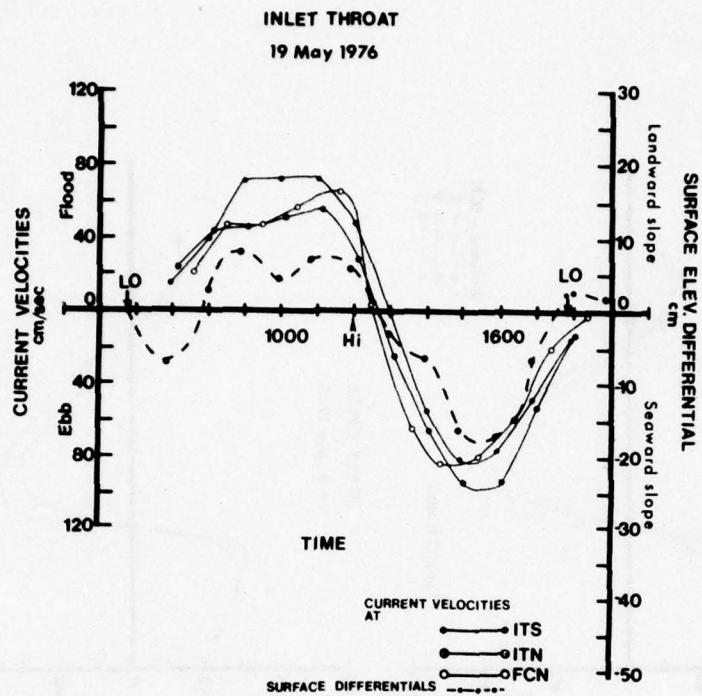


Figure B-11. Current velocity time series and surface differentials at the inlet throat and Jones Creek, 19 May 1976.

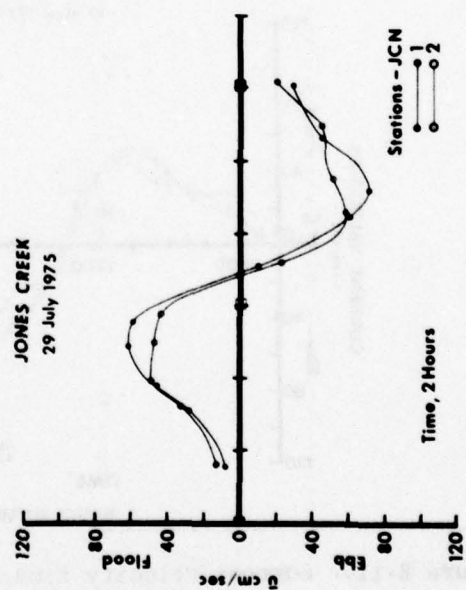
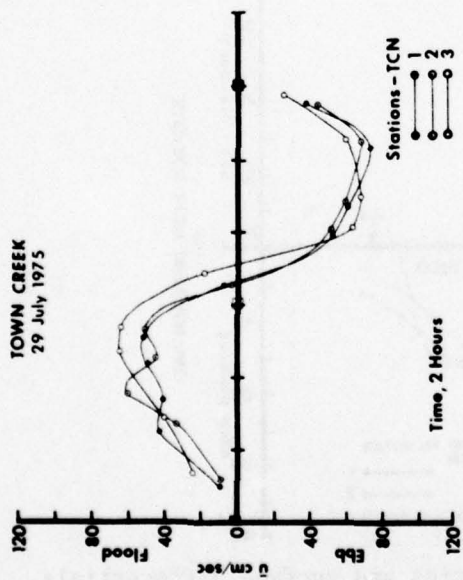
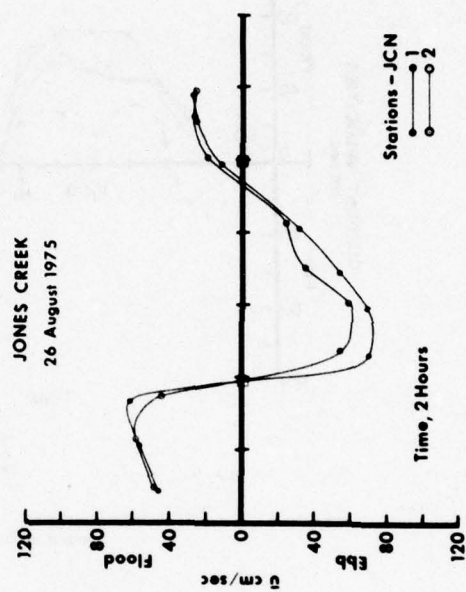
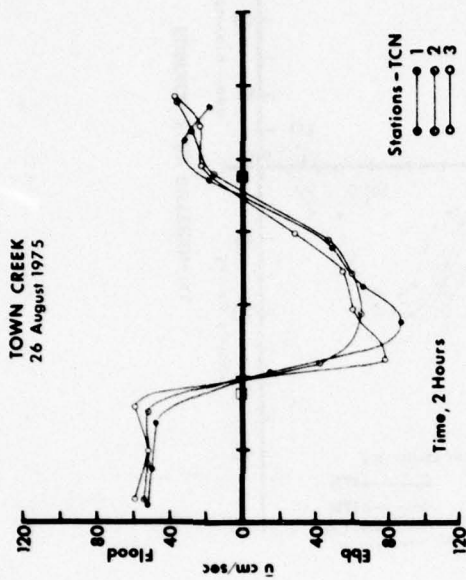


Figure B-12. Current velocity time series at Town and Jones Creeks, 29 July and 26 August 1976.

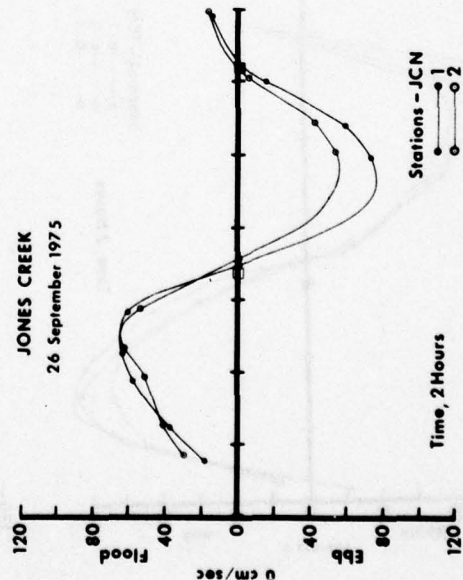
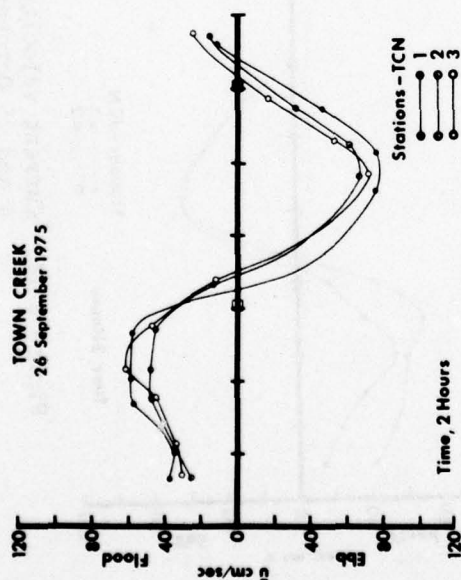
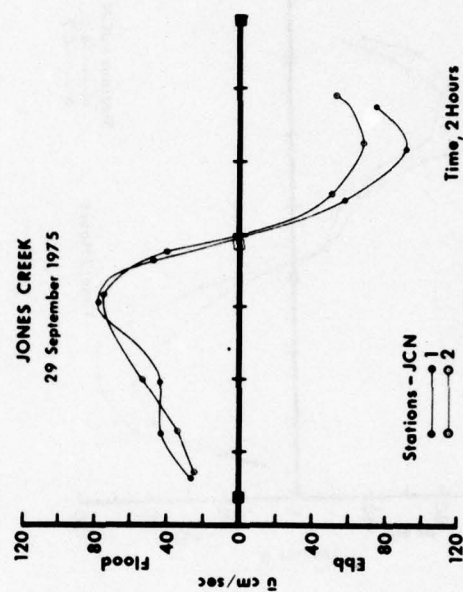
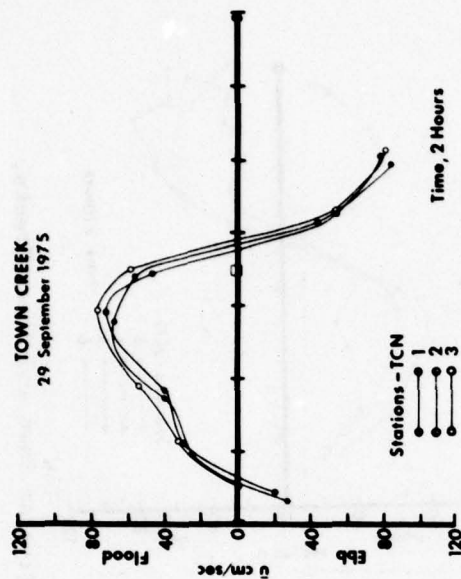


Figure B-13. Current velocity time series at Town and Jones Creeks, 26 and 29 September 1975.

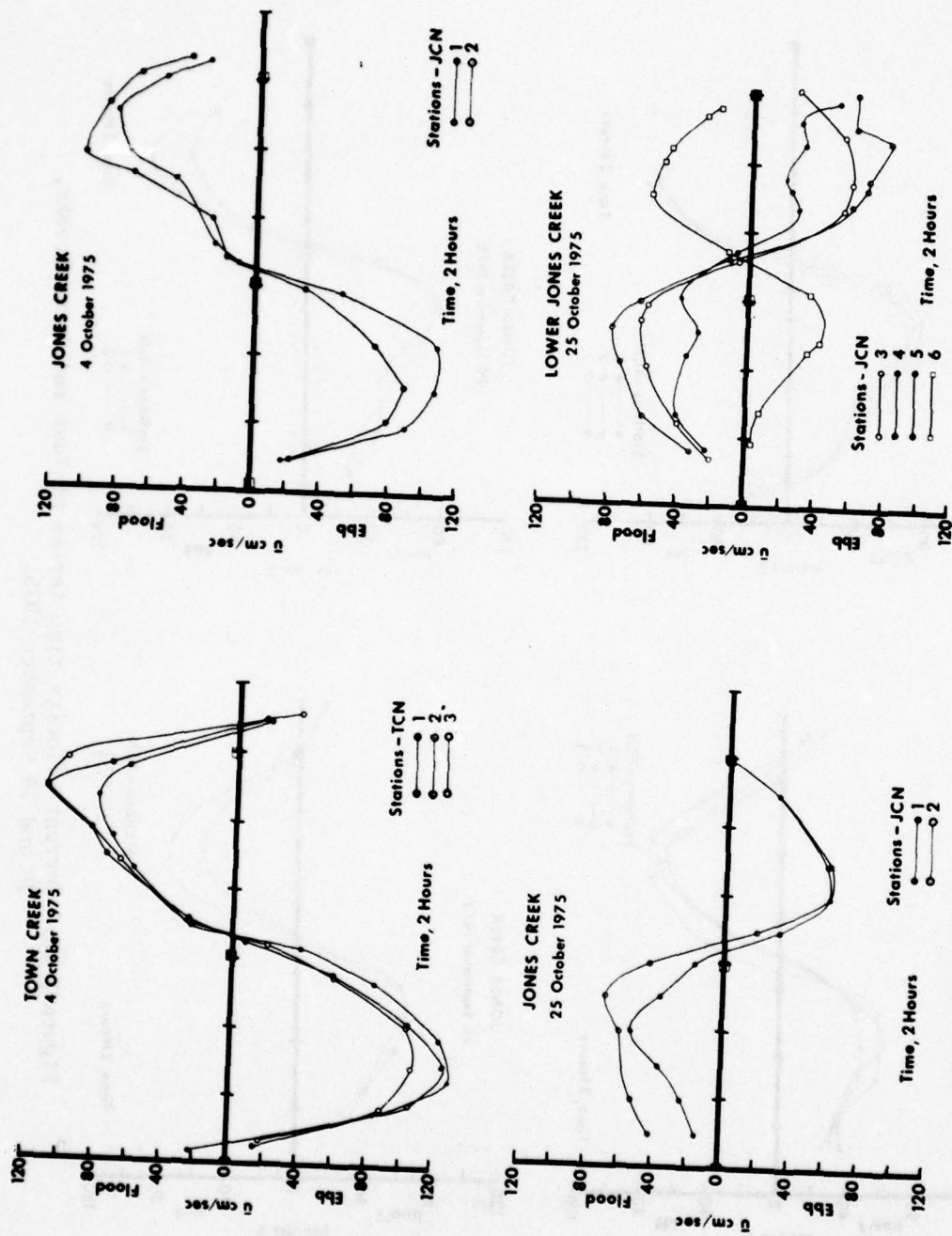


Figure B-14. Current velocity time series at Town and Jones Creeks, 4 and 25 October 1975.

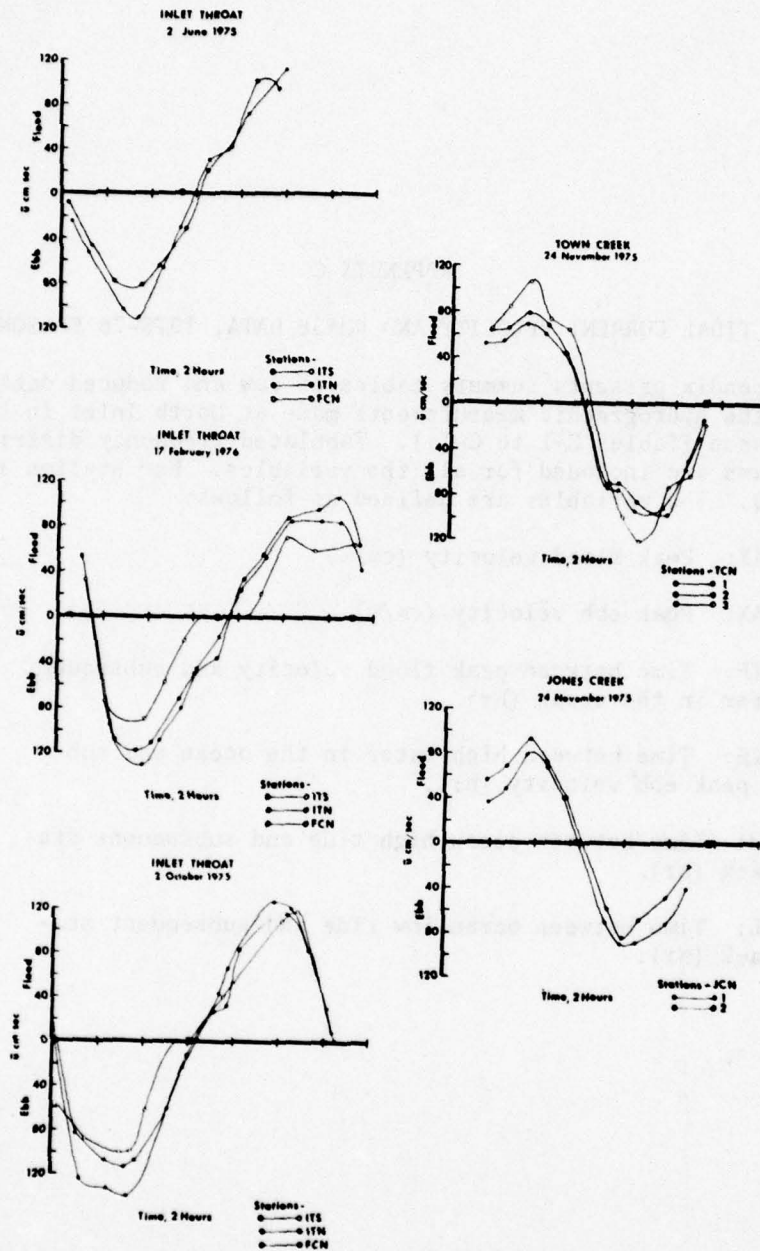


Figure B-15. Current velocity time series at the inlet throat, 2 June, 2 October 1975, and 17 February 1976, and at Town and Jones Creeks 24 November 1975.

APPENDIX C

TIDAL CURRENT VELOCITY AND PHASE DATA, 1975-76 SEASON

This appendix presents summary tables of raw and reduced data pertaining to the hydrographic measurements made at North Inlet in the 1975-76 field season (Tables C-1 to C-11). Tabulated frequency distributions and histograms are included for all the variables. For station locations, see Figure 9. The variables are defined as follows:

VFMAX: Peak flood velocity (cm/s)

VEMAX: Peak ebb velocity (cm/s)

DELTF: Time between peak flood velocity and subsequent high water in the ocean (hr).

DELTE: Time between high water in the ocean and subsequent peak ebb velocity (hr).

LAGH: Time between ocean high tide and subsequent station slack (hr).

LAGL: Time between ocean low tide and subsequent station slack (hr).

THIS PAGE IS BEST QUALITY PRACTICABLE
FROM COPY FURNISHED TO DDG

Table C-1. Measured hydraulic parameters at North Inlet.

OBS	STATION	DATE	VFMAX	VEMAX	DELTF	DELTE	LAGH	LAGL
1	ITS	51976	56	96	1.3	3.0	0.6	.
2	ITS	42776	76	.	1.4	.	.	.
3	ITS	32776	65	132	1.3	.	1.5	0.4
4	ITS	32276	62	70	1.4	2.6	0.6	.
5	ITS	31576	114	150	1.4	2.6	1.4	0.4
6	ITS	21776	105	120	0.7	3.2	1.0	0.5
7	ITS	10776	60	85	1.8	3.5	1.2	.
8	ITS	100275	114	113	1.7	3.2	0.4	0.3
9	ITS	60275	101	85	3.0	2.2	0.8	.
10	ITN	51976	75	80	1.4	3.1	0.9	.
11	ITN	42776	81	80	1.8	2.3	0.8	0.5
12	ITN	32776	64	106	0.5	.	.	0.3
13	ITN	32276	74	63	1.6	3.5	0.7	.
14	ITN	31576	125	127	1.7	4.1	0.8	0.2
15	ITN	21776	82	132	2.5	3.0	1.0	0.5
16	ITN	10776	64	96	2.8	3.7	0.9	.
17	ITN	100275	125	140	2.3	3.3	0.4	0.2
18	ITN	60275	.	114	.	.	.	0.6
19	FCN	51976	67	84	0.5	2.3	0.6	0.5
20	FCN	42776	66	108	1.0	2.3	0.6	0.1
21	FCN	32776	66	114	0.4	.	.	0.2
22	FCN	32276	56	74	1.6	1.7	0.2	.
23	FCN	31576	123	.	1.6	.	1.0	0.2
24	FCN	21776	72	92	2.9	2.3	1.0	.
25	FCN	10776	62	76	1.7	3.9	1.1	.
26	FCN	100275	117	100	1.2	3.0	0.4	.
27	JCN	51976	61	66	1.1	3.5	1.0	.
28	JCN	32475	36	54	0.9	2.6	1.0	0.6
29	JCN	31576	99	91	0.6	2.8	.	.
30	JCN	11776	64	109	0.2	2.1	0.9	0.5
31	JCN	11576	44	73	0.9	.	1.0	0.6
32	JCN	11076	24	39	0.5	3.0	0.8	.
33	JCN	112475	80	90	1.9	2.3	0.3	.
34	JCN	112575	54	60	1.9	2.0	0.4	.
35	JCN	110475	82	108	1.0	3.7	.	0.4
36	JCN	92975	78	89	1.7	2.8	0.2	.
37	JCN	92675	66	74	1.7	2.5	0.2	0.1
38	JCN	82675	63	71	0.7	1.3	.	0.6
39	JCN	72675	61	70	1.0	3.2	0.9	.
40	JCN	61775	78	.	1.0	.	0.8	.
41	JCN	61075	.	79	.	4.0	.	0.6
42	JCN	61475	76	84	0.5	3.3	1.1	0.9
43	JCS	51976	50	64	0.5	3.4	0.9	.
44	JCS	32476	38	37	0.3	2.4	1.1	0.5
45	JCS	31576	92	77	0.7	3.6	.	0.1
46	JCS	11776	72	80	0.4	2.7	1.0	0.2
47	JCS	11576	50	57	1.1	.	1.0	0.6
48	JCS	11076	30	30	1.6	3.3	0.9	.
49	JCS	112475	90	83	1.9	2.2	0.4	.
50	JCS	112575	69	62	1.0	2.4	0.7	.
51	JCS	110475	101	86	2.3	2.9	.	0.4
52	JCS	92975	74	66	1.5	2.9	0.3	.
53	JCS	92675	65	52	1.7	2.9	0.4	0.1
54	JCS	82675	60	60	1.3	1.7	0.0	0.7
55	JCS	72675	50	59	2.0	2.4	0.8	.
56	JCS	61775	86	.	1.1	.	1.1	.
57	JCS	61075	.	63	.	3.8	.	1.2
58	JCS	61475	74	72	0.0	3.9	1.2	1.0
59	TCN	32476	37	63	1.8	3.2	1.0	0.4
60	TCN	32276	42	82	1.0	2.9	1.0	.
61	TCN	11776	56	122	1.0	3.6	0.8	0.3
62	TCN	11576	66	78	1.1	.	1.2	0.5
63	TCN	11076	29	38	1.8	4.0	0.7	0.0

THIS PAGE IS BEST QUALITY PRACTICABLE
FROM COPY FURNISHED TO DDC

Table C-1. Measured hydraulic parameters at North Inlet.--
Continued

OBS	STATION	DATE	VFMAX	VEMAX	DELTF	DELTE	LAGH	LAGL
64	TCN	112475	67	86	2.3	3.1	0.2	.
65	TCN	100475	80	130	1.4	2.7	0.6	0.7
66	TCN	92975	68	.	1.7	.	0.7	.
67	TCN	92675	59	76	1.5	3.5	0.4	0.7
68	TCN	82675	.	85	.	1.9	0.4	0.6
69	TCN	72975	52	72	1.2	4.2	0.6	.
70	TCN	61775	77	102	1.3	3.6	0.9	.
71	TCN	61475	78	102	0.5	4.8	1.8	1.2
72	TCN	61075	.	87	.	3.6	0.2	0.6
73	TCM	32475	43	54	1.6	3.2	0.9	0.5
74	TCM	32276	50	81	1.0	3.1	1.3	0.5
75	TCM	11776	60	108	0.9	2.7	0.6	0.5
76	TCM	11576	59	71	1.0	.	1.4	1.0
77	TCM	11076	25	36	1.3	4.1	1.1	0.0
78	TCM	112475	77	86	2.2	4.0	0.3	.
79	TCM	100475	108	126	1.2	2.9	0.8	0.6
80	TCM	92975	71	.	1.1	.	0.6	.
81	TCM	92675	48	65	2.4	3.5	0.8	0.6
82	TCM	82675	.	66	.	2.2	0.4	0.4
83	TCN	72975	63	68	2.1	4.5	0.5	.
84	TCM	61775	82	.	0.6	.	0.9	.
85	TCM	61475	75	86	0.5	4.1	1.7	1.6
86	TCM	61075	101	76	2.0	3.5	0.5	0.8
87	TCS	32476	66	53	1.4	3.4	0.9	0.4
88	TCS	32276	56	43	0.9	3.1	1.0	.
89	TCS	11776	78	122	0.4	2.8	0.8	0.5
90	TCS	11576	68	80	1.0	.	1.4	1.2
91	TCS	11076	28	33	1.9	3.2	1.3	0.0
92	TCS	112475	104	121	2.1	2.9	0.6	.
93	TCS	100475	108	108	1.2	3.2	0.7	0.6
94	TCS	92975	78	.	1.0	.	0.9	.
95	TCS	92675	62	71	1.7	3.6	1.0	0.2
96	TCS	82675	.	79	.	0.9	0.4	0.6
97	TCS	72975	65	68	1.3	3.0	1.1	.
98	TCS	61775	94	.	1.0	.	0.9	.
99	TCS	61475	84	89	1.3	4.2	1.9	.
100	TCS	61075	.	80	.	3.6	0.5	0.8

THIS PAGE IS BEST QUALITY PRACTICABLE
FROM COPY FURNISHED TO DDG

Table C-2. Frequency distribution of maximum flood-current velocity (cm/s).

VFMAX	FREQUENCY	CUM FREQ	PERCENT	CUM PERCENT
.	8	.	.	.
24	1	1	1.087	1.087
25	1	2	1.087	2.174
28	1	3	1.087	3.261
29	1	4	1.087	4.348
30	1	5	1.087	5.435
36	1	6	1.087	6.522
37	1	7	1.087	7.609
38	1	8	1.087	8.696
42	1	9	1.087	9.783
43	1	10	1.087	10.870
44	1	11	1.087	11.957
48	1	12	1.087	13.043
50	4	16	4.348	17.391
52	1	17	1.087	18.478
54	1	18	1.087	19.565
56	4	22	4.348	23.913
59	2	24	2.174	26.087
60	3	27	3.261	29.348
61	2	29	2.174	31.522
62	3	32	3.261	34.783
63	2	34	2.174	36.957
64	2	36	2.174	39.130
65	3	39	3.261	42.391
66	5	44	5.435	47.826
67	2	46	2.174	50.000
68	2	48	2.174	52.174
69	2	50	2.174	54.348
71	1	51	1.087	55.435
72	2	53	2.174	57.609
74	3	56	3.261	60.870
75	2	58	2.174	63.043
76	2	60	2.174	65.217
77	2	62	2.174	67.391
78	5	67	5.435	72.826
80	2	69	2.174	75.000
81	1	70	1.087	76.087
82	3	73	3.261	79.348
84	1	74	1.087	80.435
86	1	75	1.087	81.522
90	1	76	1.087	82.609
92	1	77	1.087	83.696
94	1	78	1.087	84.783
99	1	79	1.087	85.870
101	3	82	3.261	89.130
104	1	83	1.087	90.217
105	1	84	1.087	91.304
108	2	86	2.174	93.478
114	2	88	2.174	95.652
117	1	89	1.087	96.739
123	1	90	1.087	97.826
125	2	92	2.174	100.000

Table C-3. Frequency distribution of maximum ebb-current velocity (cm/s).

VEMAX	FREQUENCY	CUM FREQ	PERCENT	CUM PERCENT
30	1	1	1.099	1.099
33	1	2	1.099	2.198
36	1	3	1.099	3.297
37	1	4	1.099	4.396
38	1	5	1.099	5.495
39	1	6	1.099	6.593
43	1	7	1.099	7.692
52	1	8	1.099	8.791
53	1	9	1.099	9.890
54	2	11	2.198	12.088
57	1	12	1.099	13.187
59	1	13	1.099	14.286
60	2	15	2.198	16.484
62	1	16	1.099	17.582
63	3	19	3.297	20.879
64	1	20	1.099	21.978
65	1	21	1.099	23.077
66	3	24	3.297	26.374
68	2	26	2.198	28.571
70	2	28	2.198	30.769
71	3	31	3.297	34.066
72	2	33	2.198	36.264
73	1	34	1.099	37.363
74	2	36	2.198	39.560
76	3	39	3.297	42.857
77	1	40	1.099	43.956
78	1	41	1.099	45.055
79	2	43	2.198	47.253
80	5	48	5.495	52.747
81	1	49	1.099	53.846
82	1	50	1.099	54.945
83	1	51	1.099	56.044
84	2	53	2.198	58.242
85	3	56	3.297	61.538
86	4	60	4.396	65.934
87	1	61	1.099	67.033
89	2	63	2.198	69.231
90	1	64	1.099	70.330
91	1	65	1.099	71.429
92	1	66	1.099	72.527
95	2	68	2.198	74.725
100	1	69	1.099	75.824
102	2	71	2.198	78.022
106	1	72	1.099	79.121
108	4	76	4.396	83.516
109	1	77	1.099	84.615
113	1	78	1.099	85.714
114	2	80	2.198	87.912
120	1	81	1.099	89.011
121	1	82	1.099	90.110
122	2	84	2.198	92.308
126	1	85	1.099	93.407
127	1	86	1.099	94.505
130	1	87	1.099	95.604
132	2	89	2.198	97.802
140	1	90	1.099	98.901
150	1	91	1.099	100.000

THIS PAGE IS BEST QUALITY PRACTICABLE
FROM COPY FURNISHED TO DDC

Table C-4. Frequency distribution of the time difference between peak flood velocity (at all hydrography stations) and high water in the ocean.

DELTA	FREQUENCY	CUM FREQ	PERCENT	CUM PERCENT
0	1	1	1.087	1.087
0.2	1	2	1.087	2.174
0.3	1	3	1.087	3.261
0.4	3	6	3.261	6.522
0.5	7	13	7.609	14.130
0.6	2	15	2.174	16.304
0.7	3	18	3.261	19.565
0.9	4	22	4.348	23.913
1	12	34	13.043	36.957
1.1	5	39	5.435	42.391
1.2	4	43	4.348	46.739
1.3	7	50	7.609	54.348
1.4	6	56	6.522	60.870
1.5	2	58	2.174	63.043
1.6	5	63	5.435	68.478
1.7	8	71	8.696	77.174
1.8	4	75	4.348	81.522
1.9	4	79	4.348	85.870
2	2	81	2.174	88.043
2.1	2	83	2.174	90.217
2.2	1	84	1.087	91.304
2.3	3	87	3.261	94.565
2.4	1	88	1.087	95.652
2.5	1	89	1.087	96.739
2.8	1	90	1.087	97.826
2.9	1	91	1.087	98.913
3	1	92	1.087	100.000

Table C-5. Frequency distribution of the time difference between high water in the ocean and the subsequent peak ebb velocity (at all hydrography stations).

DELTA	FREQUENCY	CUM FREQ	PERCENT	CUM PERCENT
0.9	1	1	1.220	1.220
1.3	1	2	1.220	2.439
1.7	2	4	2.439	4.878
1.9	1	5	1.220	6.098
2	1	6	1.220	7.317
2.1	1	7	1.220	8.537
2.2	3	10	3.659	12.195
2.3	5	15	6.098	18.293
2.4	3	18	3.659	21.951
2.5	1	19	1.220	23.171
2.6	3	22	3.659	26.829
2.7	3	25	3.659	30.488
2.8	3	28	3.659	34.146
2.9	6	34	7.317	41.463
3	5	39	6.098	47.561
3.1	4	43	4.878	52.439
3.2	7	50	8.537	60.976
3.3	3	53	3.659	64.634
3.4	2	55	2.439	67.073
3.5	6	61	7.317	74.390
3.6	6	67	7.317	81.707
3.7	2	69	2.439	84.146
3.8	1	70	1.220	85.366
3.9	2	72	2.439	87.805
4	3	75	3.659	91.463
4.1	3	78	3.659	95.122
4.2	2	80	2.439	97.561
4.5	1	81	1.220	98.780
4.8	1	82	1.220	100.000

THIS PAGE IS BEST QUALITY PRACTICABLE
FROM COPY FURNISHED TO DDG

Table C-6. Frequency distribution of the time lag between ocean high tide and subsequent station slack.

LAGH	FREQUENCY	CUM FREQ	PERCENT	CUM PERCENT
0	11	0		
0.1	1	1	1.124	1.124
0.2	5	6	5.618	6.742
0.3	3	9	3.371	10.112
0.4	10	19	11.236	21.348
0.5	3	22	3.371	24.719
0.6	9	31	10.112	34.831
0.7	5	36	5.618	40.449
0.8	10	46	11.236	51.685
0.9	12	58	13.483	65.169
1	13	71	14.607	79.775
1.1	6	77	6.742	86.517
1.2	3	80	3.371	89.888
1.3	2	82	2.247	92.135
1.4	3	85	3.371	95.506
1.5	1	86	1.124	96.629
1.7	1	87	1.124	97.753
1.8	1	88	1.124	98.876
1.9	1	89	1.124	100.000

Table C-7. Frequency distribution of the time lag between ocean low tide and subsequent station slack.

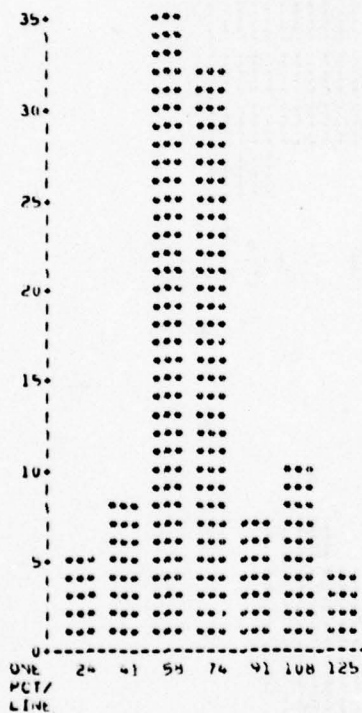
LAGL	FREQUENCY	CUM FREQ	PERCENT	CUM PERCENT
0	42	0		
0.1	3	3	5.172	5.172
0.2	4	7	6.897	12.069
0.3	6	13	10.345	22.414
0.4	3	16	5.172	27.586
0.5	7	23	12.069	39.655
0.6	11	34	18.966	58.621
0.7	11	45	18.966	77.586
0.8	3	48	5.172	82.759
0.9	3	51	5.172	87.931
1	1	52	1.724	89.655
1.1	2	54	3.448	93.103
1.2	3	57	5.172	98.276
1.6	1	58	1.724	100.000

THIS PAGE IS BEST QUALITY PRACTICABLE
FROM COPY FURNISHED TO DDC

Table C-8. Histograms and summary statistics for variables
VFMAX and VEMAX.

STATISTICS TABLE AND HISTOGRAM FOR VFMAX

NO. OF VALUES= 92
SUM= 6508
UNCORRECTED SS=308696
VARIANCE= 310.8322441306
COEF. VARIANCE=31.45093230320
NO. MISSING= 4
MEAN= 70.73912043478
CORRECTED SS= 48485.73913043
STANDARD DEVIATION=22.0015444570
STANDARD ERROR= 3.552524479746



STATISTICS TABLE AND HISTOGRAM FOR VEMAX

NO. OF VALUES= 91
SUM= 7534
UNCORRECTED SS=682763
VARIANCE= 653.8715506716
COEF. VARIANCE=30.82192448577
NO. MISSING= 9
MEAN= 82.80219780220
CORRECTED SS= 58846.63954044
STANDARD DEVIATION=25.57091219866
STANDARD ERROR= 7.185401655731

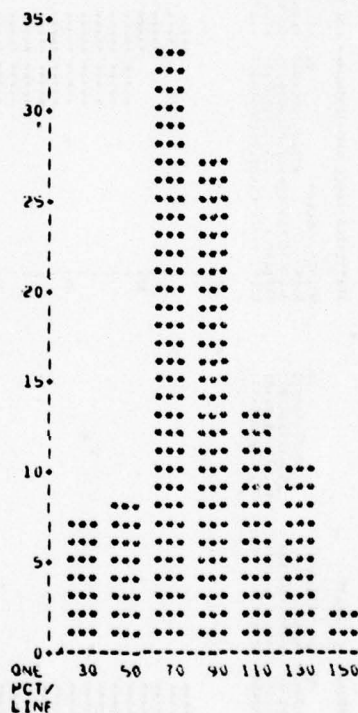
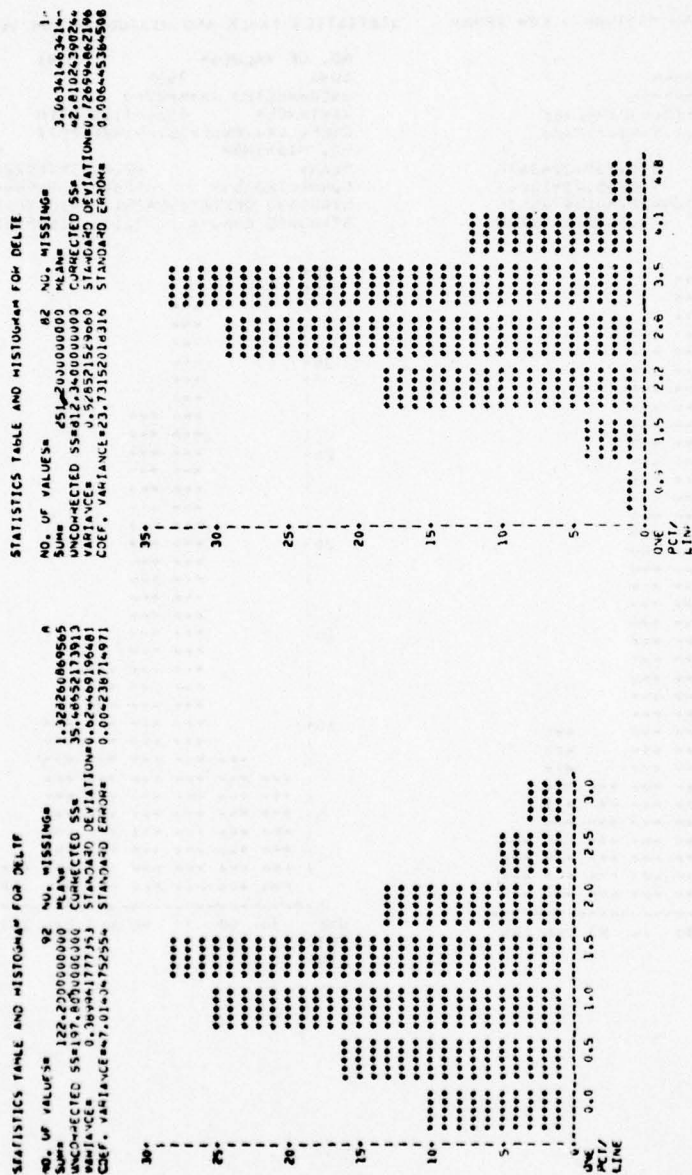
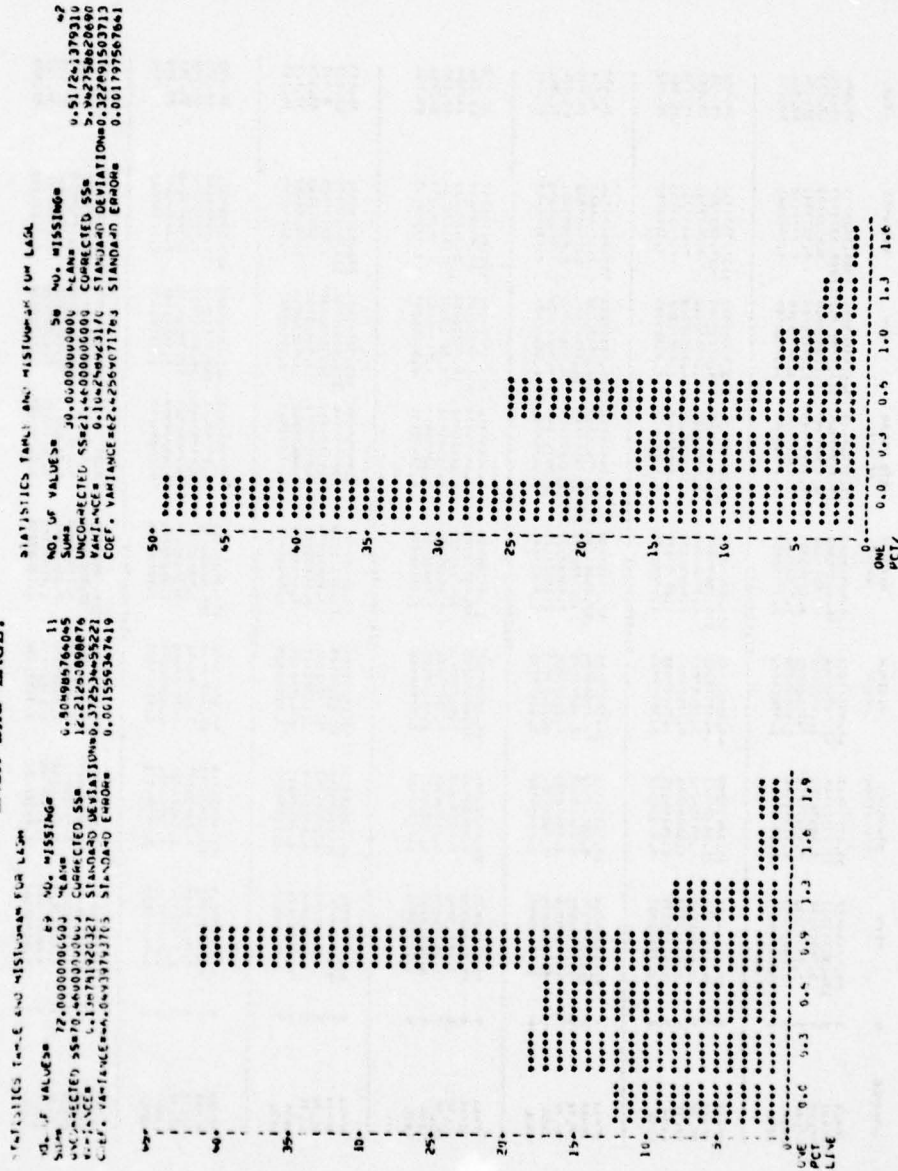


Table C-9. Histograms and summary statistics for variables
DELTF and DELTE.



THIS PAGE IS BEST QUALITY PRACTICABLE
FROM COPY FURNISHED TO DDG

Table C-10. Histograms and summary statistics for variables
LAGH and LAGL.



THIS PAGE IS BEST QUALITY PRACTICABLE
FROM COPY FURNISHED TO DDG

Table C-11. Hydraulic parameters of the North Inlet system summarized by station.

STATE	N	MEAN	STANDARD DEVIATION	MINIMUM VALUE	MAXIMUM VALUE	STD DEVE OF MEAN	SUM	VARIANCE	C.V.
ALAB	3	62.46666667	31.0050812	44.00000000	110.00000000	19.05547657	248.00000000	1089.33333333	39.021
ALAB	3	126.33333333	32.53203549	91.00000000	156.00000000	7.262176666	377.00000000	1059.33333333	26.165
ALAB	3	3.300000000	0.448743765	3.000000000	4.000000000	0.176585000	11.00000000	0.433000000	37.323
ALAB	3	3.300000000	0.448743765	3.000000000	4.000000000	0.176585000	11.00000000	0.433000000	37.323
ALAB	3	1.000000000	0.591619295	1.000000000	2.000000000	0.31792923	3.00000000	0.270000000	47.238
ALAB	2	0.400000000	0.606916765	0.300000000	1.000000000	0.30000000	1.30000000	0.25000000	76.150
STATISTICS									
WYOM	3	97.00000000	31.726137000	66.00000000	130.00000000	19.47777642	283.00000000	1137.33333333	38.669
WYOM	3	97.00000000	31.726137000	66.00000000	130.00000000	19.47777642	283.00000000	1137.33333333	38.669
WYOM	3	3.000000000	0.501172230	3.000000000	4.000000000	0.200553276	12.00000000	0.4333333333	44.654
WYOM	3	1.333333333	0.642931095	1.000000000	2.000000000	0.371184229	4.00000000	0.4333333333	44.654
WYOM	3	0.700000000	0.251661115	0.700000000	1.000000000	0.145294553	2.00000000	0.0733333333	26.964
WYOM	2	0.700000000	0.595489562	0.300000000	1.000000000	0.400000000	1.60000000	0.300000000	80.812
STATISTICS									
WYOM	7	57.16268716	10.70136151	34.00000000	77.00000000	7.666479716	400.00000000	382.16268716	36.477
WYOM	6	86.33333333	5.440776647	78.00000000	92.00000000	2.319032302	508.00000000	30.26644667	6.736
WYOM	6	0.375000000	0.629354997	0.000000000	1.000000000	0.193300460	16.00000000	0.187000000	13.630
WYOM	5	0.400000000	0.762849223	0.100000000	2.000000000	0.302359897	8.00000000	0.1952381	69.974
WYOM	6	1.190000000	0.704764962	0.400000000	1.800000000	0.352117791	4.00000000	0.24000000	77.866
STATISTICS									
WYOM	7	70.57162687	21.64203716	44.00000000	96.00000000	9.11182766	426.00000000	468.6196762	39.612
WYOM	5	76.61333333	7.406116466	65.00000000	86.00000000	0.220000000	18.00000000	0.24000000	10.566
WYOM	5	3.300000000	0.491916066	2.600000000	3.800000000	0.220000000	16.00000000	0.24000000	10.566
WYOM	7	2.65716269	0.513163699	0.700000000	2.600000000	0.23182212	10.20000000	0.37619066	42.992
WYOM	6	0.292000000	0.30311502	0.000000000	1.000000000	0.13666666	4.00000000	0.20000000	36.990
WYOM	6	1.190000000	0.704911662	0.500000000	2.000000000	0.36675733	4.60000000	0.52333333	66.653
STATISTICS									
WYOM	5	42.37600000	14.63166666	21.00000000	61.00000000	5.84259368	499.00000000	276.83024571	26.675
WYOM	7	90.31250000	8.210000000	82.00000000	98.00000000	4.20217764	679.00000000	123.0076190	11.530
WYOM	5	3.000000000	0.20465762	2.000000000	4.000000000	0.23182212	15.00000000	0.04000000	8.177
WYOM	7	1.45716269	0.613363699	1.000000000	2.000000000	0.31927616	3.00000000	0.08200000	37.255
WYOM	3	0.633333333	0.206850911	0.600000000	0.900000000	0.04432760	3.00000000	0.02466667	32.150
WYOM	3	0.700000000	0.100000000	0.600000000	0.800000000	0.05773503	2.10000000	0.01000000	14.285
STATISTICS									
WYOM	5	42.37600000	14.63166666	21.00000000	61.00000000	5.84259368	499.00000000	276.83024571	26.675
WYOM	7	90.31250000	8.210000000	82.00000000	98.00000000	4.20217764	679.00000000	123.0076190	11.530
WYOM	5	3.000000000	0.20465762	2.000000000	4.000000000	0.23182212	15.00000000	0.04000000	8.177
WYOM	7	1.45716269	0.613363699	1.000000000	2.000000000	0.31927616	3.00000000	0.08200000	37.255
WYOM	3	0.633333333	0.206850911	0.600000000	0.900000000	0.04432760	3.00000000	0.02466667	32.150
WYOM	3	0.700000000	0.100000000	0.600000000	0.800000000	0.05773503	2.10000000	0.01000000	14.285
STATISTICS									
WYOM	5	42.37600000	14.63166666	21.00000000	61.00000000	5.84259368	499.00000000	276.83024571	26.675
WYOM	7	90.31250000	8.210000000	82.00000000	98.00000000	4.20217764	679.00000000	123.0076190	11.530
WYOM	5	3.000000000	0.20465762	2.000000000	4.000000000	0.23182212	15.00000000	0.04000000	8.177
WYOM	7	1.45716269	0.613363699	1.000000000	2.000000000	0.31927616	3.00000000	0.08200000	37.255
WYOM	3	0.633333333	0.206850911	0.600000000	0.900000000	0.04432760	3.00000000	0.02466667	32.150
WYOM	3	0.700000000	0.100000000	0.600000000	0.800000000	0.05773503	2.10000000	0.01000000	14.285
STATISTICS									
WYOM	5	42.37600000	14.63166666	21.00000000	61.00000000	5.84259368	499.00000000	276.83024571	26.675
WYOM	7	90.31250000	8.210000000	82.00000000	98.00000000	4.20217764	679.00000000	123.0076190	11.530
WYOM	5	3.000000000	0.20465762	2.000000000	4.000000000	0.23182212	15.00000000	0.04000000	8.177
WYOM	7	1.45716269	0.613363699	1.000000000	2.000000000	0.31927616	3.00000000	0.08200000	37.255
WYOM	3	0.633333333	0.206850911	0.600000000	0.900000000	0.04432760	3.00000000	0.02466667	32.150
WYOM	3	0.700000000	0.100000000	0.600000000	0.800000000	0.05773503	2.10000000	0.01000000	14.285
STATISTICS									
WYOM	5	42.37600000	14.63166666	21.00000000	61.00000000	5.84259368	499.00000000	276.83024571	26.675
WYOM	7	90.31250000	8.210000000	82.00000000	98.00000000	4.20217764	679.00000000	123.0076190	11.530
WYOM	5	3.000000000	0.20465762	2.000000000	4.000000000	0.23182212	15.00000000	0.04000000	8.177
WYOM	7	1.45716269	0.613363699	1.000000000	2.000000000	0.31927616	3.00000000	0.08200000	37.255
WYOM	3	0.633333333	0.206850911	0.600000000	0.900000000	0.04432760	3.00000000	0.02466667	32.150
WYOM	3	0.700000000	0.100000000	0.600000000	0.800000000	0.05773503	2.10000000	0.01000000	14.285
STATISTICS									
WYOM	5	42.37600000	14.63166666	21.00000000	61.00000000	5.84259368	499.00000000	276.83024571	26.675
WYOM	7	90.31250000	8.210000000	82.00000000	98.00000000	4.20217764	679.00000000	123.0076190	11.530
WYOM	5	3.000000000	0.20465762	2.000000000	4.000000000	0.23182212	15.00000000	0.04000000	8.177
WYOM	7	1.45716269	0.613363699	1.000000000	2.000000000	0.31927616	3.00000000	0.08200000	37.255
WYOM	3	0.633333333	0.206850911	0.600000000	0.900000000	0.04432760	3.00000000	0.02466667	32.150
WYOM	3	0.700000000	0.100000000	0.600000000	0.800000000	0.05773503	2.10000000	0.01000000	14.285
STATISTICS									
WYOM	5	42.37600000	14.63166666	21.00000000	61.00000000	5.84259368	499.00000000	276.83024571	26.675
WYOM	7	90.31250000	8.210000000	82.00000000	98.00000000	4.20217764	679.00000000	123.0076190	11.530
WYOM	5	3.000000000	0.20465762	2.000000000	4.000000000	0.23182212	15.00000000	0.04000000	8.177
WYOM	7	1.45716269	0.613363699	1.000000000	2.000000000	0.31927616	3.00000000	0.08200000	37.255
WYOM	3	0.633333333	0.206850911	0.600000000	0.900000000	0.04432760	3.00000000	0.02466667	32.150
WYOM	3	0.700000000	0.100000000	0.600000000	0.800000000	0.05773503	2.10000000	0.01000000	14.285
STATISTICS									
WYOM	5	42.37600000	14.63166666	21.00000000	61.00000000	5.84259368	499.00000000	276.83024571	26.675
WYOM	7	90.31250000	8.210000000	82.00000000	98.00000000	4.20217764	679.00000000	123.0076190	11.530
WYOM	5	3.000000000	0.20465762	2.000000000	4.000000000	0.23182212	15.00000000	0.04000000	8.177
WYOM	7	1.45716269	0.613363699	1.000000000	2.000000000	0.31927616	3.00000000	0.08200000	37.255
WYOM	3	0.633333333	0.206850911	0.600000000	0.900000000	0.04432760	3.00000000	0.02466667	32.150
WYOM	3	0.700000000	0.100000000	0.600000000	0.800000000	0.05773503	2.10000000	0.01000000	14.285
STATISTICS									
WYOM	5	42.37600000	14.63166666	21.00000000	61.00000000	5.84259368	499.00000000	276.83024571	26.675
WYOM	7	90.31250000	8.210000000	82.00000000	98.00000000	4.20217764	679.00000000	123.0076190	11.530
WYOM	5	3.000000000	0.20465762	2.000000000	4.000000000	0.23182212	15.00000000	0.04000000	8.177
WYOM	7	1.45716269	0.613363699	1.000000000	2.000000000	0.31927616	3.00000000	0.08200000	37.255
WYOM	3	0.633333333	0.206850911	0.600000000	0.900000000	0.04432760	3.00000000	0.02466667	32.150
WYOM	3	0.700000000	0.100000000	0.600000000	0.800000000	0.05773503	2.10000000	0.01000000	14.285
STATISTICS									
WYOM	5	42.37600000	14.63166666	21.00000000	61.00000000	5.84259368	499.00000000	276.83024571	26.675
WYOM	7	90.31250000	8.210000000	82.00000000	98.00000000	4.20217764	679.00000000	123.0076190	11.530
WYOM	5	3.000000000	0.20465762	2.000000000	4.000000000	0.23182212	15.00000000	0.04000000	8.177
WYOM	7	1.45716269	0.613363699	1.000000000	2.000000000	0.31927616	3.00000000	0.08200000	37.255
WYOM	3	0.633333333	0.206850911	0.600000000	0.900000000	0.04432760	3.00000000	0.02466667	32.150
WYOM	3	0.700000000	0.100000000	0.600000000	0.800000000	0.05773503	2.10000000	0.01000000	14.285
STATISTICS									
WYOM	5	42.37600000	14.63166666	21.00000000	61.00000000	5.84259368	499.00000000	276.83024571	26.675
WYOM	7	90.31250000	8.210000000	82.00000000	98.00000000	4.20217764	679.00000000	123.0076190	11.530
WYOM	5	3.000000000	0.20465762	2.000000000	4.000000000	0.23182212	15.00000000	0.04000000	8.177
WYOM	7	1.45716269	0.613363699	1.000000000	2.000000000	0.31927616	3.000		

APPENDIX D

TIDAL CURRENT VELOCITY AND PHASE DATA, 1974-75 SEASON

This appendix presents summary tables of raw and reduced data pertaining to the hydrographic measurements made at North Inlet in the 1974-75 field season. Tabulated frequency distributions and histograms are included for all the variables (Tables D-1 to D-11). For station locations, see Figure 9. The variables are defined as follows:

VFMAX: Peak flood velocity (cm/s)

VEMAX: Peak ebb velocity (cm/s)

DELTF: Time between peak flood velocity and subsequent high water in the ocean (hr).

DELTE: Time between high water in the ocean and subsequent peak ebb velocity (hr).

LAGH: Time between ocean high tide and subsequent station slack (hr).

LAGL: Time between ocean low tide and subsequent station slack (hr).

THIS PAGE IS BEST QUALITY PRACTICABLE
 FROM COPY FURNISHED TO DDG

Table D-1. Measured hydraulic parameters at North Inlet.

OBS	STATION	DATE	VFMAX	VEMAX	DELTF	DELTE	LAGH	LAGL
1	ITN	91974	110	156	2.1	3.1	0.8	1.0
2	ITN	32175	46	91	2.0	3.6	0.8	.
3	ITN	42675	92	126	1.1	4.4	1.7	0.3
4	ITS	91974	111	118	1.7	3.6	0.7	1.1
5	ITS	32175	49	78	1.9	3.2	1.2	.
6	ITS	42675	103	103	0.7	4.2	0.9	0.3
7	TCN1	82474	65	91	1.7	3.3	0.8	0.8
8	TCN1	91574	88	105
9	TCN1	92174	50	104	2.2	3.3	0.6	.
10	TCN1	92774	62	.	2.9	.	.	0.6
11	TCN1	22275	61	99	1.4	3.9	0.9	.
12	TCN1	31975	42	81	1.5	3.2	0.4	.
13	TCN1	32275	47	82	2.2	3.2	0.4	.
14	TCN1	32475	84	108	1.1	.	0.7	0.7
15	TCN2	82474	90	96	1.6	3.7	1.1	.
16	TCN2	91574	128	88
17	TCN2	92174	81	96	1.4	3.2	0.8	.
18	TCN2	92774	77	.	2.7	.	.	0.6
19	TCN2	22275	67	81	0.7	2.6	1.2	.
20	TCN2	31975	60	72	1.9	3.9	0.8	.
21	TCN2	32275	60	69	1.9	3.0	0.6	.
22	TCN2	32475	78	100	2.1	.	0.8	1.1
23	TCN3	82474	72	87	1.5	3.8	1.2	.
24	TCN3	91574	116	96
25	TCN3	92174	81	78	0.7	3.2	0.8	.
26	TCN3	92774	73	.	1.8	.	.	0.3
27	TCN3	22275	70	76	0.5	4.2	1.4	.
28	TCN3	31975	59	74	2.0	3.6	0.4	0.3
29	TCN3	32275	60	65	1.9	3.2	0.7	.
30	TCN3	32475	75	97	2.0	.	0.9	1.1
31	JCN1	82474	72	84	0.2	3.5	1.4	1.7
32	JCN1	92174	77	89	0.6	3.3	1.0	.
33	JCN1	92774	74	.	2.1	.	.	0.7
34	JCN1	22275	68	84	0.4	3.2	2.0	.
35	JCN1	31975	34	76	2.2	3.6	0.4	0.4
36	JCN1	32275	36	81	1.1	2.5	0.1	.
37	JCN1	32475	39	92	1.4	.	.	1.8
38	JCN2	82474	58	75	0.7	3.7	1.0	2.1
39	JCN2	92174	94	78	0.9	3.2	1.1	.
40	JCN2	92774	90	.	1.7	.	.	0.5
41	JCN2	22275	91	85	1.1	3.6	1.0	.
42	JCN2	31975	44	65	2.4	3.8	0.6	0.5
43	JCN2	32275	47	69	1.4	2.6	0.4	.
44	JCN2	32475	70	83	2.0	.	.	1.5
45	JCN3	31975	26	59	1.1	3.9	0.5	.

THIS PAGE IS BEST QUALITY PRACTICABLE
FROM COPY FURNISHED TO DDC

Table D-2. Frequency distribution of maximum flood-current velocity (cm/s).

VFMAX	FREQUENCY	CUM FREQ	PERCENT	CUM PERCENT
26	1	1	2.222	2.222
34	1	2	2.222	4.444
36	1	3	2.222	6.667
39	1	4	2.222	8.889
42	1	5	2.222	11.111
44	1	6	2.222	13.333
46	1	7	2.222	15.556
47	2	9	4.444	20.000
49	1	10	2.222	22.222
50	1	11	2.222	24.444
58	1	12	2.222	26.667
59	1	13	2.222	28.889
60	3	16	6.667	35.556
61	1	17	2.222	37.778
62	1	18	2.222	40.000
65	1	19	2.222	42.222
67	1	20	2.222	44.444
68	1	21	2.222	46.667
70	2	23	4.444	51.111
72	2	25	4.444	55.556
73	1	26	2.222	57.778
74	1	27	2.222	60.000
75	1	28	2.222	62.222
77	2	30	4.444	66.667
78	1	31	2.222	68.889
81	2	33	4.444	73.333
84	1	34	2.222	75.556
88	1	35	2.222	77.778
90	2	37	4.444	82.222
91	1	38	2.222	84.444
92	1	39	2.222	86.667
94	1	40	2.222	88.889
103	1	41	2.222	91.111
110	1	42	2.222	93.333
111	1	43	2.222	95.556
116	1	44	2.222	97.778
128	1	45	2.222	100.000

THIS PAGE IS BEST QUALITY PRACTICABLE
FROM COPY FURNISHED TO DDG

Table D-3. Frequency distribution of maximum ebb-current velocity (cm/s).

VE MAX	FREQUENCY	CUM FREQ	PERCENT	CUM PERCENT
59	1	1	2.500	2.500
65	2	3	5.000	7.500
69	2	5	5.000	12.500
72	1	6	2.500	15.000
74	1	7	2.500	17.500
75	1	8	2.500	20.000
76	2	10	5.000	25.000
78	3	13	7.500	32.500
81	3	16	7.500	40.000
82	1	17	2.500	42.500
83	1	18	2.500	45.000
84	2	20	5.000	50.000
85	1	21	2.500	52.500
87	1	22	2.500	55.000
88	1	23	2.500	57.500
89	1	24	2.500	60.000
91	2	26	5.000	65.000
92	1	27	2.500	67.500
95	3	30	7.500	75.000
97	1	31	2.500	77.500
99	1	32	2.500	80.000
100	1	33	2.500	82.500
103	1	34	2.500	85.000
104	1	35	2.500	87.500
105	1	36	2.500	90.000
108	1	37	2.500	92.500
118	1	38	2.500	95.000
126	1	39	2.500	97.500
156	1	40	2.500	100.000

Table D-4. Frequency distribution of the time difference between peak flood velocity (at all hydrography stations) and high water in the ocean.

DELTF	FREQUENCY	CUM FREQ	PERCENT	CUM PERCENT
0.2	1	1	2.381	2.381
0.4	1	2	2.381	4.762
0.5	1	3	2.381	7.143
0.5	1	4	2.381	9.524
0.7	4	8	9.524	19.048
0.9	1	9	2.381	21.429
1.1	5	14	11.905	33.333
1.4	4	18	9.524	42.857
1.5	2	20	4.762	47.619
1.6	1	21	2.381	50.000
1.7	3	24	7.143	57.143
1.8	1	25	2.381	59.524
1.9	4	29	9.524	69.048
2	4	33	9.524	78.571
2.1	3	36	7.143	85.714
2.2	3	39	7.143	92.857
2.4	1	40	2.381	95.238
2.7	1	41	2.381	97.619
2.9	1	42	2.381	100.000

THIS PAGE IS BEST QUALITY PRACTICABLE
FROM COPY FURNISHED TO DDC

Table D-5. Frequency distribution of the time difference between high water in the ocean and the subsequent peak ebb velocity (at all hydrography stations).

DELTE	FREQUENCY	CUM FREQ	PERCENT	CUM PERCENT
.	13	.	.	.
2.5	1	1	3.125	3.125
2.6	2	3	6.250	9.375
3	1	4	3.125	12.500
3.1	1	5	3.125	15.625
3.2	8	13	25.000	40.625
3.3	3	16	9.375	50.000
3.5	1	17	3.125	53.125
3.6	5	22	15.625	68.750
3.7	2	24	6.250	75.000
3.8	2	26	6.250	81.250
3.9	3	29	9.375	90.625
4.2	2	31	6.250	96.875
4.4	1	32	3.125	100.000

Table D-6. Frequency distribution of the time lag between ocean high tide and subsequent station slack.

LAGH	FREQUENCY	CUM FREQ	PERCENT	CUM PERCENT
.	10	.	.	.
0.1	1	1	2.857	2.857
0.4	5	6	14.286	17.143
0.5	1	7	2.857	20.000
0.6	3	10	8.571	28.571
0.7	3	13	8.571	37.143
0.8	7	20	20.000	57.143
0.9	3	23	8.571	65.714
1	3	26	8.571	74.286
1.1	2	28	5.714	80.000
1.2	3	31	8.571	88.571
1.4	2	33	5.714	94.286
1.7	1	34	2.857	97.143
2	1	35	2.857	100.000

Table D-7. Frequency distribution of the time lag between ocean low tide and subsequent station slack.

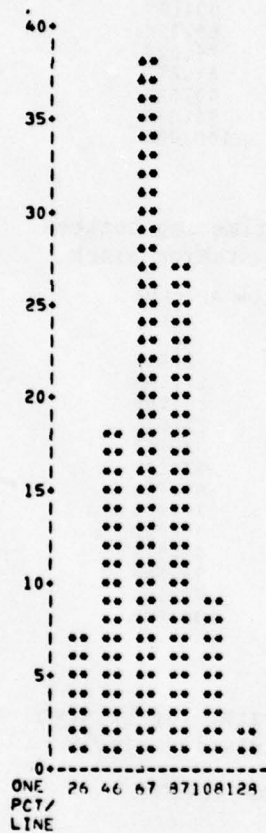
LAGL	FREQUENCY	CUM FREQ	PERCENT	CUM PERCENT
.	25	.	.	.
0.3	4	4	20.000	20.000
0.4	1	5	5.000	25.000
0.5	2	7	10.000	35.000
0.6	2	9	10.000	45.000
0.7	2	11	10.000	55.000
0.8	1	12	5.000	60.000
1	1	13	5.000	65.000
1.1	3	16	15.000	80.000
1.5	1	17	5.000	85.000
1.7	1	18	5.000	90.000
1.8	1	19	5.000	95.000
2.1	1	20	5.000	100.000

THIS PAGE IS BEST QUALITY PRACTICABLE
FROM COPY FURNISHED TO DDC

Table D-8. Histograms and summary statistics for variables VFMAX and VEMAX.

STATISTICS TABLE AND HISTOGRAM FOR VFMAX

NO. OF VALUES= 45
SUM= 3177
UNCORRECTED SS=247445
VARIANCE= 526.1090909091
COEF. VARIANCE=32.4897649486
NO. MISSING= 0
MEAN= 70.600000000000
CORRECTED SS= 23148.800000000
STANDARD DEVIATION=22.93706805390
STANDARD ERROR= 11.69131313131



STATISTICS TABLE AND HISTOGRAM FOR VEMAX

NO. OF VALUES= 40
SUM= 3537
UNCORRECTED SS=325543
VARIANCE= 327.7891025641
COEF. VARIANCE=20.47491875445
NO. MISSING= 5
MEAN= 88.425000000000
CORRECTED SS= 12783.775000000
STANDARD DEVIATION=18.10496690862
STANDARD ERROR= 8.194727564103

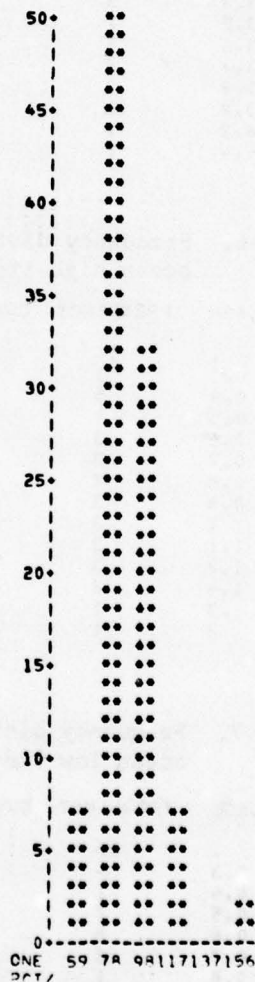


Table D-9. Histograms and summary statistics for variables
DELTF and DELTE.

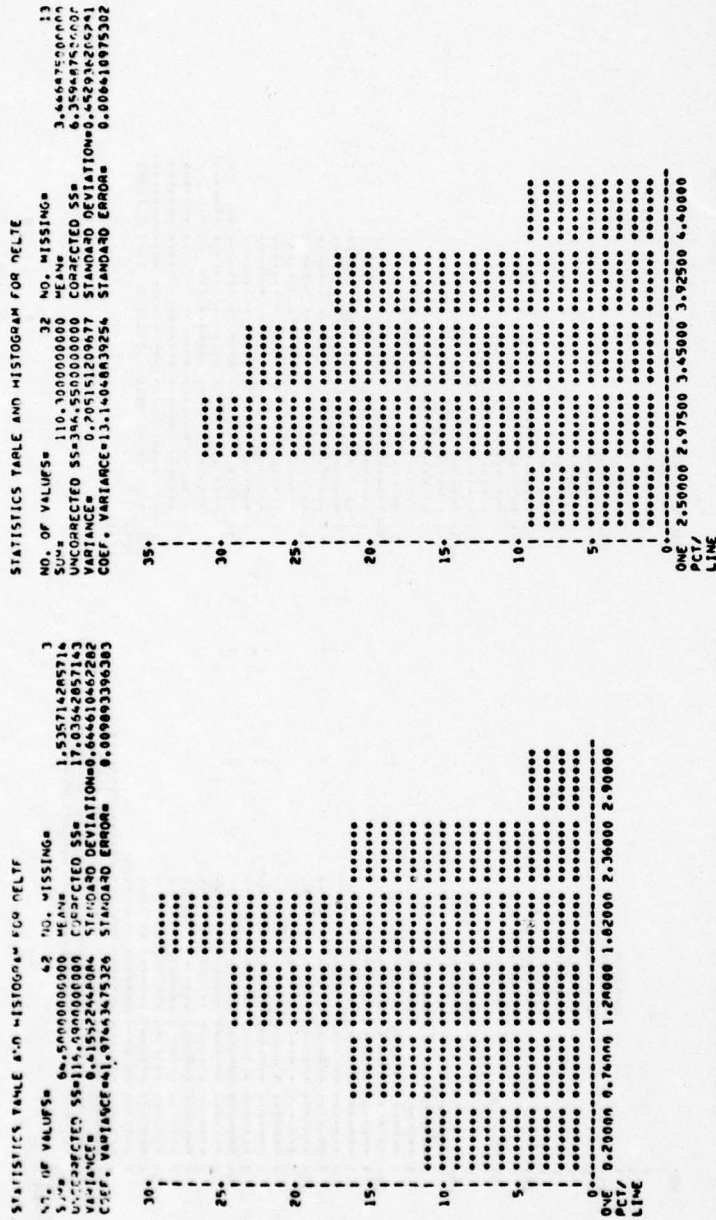
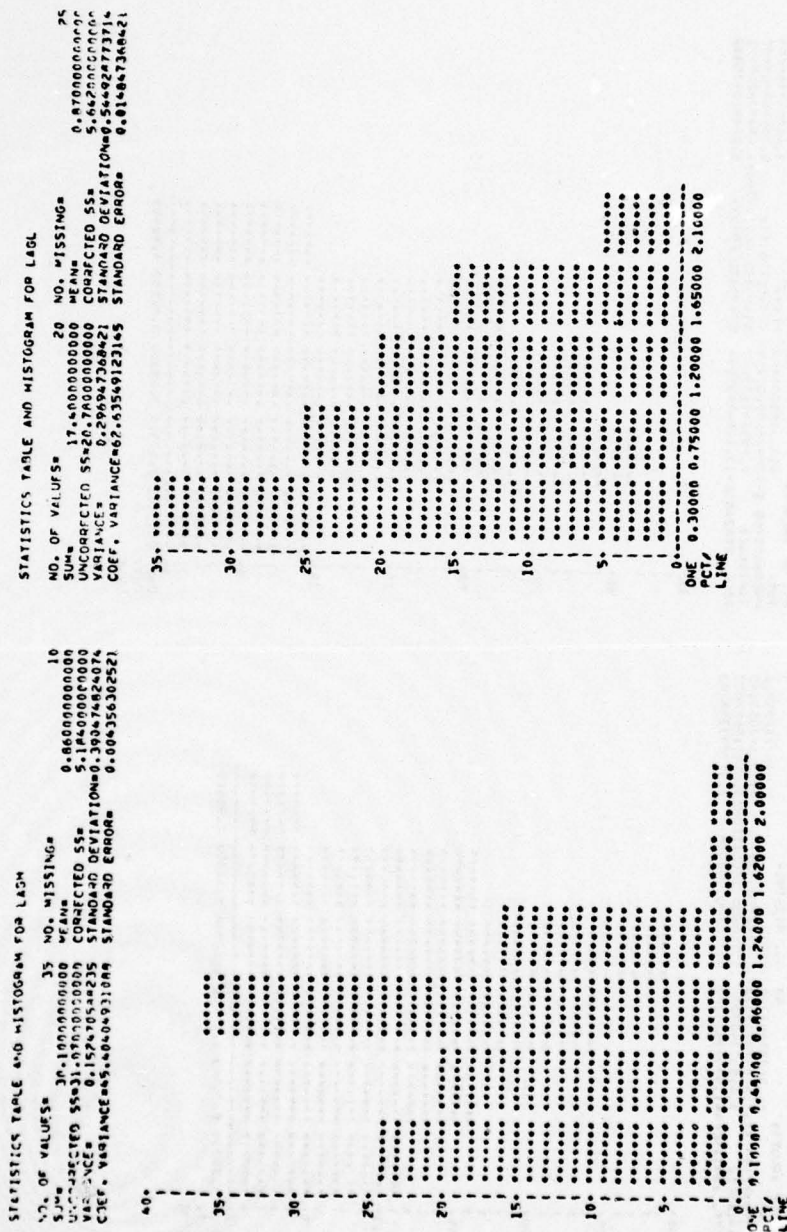


Table D-10. Histograms and summary statistics for variables LAGH and LAGL.



THIS PAGE IS BEST QUALITY PRACTICABLE
FROM COPY FURNISHED TO DDG

165

APPENDIX E

HOURLY CURRENT VELOCITY READINGS AND WATER SURFACE DIFFERENTIALS

This appendix presents hourly velocity readings (integrated means through a vertical column) at all North Inlet hydrography stations for the 1975-1976 field season (Tables E-1 and E-2). The hourly water surface differentials were obtained from simultaneous tide records at the ocean, Jones Creek, and Town Creek gages (Figs. E-1, E-2, and E-3). The numerical raw data in this appendix correspond to the graphical presentation in Appendix B. For station locations see Figure 9. The variables are defined as follows:

DATE: Date of observation

TIME: Hour of observation (e.s.t.)

OCEAN: Water surface elevation at ocean gage (in cm relative to datum).

TOWN: Water surface elevation at Town Creek gage (in cm relative to datum).

JONES: Water surface elevation at Jones Creek gage (in cm relative to datum).

TCN1-FCN: Current velocity at the representative observation station.

DELTOW: Instantaneous water surface elevation difference between ocean gage and Town Creek gage (cm). Positive differential implies landward slope.

DELJON: Instantaneous water surface elevation differential between ocean gage and Jones Creek gage (cm).

VELT: Mean velocity of all three Town Creek stations (cm/s).

VELJ: Mean velocity of both Jones Creek stations (cm/s).

VELM: Mean velocity of all three inlet throat stations (cm/s).

DIFT: Absolute value of DELTOW (cm)

DIFJ: Absolute value of DELJON (cm)

AVELT: Absolute value of VELT (cm/s)

AVELJ: Absolute value of VELJ (cm/s)

THIS PAGE IS BEST QUALITY PRACTICABLE
FROM COPY FURNISHED TO DDC

Table E-1. Current velocity readings (integrated means) at each station (cm/s), water surface elevations (cm), and elevation differentials (cm).

[illegible]

THIS PAGE IS BEST QUALITY PRACTICABLE
FROM COPY FURNISHED TO DDG

Table E-1. Current velocity readings (integrated means) at each station (cm/s), water surface elevations (cm), and elevation differentials (cm).--
Continued

[illegible]

THIS PAGE IS BEST QUALITY PRACTICABLE
FROM COPY FURNISHED TO DDC

Table E-1. Current velocity readings (integrated means) at each station (cm/s), water surface elevations (cm), and elevation differentials (cm).--
Continued

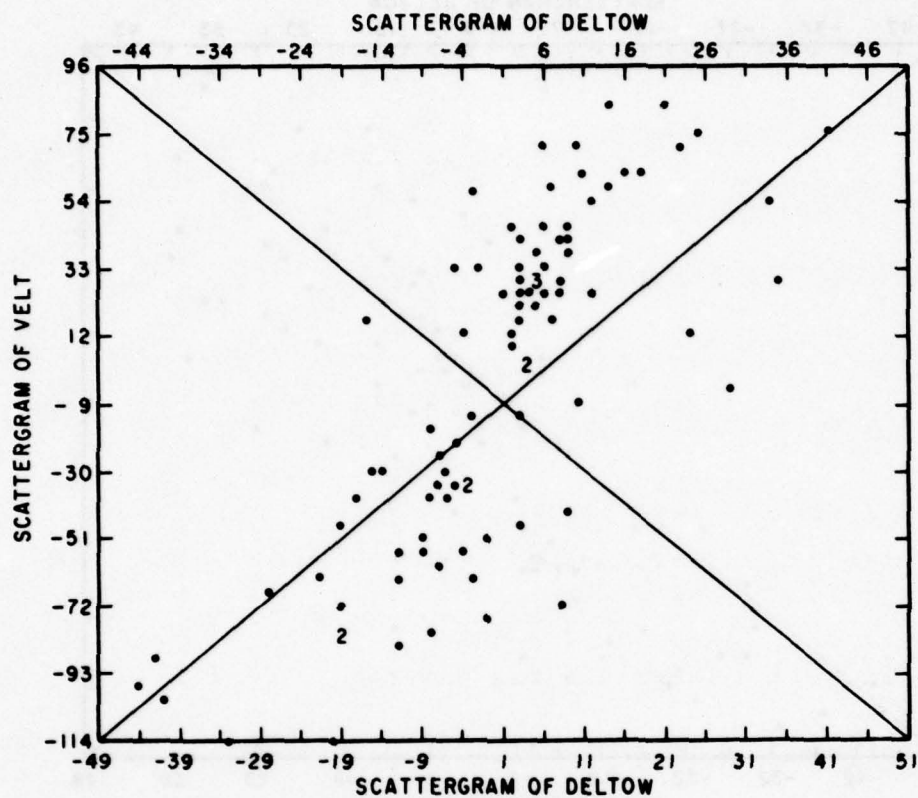
DATE	TIME	OCEN	TO-M	JONES	TC1	TC2	TC3	TC4	TC5	ITS	ITM	FCR	DELTA	DELTA	VEL	VEL	VEL
32476	1000	-29	-29	-34	10	4	8	4	4	0	0	0	0	5	7	4	0
32476	1100	-14	-17	-21	18	18	18	18	18	0	0	0	3	7	18	18	0
32476	1200	14	9	0	32	35	30	22	27	0	0	0	5	14	32	25	0
32476	1300	39	34	28	38	43	43	30	34	0	0	0	5	11	41	32	0
32476	1400	63	55	50	36	42	47	35	35	0	0	0	8	13	42	35	0
32476	1500	74	66	64	25	29	34	27	36	0	0	0	8	10	29	32	0
32476	1600	66	66	64	0	-3	-3	-2	0	0	0	0	0	2	-2	-1	0
32476	1700	50	51	53	-52	-48	-41	-46	-32	0	0	0	-1	-3	-47	-39	0
32476	1800	21	28	30	-62	-56	-53	-56	-36	0	0	0	-7	-9	-57	-46	0
32476	1900	-6	3	3	-60	-50	-41	-48	-30	0	0	0	-9	-9	-50	-39	0
32476	2000	-27	-23	-24	-38	-30	-30	-34	-19	0	0	0	-4	-3	-33	-27	0
32476	2100	-40	-41	-40	0	0	0	0	0	0	0	0	1	0	0	0	0
32476	2200	-38	-40	-45	0	0	0	0	0	0	0	0	2	7	0	0	0
32776	600	46	88	88	0	0	0	0	0	-68	-46	-78	0	-6	0	0	-64
32776	700	72	72	78	0	0	0	0	0	-118	-98	-106	-9	-18	0	0	-107
32776	800	36	45	54	0	0	0	0	0	-128	-106	-110	-10	-17	0	0	-115
32776	900	3	13	20	0	0	0	0	0	-105	-85	-64	-3	-14	0	0	-85
32776	1000	-28	-25	-14	0	0	0	0	0	-56	-48	-15	0	-6	0	0	-40
32776	1100	-52	-52	-46	0	0	0	0	0	0	0	0	3	0	7	0	0
32776	1200	-49	-49	-56	0	0	0	0	0	32	22	16	-1	9	0	0	23
32776	1300	-33	-32	-42	0	0	0	0	0	38	41	42	-1	10	0	0	40
32776	1400	-4	-3	-14	0	0	0	0	0	46	64	48	0	10	0	0	53
32776	1500	27	27	17	0	0	0	0	0	66	63	53	2	9	0	0	61
32776	1600	58	56	49	0	0	0	0	0	58	64	66	14	18	0	0	63
32776	1700	88	74	70	0	0	0	0	0	41	46	55	8	9	0	0	47
32776	1800	89	81	80	0	0	0	0	0	-10	0	26	6	4	0	0	5
32776	1900	76	70	72	0	0	0	0	0	0	0	0	0	-2	0	0	0
32776	2000	66	66	68	0	0	0	0	0	0	0	0	0	0	0	0	0
32776	600	92	83	84	0	0	0	0	0	0	0	0	3	7	0	0	11
32776	700	92	84	85	0	0	0	0	0	0	0	0	0	0	0	0	0
32776	800	88	74	65	0	0	0	0	0	-56	-76	-20	-3	0	0	0	-44
32776	900	25	45	28	0	0	0	0	0	-84	-110	-20	-3	0	0	0	-65
32776	1000	-12	8	-3	0	0	0	0	0	-78	-42	-20	-9	0	0	0	-57
32776	1100	-33	-26	-35	0	0	0	0	0	-50	-42	-7	2	0	0	0	-31
32776	1200	-44	-44	-46	0	0	0	0	0	-16	18	0	2	0	0	0	1
32776	1300	-33	-32	-29	0	0	0	0	0	0	20	30	-1	-4	0	0	17
32776	1400	-13	-12	-7	0	0	0	0	0	0	44	36	-1	-6	0	0	27
32776	1500	22	17	25	0	0	0	0	0	64	76	52	5	-3	0	0	64
32776	1600	60	53	56	0	0	0	0	0	62	80	30	7	4	0	0	57
32776	1700	84	74	75	0	0	0	0	0	73	83	51	10	9	0	0	69
32776	1800	97	93	90	0	0	0	0	0	74	65	65	4	7	0	0	68
32776	1900	97	97	94	0	0	0	0	0	23	25	0	0	3	0	0	16
32776	2000	79	83	88	0	0	0	0	0	0	0	0	-6	-1	0	0	0
32776	2100	40	54	52	0	0	0	0	0	0	0	0	-19	-12	0	0	0
51976	600	-67	-65	-67	0	0	0	0	0	0	0	0	-2	0	0	0	0
51976	700	-55	-48	-52	0	0	0	0	0	20	16	0	-7	-3	0	0	12
51976	800	-23	-26	-29	0	0	0	14	16	42	42	35	3	6	0	15	40
51976	900	13	5	6	0	0	0	22	30	48	75	49	8	7	0	26	57
51976	1000	47	41	37	0	0	0	42	35	52	75	55	4	10	0	39	61
51976	1100	75	68	62	0	0	0	50	45	58	76	65	7	13	0	48	66
51976	1200	85	79	76	0	0	0	40	44	38	55	62	6	9	0	42	52
51976	1300	71	74	74	0	0	0	-1	0	-14	4	-30	-3	-3	0	-1	-13
51976	1400	53	57	58	0	0	0	-36	-39	-60	-50	-75	-6	-5	0	-38	-62
51976	1500	16	32	29	0	0	0	-66	-56	-90	-80	-84	-16	-13	0	-61	-85
51976	1600	-18	-1	-1	0	0	0	-62	-48	-98	-78	-70	-17	-17	0	-55	-82
51976	1700	-38	-32	-33	0	0	0	-44	-30	-58	-50	-40	-6	-5	0	-37	-49
51976	1800	-42	-45	-47	0	0	0	-30	-16	-18	-16	-10	3	5	0	-23	-15
51976	1900	-36	-38	-42	0	0	0	0	0	0	0	0	2	6	0	0	0
51976	2000	-25	-26	-30	0	0	0	0	0	0	0	0	1	5	0	0	0
51976	2100	4	-2	0	0	0	0	0	0	0	0	0	6	4	0	0	0
51976	2200	33	26	28	0	0	0	0	0	0	0	0	7	5	0	0	0

THIS PAGE IS BEST QUALITY PRACTICABLE
FROM COPY FURNISHED TO DDC

Table E-2. Correlation matrix for current velocity observations.

	VELT	VELJ	VELM	TCN1	TCN2	TCN3	JCN1	JCN2	ITS	ITN	FCN
VELT	1.0000 (.01) S=0.001	0.9760 (.66) S=0.001	0.9498 (.11) S=0.001	0.9764 (.90) S=0.001	0.9929 (.91) S=0.001	0.9908 (.89) S=0.001	0.9726 (.65) S=0.001	0.9713 (.64) S=0.001	0.9686 (.11) S=0.001	0.9378 (.11) S=0.001	0.9159 (.10) S=0.001
VELJ	0.9760 (.66) S=0.001	1.0000 (.01) S=0.001	0.9844 (.22) S=0.001	0.9849 (.62) S=0.001	0.9891 (.64) S=0.001	0.9849 (.65) S=0.001	0.9960 (.89) S=0.001	0.9956 (.87) S=0.001	0.9776 (.22) S=0.001	0.9745 (.22) S=0.001	0.9646 (.21) S=0.001
VELM	0.9498 (.11) S=0.001	0.9844 (.22) S=0.001	1.0000 (.01) S=0.001	0.9613 (.11) S=0.001	0.9232 (.11) S=0.001	0.9833 (.10) S=0.001	0.9783 (.22) S=0.001	0.9855 (.21) S=0.001	0.9921 (.61) S=0.001	0.9890 (.67) S=0.001	0.9660 (.65) S=0.001
TCN1	0.9764 (.90) S=0.001	0.9849 (.62) S=0.001	0.9613 (.11) S=0.001	1.0000 (.01) S=0.001	0.9881 (.87) S=0.001	0.9809 (.84) S=0.001	0.9851 (.81) S=0.001	0.9766 (.62) S=0.001	0.9756 (.11) S=0.001	0.9430 (.11) S=0.001	0.9383 (.10) S=0.001
TCN2	0.9929 (.91) S=0.001	0.9891 (.64) S=0.001	0.9232 (.11) S=0.001	0.9881 (.87) S=0.001	1.0000 (.01) S=0.001	0.9864 (.88) S=0.001	0.9858 (.88) S=0.001	0.9841 (.63) S=0.001	0.9448 (.11) S=0.001	0.9080 (.11) S=0.001	0.8881 (.10) S=0.001
TCN3	0.9908 (.89) S=0.001	0.9849 (.62) S=0.001	0.9833 (.10) S=0.001	0.9809 (.84) S=0.001	0.9864 (.88) S=0.001	1.0000 (.01) S=0.001	0.9810 (.64) S=0.001	0.9801 (.63) S=0.001	0.9930 (.10) S=0.001	0.9713 (.10) S=0.001	0.9746 (.9) S=0.001
JCN1	0.9726 (.65) S=0.001	0.9960 (.89) S=0.001	0.9783 (.22) S=0.001	0.9851 (.81) S=0.001	0.9858 (.88) S=0.001	0.9810 (.64) S=0.001	1.0000 (.01) S=0.001	0.9834 (.86) S=0.001	0.9735 (.22) S=0.001	0.9675 (.21) S=0.001	0.9577 (.21) S=0.001
JCN2	0.9713 (.64) S=0.001	0.9956 (.87) S=0.001	0.9855 (.21) S=0.001	0.9766 (.62) S=0.001	0.9841 (.86) S=0.001	0.9801 (.63) S=0.001	0.9834 (.86) S=0.001	1.0000 (.01) S=0.001	0.9761 (.21) S=0.001	0.9765 (.21) S=0.001	0.9715 (.20) S=0.001
ITS	0.9686 (.11) S=0.001	0.9776 (.22) S=0.001	0.9921 (.61) S=0.001	0.9756 (.11) S=0.001	0.9448 (.11) S=0.001	0.9930 (.10) S=0.001	0.9735 (.22) S=0.001	0.9761 (.21) S=0.001	1.0000 (.01) S=0.001	0.9854 (.59) S=0.001	0.9544 (.57) S=0.001
ITN	0.9378 (.11) S=0.001	0.9745 (.22) S=0.001	0.9890 (.67) S=0.001	0.9430 (.11) S=0.001	0.9080 (.11) S=0.001	0.9713 (.10) S=0.001	0.9675 (.22) S=0.001	0.9765 (.21) S=0.001	0.9854 (.59) S=0.001	1.0000 (.01) S=0.001	0.9493 (.62) S=0.001
FCN	0.9159 (.10) S=0.001	0.9646 (.21) S=0.001	0.9660 (.65) S=0.001	0.9383 (.10) S=0.001	0.8881 (.10) S=0.001	0.9746 (.9) S=0.001	0.9577 (.21) S=0.001	0.9735 (.20) S=0.001	0.9544 (.57) S=0.001	0.9493 (.62) S=0.001	1.0000 (.01) S=0.001

(COEFFICIENT / (CASES) / SIGNIFICANCE) (A VALUE OF 99.0000 IS PRINTED IF A COEFFICIENT CANNOT BE COMPUTED)

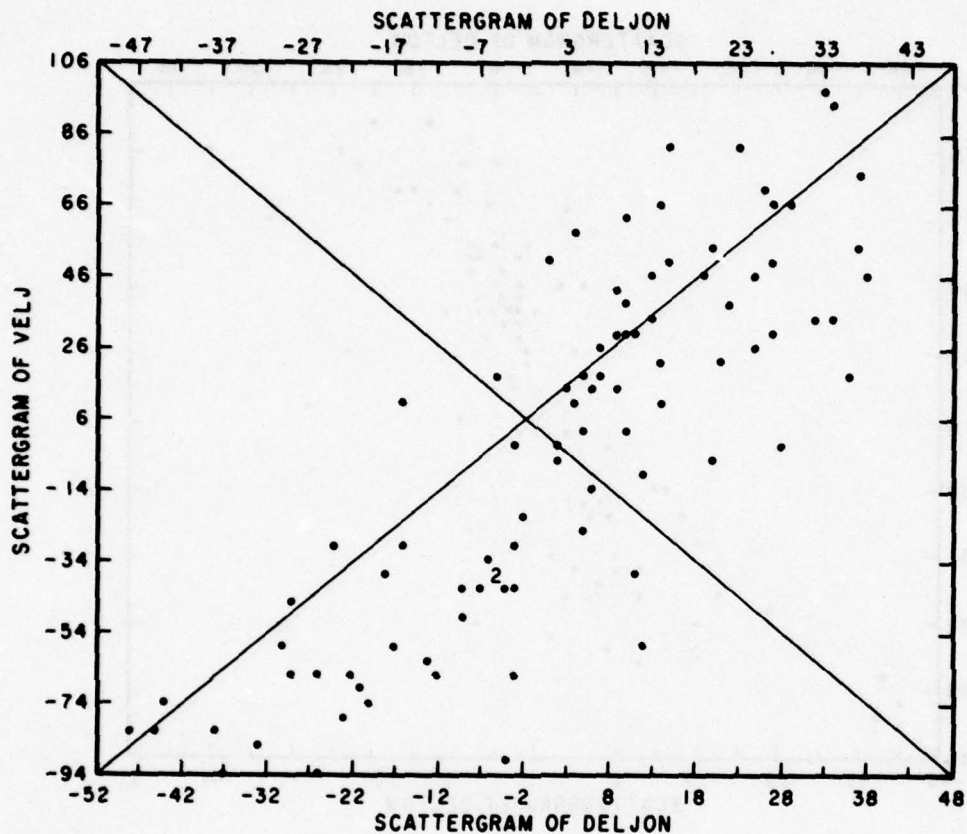


STATISTICAL PACKAGE FOR THE SOCIAL SCIENCES SPSSH-RELEASE 6.02 11/24/76

STATISTICS:

CORRELATION (R)- 0.77764 R SQUARED - 0.60472 SIGNIFICANCE - 0.00001
 STD ERR OF EST -32.85753 INTERCEPT (A) -2.10095 SLOPE (B) - 2.61776
 PLOTTED VALUES -91 EXCLUDED VALUES - 0 MISSING VALUES -117

Figure E-1. Scatter diagram of current velocity at Town Creek (VELT) versus the instantaneous water surface elevation differential between the ocean and Town Creek gages.

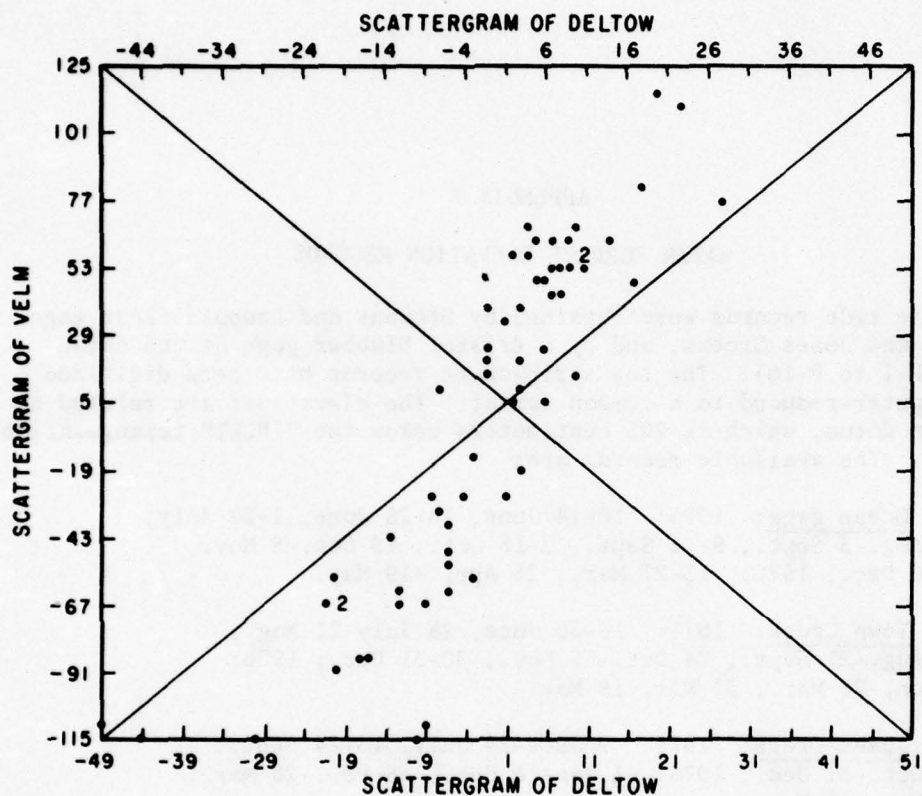


STATISTICAL PACKAGE FOR THE SOCIAL SCIENCES SPSSH-RELEASE 6.02 11/24/76

STATISTICS:

CORRELATION (R) - 0.83751	R SQUARED - 0.70142	SIGNIFICANCE - 0.00001
STD ERR OF EST - 28.18429	INTERCEPT (A) - 6.37400	SLOPE (B) - 2.04415
PLOTTED VALUES - 89	EXCLUDED VALUES - 0	MISSING VALUES - 119

Figure E-2. Scatter diagram of current velocity at Jones Creek (VELJ) versus the instantaneous water surface elevation differential between the ocean and Jones Creek gages.



STATISTICAL PACKAGE FOR THE SOCIAL SCIENCES SPSSH-RELEASE 6.02 11/24/76

STATISTICS:

CORRELATION (R)- 0.86393 R SQUARED - 0.74637 SIGNIFICANCE - 0.00001
 STD ERR OF EST -31.83394 INTERCEPT (A) - 6.77610 SLOPE (B) - 3.84794
 PLOTTED VALUES -64 EXCLUDED VALUES - 0 MISSING VALUES -144

Figure E-3. Scatter diagram of current velocity at the inlet throat (VELM) versus the instantaneous water surface elevation differential between the ocean and Town Creek gages.

APPENDIX F

WATER SURFACE ELEVATION RECORDS

These tide records were obtained by Stevens and Leupold float gages at Town and Jones Creeks, and by a Bristol blubber gage at the ocean (Figs. F-1 to F-16). The raw strip-chart records have been digitized and computer-reduced to a common format. The elevations are related to a common datum, which is 205 centimeters below the "INLET" triangulation station. The available records are:

Ocean gage: 1975: 10-14 June, 16-28 June, 1-28 July,
27 Aug.-3 Sept., 9-23 Sept., 2-15 Oct., 18 Oct.-8 Nov.,
7-28 Dec.; 1976: 13-27 Mar., 25 Apr. -19 May.

Town Creek: 1975: 10-30 June, 28 July-21 Aug.,
30 Aug.-21 Sept., 24 Oct.-30 Nov., 30-31 Dec.; 1976:
1 Jan.-28 Mar., 31 Mar.-19 May.

Jones Creek: 1975: 9 June-24 July, 13-24 Sept.,
25 Oct.-31 Dec.; 1976: 1 Jan-16 Feb., 18 Feb.-28 Mar.,
31 Mar.-17 May.

NOTE:--The Jones Creek record for the period of 1 Nov.-31 Dec. 1975 is included as Figure 12.

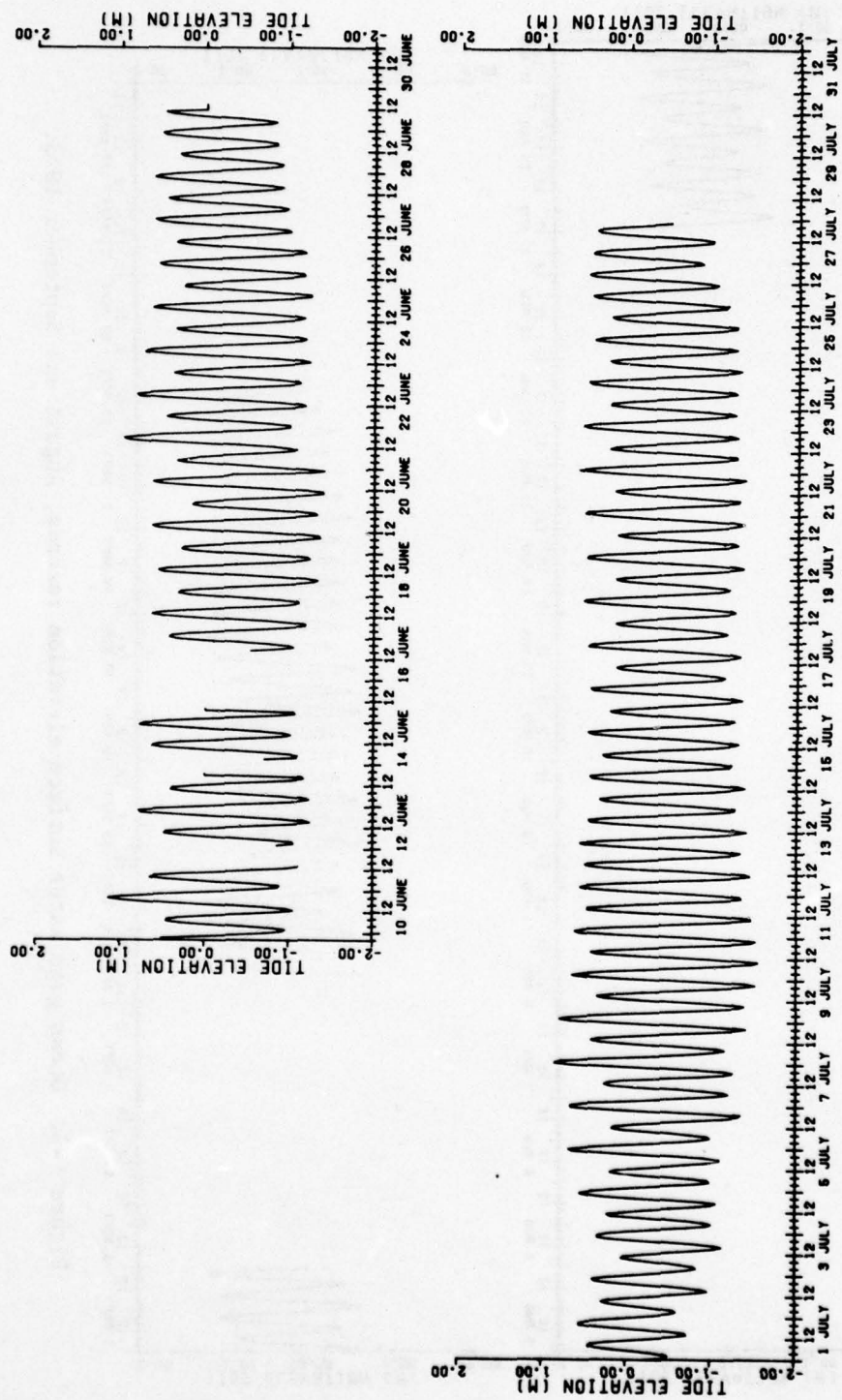


Figure F-1. Ocean gage water surface elevation records, June and July 1975.

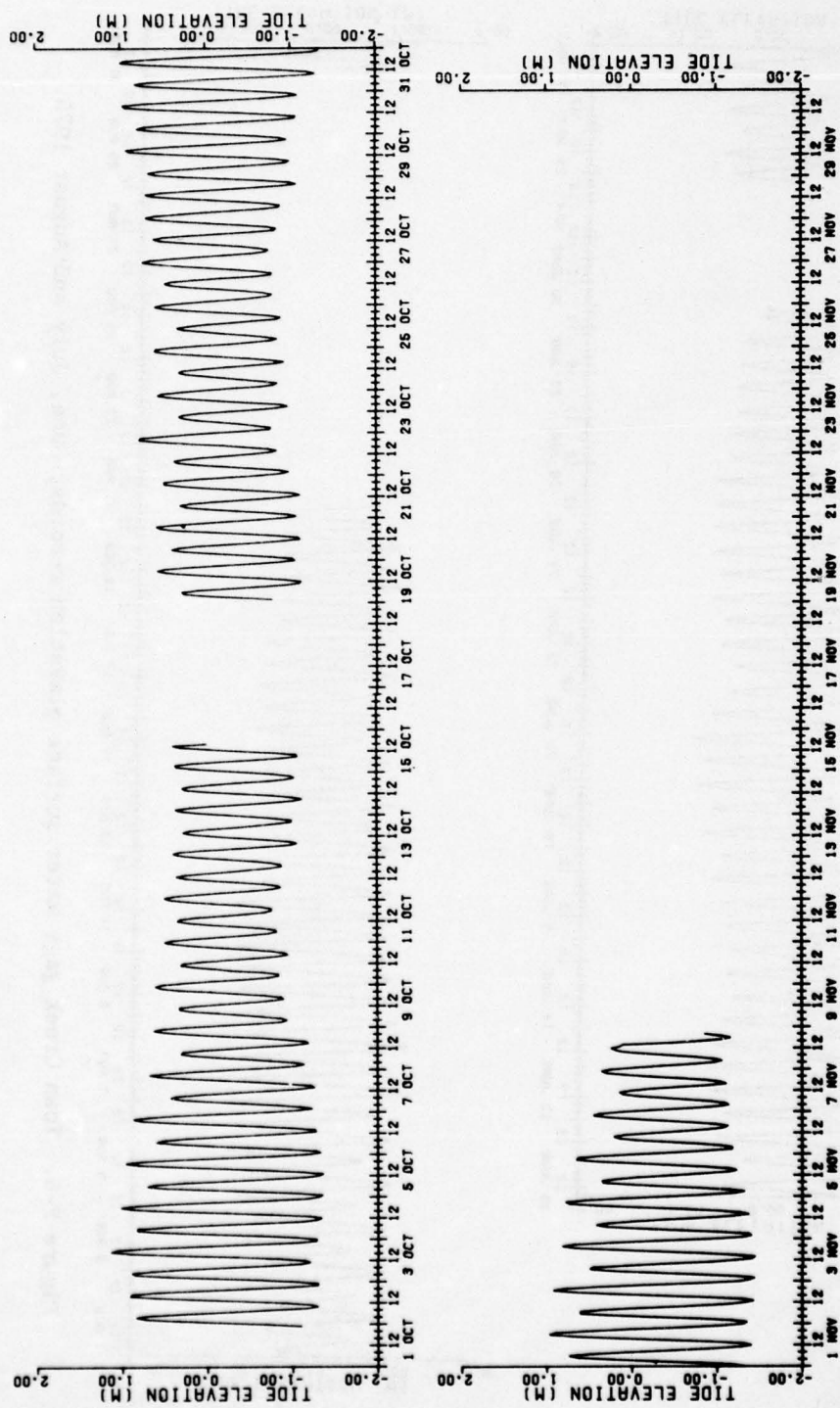


Figure F-3. Ocean gage water surface elevation records, October and November 1975.

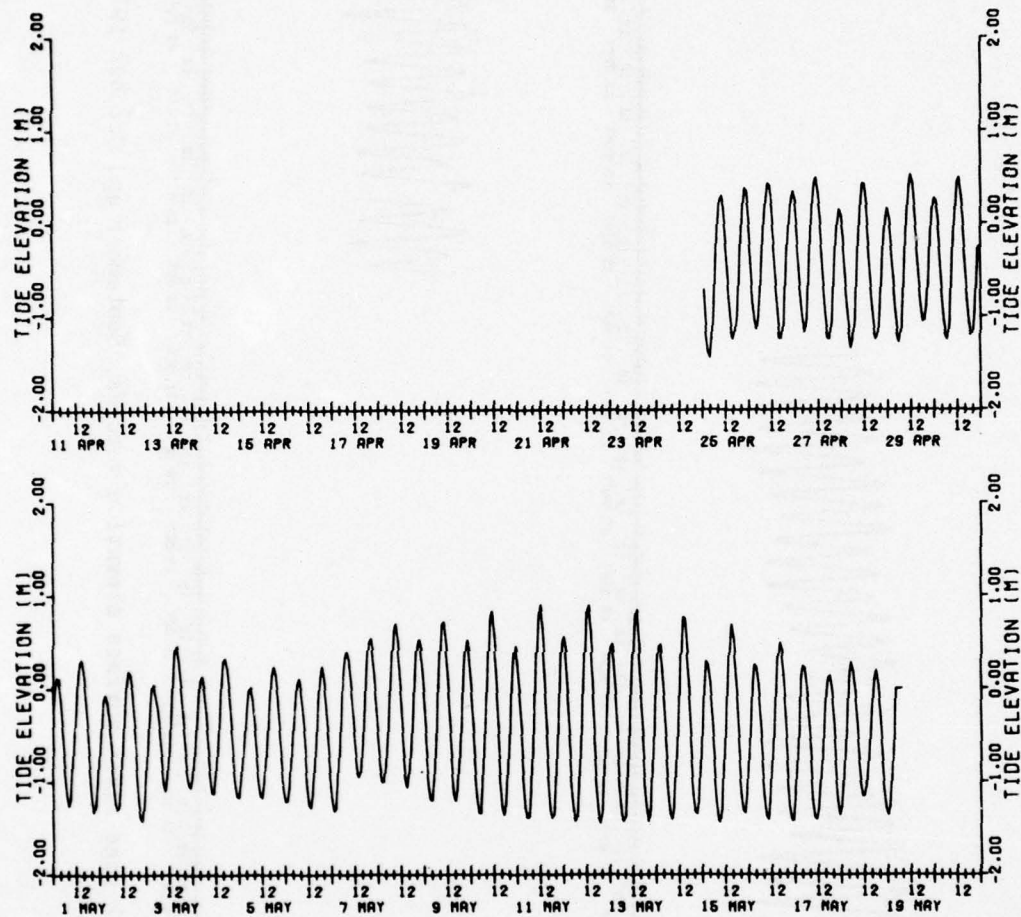


Figure F-5. Ocean gage water surface elevation records, April and May 1976.

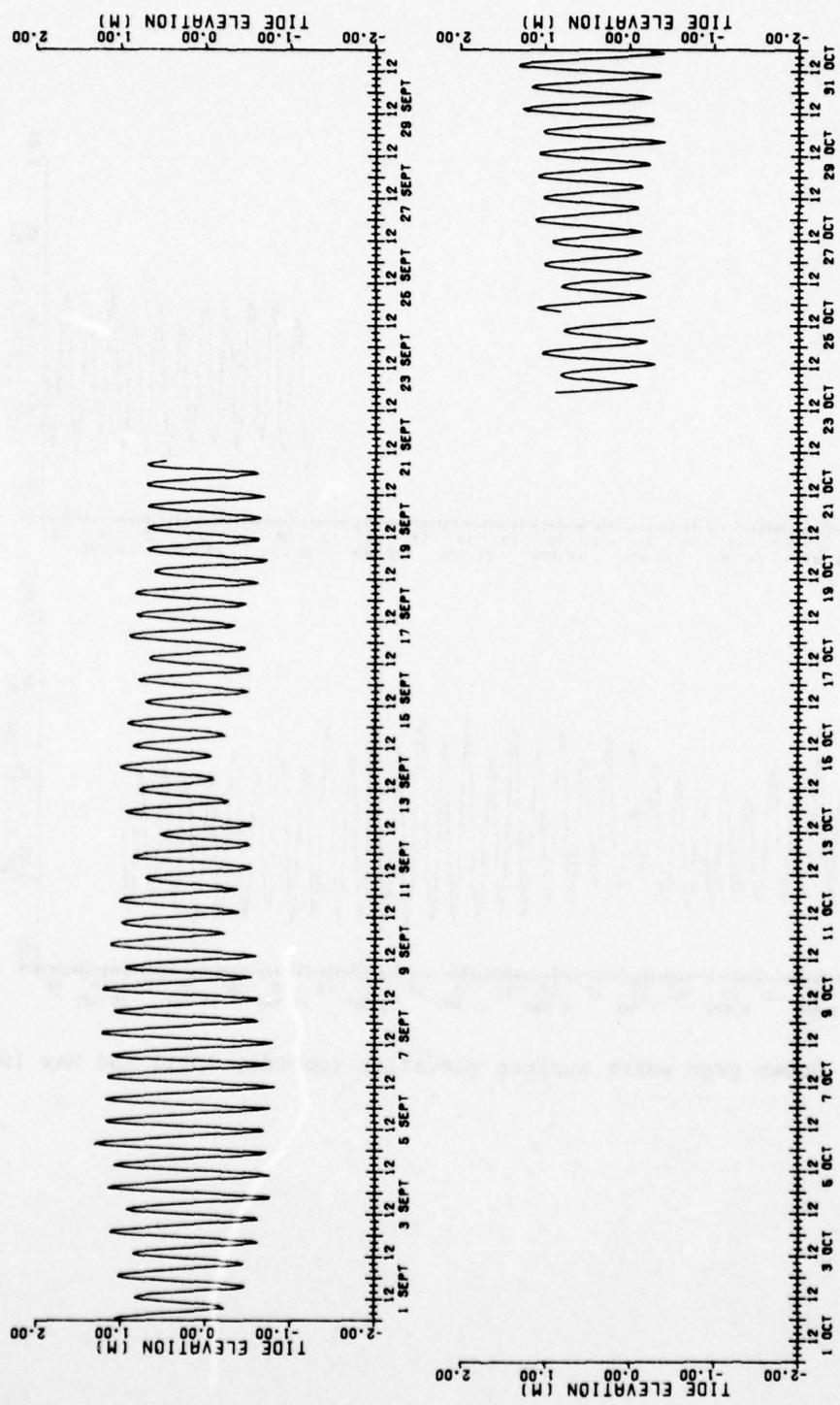


Figure F-7. Town Creek gage water surface elevation records, September and October 1975.

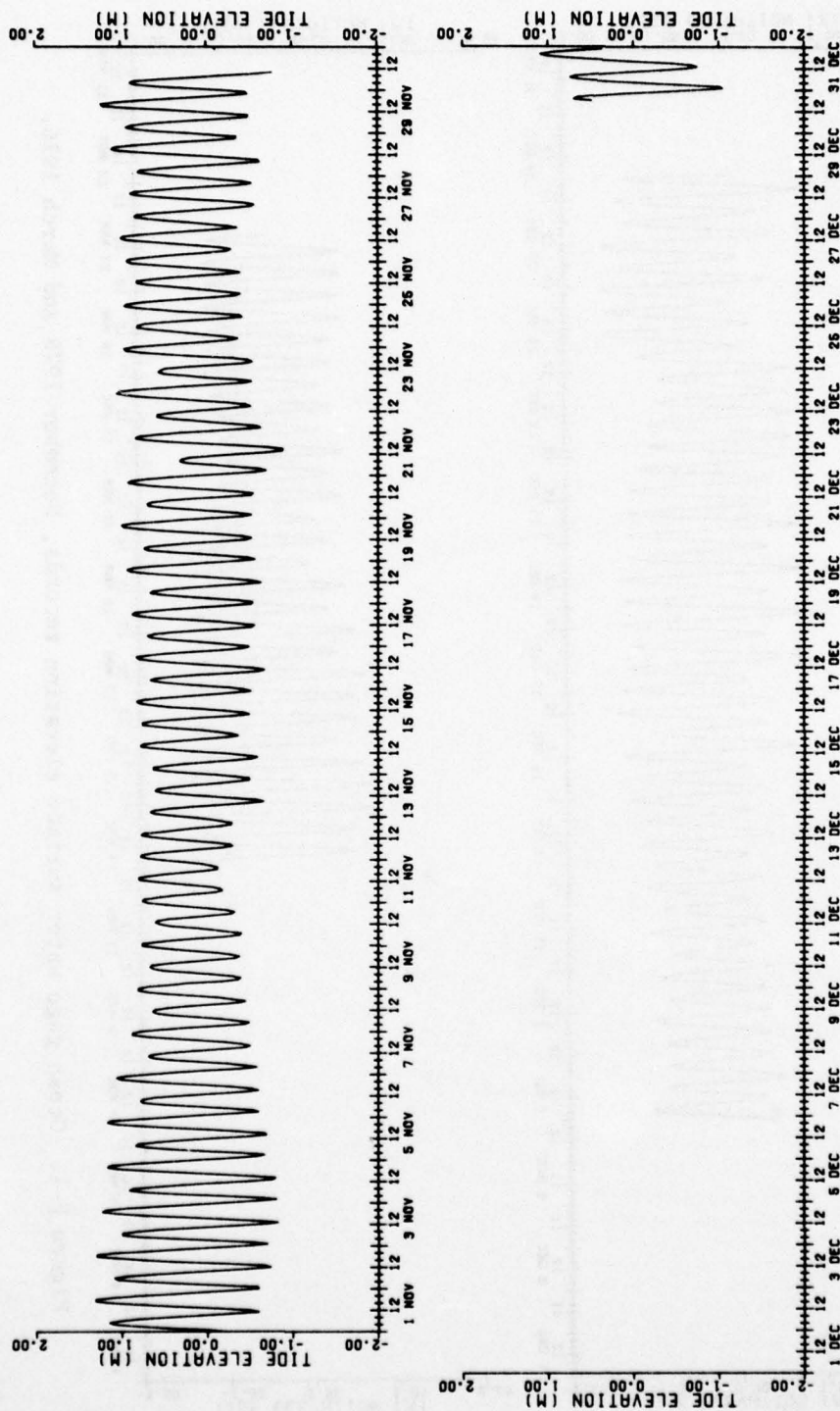


Figure F-8. Town Creek gage water surface elevation records, November and December 1975.

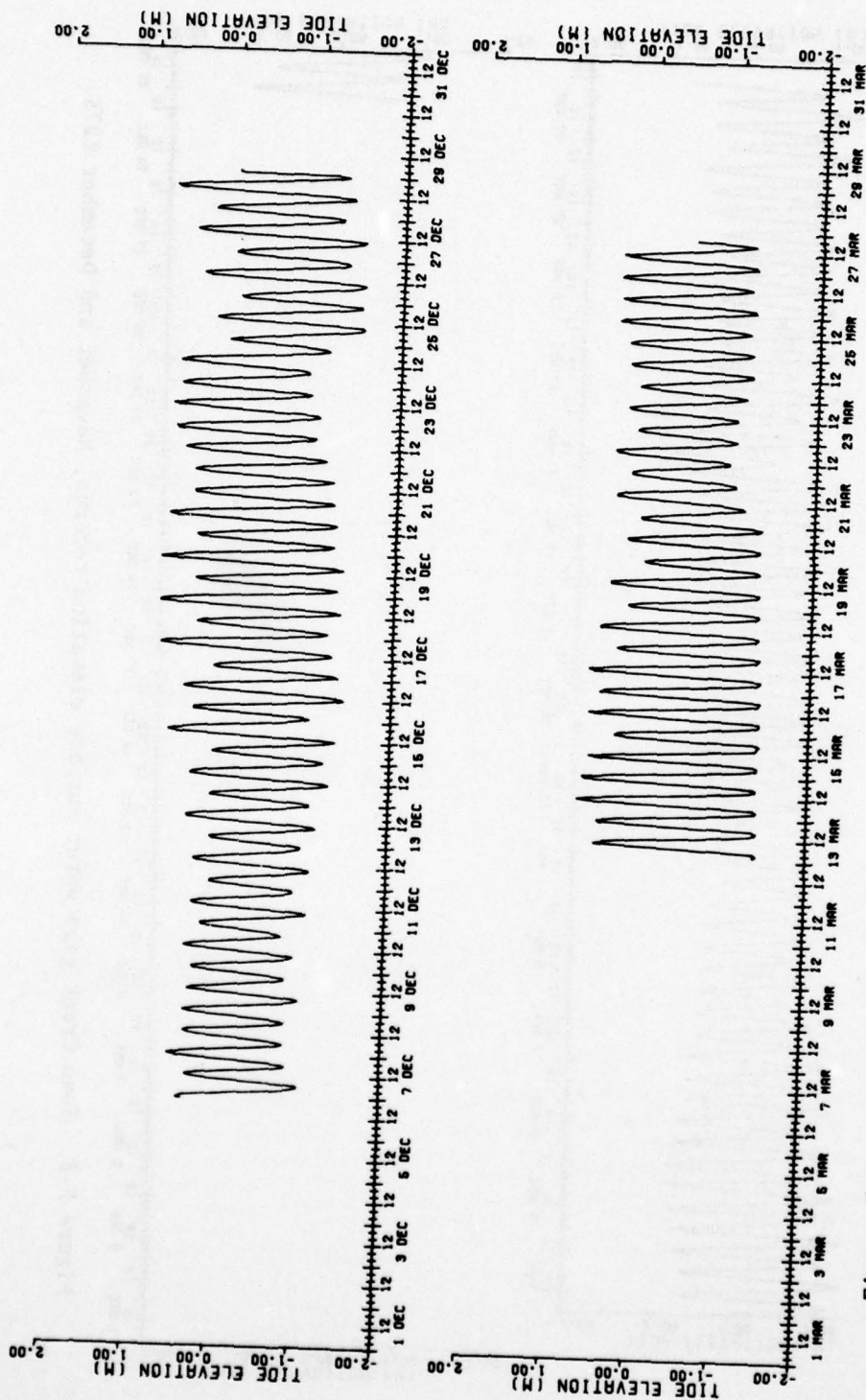


Figure F-4. Ocean gage water surface elevation records, December 1975 and March 1976.

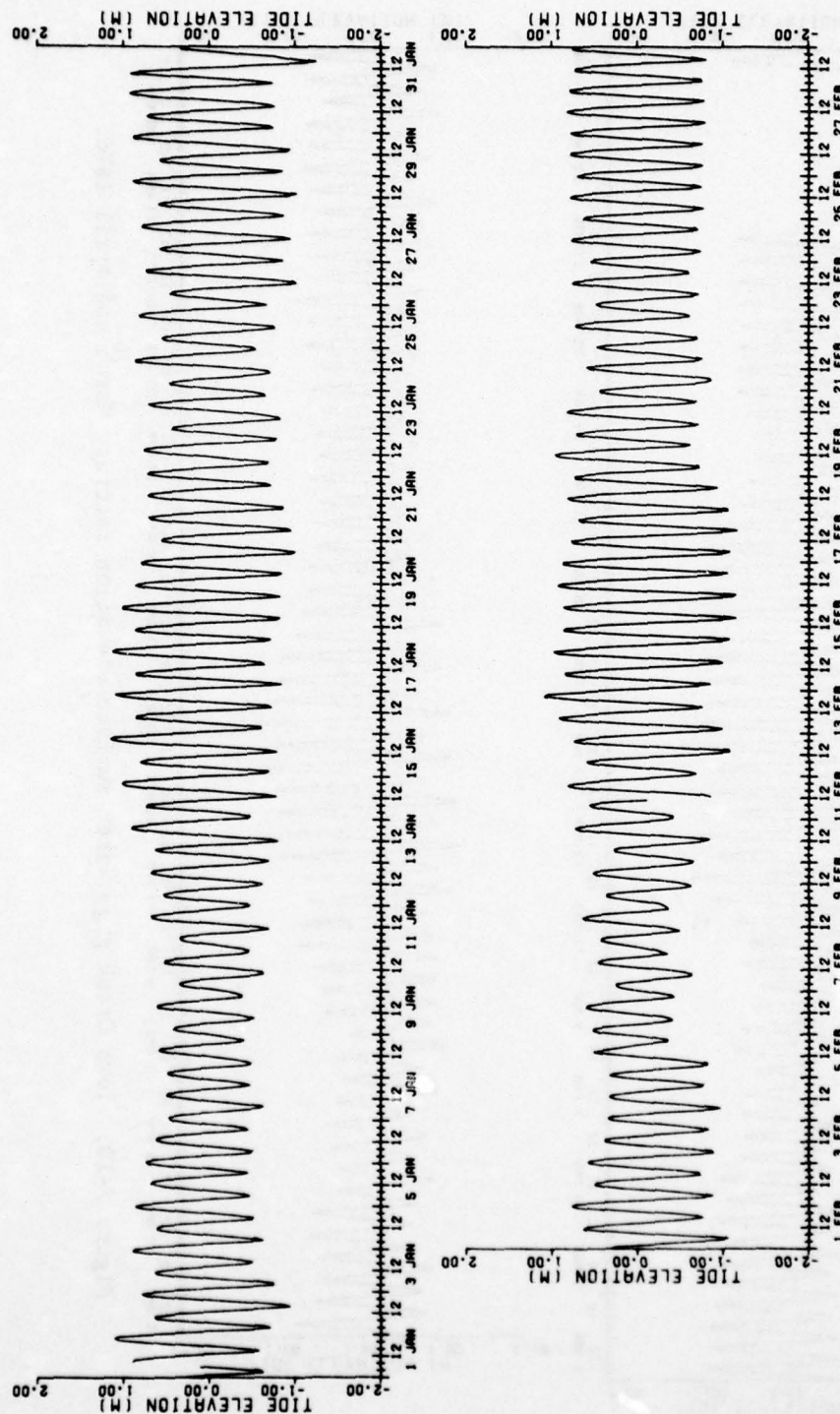


Figure F-9. Town Creek gage water surface elevation records, January and February 1976.

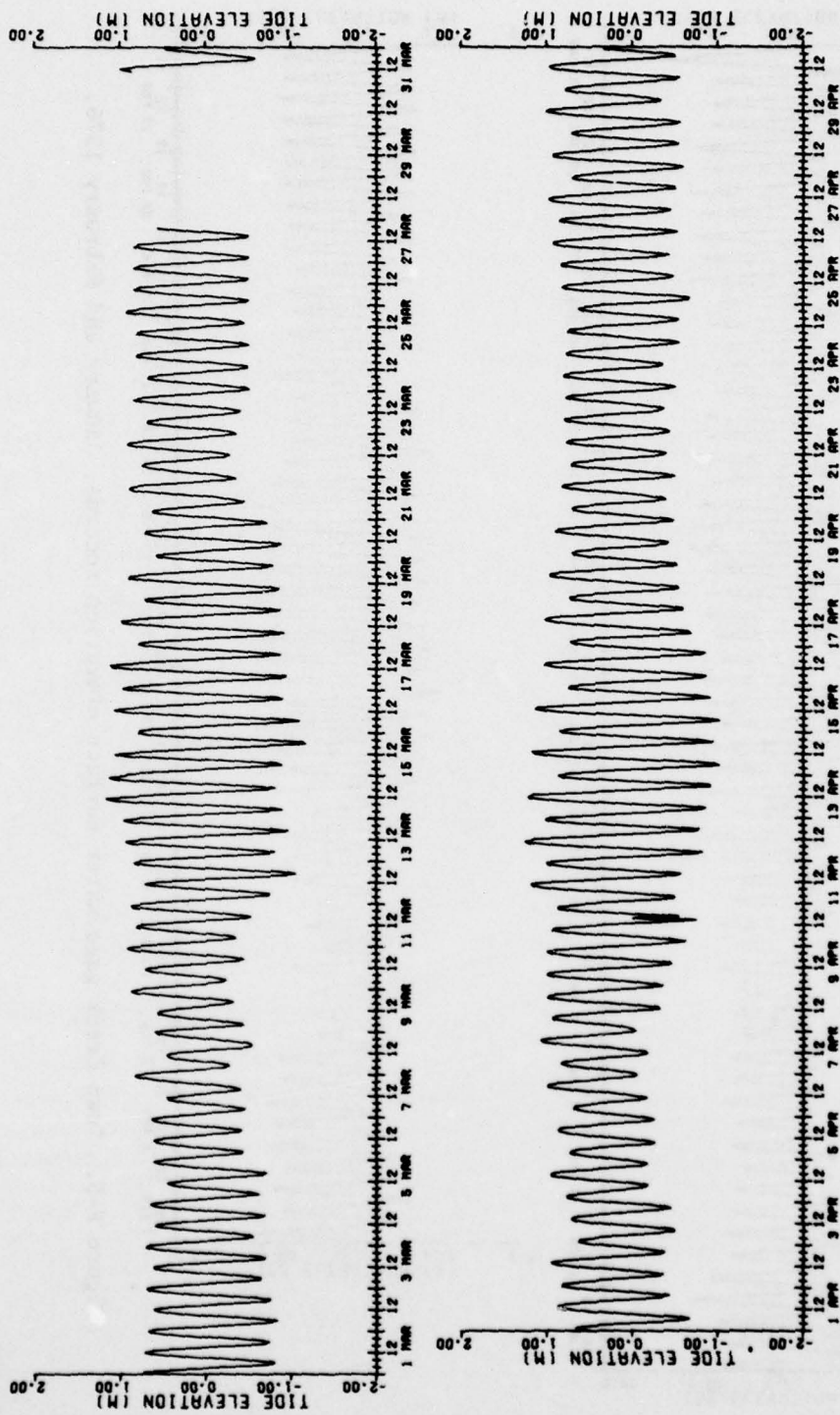


Figure F-10. Town Creek gage water surface elevation records, March and April 1976.

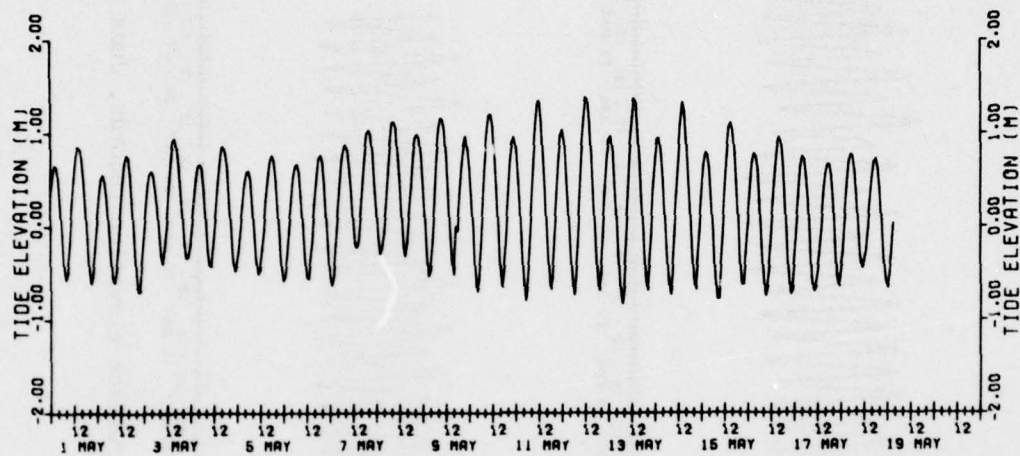


Figure F-11. Town Creek gage water surface elevation records, May 1976.

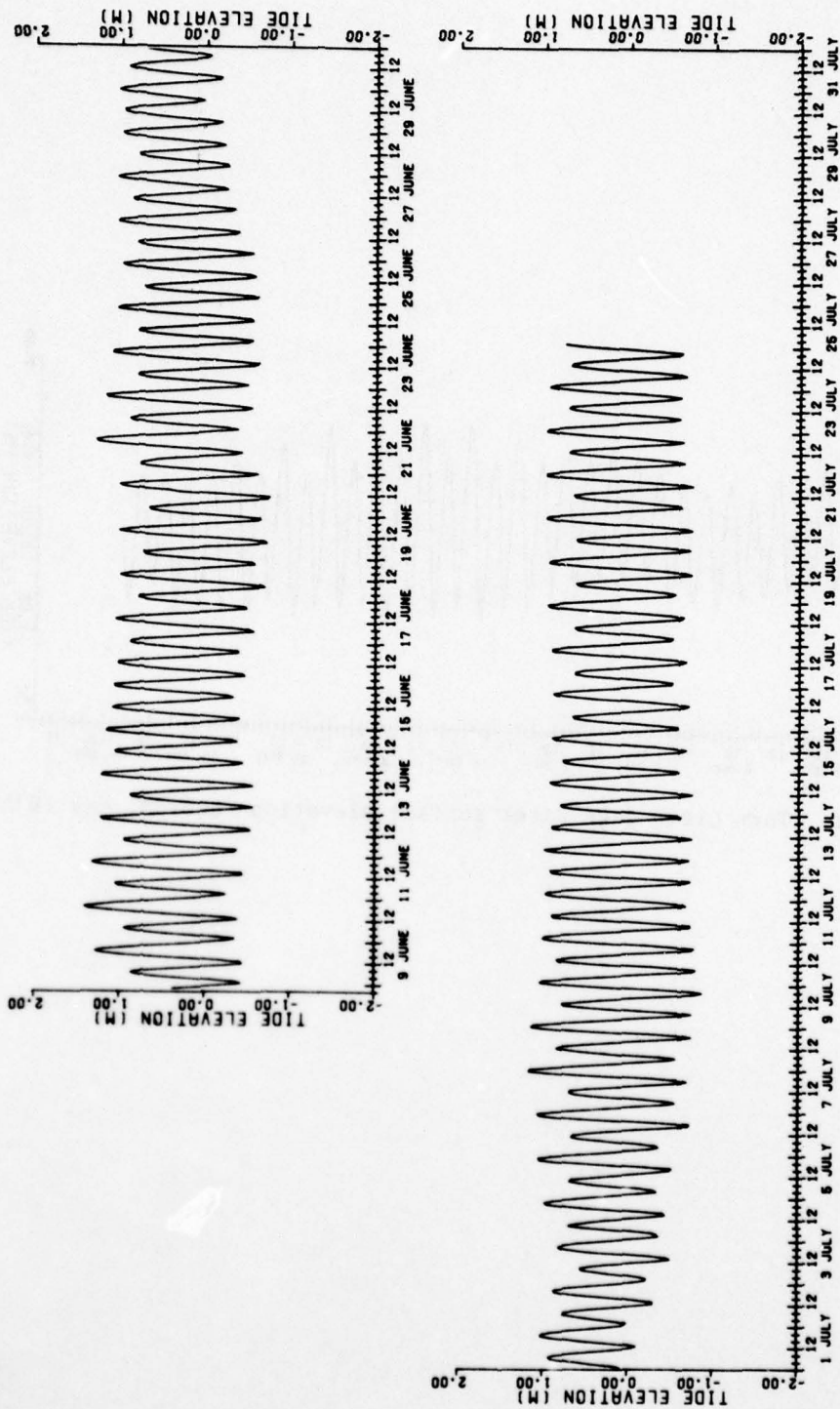


Figure F-12. Jones Creek gage water surface elevation records, June and July 1975.

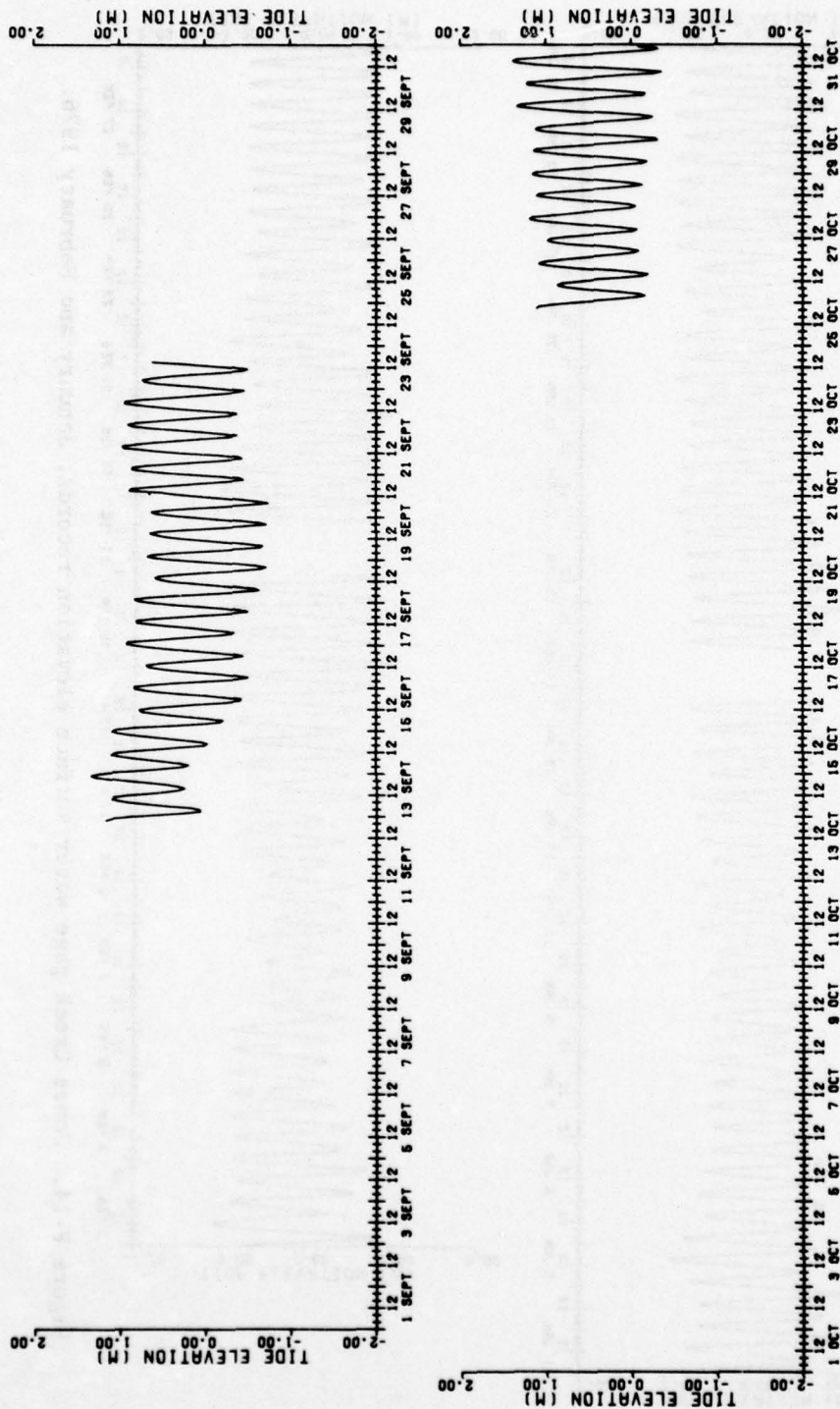


Figure F-13. Jones Creek gage water surface elevation records, September and October 1975.

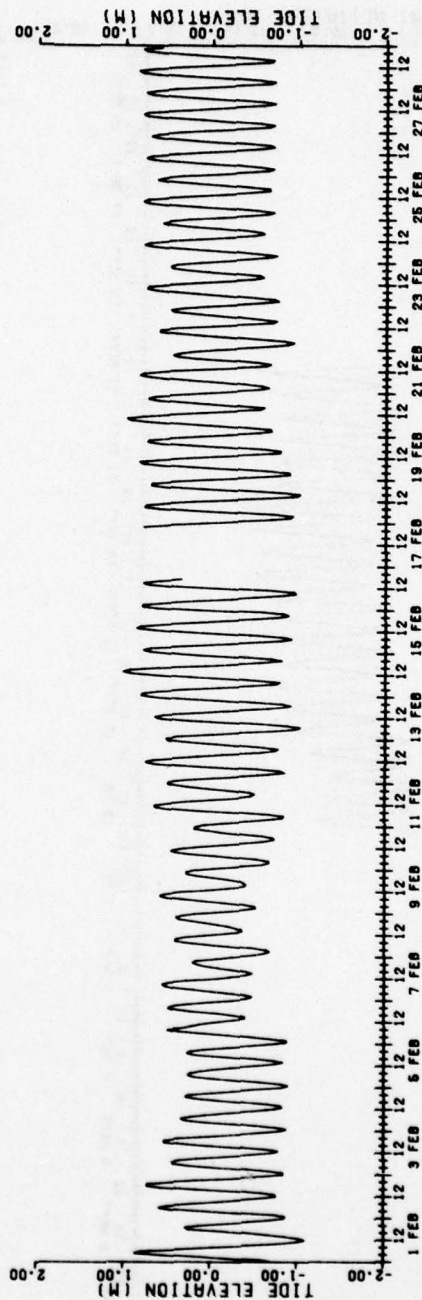
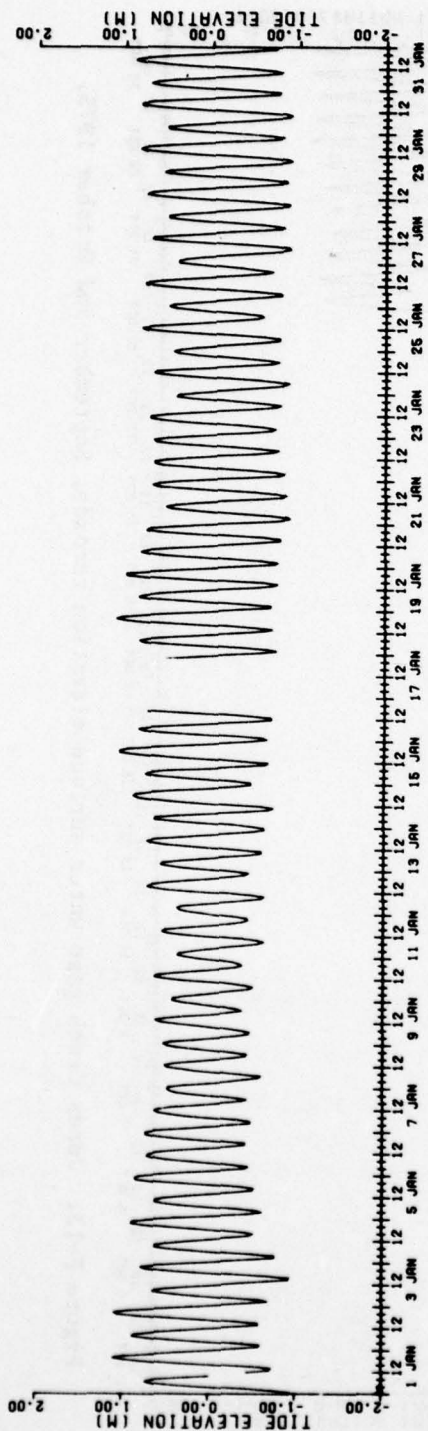


Figure F-14. Jones Creek gage water surface elevation records, January and February 1976.

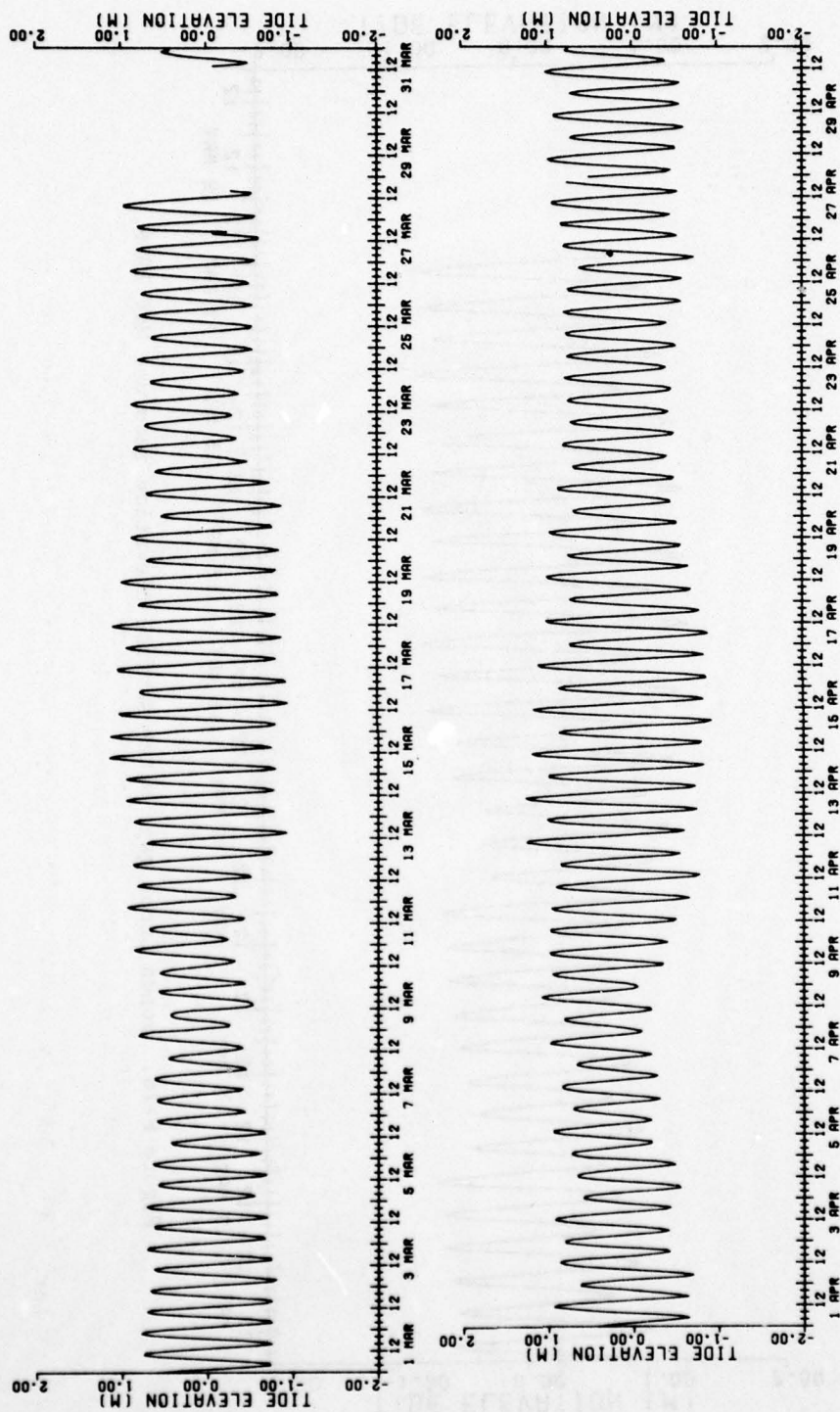


Figure F-15. Jones Creek gage water surface elevation records, March and April 1976.

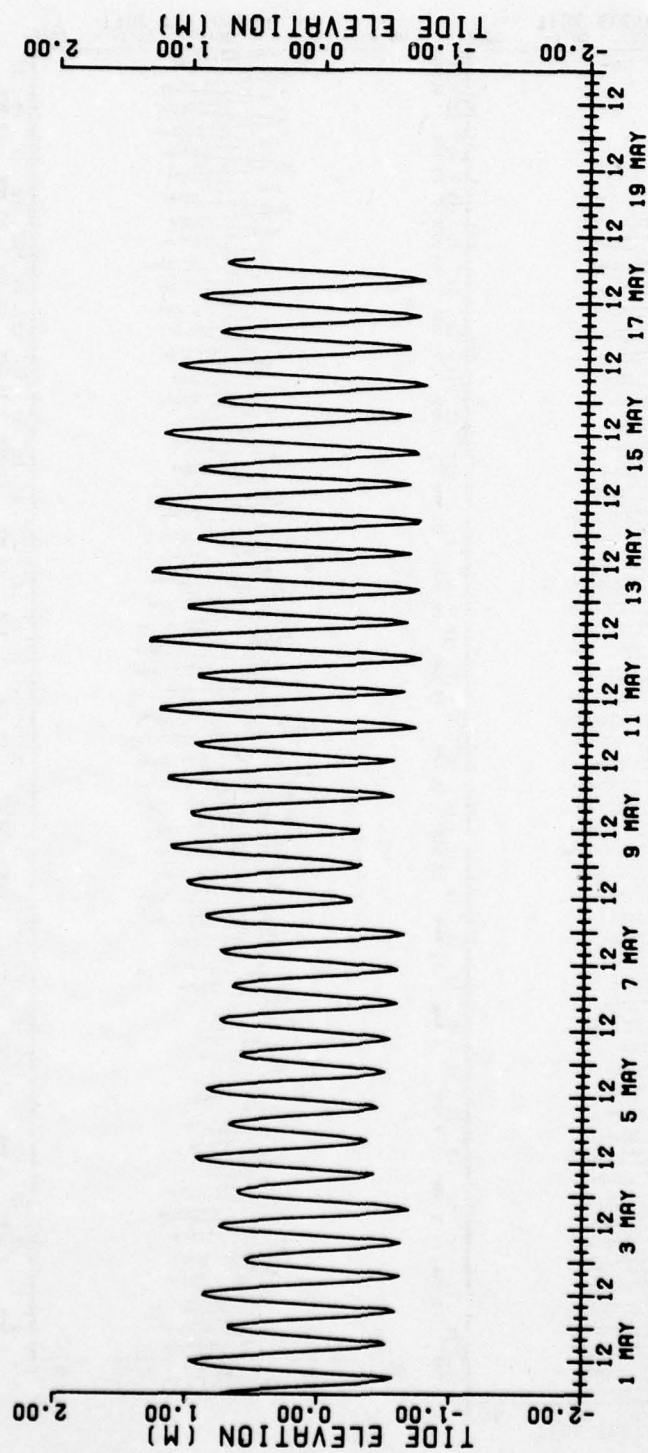


Figure F-16. Jones Creek gage water surface elevation records, May 1976.

APPENDIX G

SPECTRA OF 2-WEEK WATER SURFACE ELEVATION RECORDS

Spectra (Figs. G-1 to G-5) were calculated by applying the Statistical Analysis System (SAS) "SPECTRA" procedure to the water surface elevation records presented in Appendix F.

AD-A063 986

SOUTH CAROLINA UNIV COLUMBIA COASTAL RESEARCH DIV
HYDRAULICS AND DYNAMICS OF NORTH INLET, SOUTH CAROLINA, 1975-76--ETC(U)
SEP 78 D NUMMEDAL, S M HUMPHRIES

F/G 8/3

DACW72-72-C-0032

UNCLASSIFIED

WES-GITI-16

NL

3 OF 3
ADA
063986

SEE
COPY



END
DATE
FILMED

4 -79
DDC

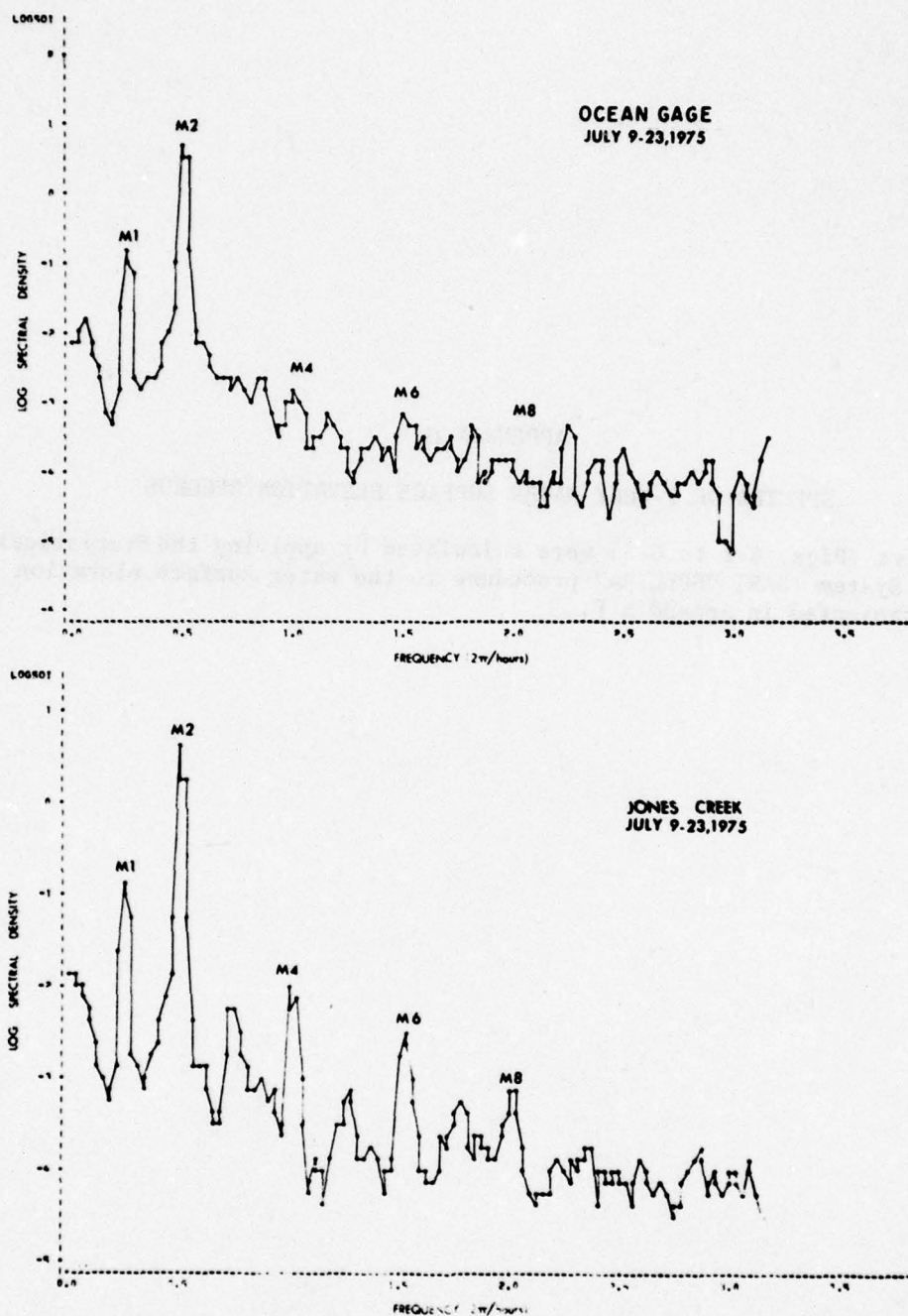


Figure G-1. Spectra of the ocean and Jones Creek gage water surface records, 9-23 July 1975.

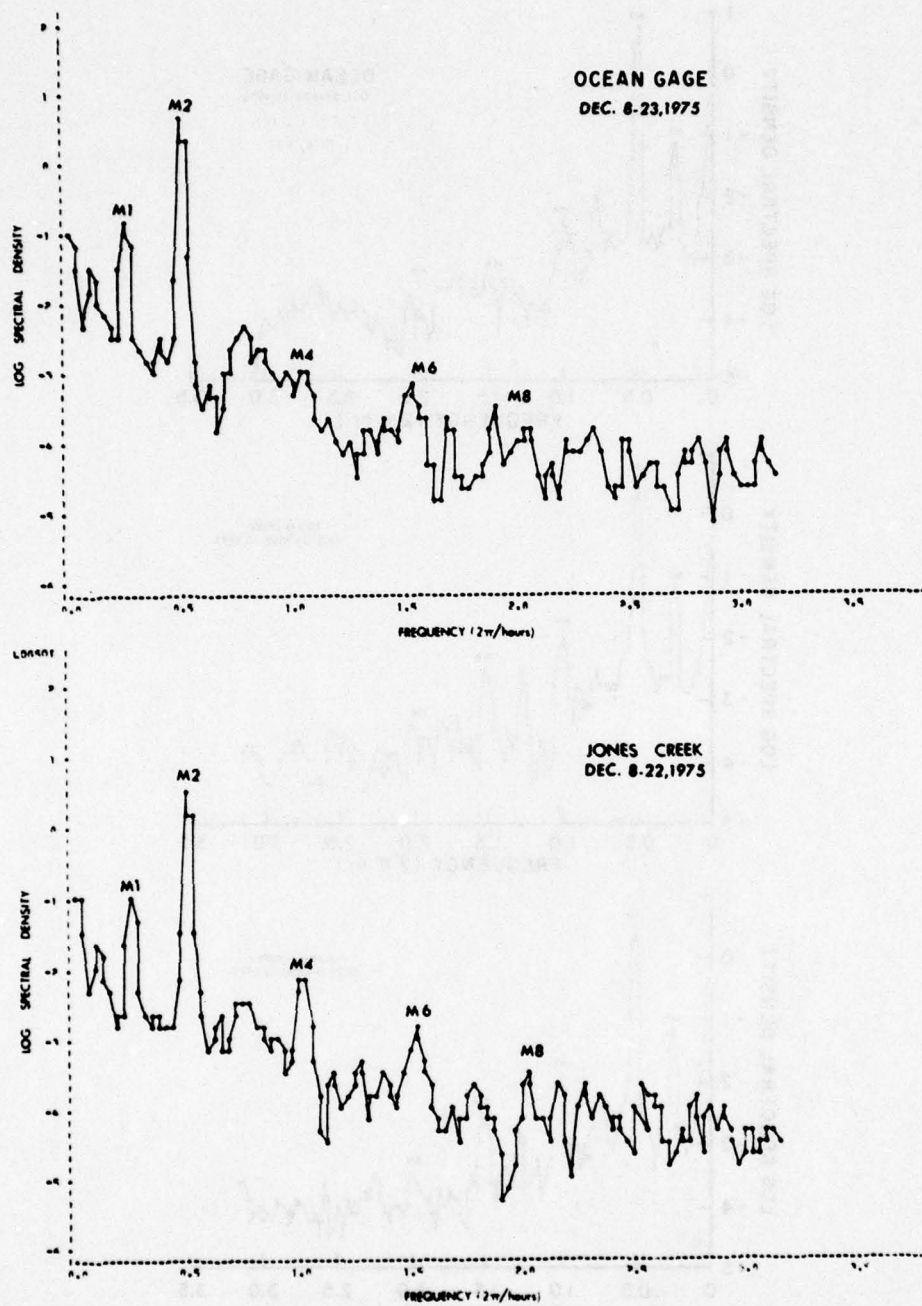


Figure G-3. Spectra of the ocean and Jones Creek gage water surface records, 8-23 December 1975.

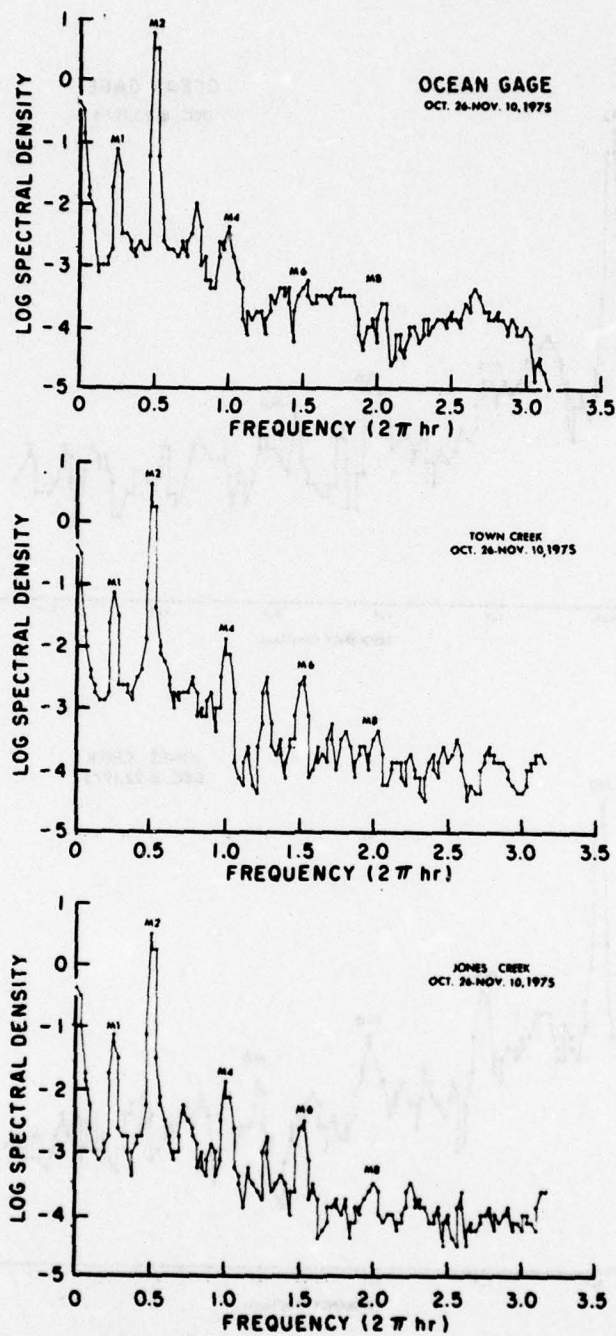


Figure G-2. Spectra of the ocean, Town Creek, and Jones Creek gage water surface records, 26 October-10 November 1975.

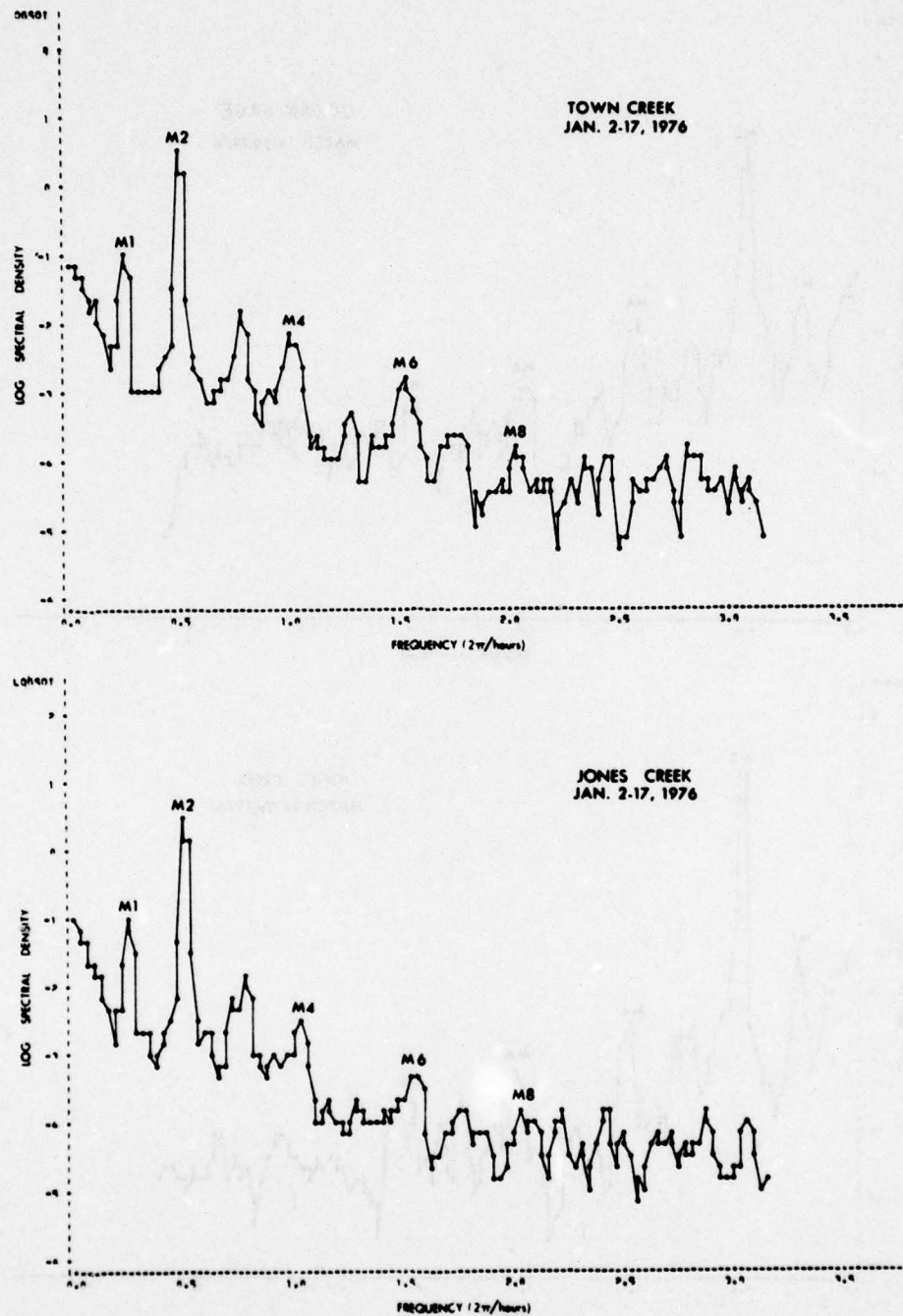


Figure G-4. Spectra of the Town Creek and Jones Creek gage water surface records, 2-17 January 1975.

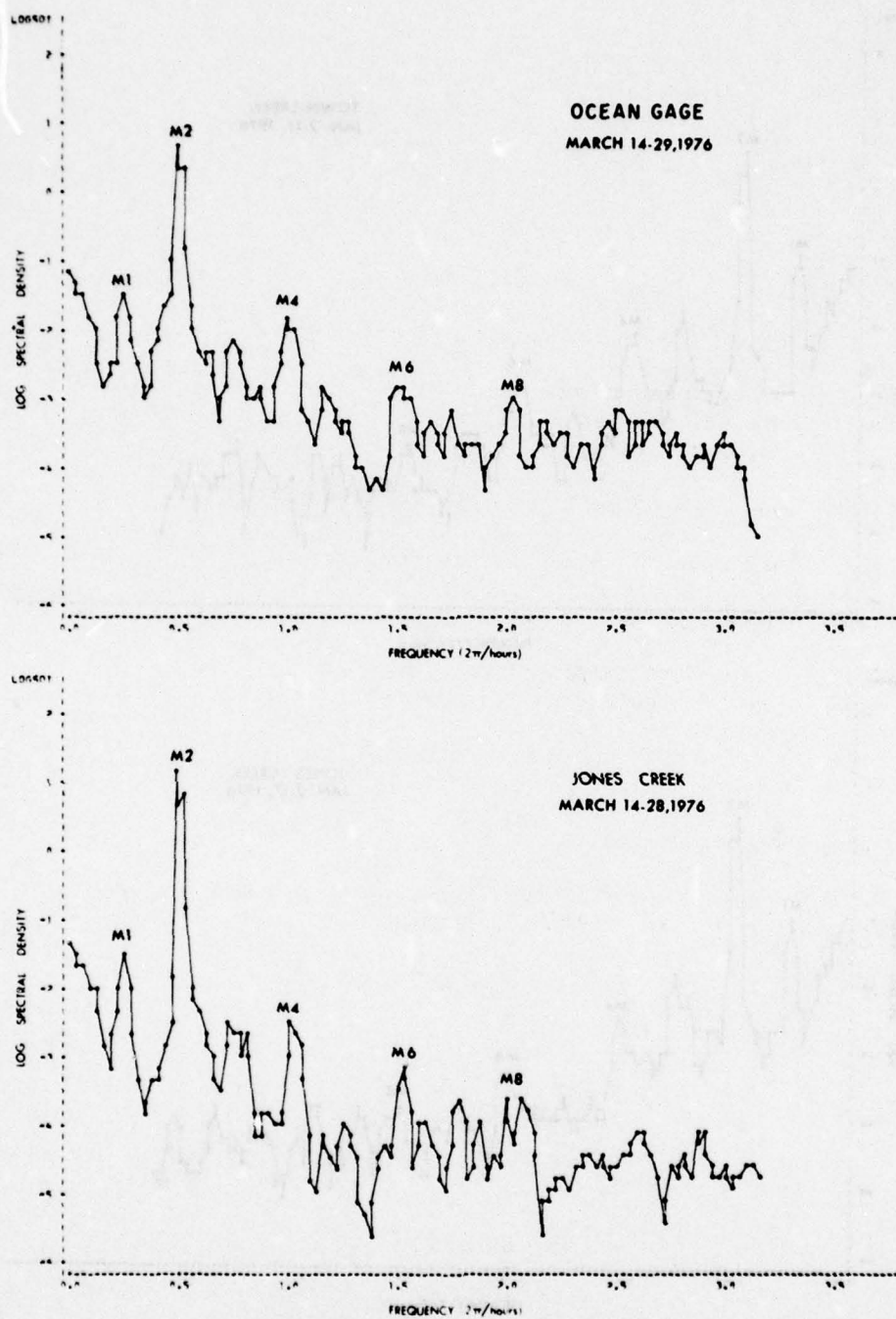


Figure G-5. Spectra of the ocean and Jones Creek gage water surface records, 14-29 March 1976.

APPENDIX H

DESCRIPTIVE STATISTICS OF LITTORAL PROCESS PARAMETERS

Measurements were made by observers on the beach (Tables H-1, H-2, and H-3). The techniques used were described in some detail by Finley (1976, p. 37). The parameters are defined as follows:

VEL: Longshore current velocity (cm/s)

WIND: Windspeed, 2 meters above ground

DIR: Wind direction (azimuth)

WINDL: Longshore component of windspeed (in tenths of miles per hour). Negative sign indicates that the wind was blowing from right to left.

HGT: Primary breaker height (cm)

PER: Breaker period (s)

ANGL: Wave orthogonal angle relative to the beach. Zero degrees is the strike of the beach toward the left.

THIS PAGE IS BEST QUALITY PRACTICABLE
FROM COPY FURNISHED TO DDG

Table H-1. Summary table of littoral process parameters at station DBI-25.

	NUMBER	VFL	WIND	OIR	WINDL	HGT	PER	ANGL
June 1975	101	66	5	66	33	65	65	84
	102	45	10	70	50	55	65	82
	103	45	10	70	62	50	65	85
	104	44	10	90	31	70	55	90
	105	-9	10	106	3	100	55	90
	106	-2	3	110	-1	90	55	94
	108	39	11	35	105	70	75	90
	109	85	16	70	99	50	55	82
	110	71	18	78	90	60	55	80
	111	103	26	60	193	150	60	84
	112	74	21	81	95	75	74	114
	115	37	8	92	22	74	120	65
	116	-22	8	100	11	110	100	70
	117	-4	8	95	18	60	85	80
	118	-3	8	126	-25	80	93	90
	119	-10	5	225	-45	56	105	92
	122	-25	10	233	-82	50	65	90
	123	-8	5	212	-49	40	65	90
	124	-2	5	230	-42	60	62	90
	125	-1	7	270	-22	50	85	90
	126	0	5	300	10	40	75	90
	127	16	5	0	48	50	82	90
	128	0	9	164	-75	30	85	90
	129	-17	9	154	-65	40	70	98
	131	20	5	310	19	60	85	95
	132	-2	4	308	14	62	85	90
	133	-1	3	110	-1	64	85	90
	134	-23	12	170	-106	40	88	80
	135	-10	9	206	-89	50	79	92
	136	-12	7	216	-67	40	75	90
	137	-9	9	176	-83	50	69	88
	138	-30	10	176	-93	35	66	95
	139	-34	12	182	-115	40	73	93
	140	-29	10	180	-95	30	70	93
	141	-7	6	242	-43	42	80	90
	142	-28	7	242	-50	48	80	90
	144	-24	14	196	-140	60	110	115
	145	-59	15	194	-150	54	82	103
	146	-47	12	190	-119	38	70	107
	147	-7	3	244	-21	42	65	92
	148	-18	3	221	-28	60	70	94
	149	-56	10	180	-95	54	106	120
	150	-12	10	170	-88	58	75	92
	151	-27	14	198	-140	53	80	96
	152	-31	12	195	-120	61	100	94
	153	-38	12	212	-116	47	105	124
	157	-20	10	180	-95	60	90	105
	158	-26	10	176	-93	44	70	96
	159	-17	6	180	-57	34	105	100
	160	1	8	0	0	40	106	90
	163	-25	5	280	-7	43	80	90
	164	-31	12	180	-114	49	85	96
	166	-23	9	203	-90	52	90	94
	167	8	4	294	4	57	110	90
	169	-40	12	164	-102	45	90	110
	170	29	9	280	-13	50	95	80
	171	46	13	18	130	72	75	70
	172	48	14	26	139	60	70	72
	173	79	16	66	107	68	85	70
	174	54	19	80	89	90	70	74
September 1975	201	-21	5	60	37	41	67	96
	202	-6	10	56	79	52	41	100
	203	-14	10	46	88	46	45	92

THIS PAGE IS BEST QUALITY PRACTICABLE
FROM COPY FURNISHED TO DDC

Table H-1. Summary table of littoral process parameters at station DBI-25.--Continued

NUMBER	VFL	WIND	DIR	WINDL	HGT	PER	ANGL
204	-17	13	180	-124	44	52	95
205	-56	15	178	-141	44	45	93
206	-15	13	180	-124	61	40	94
207	-46	15	178	-141	70	40	93
208	-47	16	180	-152	68	40	90
209	-53	17	180	-162	72	76	96
210	-18	16	180	-152	76	90	92
211	-26	10	205	-99	56	81	98
212	-19	10	180	-95	70	95	95
213	-14	13	180	-124	46	46	93
214	-15	9	190	-89	63	107	93
215	13	4	305	12	62	82	90
216	40	3	15	30	65	120	90
217	25	8	40	74	90	104	90
218	28	7	35	67	86	90	93
220	-35	6	225	-54	96	125	91
222	25	10	0	95	52	115	40
223	6	5	0	48	30	90	86
224	13	5	80	24	42	100	87
225	16	5	90	16	30	90	85
226	-20	4	135	-18	34	107	93
227	13	3	0	29	70	90	90
228	40	3	35	29	70	120	90
229	90	20	45	178	130	90	78
230	8	2	270	-6	50	120	90
231	47	15	50	127	65	110	60
232	50	21	45	187	130	115	76
233	108	22	50	187	140	104	73
234	48	22	45	196	75	120	60
235	141	24	35	268	65	0	85
236	93	16	30	156	140	40	94
237	80	15	45	134	90	63	85
238	70	13	30	127	93	66	75
239	69	10	0	95	75	91	82
240	15	6	45	54	63	70	88
241	26	10	45	89	52	101	85
242	23	13	45	116	82	120	83
243	55	13	45	116	70	110	85
244	59	10	60	74	74	120	87
245	8	5	45	45	41	122	90
246	36	13	45	116	72	83	74
247	7	13	45	116	80	107	80
248	45	14	45	125	63	88	78
249	13	12	45	107	75	98	85
250	37	8	40	74	78	92	90
251	11	2	270	-6	73	40	88
252	13	4	315	18	60	130	90
253	5	8	327	50	54	115	90
254	11	10	0	95	64	115	88
255	35	7	0	67	30	100	83
257	45	27	35	258	85	42	45
258	34	30	30	293	91	73	73
259	42	19	35	181	64	90	76
260	39	18	30	176	75	90	80
261	34	17	10	168	102	110	78
262	56	13	30	127	115	55	82
263	73	7	46	61	68	92	83
264	47	15	47	131	61	92	80
264A	58	15	47	131	73	103	82
267	28	14	89	46	85	93	88
268	73	7	0	67	96	63	72
269	71	4	30	39	40	101	81

THIS PAGE IS BEST QUALITY PRACTICABLE
FROM COPY FURNISHED TO DDC

Table H-1. Summary table of littoral process parameters at station DBI-25.--Continued

	NUMBER	VFL	WIND	DIR	WINDL	HGT	PER	ANGL
January 1976	301	105	16	32	155	85	70	85
	302	93	12	45	107	75	70	90
	303	72	8	50	88	55	75	75
	304	28	7	45	62	40	75	80
	305	71	23	5	224	100	60	70
	306	99	24	10	238	125	65	65
	307	68	20	20	200	110	80	80
	308	49	17	45	152	100	64	75
	310	19	7	40	65	100	69	90
	311	27	3	0	29	95	72	95
	312	33	2	45	18	65	78	95
	313	17	1	45	9	60	72	100
	314	-20	0	0	55	69	95	95
	315	10	10	280	-14	80	85	95
	316	4	9	303	23	80	80	90
	318	8	10	320	53	35	80	90
	319	43	7	0	67	45	78	70
	320	48	13	5	127	40	81	70
	321	21	7	350	62	60	84	70
	322	14	5	15	50	75	87	80
	323	17	3	350	27	40	95	85
	324	7	2	345	17	35	102	95
	325	-4	2	340	16	40	97	95
	326	14	5	65	34	40	87	90
	328	16	8	135	-36	45	90	90
	329	-2	2	330	13	35	92	84
	330	-3	1	170	-9	35	80	85
	331	-15	7	205	-69	40	95	88
	332	1	4	190	-89	50	100	100
	333	-9	2	330	13	30	80	90
	334	6	2	42	14	34	88	90
	335	-6	5	110	-2	40	84	90
	336	5	7	110	-2	33	130	90
	337	-12	3	180	-29	35	90	90
	338	-9	1	30	10	40	65	93
	339	-7	1	30	10	30	85	92
	340	-17	4	150	-27	40	72	93
	342	-11	5	210	-49	35	95	90
	343	-49	6	270	-19	40	97	93
	344	12	15	9	148	35	100	92
	345	13	7	345	59	40	92	98
	346	51	15	30	147	30	95	88
	347	25	7	345	59	35	87	90
	348	-3	5	0	48	35	90	90
	349	46	20	60	149	50	60	78
	350	44	15	30	147	50	105	82
	351	35	10	45	89	54	85	80
	352	27	9	0	86	58	82	85
	353	17	9	74	50	72	85	85
	354	31	8	105	4	60	87	90
	359	-2	5	270	-16	40	88	91
	360	5	5	315	23	70	80	75
	361	47	5	330	34	80	95	75
	362	43	12	270	-37	35	87	85
	363	27	15	0	143	35	70	73
	364	66	10	350	88	70	60	75
	365	41	12	0	114	47	80	85
	366	46	15	20	150	70	73	65
	367	103	12	30	117	60	80	78
	368	23	10	20	100	45	68	73
March 1976	401	9	3	20	30	56	95	89
	402	2	4	45	53	56	87	89
	403	9	12	45	107	53	95	87

THIS PAGE IS BEST QUALITY PRACTICABLE
FROM COPY FURNISHED TO DDG

Table H-1. Summary table of littoral process parameters at station DBI-25.--Continued

NUMBER	VFL	WIND	DIA	WINDL	HGT	PEP	ANGL
404	23	10	45	89	54	90	87
405	17	4	112	-3	52	89	80
406	3	9	90	28	61	97	84
407	-49	12	225	-107	72	95	105
408	-54	13	225	-116	68	50	90
412	-1	4	250	-75	42	123	94
413	-1	3	270	-9	43	105	90
418	31	4	0	38	50	50	75
419	39	7	0	67	63	60	79
420	25	5	0	48	50	52	77
421	24	9	40	83	34	61	82
422	1	10	180	-95	50	75	90
423	-26	15	180	-143	45	80	102
424	-14	4	245	-27	48	105	105
425	2	5	225	-45	52	95	100
426	5	10	180	-95	49	125	90
427	-21	11	180	-104	43	90	91
428	-3	10	180	-95	30	95	95
429	-1	10	180	-95	54	94	100
430	-26	0	0	0	57	85	99
432	-54	13	205	-129	65	75	98
433	-43	13	180	-124	51	75	96
434	-46	18	225	-160	42	65	93
435	-13	12	225	-107	50	95	100
436	-41	10	225	-89	70	80	100
437	-61	15	225	-134	70	70	70
438	-62	12	180	-114	80	85	100
439	-51	14	135	-64	60	95	100
440	-63	12	180	-114	64	80	105
441	-73	12	225	-107	78	85	102
442	18	10	0	95	44	51	71
443	88	14	0	133	80	80	65
444	89	12	0	114	56	93	73
445	46	11	0	105	50	72	85
446	27	2	0	19	35	120	82
447	39	18	45	160	60	70	90
448	31	21	0	200	36	105	78
449	44	20	15	200	70	59	84
450	82	14	67	92	100	60	85
451	42	15	67	99	60	100	84
452	31	4	45	36	35	58	87
453	14	11	67	72	40	55	87
454	17	11	90	34	34	90	85
455	17	14	112	-10	39	100	87
456	31	15	90	45	56	100	89
457	-7	12	135	-55	48	75	90
458	-18	4	270	-12	68	100	90
459	-3	2	270	-6	67	105	90
460	0	5	292	4	37	92	90
461	2	7	270	-22	55	115	90
462	-9	7	270	-22	40	102	88
463	-10	9	225	-80	50	85	90
467	-27	7	135	-32	35	115	90
470	-25	9	202	-90	50	96	96
471	-41	10	202	-100	36	70	91
472	-17	10	180	-95	52	121	99
473	-33	10	180	-95	44	91	92
474	-73	12	180	-114	80	60	100
475	-44	15	135	-88	80	85	105
476	-27	12	180	-114	45	75	98

THIS PAGE IS BEST QUALITY PRACTICABLE
FROM COPY FURNISHED TO DDG

Table H-2. Frequency distribution of longshore current velocities at station DBI-25. Negative sign indicates current to the left (north), positive currents flow to the right (south).

VEL	FREQUENCY	CUM FREQ	PERCENT	CUM PERCENT	VEL	FREQUENCY	CUM FREQ	PERCENT	CUM PERCENT
-73	2	2	0.806	0.806	14	3	140	1.210	56.452
-63	1	3	0.403	1.210	15	1	141	0.403	56.855
-62	1	4	0.403	1.613	16	3	144	1.210	58.065
-61	1	5	0.403	2.016	17	6	150	2.419	60.484
-59	1	6	0.403	2.419	18	1	151	0.403	60.887
-56	2	8	0.806	3.225	19	1	152	0.403	61.290
-54	2	10	0.806	4.032	20	1	153	0.403	61.694
-53	1	11	0.403	4.435	21	1	154	0.403	62.097
-51	1	12	0.403	4.839	23	3	157	1.210	63.306
-49	2	14	0.806	5.645	24	1	158	0.403	63.710
-47	2	16	0.806	6.452	25	4	162	1.613	65.323
-46	2	18	0.806	7.258	26	1	163	0.403	65.726
-44	1	19	0.403	7.661	27	4	167	1.613	67.339
-43	1	20	0.403	8.065	28	3	170	1.210	68.548
-41	2	22	0.806	8.871	29	1	171	0.403	68.952
-40	1	23	0.403	9.274	31	5	176	2.016	70.968
-39	1	24	0.403	9.677	32	2	178	0.806	71.774
-35	1	25	0.403	10.081	34	2	180	0.806	72.581
-34	1	26	0.403	10.484	35	2	182	0.806	73.387
-33	1	27	0.403	10.887	36	1	183	0.403	73.790
-31	2	29	0.806	11.694	37	2	185	0.806	74.597
-30	1	30	0.403	12.097	38	1	186	0.403	75.000
-29	1	31	0.403	12.500	39	3	189	1.210	76.210
-29	1	32	0.403	12.903	40	2	191	0.806	77.014
-27	3	35	1.210	14.113	41	1	192	0.403	77.419
-26	4	39	1.613	15.726	42	2	194	0.806	78.226
-25	3	42	1.210	16.935	43	2	196	0.806	79.032
-24	1	43	0.403	17.339	44	2	198	0.806	79.839
-23	2	45	0.806	18.145	45	3	201	1.210	81.048
-22	1	46	0.403	18.548	46	2	203	0.806	81.855
-21	2	48	0.806	19.354	47	3	206	1.210	83.065
-20	3	51	1.210	20.565	48	3	209	1.210	84.274
-19	1	52	0.403	20.968	49	1	210	0.403	84.677
-18	3	55	1.210	22.177	50	1	211	0.403	85.081
-17	5	60	2.016	24.194	51	1	212	0.403	85.484
-16	2	62	0.806	25.000	54	1	213	0.403	85.887
-15	3	65	1.210	26.210	55	1	214	0.403	86.290
-14	1	66	0.403	26.613	58	1	215	0.403	86.694
-13	1	67	0.403	27.016	59	1	216	0.403	87.097
-12	3	70	1.210	28.226	64	1	217	0.403	87.500
-11	1	71	0.403	28.629	65	1	218	0.403	87.903
-10	3	74	1.210	29.839	66	4	222	1.613	89.516
-9	5	79	2.016	31.855	68	1	223	0.403	89.919
-8	1	80	0.403	32.258	69	1	224	0.403	90.323
-7	4	84	1.613	33.871	70	1	225	0.403	90.726
-6	2	86	0.806	34.677	71	3	228	1.210	91.935
-4	2	88	0.806	35.484	72	1	229	0.403	92.339
-3	5	93	2.016	37.500	73	2	231	0.806	93.145
-2	5	98	2.016	39.516	74	1	232	0.403	93.548
-1	5	103	2.016	41.532	79	1	233	0.403	93.952
0	3	106	1.210	42.742	80	1	234	0.403	94.355
1	3	109	1.210	43.952	82	1	235	0.403	94.758
2	3	112	1.210	45.161	85	1	236	0.403	95.161
3	1	113	0.403	45.565	86	1	237	0.403	95.565
4	1	114	0.403	45.968	88	1	238	0.403	95.968
5	4	118	1.613	47.581	89	1	239	0.403	96.371
6	2	120	0.806	48.387	90	1	240	0.403	96.774
7	2	122	0.806	49.194	93	2	242	0.806	97.581
8	4	126	1.613	50.806	99	1	243	0.403	97.984
9	2	128	0.806	51.613	103	2	245	0.806	98.790
10	1	129	0.403	52.016	105	1	246	0.403	99.194
11	2	131	0.806	52.823	108	1	247	0.403	99.597
12	1	132	0.403	53.226	141	1	248	0.403	100.000
13	5	137	2.016	55.242					

THIS PAGE IS BEST QUALITY PRACTICABLE
FROM COPY FURNISHED TO DDC

Table H-3. Frequency distribution of wave heights at station DBI-25.

HGT	FREQUENCY	CUM FREQ	PERCENT	CUM PERCENT
30	9	9	3.629	3.629
33	1	10	0.403	4.032
34	4	14	1.613	5.645
35	15	29	6.048	11.694
36	2	31	0.806	12.500
37	1	32	0.403	12.903
38	2	34	0.806	13.710
39	1	35	0.403	14.111
40	20	55	8.065	22.177
41	2	57	0.806	22.984
42	5	62	2.016	25.000
43	3	65	1.210	26.210
44	1	66	0.403	26.613
45	6	72	2.419	29.032
46	4	76	1.613	30.645
47	2	78	0.806	31.452
48	5	83	2.016	33.468
49	1	84	0.403	33.871
50	20	104	8.065	41.936
51	1	105	0.403	42.339
52	7	112	2.823	45.161
53	2	114	0.806	45.968
54	5	119	2.016	47.984
55	3	122	1.210	49.194
56	6	128	2.419	51.613
57	2	130	0.806	52.419
58	3	133	1.210	53.629
60	17	150	6.855	60.484
61	4	154	1.613	62.097
62	2	156	0.806	62.903
63	4	160	1.613	64.516
64	4	164	1.613	66.129
65	6	170	2.419	68.548
66	1	171	0.403	68.952
67	1	172	0.403	69.355
68	5	177	2.016	71.371
69	1	178	0.403	71.774
70	13	191	5.242	77.016
72	5	196	2.016	79.032
73	2	198	0.806	79.839
74	2	200	0.806	80.645
75	7	207	2.823	83.468
76	1	208	0.403	83.871
78	2	210	0.806	84.677
80	9	219	3.629	88.306
82	1	220	0.403	88.710
85	3	223	1.210	89.919
86	1	224	0.403	90.323
90	4	228	1.613	91.936
91	1	229	0.403	92.339
93	1	230	0.403	92.742
95	1	231	0.403	93.145
96	2	233	0.806	93.952
100	5	238	2.016	95.968
102	1	239	0.403	96.371
110	2	241	0.806	97.177
115	1	242	0.403	97.581
125	1	243	0.403	97.984
130	2	245	0.806	98.790
140	2	247	0.806	99.597
150	1	248	0.403	100.000

THIS PAGE IS NOT QUALITY REPRODUCED
FROM COPY FURNISHED TO YOU

Table I. Summary of distribution of wave heights at station 101-10.

Wave Height (ft)	Frequency (%)	Wave Height (ft)	Frequency (%)
0.0-0.5	1.0	1.5-2.0	1.0
0.5-1.0	1.0	2.0-2.5	1.0
1.0-1.5	1.0	2.5-3.0	1.0
1.5-2.0	1.0	3.0-3.5	1.0
2.0-2.5	1.0	3.5-4.0	1.0
2.5-3.0	1.0	4.0-4.5	1.0
3.0-3.5	1.0	4.5-5.0	1.0
3.5-4.0	1.0	5.0-5.5	1.0
4.0-4.5	1.0	5.5-6.0	1.0
4.5-5.0	1.0	6.0-6.5	1.0
5.0-5.5	1.0	6.5-7.0	1.0
5.5-6.0	1.0	7.0-7.5	1.0
6.0-6.5	1.0	7.5-8.0	1.0
6.5-7.0	1.0	8.0-8.5	1.0
7.0-7.5	1.0	8.5-9.0	1.0
7.5-8.0	1.0	9.0-9.5	1.0
8.0-8.5	1.0	9.5-10.0	1.0

APPENDIX I

BEACH PROFILES AT DUBIDUE AND NORTH ISLANDS

Beach profiles (Figs. I-1 to I-10) were measured from the backshore to approximately 2 feet below the waterline. The backshore reference height remained invariant over time. A map of profile locations is given in Figure 28.

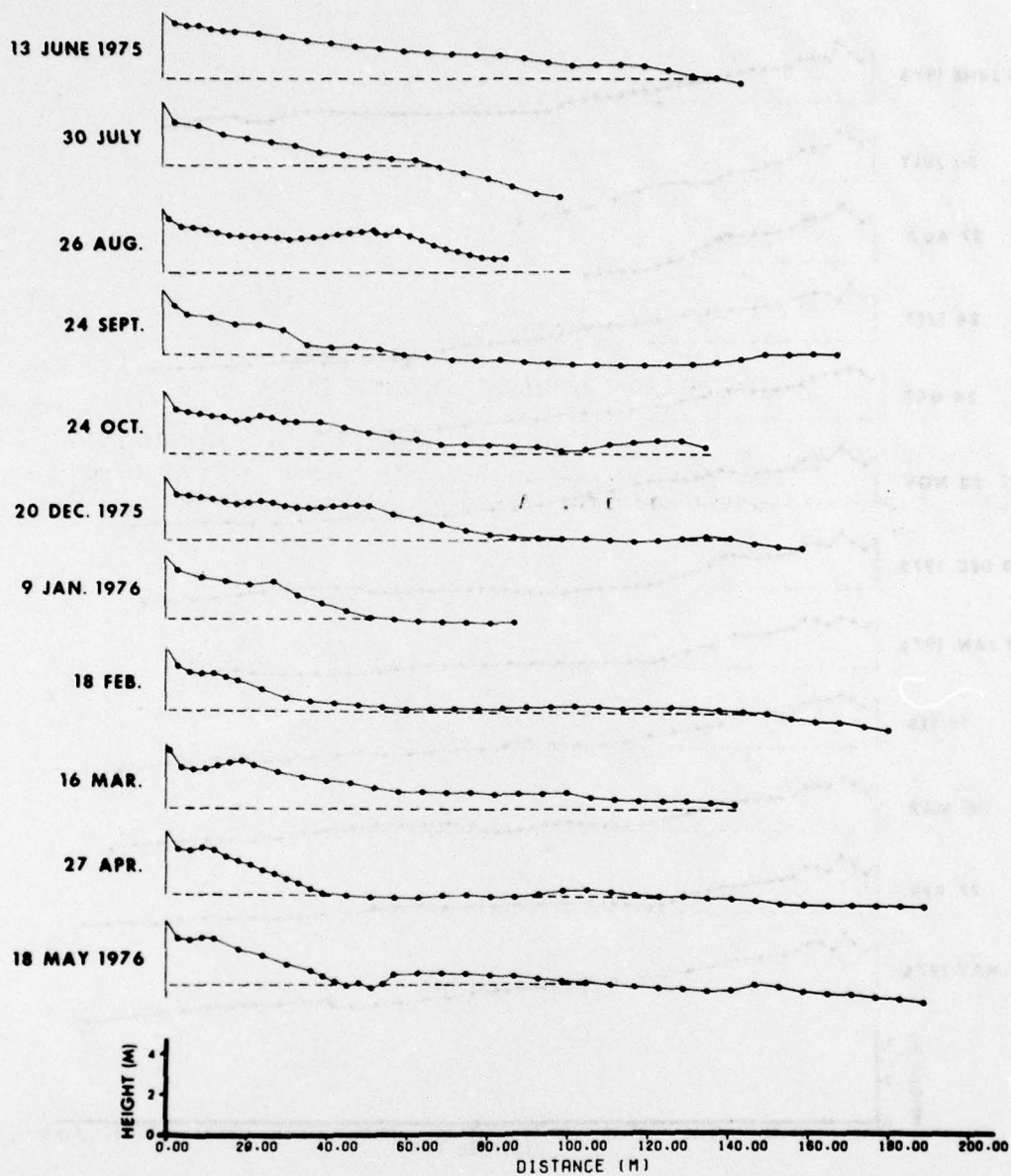


Figure I-1. Beach profiles at station DBI-6, 13 June 1975 to 18 May 1976.

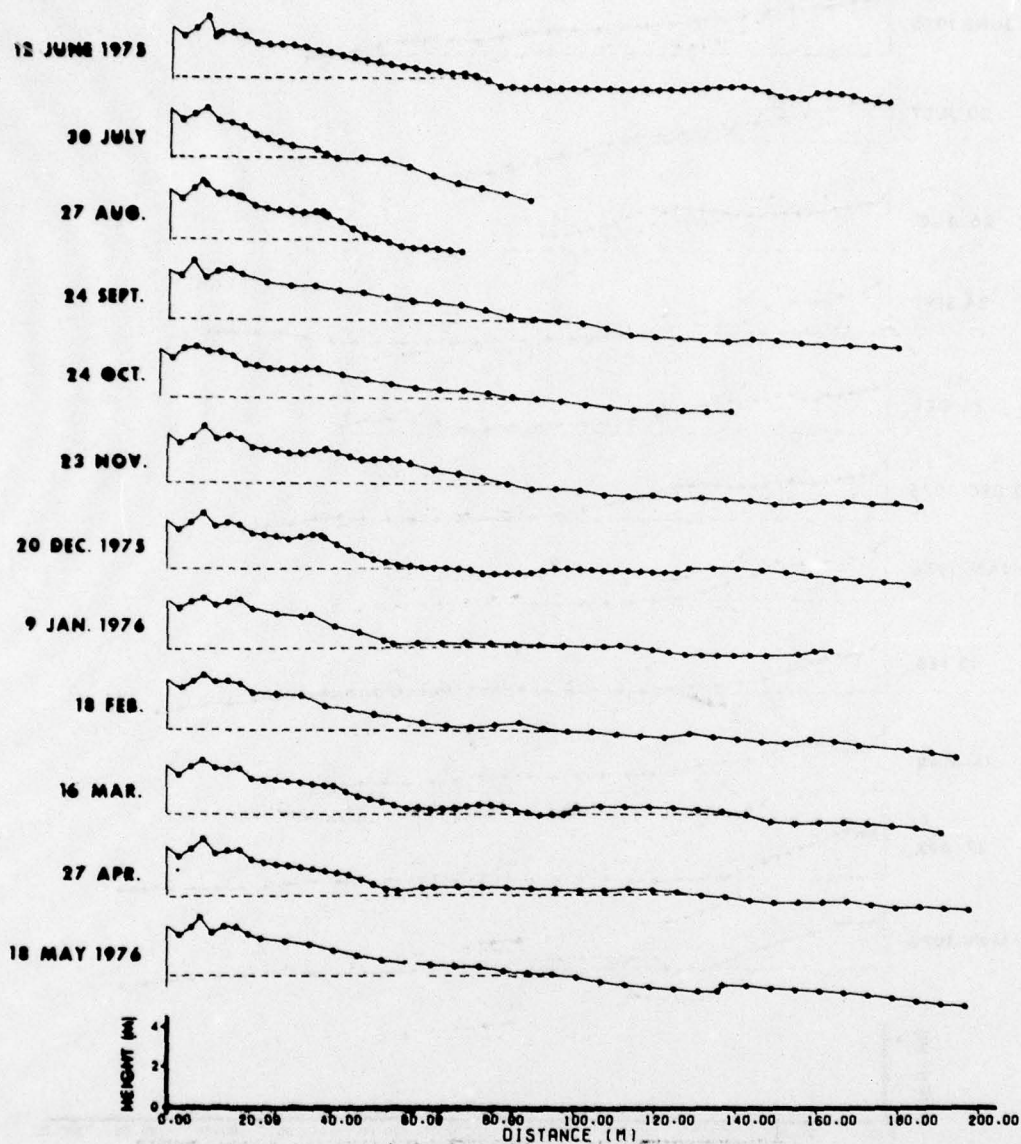


Figure I-2. Beach profiles at station DBI-8, 12 June 1975 to 18 May 1976.

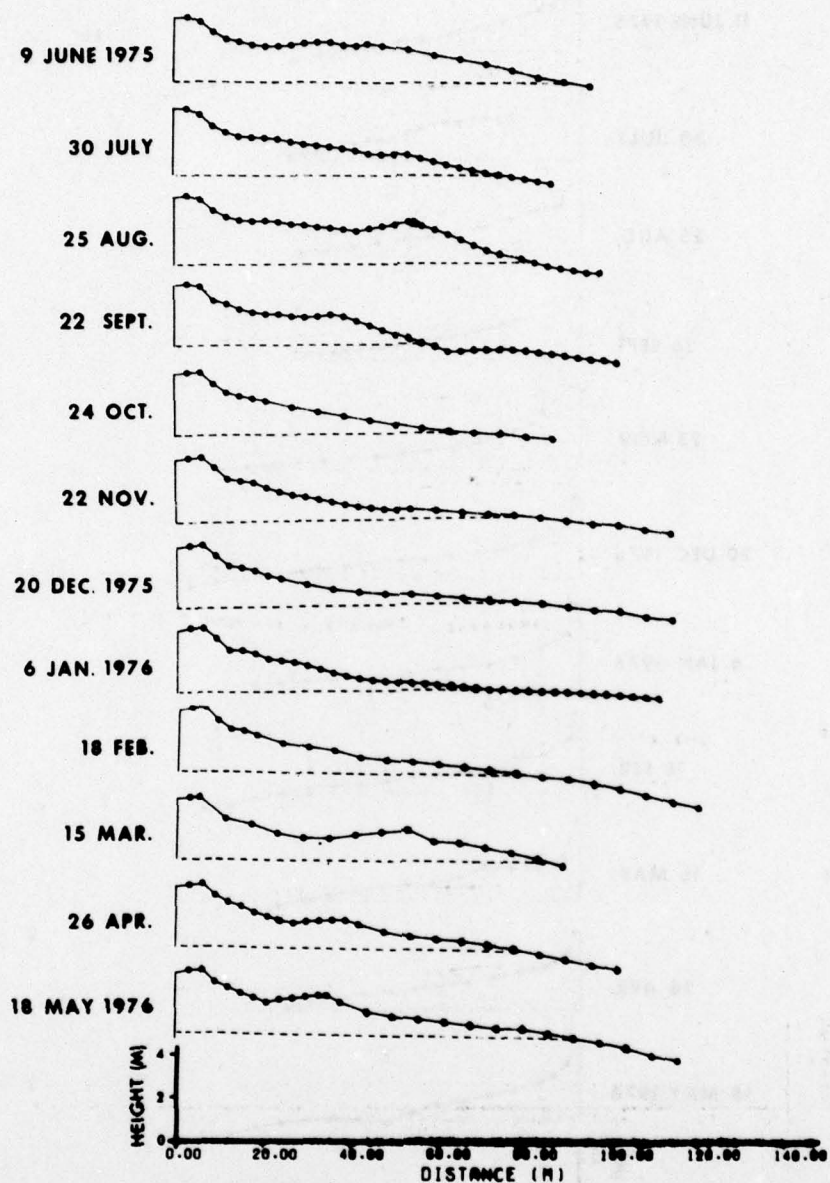


Figure I-3. Beach profiles at station DBI-10, 9 June 1975 to 18 May 1976.

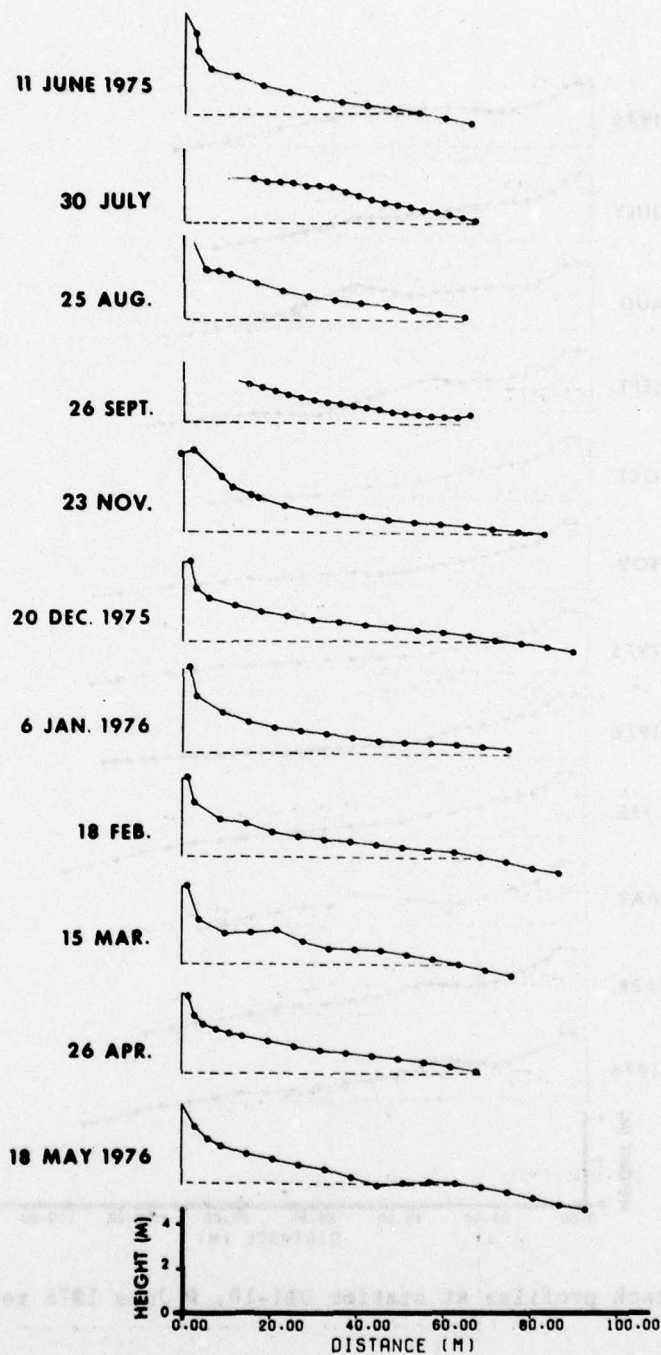


Figure I-4. Beach profiles at station DBI-20, 11 June 1975 to 18 May 1976.

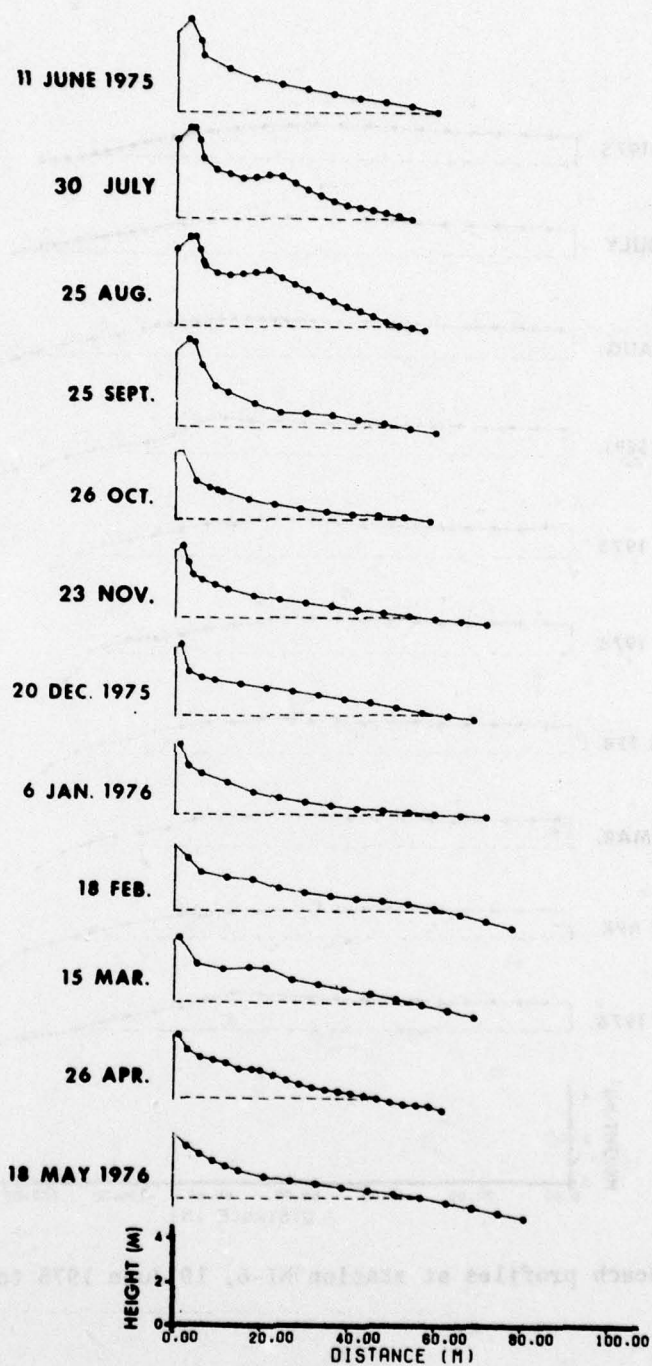


Figure I-5. Beach profiles at station DBI-25, 11 June 1975 to 18 May 1976.

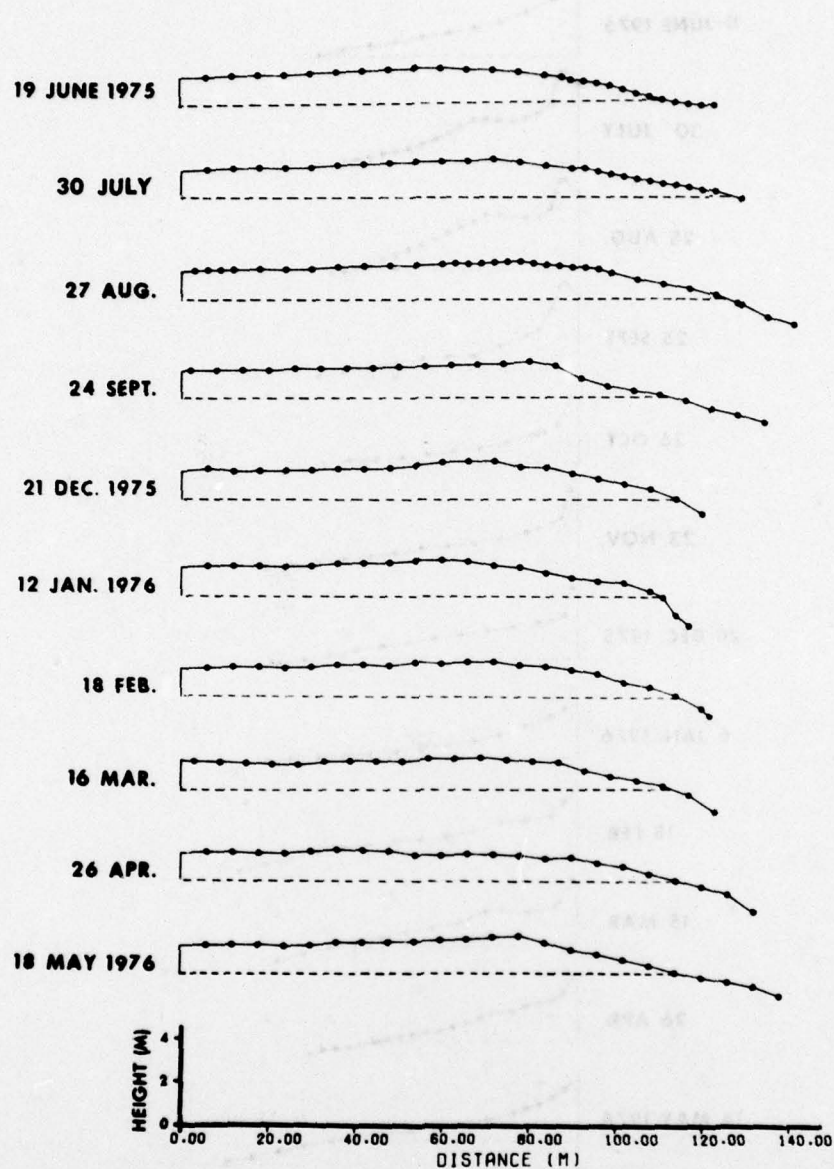


Figure I-6. Beach profiles at station NI-6, 19 June 1975 to 18 May 1976.

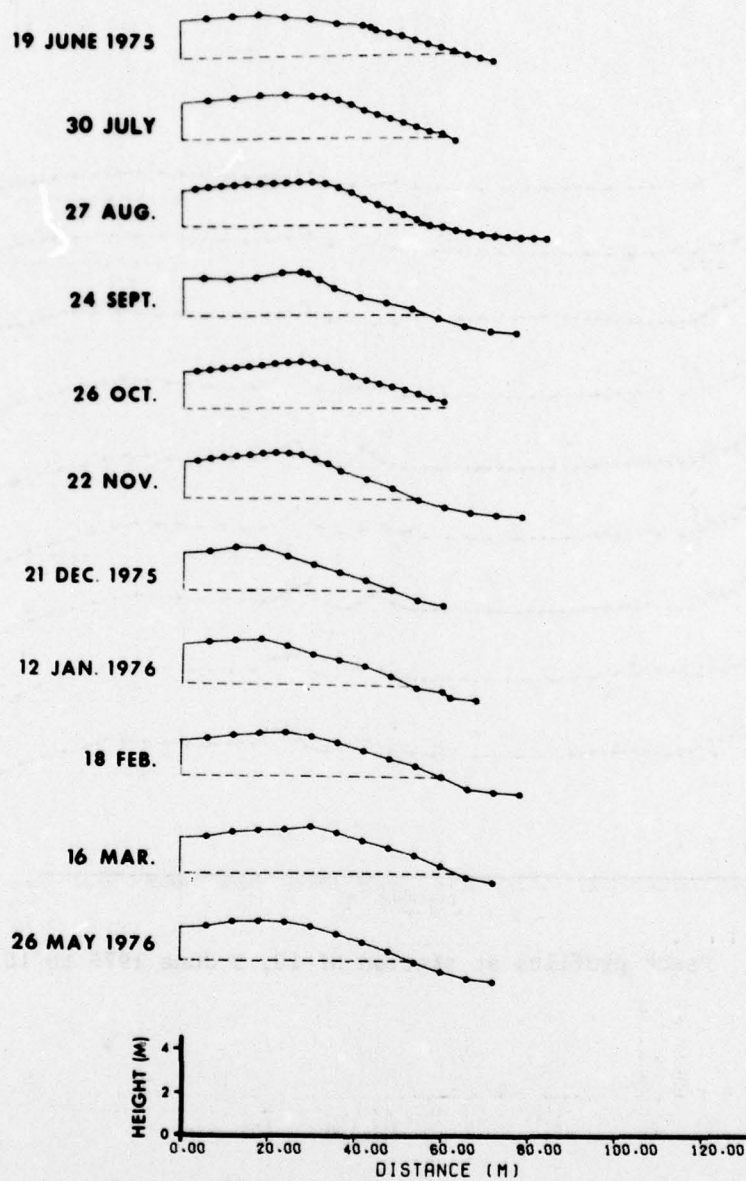


Figure I-7. Beach profiles at station NI-8, 19 June 1975 to 26 May 1976.

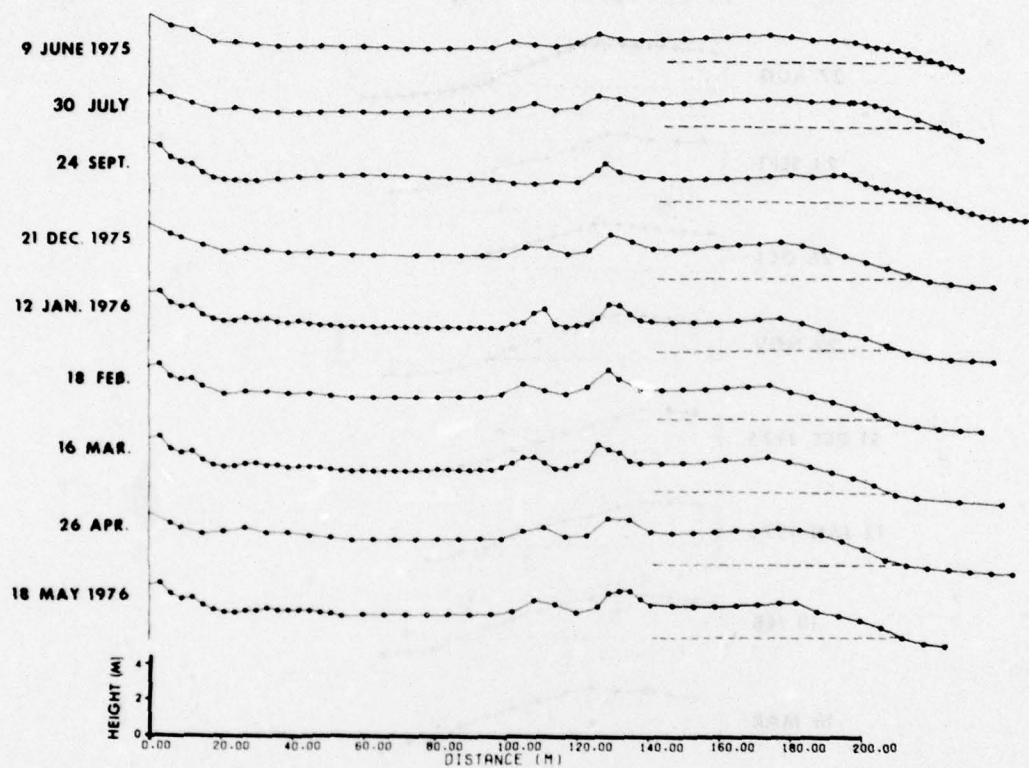


Figure I-8. Beach profiles at station NI-10, 9 June 1975 to 18 May 1976.

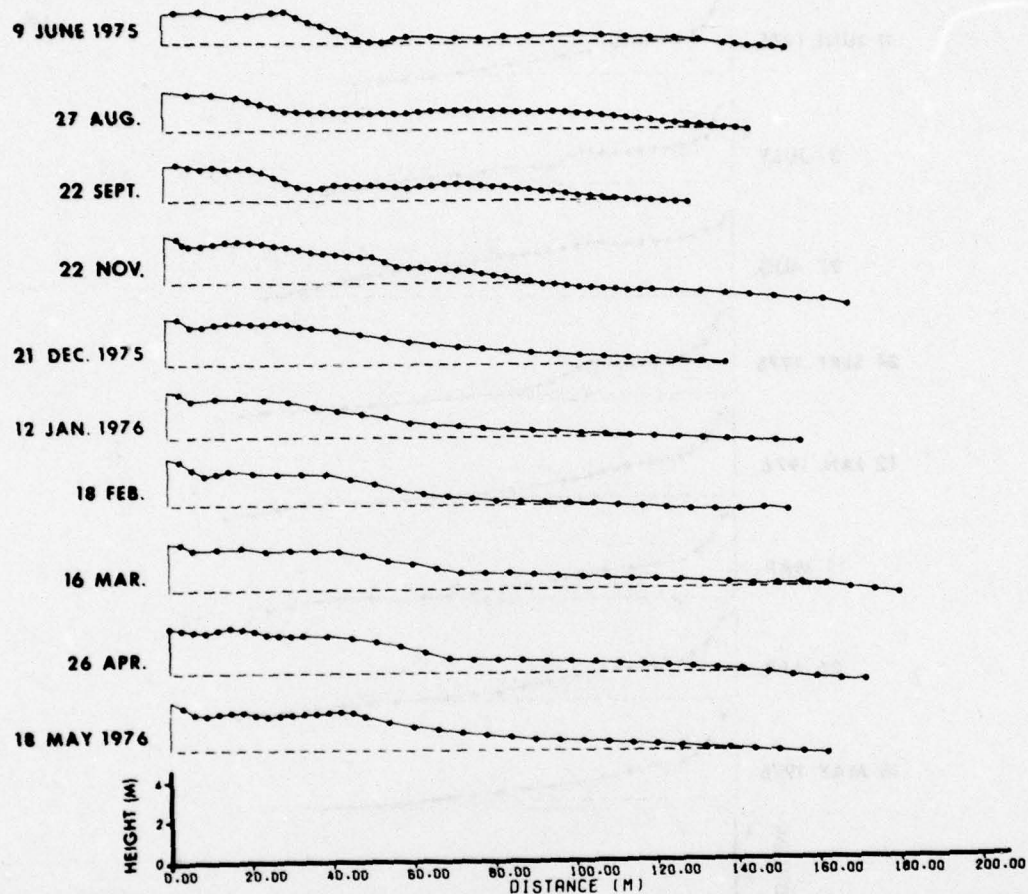


Figure I-9. Beach profiles at station NI-14, 9 June 1975 to 18 May 1976.

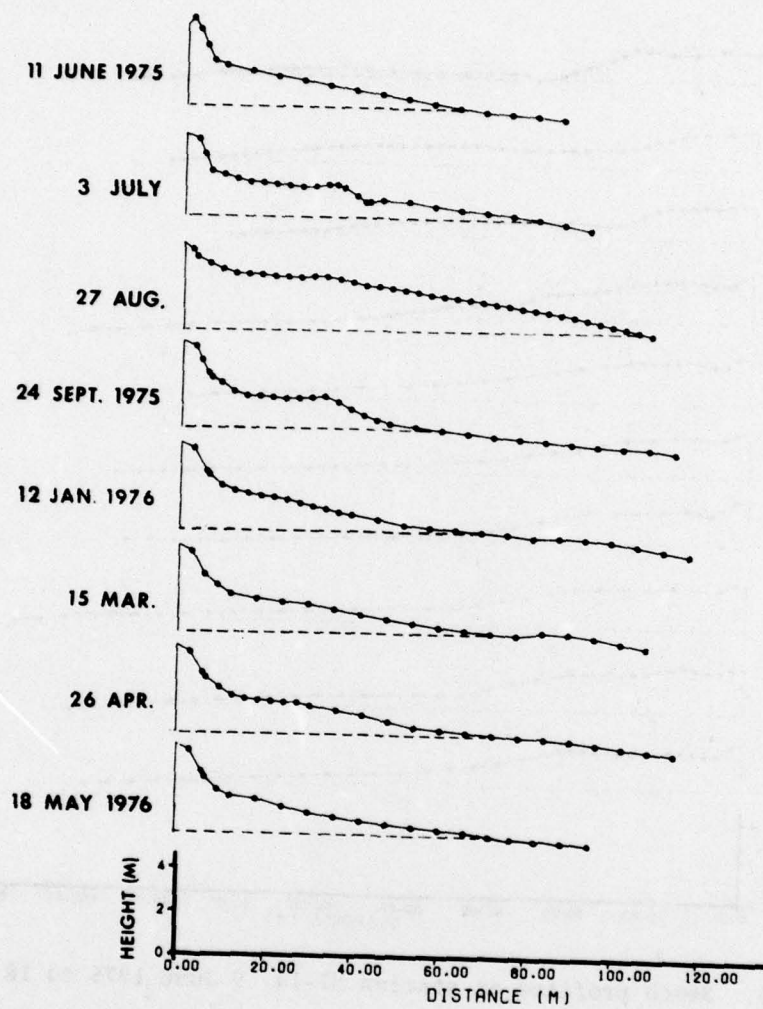


Figure I-10. Beach profiles at station NI-20, 11 June 1975 to 18 May 1976.

Finley, Robert J.

Hydraulics and dynamics of North Inlet, South Carolina, 1974-75 /
by Robert J. Finley. - Fort Belvoir, Va. : U.S. Coastal Engineering
Research Center, 1976.

188 p. : ill. (GITI report 10) Also (Contracts - Coastal Engineer-
ing Research Center : DACW72-72-C-0032 and DACW72-74-C-0018)

Bibliography : p. 126.

Variation in wave parameters, beach and inlet morphology, and tidal
hydraulics are discussed in relation to climatic patterns at North
Inlet, South Carolina.

1. North Inlet, South Carolina. 2. Tidal hydraulics. 3. Tidal
inlets. 4. Coastal morphology. I. Title. II. South Carolina.

University. III. Series : U.S. Army Corps of Engineers. GITI report

10. IV. U.S. Coastal Engineering Research Center. Contract DACW72-
72-C-0032. V. U.S. Coastal Engineering Research Center. Contract
DACW72-74-C-0018.

GB454

.15

US81r

no.10

551.4

Finley, Robert J.

Hydraulics and dynamics of North Inlet, South Carolina, 1974-75 /
by Robert J. Finley. - Fort Belvoir, Va. : U.S. Coastal Engineering
Research Center, 1976.

188 p. : ill. (GITI report 10) Also (Contracts - Coastal Engineer-
ing Research Center : DACW72-72-C-0032 and DACW72-74-C-0018)

Bibliography : p. 126.

Variation in wave parameters, beach and inlet morphology, and tidal
hydraulics are discussed in relation to climatic patterns at North
Inlet, South Carolina.

1. North Inlet, South Carolina. 2. Tidal hydraulics. 3. Tidal
inlets. 4. Coastal morphology. I. Title. II. South Carolina.

University. III. Series : U.S. Army Corps of Engineers. GITI report

10. IV. U.S. Coastal Engineering Research Center. Contract DACW72-
72-C-0032. V. U.S. Coastal Engineering Research Center. Contract
DACW72-74-C-0018.

GB454

.15

US81r

no.10

551.4

Finley, Robert J.

Hydraulics and dynamics of North Inlet, South Carolina, 1974-75 /
by Robert J. Finley. - Fort Belvoir, Va. : U.S. Coastal Engineering
Research Center, 1976.

188 p. : ill. (GITI report 10) Also (Contracts - Coastal Engineer-
ing Research Center : DACW72-72-C-0032 and DACW72-74-C-0018)

Bibliography : p. 126.

Variation in wave parameters, beach and inlet morphology, and tidal
hydraulics are discussed in relation to climatic patterns at North
Inlet, South Carolina.

1. North Inlet, South Carolina. 2. Tidal hydraulics. 3. Tidal
inlets. 4. Coastal morphology. I. Title. II. South Carolina.

University. III. Series : U.S. Army Corps of Engineers. GITI report

10. IV. U.S. Coastal Engineering Research Center. Contract DACW72-
72-C-0032. V. U.S. Coastal Engineering Research Center. Contract
DACW72-74-C-0018.

GB454

.15

US81r

no.10

551.4

Finley, Robert J.

Hydraulics and dynamics of North Inlet, South Carolina, 1974-75 /
by Robert J. Finley. - Fort Belvoir, Va. : U.S. Coastal Engineering
Research Center, 1976.

188 p. : ill. (GITI report 10) Also (Contracts - Coastal Engineer-
ing Research Center : DACW72-72-C-0032 and DACW72-74-C-0018)

Bibliography : p. 126.

Variation in wave parameters, beach and inlet morphology, and tidal
hydraulics are discussed in relation to climatic patterns at North
Inlet, South Carolina.

1. North Inlet, South Carolina. 2. Tidal hydraulics. 3. Tidal
inlets. 4. Coastal morphology. I. Title. II. South Carolina.

University. III. Series : U.S. Army Corps of Engineers. GITI report

10. IV. U.S. Coastal Engineering Research Center. Contract DACW72-
72-C-0032. V. U.S. Coastal Engineering Research Center. Contract
DACW72-74-C-0018.

GB454

.15

US81r

no.10

551.4